Supplementary Materials for

Design of SARS-CoV-2 papain-like protease inhibitor with antiviral efficacy in a mouse model

Bin Tan[1*], Xiaoming Zhang[2*], Ahmadullah Ansari[3,4*], Prakash Jadhav[1*], Haozhou Tan[1], Kan Li[1], Ashima Chopra[3,4], Alexandra Ford[5], Xiang Chi[2], Francesc Xavier Ruiz[3,4]†, Eddy Arnold[3,4]†, Xufang Deng[2,6]†, Jun Wang[1]†

[1]Department of Medicinal Chemistry, Ernest Mario School of Pharmacy, Rutgers, the State University of New Jersey, Piscataway, NJ, 08854, USA

[2]Department Physiological Sciences, College of Veterinary Medicine, Oklahoma State University, Stillwater, OK, 74078, USA

[3]Center for Advanced Biotechnology and Medicine, Rutgers, the State University of New Jersey, Piscataway, NJ, 08854, USA

[4]Department of Chemistry and Chemical Biology, Rutgers, the State University of New Jersey, Piscataway, NJ, 08854, USA

[5]Deprtment of Veterinary Pathobiology, College of Veterinary Medicine, Oklahoma State University, Stillwater, OK, 74078, USA

[6]Oklahoma Center for Respiratory and Infectious Diseases, Oklahoma State University, Stillwater, OK, 74078, USA

[*]These authors contributed equally to this work

†Corresponding author. Email: junwang@pharmacy.rutgers.edu (J.W.); xufang.deng@okstate.edu (X.D.); arnold@cabm.rutgers.edu (E.A.); xavier@cabm.rutgers.edu (F.X.R.)

The PDF file includes:

Materials and Methods

Cell lines and virus

A Vero-E6 cell line, a gift from Dr. Susan Baker (Loyola University Chicago), was grown in Dulbecco's modified Eagle medium (DMEM) (Corning, 10013CM) containing 10% heat-inactivated fetal bovine serum (FBS) (Gibco, 10-438-026), 1% Pen/Strep (30-001-CI), 1× nonessential amino acid (NEAA) (Cytiva HyClone, SH30238.01). A Vero-E6 line expressing human angiotensin-converting enzyme 2 (hACE2) and human transmembrane protease, serine 2 (hTMPRSS2) (Vero-AT), obtained through NIH-BEI Resources (NR-54970) were grown in DMEM containing 10% FBS, 1% Pen/Strep, 1× NEAA, and 10 μg/mL puromycin (InVivogen, ant-pr-1) to maintain the expression of hTMPRSS2 and hACE2. A Caco-2 line expressing hACE2 and hTMPRSS2 (Caco2-AT) (*37*), a gift from Dr. Mohsan Saeed (Boston University), was propagated in DMEM containing 10% FBS, 1% Pen/Strep, 1× NEAA, 1 μg/mL puromycin, and 1 μg/mL blasticidin (InVivogen, ant-bl-05).

The mouse-adapted SARS2-N501Y$_{MA30}$ virus, a gift from Dr. Stanley Perlman (University of Iowa), was propagated once with Vero-AT cells and titrated with Vero-E6 cells. The following SARS-CoV-2 strains/isolates were obtained through BEI Resources, NIAID, NIH: Washington strain 1 (WA1) (NR-52281), recombinant SARS-CoV-2 expressing nano-luciferase reporter (icSARS-CoV-2-nLuc) (NR-54003), Delta strain (NR-55672), Omicron BA.2 strain (NR-56520). These viruses were propagated once with Vero-AT cells to obtain large viral stocks and were titrated with Vero-AT cells. The following recombinant SARS-CoV-2 viruses were generated previously (PMID: 37637734) or in this study using a reverse genetics system developed by Dr. Ralph Baric's group at the University of North Carolina at Chapel Hill (BEI, NR-52281): recombinant wild-type SARS-CoV-2 WA1 strain (rSARS-CoV-2), and recombinant Nsp5/Mpro mutant viruses (rNsp5^{S144M}, rNsp5$^{L50F/E166V}$, and rNsp5$^{L50F/E166V/L167F}$). These viruses were titrated with Vero-E6 cells and full-genome sequenced using the ARTIC method (*38, 39*).

Biocontainment

All procedures with live SARS-CoV-2 were performed in certified biosafety level 3 (BSL3) facilities at Oklahoma State University using biosafety protocols approved by the Institutional Biosafety Committee (IBC), which comprises scientists, biosafety and compliance experts, and members of the local community. All research personnel received rigorous biosafety, biosecurity, and BSL3 training before participating in experiments. Personal protective equipment, including scrubs, disposable overalls, shoe covers, double-layered gloves, and powered air-purifying respirators, were used. Biosecurity measures are built in the environment through building and security systems and are reinforced through required training programs, standing meetings, and emergency exercises. The researchers involved in working with live viruses received the SARS-CoV-2 mRNA vaccine before the study was started. Finally, all researchers were medically cleared by the Oklahoma State University Occupational Health Program.

Enzymatic Assays

The SARS-CoV-2 PL^{pro} enzymatic assays were carried out as follows: The assay was carried out in 96-well plates with 100 μL of 200 nM PL^{pro} protein in PL^{pro} reaction buffer [50 mM HEPES (pH 7.5), 0.01% Triton X-100, and 5 mM DTT]. Then, 1 μl of testing compound at various concentrations was added to each well and incubated at 30°C for 30 min. The enzymatic reaction

was initiated by adding 1 μL of 1 mM FRET substrate Dabcyl-FTLRGG/APTKV-Edans (the final substrate concentration is 10 μM). The reaction was monitored in a Cytation 5 image reader with filters for excitation at 360/40 nm and emission at 460/40 nm at 30°C for 1 hour. The initial velocity of the enzymatic reaction with and without testing compounds was calculated by linear regression for the first 15 min of the kinetic progress curve. The IC_{50} values were calculated by plotting the initial velocity against various concentrations of testing compounds with a dose-response function in Prism 8 software.

For determination of K_m and V_{max}, PL^{pro} was diluted in the reaction buffer (50 mM Hepes (pH 7.5), 0.01% Triton X-100, and 5 mM DTT) to the final concentration of 200 nM, and various concentrations (1.5625, 3.125, 6.25, 12.5, 25, 50, 100, 200 μM) of PL^{pro} FRET substrate were added to initiate the reaction. The reaction was monitored every 71 seconds for 1 hour at 30 °C in Cytation 5 image reader with excitation wavelength at 360/40 nm and emission wavelength at 460/40 nm. The initial velocity of the enzymatic reaction at each concentration of FRET substrate was determined in the first 15 min by linear regression. The K_m and V_{max} were determined by fitting the curves with nonlinear regression of initial velocity vs. concentration of FRET substrate using the Michaelis-Menten equation in Prism 8.

For the K_i measurement, 10 μL 200 nM SARS-CoV-2 PL^{pro} protein was added to 190 μl of PL^{pro} reaction buffer containing testing compound and the FRET substrate, and the reaction was monitored for 2 h. The final FRET substrate concentration in this assay is 20 μM. Detailed curve fitting and K_i determination was described previously (*40, 41*). The equation used for Morrison plot curve fitting is: $Y=V_o*(1-((((E_t + X+(K_i*(1+(S/K_m))))-(((E_t + X+(K_i*(1+(S/K_m))))^2)-4*E_t*X)^0.5))/(2*E_t)))$. Y: enzyme activity; V_0: velocity in the absence of inhibitor; E_t: enzyme concentration (0.2 μM); X: concentration of inhibitor (μM); K_i: dissociation of inhibitor (μM); S: substrate concentration (20 μM); K_m: the concentration of substrate which permits the enzyme to achieve half V_{max} (34.08 μM).

The enzymatic assay of SARS-CoV-2 PL^{pro} with Ub-AMC (UBPBIO, M3010) substrate was carried out in 384-well plate format. compound with various concentrations was mixed with 50 nM SARS-CoV-2 PL^{pro} dissolved in PL^{pro} reaction buffer. After incubation at 30°C for 15 min, the reaction was initiated by adding 2.5 μM Ub-AMC substrate. The fluorescence was monitored using the excitation of 360/40nm and emission of 460/40nm at 30°C for 1 hour. The first 1000 seconds of initial velocity was calculated for plotting IC_{50}. For the K_i measurement, compound with various concentrations was mixed with 2.5 μM Ub-AMC substrate in PL^{pro} reaction buffer, and the reaction was initiated by the addition of 10 nM SARS-CoV-2 PL^{pro}. The fluorescence was monitored immediately in the plate reader for 4 hours. The first 4000 seconds of initial velocity was calculated for plotting the K_i.

The enzymatic assay of SARS-CoV-2 PL^{pro} with ISG15-AMC (R&D, UL553050) substrate was carried out in 384-well plate format. Compound with various concentrations was mixed with 2 nM SARS-CoV-2 PL^{pro} in PL^{pro} reaction buffer. After incubation at 30°C for 15 min, the reaction was initiated by adding 0.5 μM ISG15-AMC substrate. The fluorescence was monitored using the excitation of 360/40nm and emission of 460/40nm at 30°C for 1 hour. The first 500 seconds of initial velocity was calculated for plotting the IC_{50}. For the K_i measurement, compound with various concentrations was mixed with 0.1 μM ISG15-AMC substrate in PL^{pro} reaction buffer, and the reaction was initiated by adding 0.2 nM SARS-CoV-2 PL^{pro}. The fluorescence was monitored immediately in the plate reader with the same condition for 4 hours. The first 2500 seconds of initial velocity was calculated for plotting the K_i.

The counter screening of the compound against USP7(R&D, E519025) and USP14 (Enzo, BMLUW98400100) were performed in 384-well plate format. For the USP7 assay, compound with various concentrations was mixed with 40 nM USP7 dissolved in the USP7 reaction buffer (HEPES 50 mM, pH 7.5, BSA 0.1 mg/mL, Triton X-100 0.01%, DTT 5mM, Glycerol 5%). After incubation at 30°C for 15 min, the reaction was initiated by adding 5 μM Ub-AMC substrate. For the USP14 assay, the procedure was similar, with 1.7 μM of USP14 assayed and 4 μM Ub-AMC. The fluorescence was monitored in Cytation 5 plate reader with excitation of 360/40nm and emission of 460/40nm at 30°C for 1 hour. For both assays, the 3000 seconds of initial velocity was calculated and normalized with that of the DMSO-treated group to determine the percentage inhibition.

Differential Scanning Fluorimetry (DSF)

The thermal shift assay was performed using Thermo Fisher QuantStudio 5 Real-time PCR system. Compounds with various concentrations were mixed with 4 μM SARS-CoV-2 PL^{pro} in the reaction buffer (HEPES 50mM, pH 7.5, DTT 5mM, and Triton X-100 0.01%). After incubation at 30°C for 1 hour, 1x SYPRO orange dye was added. The fluorescence was monitored under a temperature gradient from 25 °C to 95 °C at an increment of 0.05 °C/s. The melting temperature (T_m) was determined by the mid-log of the transition phase from the native to denatured protein by the Boltzmann model in Protein Thermal Shift Software v1.3.

Cell-Based FlipGFP-PL^{pro} Assay

Plasmid pcDNA3-TEV-flipGFP-T2A-mCherry was ordered from Addgene (catalog no.124429). SARS-CoV-2 PL^{pro} cleavage site LRGGAPTK was introduced into pcDNA3-FlipGFP-T2A-mCherry via overlapping PCRs to generate a fragment with SacI and *Hin*dIII sites at the ends. SARS-CoV-2 PL^{pro} expression plasmid pcDNA3.1 SARS2 PL^{pro} was ordered fromGenscript (Piscataway NJ) with codon optimization. For transfection, 96-well Greiner plate (catalog no. 655090) was seeded with HEK293T cells to overnight 70-80% confluency. A total of 9 μL of Opti-MEM, 0.1 μL of 500 ng/μL pcDNA3-flipGFP-T2A-mCherry plasmid, 0.1 μL of 500 ng/μL protease expression plasmid pcDNA3.1, and 0.3 μL of transIT-293 (Mirus) were used each well of a 96-well plate. Three hours after transfection in a cell culture incubator (humidified, 5% CO_2/95% air, 37°C), 1 μL of testing compound was added to each well at 100-fold dilution. Images were acquired 48h after transfection with a Celigo Image Cytometer (Nexcelom) and were analyzed with Gen5 3.10 software (Biotek). SARS-CoV-2 PL^{pro} protease activity was calculated by the ratio of GFP signal sum intensity over the mCherry signal sum intensity. The FlipGFP- PL^{pro} assay IC_{50} value was calculated by plotting the GFP/mCherry signal over the applied compound concentration with a four-parameter dose-response function in Prism 8. The mCherry signal alone was utilized to determine the compound cytotoxicity (*28*).

Antiviral assays with live SARS-CoV-2

Three assays were employed for antiviral effect evaluation: cell viability assay, reporter virus assay, and antiviral plaque assay. For the cell viability assay, Vero-AT cells at a density of $1.5x10^4$ cells/well were batched inoculated with SARS-CoV-2 at a multiplicity of infection (MOI) of 0.2 and then added to 96-well plates (Corning, #3598) in 50 μL per well of DMEM containing 4% FBS and 2μM CP-100356, a P-glycoprotein inhibitor. For the reporter virus assay, Caco2-AT cells at a density of $1.5x10^4$ cells/well were batched inoculated with icSARS-CoV-2-nLuc at a MOI of 0.2 and then added to 96-well plates in 50 μL per well of DMEM containing 4% FBS and 2 μM

CP-100356. To prepare compound solutions, the test compounds and positive control (nirmatrelvir) were 3-fold serially diluted in DMEM, starting at 30 μM final concentration for the test compounds or 3.3 μM for the positive control. After dilution, 50 μL diluted compound was transferred and mixed (1:1 volume ratio) with the cell-virus mixture that was pre-seeded in 96-well plates. Cells were incubated for 24 hours (Caco2-AT) or 48 hours (Vero-AT) at 37 °C with 5% CO_2 and then subjected to a Celltiter-Glo cell viability assay (Promega, G9243) or Nano-Glo Luciferase assay (Promega, N1130) on a Promega GloMax Discover microplate reader (Promega, GM3000) following the instruction of the manufacturer.

For the antiviral plaque assay, Vero-AT cells were seeded in 12-well plates a day prior to infection and the drug dissolved in DMSO was serially diluted in DMEM with 3-fold dilutions between test concentrations, starting at 10 μM final concentration. Cells in 12-well plates were incubated with approximately 20 plaque-forming units (PFUs) per well of each virus for 1 hour. After incubation, the inoculum was removed and 1 mL 1X DMEM-1.2% Avicel (FMC polymers) mixture containing serially-diluted compound and 2uM P-glycoprotein inhibitor, CP-100356 was added to each well. After 48 hours of incubation at 37°C, the DMEM-Avicel mixture was removed and the cells were stained using 0.1% crystal violet solution. Plates were photographed and measured for the area of cells affected by infection using ImageJ.

Mouse experiments

All mouse experiments with SARS-CoV-2 were performed in a certified biosafety level 3 (BSL3) facility at Oklahoma State University. All animal studies were reviewed and approved by the Oklahoma State University Animal Care and Use Committee and met stipulations of the Guide for the Care and Use of Laboratory Animals. Nine to twelve-week-old female Balb/c mice (Strain #: 000651) were procured from the Jackson laboratory. Mice were briefly anesthetized with isoflurane and inoculated intranasally (i.n.) with 5600 PFUs of SARS2-N501Y_{MA30} in a total volume of 50 μl DMEM. PLpro inhibitor (Jun-12-68-2) was dissolved with 0.5% methylcellulose solution containing 2% Tween-80 and was administered via oral gavage using 20G/30mm plastic feeding tubes (Instech, FTP203050) for 3 or 5 days after virus inoculation. Animal weight and health were monitored daily. A group of 5 mice for each treatment were euthanized at 2- and 4 days post-infection (DPI) for necropsy. The left lungs were collected in pre-filled bead tubes (Fisher Scientific, 15-340-153) filled with 1 mL DMEM for viral load determination, and the rest of the lungs were transfused with 1 mL zinc-buffered formalin solution (Fisher Scientific, STLBFZ1) and then removed and fixed with 30 ml zinc-buffered formalin solution for at least two days before removal from BSL3 in accordance with an approved IBC protocol.

Lung viral titer by plaque assay

The lung tissues were homogenized in pre-filled bead tubes using an automated homogenizer (Fisherbrand™, 15-340-164), and followed by centrifugation (400 xg for 5 minutes). The clarified tissue homogenate supernatants were aliquoted and stored at -80 °C or subjected to standard plaque assay with Vero-AT cells. The supernatants were serially diluted in DMEM and inoculated onto Vero-AT cells in twelve-well plates and maintained at 37 °C in 5% CO_2 for 1 hour with gentle rocking every 15 min. After removing the inoculum, plates were overlaid with 1.2 % agarose (Fisherbrand, BP160-500)-1X DMEM mix containing 2% FBS. After 2 days, overlays were removed, and plaques were visualized by staining with 0.1% crystal violet. Viral titers were quantified as PFUs per ml tissue.

Histology and immunohistochemistry (IHC)

Fixed tissues were trimmed, and processed using a Leica ASP300s processor (Leica Biosystems, Leico Biosystems Inc., 1700 Leider Lane, Buffalo Grove, IL 60089 United States) on a delayed short cycle program and embedded in paraffin (Leica Surgipath Paraplast Infiltration and Embedding Medium; Leica Biosystems). Paraffin blocks were cut into 4 µm-thick sections and mounted on VistaVision HistoBond adhesive glass slides from VWR (Radnor, PA). Hematoxylin and eosin (H&E) staining was performed following standard operating procedures with the Sakura Finetek DRS601 (Sakura Finetek USA, Inc., 1750 West 214th Street, Torrance, CA 90501). For IHC, slides were rehydrated with water, following HIER (Heat Induced Epitope Retrieval) performed at 95C^{o} for 20 minutes in Citrate Unmasking solution (H-3300, Vector Laboratories, Newark, CA). SARS-CoV-2 Nucleocapsid antibody [HL448] (Genetex, GTX635686) was diluted 1:5000 in TBS-Tween 20 buffer with 10% normal goat serum and slides were incubated for 1 hour at room temperature (RT). Slides were washed in TBS-Tween 20 buffer and then quenched of endogenous peroxidase using 0.3% H_2O_2 for 10 minutes. Slides were washed and detection was carried out using VECTASTAIN® Elite® ABC-HRP Kit, Peroxidase (Rabbit IgG) (Vector Laboratories, PK-6101) per the manufacturer's instructions. Hematoxylin diluted 1:10 was used as a counterstain. HE stained tissues were evaluated by a board-certified veterinary pathologist for three parameters: presence of edema or hyaline membranes, perivascular lymphoid inflammation, and interstitial pneumonia. Edema or hyaline membranes were evaluated using a distribution-based ordinal scoring with 0, none; 1, <25%; 2, 26-50%, 3, 51-75%, 4, >75% of tissue affected. Perivascular lymphoid inflammation and interstitial pneumonia were evaluated using a severity-based ordinal scoring system on a scale of zero to three: 0 (absent), 1 (mild), 2 (moderate), 3 (severe). IHC was ordinally scored on the percentage distribution of staining in the tissues: 0, absent; 1, 0–25%; 2, 26–50%; 3, 51–75%; 4, >75% of tissue.

RNA extraction and Real-time PCR quantification

Total RNA was extracted from the lung homogenate supernatants using TRIzol (Invitrogen, 15596018) and followed by RNA purification using the ReliaPrep™ RNA Cleanup/Concentration Kit (Promega, Z1073). A total of 1000 ng RNA was used for cDNA synthesis using the RT² HT First Strand Kit (QIAGEN, 330411) which contains a component to eliminate genomic DNA contamination. Quantitative PCR was performed with specific primers (Table S1) using PowerUp SYBR Green Master mix (Fisher, A25918) on QuanStudio 6 Pro (ThermoFisher, A43160). Cycle threshold values were normalized to 18S RNA levels by using the $2^{-\Delta Ct}$ method.

Gene	Forward (5'->3')	Reverse (5'->3')
SARS-CoV-2 N gene	AAGCTGGACTTCCCTATGGTG	CGATTGCAGCATTGTTAGCAGG
Mouse IL-6	GCTACCAAACTGGATATAATCAGGA	CCAGGTAGCTATGGTACTCCAGAA
Mouse IL-1b	TGGACCTTCCAGGATGAGGACA	GTTCATCTCGGAGCCTGTAGTG
Mouse CXCL10	GCTTCCCTATGGCCCTCATT	GCCGTCATTTTCTGCCTCAT
Mouse IFN-b	TCAGAATGAGTGGTGGTTGC	GACCTTTCAAATGCAGTAGATTCA

In vitro PK studies

The *in vitro* PK studies were performed by Wuxi Apptec.

1. Plasma Protein Binding Assay-HTD Method

1. The test compounds or positive control warfarin were spiked into frozen plasma at the final concentration of 2 µM.
2. An aliquot of 150 µL of the compound-spiked plasma sample was added to one side of the chamber in a 96-well equilibrium dialysis plate (HTD dialysis), and an equal volume of dialysis buffer was added to the other side of the chamber. An aliquot of plasma sample was harvested before the incubation and used as T0 samples for recovery calculation. Triplicate incubations were performed.
3. The plate was then incubated in a humidified incubator with 5% CO_2 at 37°C for 4 hours.
4. After incubation, 50 µL samples were taken from the plasma side as well as the buffer side.
5. The plasma sample was mixed with an equal volume of blank buffer; buffer samples were mixed with an equal volume of blank plasma.
6. The matrix-matched samples were quenched with stop solution containing internal standard (IS).
7. Samples were analyzed by LC-MS/MS. Test compound concentrations in plasma and buffer samples were determined based on peak area ratio of analyte to IS without a standard curve.

2. Microsomal CYP Inhibition (IC50 determination) Using 5 in 1 Cocktail Substrates

1) CYP450 enzymatic activities were determined using 5in1 probe substrate cocktail. For each reaction, enzymatic activities in the presence of the test compound at 8 concentrations (e.g. 0.00, 0.050, 0.150, 0.500, 1.50, 5.00, 15.0, or 50.0 µM) were measured in singlet (n=1). A known inhibitor for each isoform, tested at a single concentration (3.00 µM) in duplicate (n=2), was included as positive control.
2) Incubation mixture containing pooled human liver microsomes (Corning, Xenotech, or other qualified vendors; pooled from multiple donors) at 0.200 mg/ml, probe substrates, and standard inhibitors (listed in the following table) or the test compound were warm up at 37.0°C for 10 minutes. The reactions were initiated by the addition of the NADPH (1.00 mM).

CYP isoform	Probe Substrate	Substrate Final Conc. (µM)	Standard Inhibitor	Inhibitor Final Conc. (µM)
1A2	Phenacetin	10.0	α-Naphthoflavone	3.00
2C9	Diclofenac	5.00	sulfaphenazole	3.00
2C19	S-Mephenytoin	30.0	(+)-N-3-benzylnirvanol	3.00
2D6	Dextromethorphan	5.00	quinidine	3.00
3A4	Midazolam	2.00	ketoconazole	3.00

3) After the mixture was incubated at 37.0°C for 10 minutes, ice cold acetonitrile containing the internal standard (IS) was added to terminate the reactions.
4) The metabolites generated from the probe substrates were measured by LC-MS/MS and were assessed based on peak area ratios of analyte/IS.

5) The remaining activity (expressed as % of control activity) was calculated; IC_{50} values of the test compound were determined using SigmaPlot or XLfit with 3- or 4- parameter logistic sigmoidal equation.

3. Kinetic Solubility Assay

1. The Kinetic solubility assay employs the shake flask method followed by HPLC-UV analysis. The following were the step-wise procedure:

– Weigh and dissolve the samples in 100% DMSO as the stock solution of 10 mM. About 10 µL (compound/Media) of stock solution was needed in this assay.

– Add the test compounds and controls (10 mM in DMSO, 10 µL/vial) into the buffer (490 µL/well) placed in a Mini-Uniprep filter. Vortex the samples of kinetic solubility for 2 minutes.

– Incubate and shake the solubility solutions on an orbital shaker with 800 rpm at room temperature for 24 hours.

– Centrifuge at 4000rpm, 20 ℃ for 10 min

– Transfer 400 µL (with or without dilution) of each solubility supernatant into 96- deep well for analysis after the samples were directly filtered by the syringeless filter device

– Determine the test compound concentration of the filtrate using HPLC-UV.

– Inject at least 5 UV standard solutions into HPLC from low to high concentration subsequently and then test the Kinetic solubility supernatant in duplicate.

– Use the QC samples to monitor Kinetic solubility determination process.

4. Liver Microsome Metabolic Stability Assay (NADPH)

1) Test compounds were incubated at 37.0°C with liver microsomes (pooled from multiple donors) at 1.00 µM in the presence of NADPH (~1.00 mM) at 0.500 mg/ml microsomal protein.
2) Positive controls include testosterone (3A4 substrate), propafenone (2D6) and diclofenac (2C9). They were incubated with microsomes in the presence of NADPH.
3) Time samples (0, 5, 15, 30, 45, and 60 minutes) were removed, immediately mixed with cold acetonitrile containing internal standard (IS). Test compounds incubated with microsomes without NADPH for 60 min are also included.
4) Single point for each test condition (n=1).
5) Samples were analyzed by LC/MS/MS; disappearance of test compound was assessed base on peak area ratios of analyte/IS (no standard curve).
6) Using the following equation to calculate the microsome clearance:

$$C_t = C_0 \bullet e^{-k_e \bullet t}$$

$$T_{1/2} = \frac{Ln2}{-k_e} = \frac{0.693}{-k_e}$$

$$CL_{\text{int}(mic)} = \frac{0.693}{In\ vitro\ T_{1/2}} \bullet \frac{1}{mg/mL\ microsomal\ \ protein\ in\ reaction\ system}$$

The mg microsomal protein / g liver weight is 45 for 5 species
The liver weight values will use 40 g/kg, 30 g/kg, 32 g/kg, 20 g/kg and 88 g/kg for rat, monkey, dog, human and mouse, respectively.
The liver clearance will be calculated using CLint(mic) with

$$CL_{\text{int}(liver)} = CL_{\text{int}(mic)} \bullet \frac{mg\ microsomes}{g\ liver} \bullet \frac{g\ liver}{kg\ body\ weight}$$

In vivo PK studies

The *in vivo* PK studies were performed by Pharmaron US.

Male C57BL/6J mice (approximately 6-8 weeks old, 20-30 g, supplied by SPF Biotechology Co. Ltd, Beijing, China) were used for the pharmacokinetic studies . Mice (n=3 oral or intraperitoneal per group) each received either oral gavage administration or intraperitoneal administration of test compound. The dose formulation used for oral dosing was 0.5% methylcellulose (400 cP)/2% Tween 80 in water, administered at a dose level of 50 mg/kg. Serial blood samples (ca. 25 µL blood in to tubes containing heparin-Na as anticoagulant) were collected up to h after the start of dosing via direct vein puncture of the dorsal metatarsal vein. The samples were collected via dorsal metatarsal vein at all time points. At the end of the study, the mice were euthanized by inhalation of rising concentrations of carbon dioxide. Blood was centrifuged to yield plasma. Plasma samples were stored at −75°C prior to analysis.

Plasma sample analysis

Plasma samples (10 uL for mouse) were extracted using protein precipitation with 200 µL of acetonitrile containing an analytical internal standard. An aliquot of the supernatant was analysed by reverse phase LC-MS/MS. Samples were assayed against calibration standards prepared in control plasma and the assay was qualified through inclusion of quality control (QC) samples.

PK data analysis from PK studies

PK parameters were obtained from the plasma concentration–time profiles using non-compartmental analysis with Phoenix (WinNonlin) pharmacokinetic software version 8.3.1.5014 (Pharsight, Mountain View, CA).

All the procedures related to animal handling, care, and the treatment in this study were performed according to Animal care and Use Application (AUP) approved by the Institutional Animal Care and Use Committee (IACUC) of Pharmaron following the guidance of the Association for Assessment and Accreditation of Laboratory Animal Care (AAALAC). Pharmaron's IACUC policies are compliance with laws and regulations of local government for animal research, and also compliance with the guidelines of the Guide for the Care and Use of Laboratory Animals.

Cytotoxicity assay in Vero E6 cells

The cytotoxicity of compounds was determined using the neutral red uptake assay (*22*). Briefly, 252,000 cells/mL of Vero cells grown in DMEM with 10% fetal bovine serum (FBS) were dispensed into 96-well cell culture plates at 100 µL/well. Twelve hours later, the growth DMEM medium was aspirated and washed with 100 µL PBS buffer. After aspiration, 100 µL fresh DMEM medium with 2% FBS was first added, followed by the addition of 1 µL serially diluted compounds. Another 100 µL fresh DMEM medium with 2% FBS was added as an overlay as soon as the compounds were added. After 48 hours of incubation at 37 °C, the medium was aspirated and replaced with 100 µL serum-free DMEM medium containing 40 µg/mL neutral red and incubated at 37 °C for 2 hours. After aspiration and washing with 100 µL PBS buffer, 100 µL neutral red destain solution was added to extract the neutral red from the cells. Shake the plate till a homogeneous solution formed in each well, the amount of neutral red taken up was determined by measuring the absorbance at 540 nm using a BioTek Microplate Epoch 2 Reader

(Agilent). The CC_{50} values were calculated from best-fit dose-response curves with the variable slope in Prism 9.

Recombinant protein production

The PL^{pro} bacterial expression plasmid was obtained through BEI Resources, NIAID, NIH: Vector pMCSG53 Containing the SARS-Related Coronavirus 2, Wuhan-Hu-1 Papain-Like Protease Gene, NR-52897. Protein expression and purification were done similarly as reported (*42*). Briefly, the pMCSG53-PL^{pro} plasmid was transformed into the *E. coli* BL21(DE3) strain (Invitrogen) and cultured in LB medium supplemented with ampicillin (100 µg/ml). The transformed cells were induced with 1 mM IPTG at an OD600 of 0.8, followed by expression at 16 °C for 18 hours.
Bacterial cells were harvested by centrifugation at 7000 × g and cell pellets were resuspended in a 12.5 ml lysis buffer (500 mM NaCl, 5% (v/v) glycerol, 50 mM HEPES(2-[4-(2-Hydroxyethyl)piperazin-1-yl]ethane-1-sulfonic acid) pH 8.0, 20 mM imidazole pH 8.0, 1 mM TCEP, 1 µM $ZnCl_2$) per liter culture and sonicated at 120 W for 10 min (4 s ON, 20 s OFF). The lysate was clarified by centrifugation at 37000 × g for 60 min at 4 °C. Ni-NTA purification was performed according to the manufacturer's recommendations (Qiagen, Valencia, CA USA) with the lysis buffer. Bound PL^{pro} was eluted with 20 ml of lysis buffer supplemented to 500 mM imidazole pH 7.5, followed by Tobacco Etch Virus (TEV) protease treatment at 1:25 protease:protein ratio at 4 °C overnight, and a reverse Ni-NTA purification. Size exclusion chromatography was performed on a Superdex 200 increase 10/300 GL column equilibrated in lysis buffer. Peak fractions were pooled, buffer-exchanged to a final buffer 150 mM NaCl, 50 mM tris(hydroxymethyl)aminomethane (Tris) pH 7.5, 1 µM $ZnCl_2$, 4 mM TCEP and concentrated at 20 mg/ml. In the case of the PLpro-**Jun11313** structure, the buffer used was identical, except that 20 mM HEPES pH 7.5 was utilized and PL^{pro} was concentrated at 8 mg/ml.

Crystallization of SARS-CoV-2 PL^{pro} with inhibitors

For co-crystallization of the PL^{pro}-**Jun11313** complex, 10-fold molar excess of inhibitor was added to PL^{pro} and incubated for 1-2 hr on ice. The complex was then clarified by spinning at 15,000 × g for 20 minutes before the crystallization screening. The sitting drop vapor diffusion method was dispensed with the help of an Oryx8 robot (Douglas Instruments Ltd) in 96-well Intelli-Plate (Art Robbins Instruments). Cocrystallizations were attempted with the protein-to-matrix ratio of 1:1, 2:1 and 1:2 at 4 °C and 20 °C in a focused screen based on the SARS-CoV-2 PL^{pro} PDB deposited conditions. After several crystallization optimization steps, crystals started growing in a hanging drop vapor-diffusion setup consisting of 4µl protein against 2µl well solution. After two weeks, hexagonal shaped cocrystals grew with protein at 8 mg/ml, inhibitor at 2.2 mM and a well solution containing sodium citrate dibasic trihydrate pH 6.7, ammonium sulfate 2.5 M at 4 °C, in the space group $P3_221$ with four copies of the complex in the asymmetric unit.
For cocrystallization with the rest of inhibitors, a similar initial approach was used (sitting drop), except the protein (20 mg/ml) was mixed with inhibitors at 5.7 mM (molar ratio of 2:1), and a well solution containing 0.1 M Bis-Tris pH 5.5-6.5, 200 mM zinc acetate, 8-12% PEG 8000 at 4 °C. Pyramidal shaped crystals (~150µm) grew in 1 hour, belonging to the $I4_122$ space group, with one copy of the complex in the asymmetric unit. Crystals selected for data collection were washed in the crystallization buffer supplemented with 20% glycerol and flash-cooled in liquid nitrogen.

Data collection, structure determination, and refinement

Single-wavelength X-ray diffraction data for **Jun11313**, **Jun12129**, **Jun12145**, **Jun12197** and **Jun 12162** were collected at 100K temperature at the beamline 23-ID-B at Advance Photon Source at Argonne National Laboratory (Lemont, IL), and **Jun12199**, **Jun12303**, **Jun11941** and **Jun12682** were collected at Beamline 17-ID-1(AMX) at NSLS-II at Brookhaven National Laboratory (Upton, NY), respectively. All data sets were collected remotely, followed by crystal rastering before data collection to find the best diffraction spot on the crystals.

The dataset for the PL^{pro}-**Jun11313** complex was indexed, integrated, and scaled using HKL2000 (*43*), and the rest of the data sets were processed by using Dials (*44*), Aimless (*45*) or autoPROC from Global Phasing (*46*). The structure coordinates were obtained by molecular replacement method using PDB 7NFV as a template in Phaser (*47*). The obtained initial maps were used to generate the unbiased polder difference map for the inhibitor (*36*). The inhibitor electron density was visualized and examined, and the inhibitor molecules were fitted by using Coot (*48*). To obtain a better model and converging Rwork/Rfree values, the datasets were subjected to refinement iteratively by manual model building in Coot followed by refinement in Phenix (*49*). Solvent molecules were added in the last few refinement cycles. Statistics of diffraction data processing and the model refinement are given in table S1. The inhibitor restraints were generated with the Grade online server, and the interactions were assessed with the help of the PLIP online server (*50*) and manually in Coot. PLpro-inhibitor complex structures were analyzed, and the figures showing the protein-inhibitor cocrystal structures were made with PyMOL.

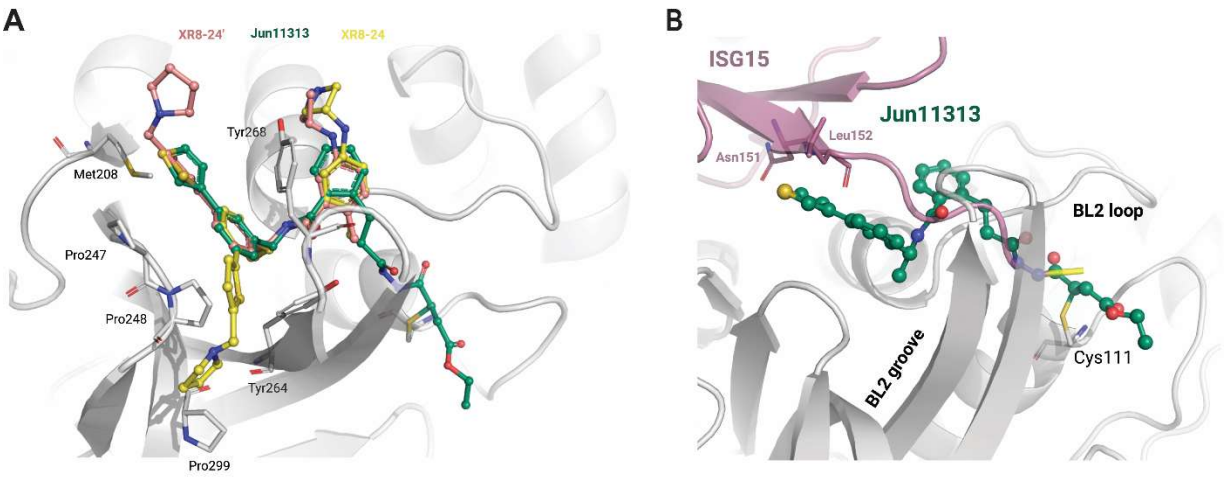

Fig. S1. Comparison of Jun11313, XR8-24, and ISG15 binding to SARS-CoV-2 PL^{pro}. (**A**) Superposition of the PL^{pro}-**Jun11313** structure to the structure of the PL^{pro}-**XR8-24** complex (PDB 7LBS), with **XR8-24** in yellow sticks and spheres, with the relevant residues for binding of both compounds indicated. Additionally, **XR8-24'** is displayed as light pink sticks and spheres, representing the docking of **XR8-24** with a phenyl-substituted moiety in the opposite direction to the experimental data, pointing towards the solvent. (**B**) Superposition of the PL^{pro}-**Jun11313** structure to the structure of SARS-CoV-2 PL^{pro} in complex with ISG15 (magenta ribbons, PDB 7RBS). The phenyl thienyl group of **Jun11313** is binding in the ISG15 binding site (analogous to the Ubiquitin binding site) of SARS-CoV-2 PL^{pro} in the region where residues Asn151^{ISG15} and Leu152^{ISG15} at the end of a β sheet in ISG15 interact with PL^{pro}. The BL2 loop and BL2 groove elements of PL^{pro} are highlighted alongside the catalytic residue Cys111.

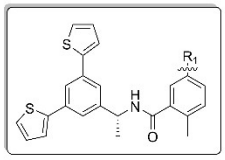

Jun11924
IC_{50} = 177.7 ± 10.0 nM
CC_{50} = 36.4 ± 1.3 μM

Jun11922
IC_{50} = 171.2 ± 14.0 nM
CC_{50} = 11.0 ± 0.4 μM

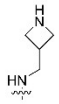

Jun1238
IC_{50} = 339.8 ± 29.0 nM
CC_{50} = 5.9 ± 0.7 μM

Jun12112
IC_{50} = 184.1 ± 22.0 nM
CC_{50} = 7.9 ± 1.4 μM

Jun1271
IC_{50} = 116.6 ± 16.0 nM
CC_{50} = 4.6 ± 0.4 μM

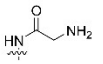

Jun11923
IC_{50} = 147.2 ± 7.0 nM
CC_{50} = 11.6 ± 0.7 μM

Jun12111
IC_{50} = 118.2 ± 12.0 nM
CC_{50} = 8.23 ± 0.26 μM

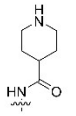

Jun11945
IC_{50} = 162.8 ± 0.5 nM
CC_{50} = 13.5 ± 0.7 μM

Jun11874
IC_{50} = 65.1 ± 1.4 nM
CC_{50} = 7.0 ± 1.1 μM

Jun11875
IC_{50} = 66.2 ± 2.0 nM
CC_{50} = 4.5 ± 1.6 μM

Jun11899
IC_{50} = 75.9 ± 2.0 nM
CC_{50} = 6.5 ± 0.3 μM

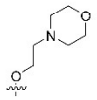

Jun118910
IC_{50} = 367.1 ± 3.0 nM
CC_{50} = 96.8 ± 3.6 μM

Jun11898
IC_{50} = 132.6 ± 4.0 nM
CC_{50} = 19.1 ± 4.2 μM

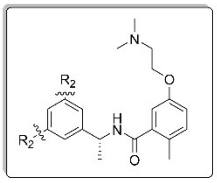

Jun11931
IC_{50} = 99.3 ± 4.0 nM
CC_{50} = 9.4 ± 1.0 μM

Jun119415
IC_{50} = 143.2 ± 9.0 nM
CC_{50} = 7.6 ± 0.3 μM

Jun11903
IC_{50} = 202.2 ± 8.0 nM
CC_{50} = 7.7 ± 0.4 μM

Jun11932
IC_{50} = 83.7 ± 6.0 nM
CC_{50} = 16.0 ± 1.2 μM

Jun11934
IC_{50} = 109.0 ± 7.0 nM
CC_{50} = 37.1 ± 4.4 μM
$T_{1/2}$ = 17.9 min

Jun11933
IC_{50} = 103.0 ± 7.0 nM
CC_{50} = 13.8 ± 1.9 μM

Jun11943
IC_{50} = 167.3 ± 7.0 nM
CC_{50} = 9.1 ± 0.3 μM

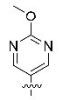

Jun1218
IC_{50} = 1.95 ± 0.08 μM
CC_{50} = 89.8 ± 3.0 μM

Jun11941
IC_{50} = 151.1 ± 4.0 nM
CC_{50} = 54.8 ± 8.3 μM
FlipGFP EC_{50} = 1.8 ± 0.2 μM
$T_{1/2}$ > 145 min

Jun11942
IC_{50} = 178.5 ± 8.0 nM
CC_{50} = 160.4 ± 59.2 μM
FlipGFP EC_{50} = 2.2 ± 0.2 μM
$T_{1/2}$ = 45.5 min

Jun1212
IC_{50} = 390.3 ± 25.0 nM
CC_{50} = 17.8 ± 0.3 μM

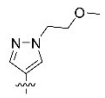

Jun1215
IC_{50} = 181.7 ± 6.0 nM
CC_{50} = 77.6 ± 5.5 μM
FlipGFP EC_{50} = 4.7 ± 0.4 μM

Jun1247
IC_{50} = 165.3 ± 9.0 nM
CC_{50} > 125 μM
FlipGFP EC_{50} > 60 μM

Jun12382
IC_{50} = 443.4 ± 44.0 nM
CC_{50} = 31.0 ± 2.1 μM

Jun1246
IC_{50} = 463.6 ± 39.1 nM
CC_{50} = 39.6 ± 4.7 μM

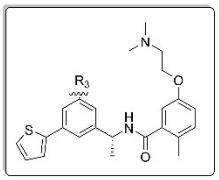

Jun1211
IC_{50} = 152.7 ± 6.0 nM
CC_{50} = 9.8 ± 1.0 μM

Jun1244
IC_{50} = 81.9 ± 8.0 nM
CC_{50} = 9.0 ± 0.7 μM
$T_{1/2}$ = 6.6 min

Jun1251
IC_{50} = 74.7 ± 4.0 nM
CC_{50} = 7.6 ± 0.4 μM
$T_{1/2}$ = 25 min

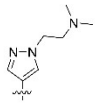

Jun1252
IC_{50} = 116.4 ± 10.0 nM
CC_{50} = 8.2 ± 0.2 μM
$T_{1/2}$ = 66.8 min

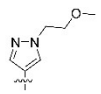

Jun1254
IC_{50} = 111.8 ± 11.0 nM
CC_{50} = 9.7 ± 2.2 μM

Jun1257
IC_{50} = 113.5 ± 8.0 nM
CC_{50} = 18.0 ± 1.6 μM
$T_{1/2}$ = 55.6 min

Jun121210
IC_{50} = 81.9 ± 5.7 nM
CC_{50} > 125 μM
FlipGFP EC_{50} = 13.6 ± 1.9 μM

Jun12149
IC_{50} = 73.8 ± 3.0 nM
CC_{50} = 6.3 ± 1.1 μM

Jun12129
IC_{50} = 90.9 ± 4.6 nM
CC_{50} = 8.3 ± 1.2 μM

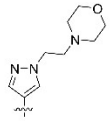

Jun121910
IC_{50} = 66.4 ± 3.0 nM
CC_{50} = 17.7 ± 2.1 μM
FlipGFP EC_{50} = 1.1 ± 0.2 μM
$T_{1/2}$ = 28.5 min

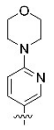

Jun12511
IC_{50} = 91.5 ± 17.0 nM
CC_{50} = 6.2 ± 0.2 μM
$T_{1/2}$ = 91.2 min

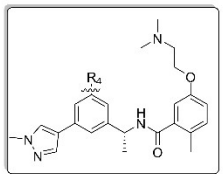

Jun12145
IC_{50} = 108.5 ± 6.2 nM
CC_{50} = 31.3 ± 5.4 μM
FlipGFP EC_{50} = 1.3 ± 0.3 μM
$T_{1/2}$ = 26.3 min

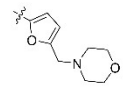

Jun12681
IC_{50} = 120.2 ± 5.1 nM
CC_{50} = 114.5 ± 3.4 μM
FlipGFP EC_{50} = 1.8 ± 0.3 μM

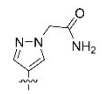

Jun121911
IC_{50} = 73.2 ± 3.2 nM
CC_{50} > 125 μM
FlipGFP EC_{50} > 60 μM

Jun12336
IC_{50} = 118.2 ± 6.4 nM
CC_{50} > 125 μM
$T_{1/2}$ < 2.5 min

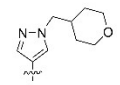

Jun12467
IC_{50} = 73.26 ± 6 nM
CC_{50} = 165.2 ± 26.5 μM
FlipGFP EC_{50} = 1.7 ± 0.4 μM
$T_{1/2}$ = 139.1 min

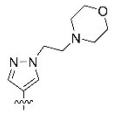

Jun12351
IC_{50} = 98.8 ± 5.2 nM
CC_{50} > 125 μM
FlipGFP EC_{50} = 2.0 ± 0.4 μM
$T_{1/2}$ > 145 min

Jun12199
IC_{50} = 108.8 ± 10.2 nM
CC_{50} = 63.2 ± 11.3 μM
FlipGFP EC_{50} = 0.8 ± 0.1 μM
$T_{1/2}$ = 79.7 min

Jun12197
IC_{50} = 102.7 ± 10.2 nM
CC_{50} = 43.7 ± 5.1 μM
FlipGFP EC_{50} = 0.6 ± 0.1 μM
$T_{1/2}$ = 116.0 min

Jun12603
IC_{50} = 112.2 ± 6.0 nM
CC_{50} = 61.0 ± 19.3 μM
FlipGFP EC_{50} = 2.4 ± 0.4 μM

Jun12446
IC_{50} = 132.5 ± 4.2 nM
CC_{50} = 8.6 ± 0.5 μM

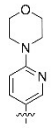

Jun12278
IC_{50} = 88.1 ± 11.5 nM
CC_{50} = 37.3 ± 3.8 μM
FlipGFP EC_{50} = 1.0 ± 0.2 μM
$T_{1/2}$ = 71.3 min

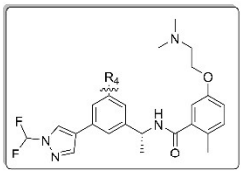

Jun12162
IC_{50} = 98.3 ± 7.0 nM
CC_{50} = 42.3 ± 2.3 μM
FlipGFP EC_{50} = 2.1 ± 0.2 μM
$T_{1/2}$ = 76.7 min
SARS-CoV-2
EC_{50} = 0.33 μM (A549)

Jun12208
IC_{50} = 91.6 ± 6.0 nM
CC_{50} = 167.8 ± 15.8 μM
FlipGFP EC_{50} = 16.9 ± 3.3 μM

Jun12235
IC_{50} = 162.2 ± 10.0 nM
CC_{50} = 16.5 ± 6.8 μM

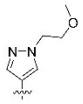

Jun12281
IC_{50} = 111.9 ± 9.0 nM
CC_{50} = 59.2 ± 10.0 μM
FlipGFP EC_{50} = 1.8 ± 0.5 μM
$T_{1/2}$ = 75.6 min

Jun12303
IC_{50} = 121.5 ± 4.0 nM
CC_{50} = 56.8 ± 7.4 μM
FlipGFP EC_{50} = 2.6 ± 0.2 μM
$T_{1/2}$ = 136 min

Jun12284
IC_{50} = 96.6 ± 6.0 nM
CC_{50} = 30.4 ± 9.5 μM
FlipGFP EC_{50} = 2.1 ± 0.4 μM

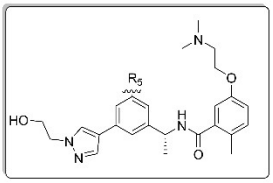

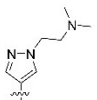

Jun12165
IC_{50} = 145.0 ± 10.0 nM
CC_{50} > 125 μM

Jun12168
IC_{50} = 72.4 ± 3.0 nM
CC_{50} = 34.5 ± 10.2 μM
FlipGFP EC_{50} = 9.7 ± 1.5 μM

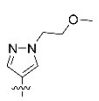

Jun12163
IC_{50} = 102.0 ± 7.0 nM
CC_{50} > 125 μM

Jun12164
IC_{50} = 92.4 ± 4.0 nM
CC_{50} > 125 μM

Jun12198
IC_{50} = 142.0 ± 19.0 nM
CC_{50} > 125 μM

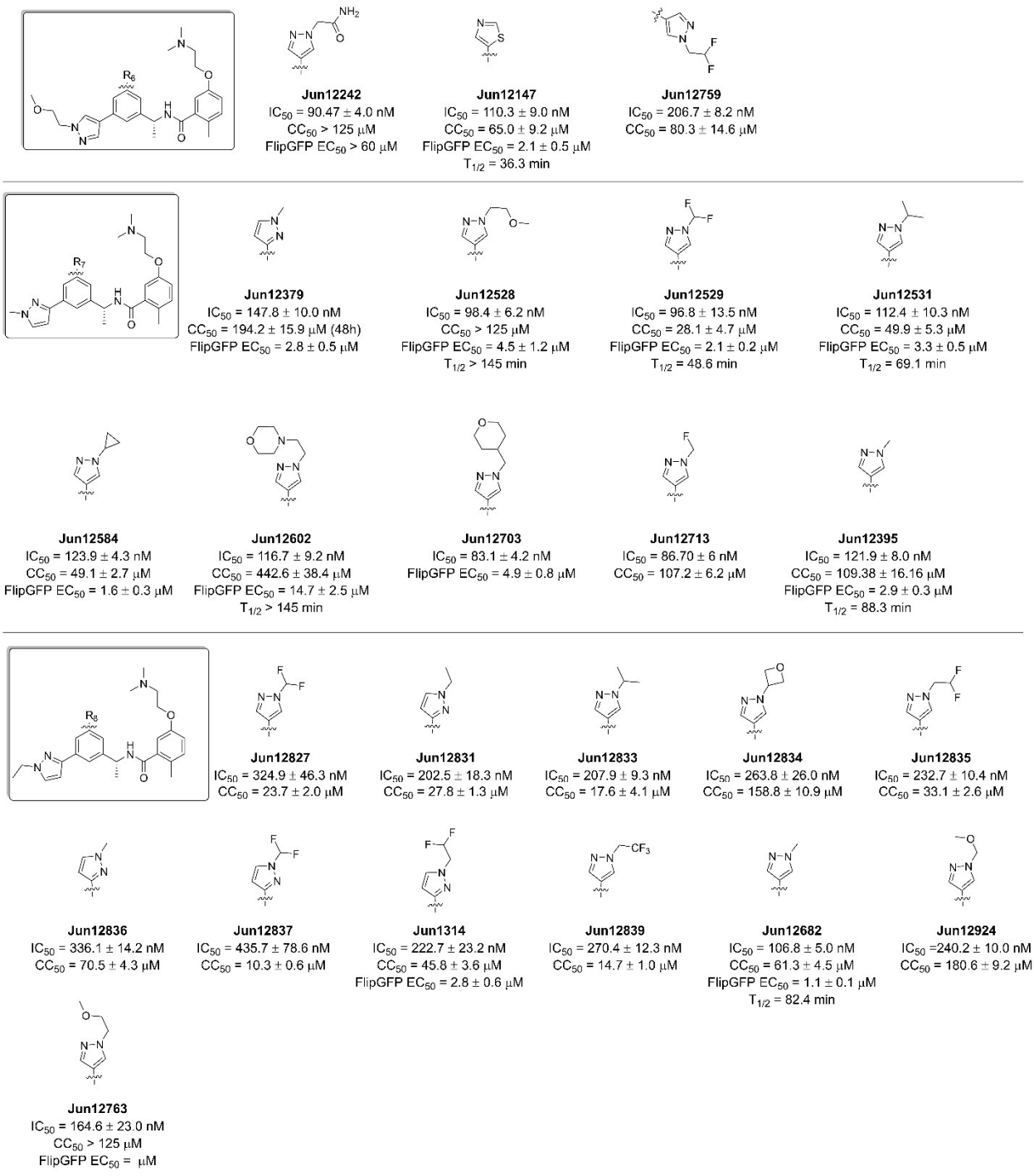

Fig. S2. Lead optimization of biarylphenyl series of SARS-CoV-2 PL^{pro} inhibitors. IC_{50} values were obtained in the FRET-based enzymatic assay as described in the materials and methods section. CC_{50} values were determined using the neutral red method in Vero E6 cells with a 48 h incubation. FlipGFP EC_{50} values were measured in 293T cells transfected with the pcDNA3-flipGFP-T2A-mCherry plasmid and PL^{pro} expression plasmid pcDNA3.1. The results are mean ± standard deviation of three replicates.

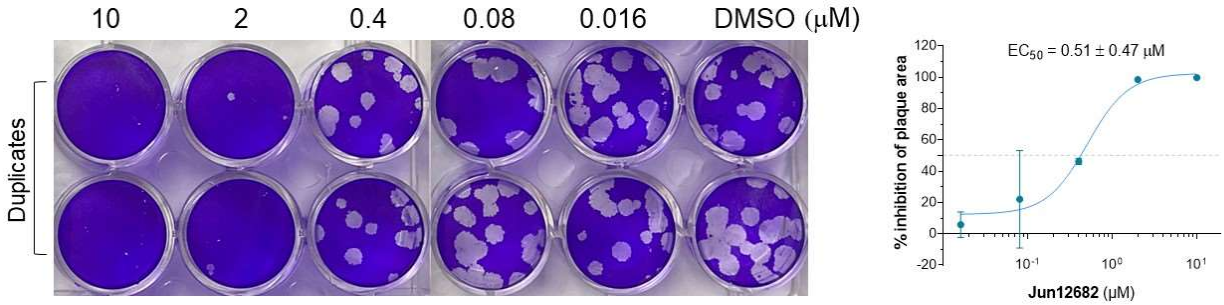

Fig. S3. Plaque assay of Jun12682 against SARS-CoV-2. Vero-AT cells were seeded in 12-well plates a day prior to infection and the drug dissolved in DMSO was serially diluted in DMEM with 3-fold dilutions between test concentrations.

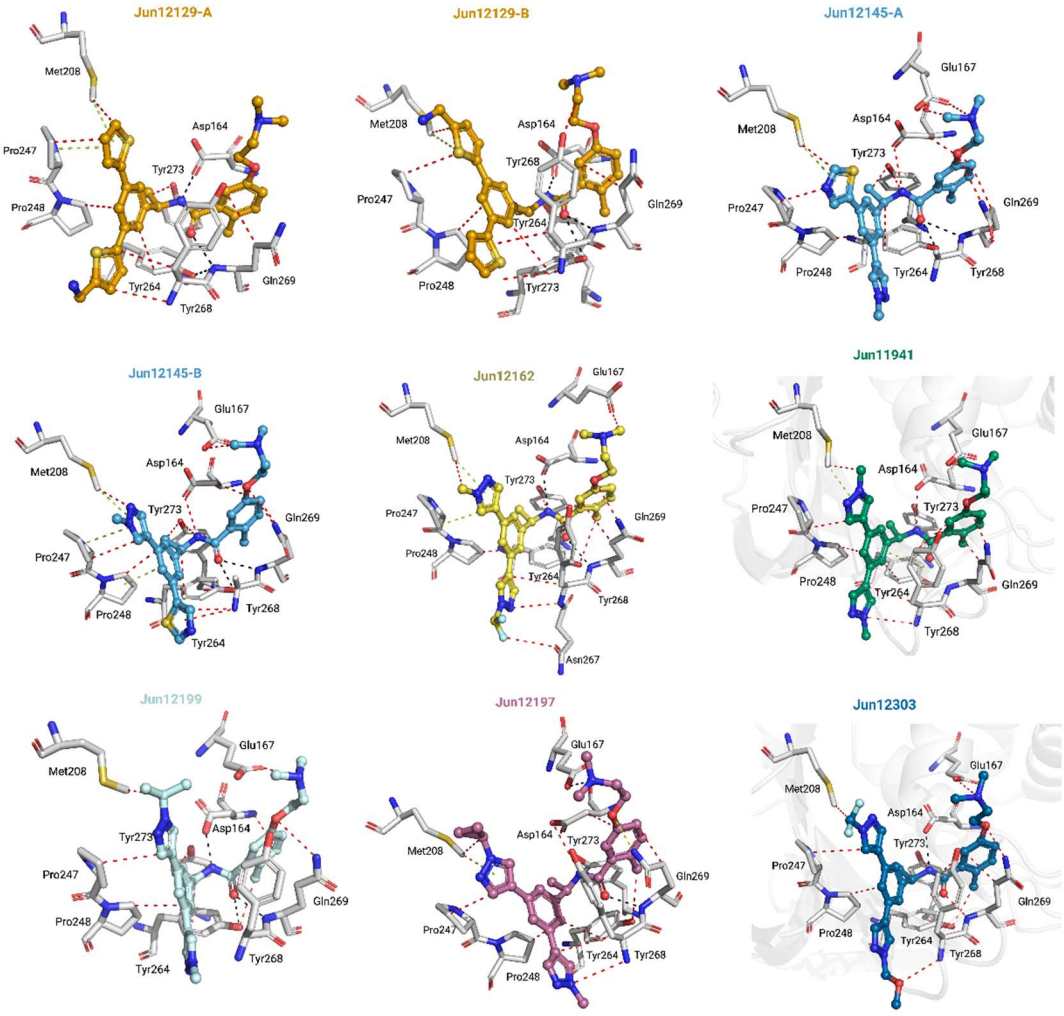

Fig. S4. Binding of biarylphenyl benzamides to SARS-CoV-2 PL^{pro}. Interactions of **Jun 12682** derivatives with the PL^{pro} protein are almost conserved. Hydrogen bonds are represented in black dashed lines, van der Waals contacts as red dashed lines, and π–π interactions as light green dashed. PL^{pro} complex structures of **Jun12129** and **Jun12145** possess two conformations of the inhibitor, designated by A and B conformers. The occupancies for **Jun 12129** conformations A and B are 0.64 and 0.36, and **Jun12145** are 0.67 and 0.33.

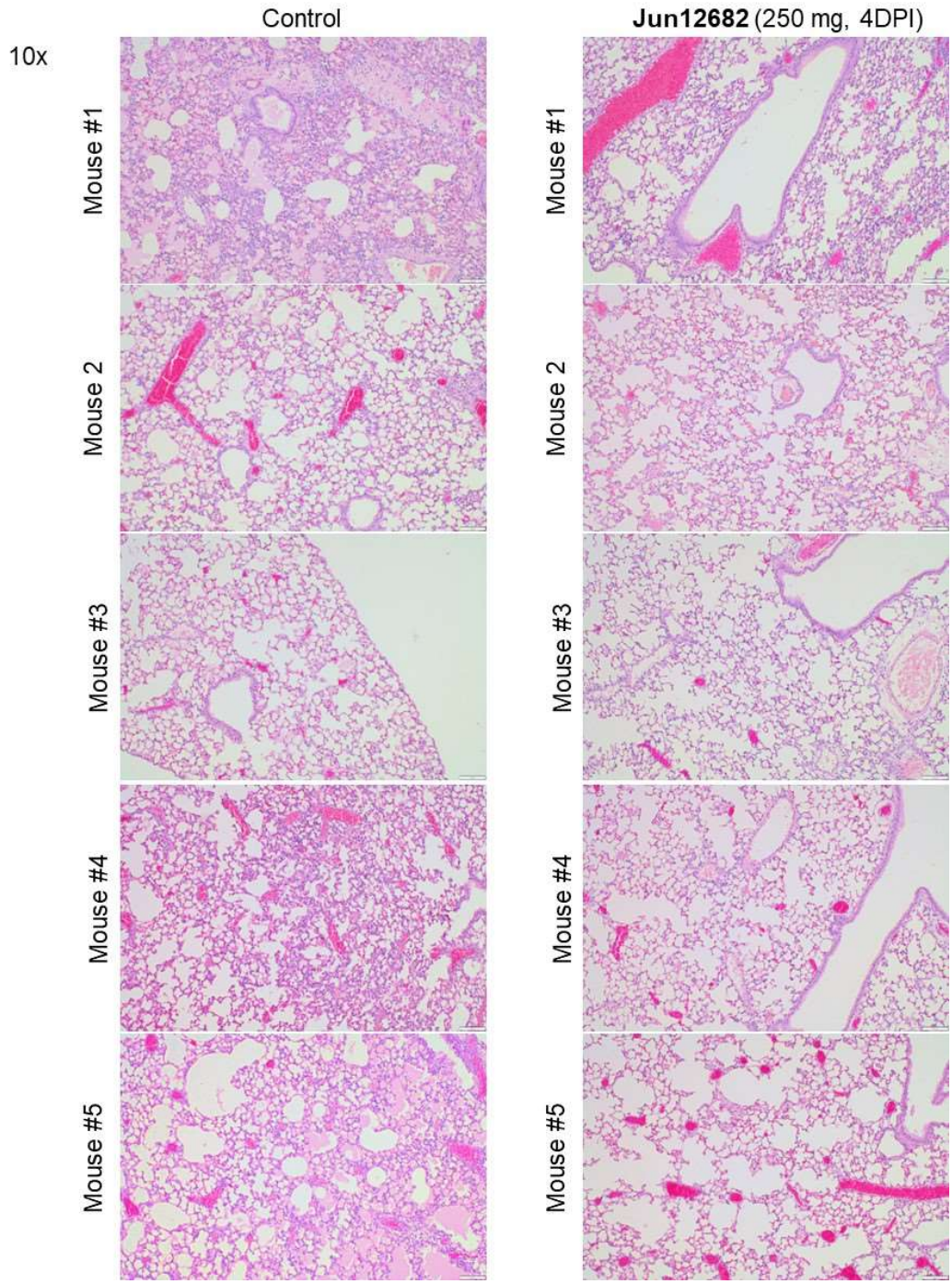

Fig. S5. H&E staining of individual mouse lung sections. Lungs collected at 4 DPI from vehicle- or 250mg/kg **Jun12682**-treated mice (n=5 each group) were stained with haematoxylin and eosin (H&E). Scale bars, 50 μm (10X).

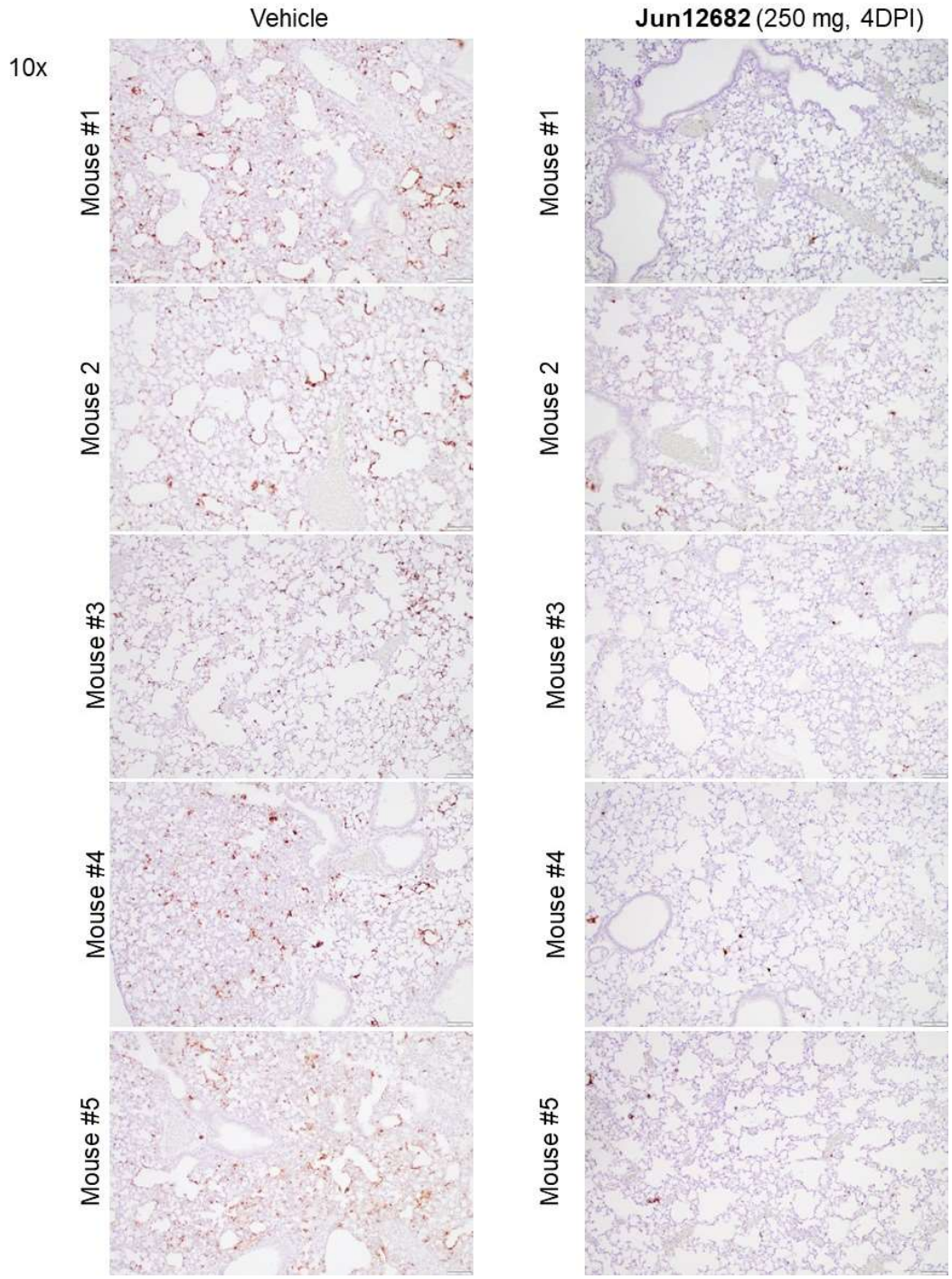

Fig. S6. Viral antigen staining of individual mouse lung sections. Lungs collected at 4 DPI from vehicle- or 250mg/kg **Jun12682**-treated mice (n=5 each group) were stained with a monoclonal antibody against SARS-CoV-2 nucleocapsid protein. Scale bars, 50 μm (10X).

Table S1. X-ray data collection and refinement statistics

PDB Accession code	8UUW	8UUY	8UUV	8UUU
Inhibitor	**Jun12145**	**Jun12129**	**Jun12197**	**Jun12162**
Data Statistics				
Wavelength	1.033	1.033	1.033	1.033
Resolution range	109.18 - 3.20 (3.42-3.20)	100.92 - 3.05 (3.26 - 3.051)	29.05 - 3.01 (3.19 - 3.01)	29.35 - 3.01 (3.19 - 3.01)
Space group	I 4_1 2 2	I 4_1 2 2	I 4_1 2 2	I 4_1 2 2
Unit cell dimensions a b c [Å]	115.028 115.028 218.357	113.68 113.68 219.955	114.212 114.212 218.533	115.393 115.393 220.691
Unit cell dimensions α β γ (°)	90 90 90	90 90 90	90 90 90	90 90 90
Unique reflections	12514 (2233)	14155 (2508)	14671 (2235)	15235 (2404)
Multiplicity	9.6 (8.3)	26.4 (27.2)	25.5 (24.6)	25.6 (25.4)
Completeness (%)	99.9 (99.80)	100.0 (100)	99.3 (96.3)	99.7 (99.1)
Mean I/sigma(I)	4.5 (1.5)	6.8 (1.0)	19.1 (4.60)	17.03 (5.1)
Wilson B-factor	68.26	86.1	74.45	65.43
R-merge	0.620 (3.791)	0.508(5.381)	0.148 (0.838)	0.189 (0.813)
R-meas	0.656 (4.055)	0.518(5.482)	0.151 (0.856)	0.192 (0.830)
R-pim	0.209 (1.403)	0.100(1.037)	0.030 (0.170)	0.038 (0.162)
CC1/2	0.931 (0.434)	0.997(0.677)	0.999 (0.975)	0.998 (0.954)
Refinement Statistics				
Reflections used in refinement	12339 (1183)	14106 (1379)	14644 (1357)	15190 (1506)
Reflections used for R-free	613 (58)	704 (65)	715 (49)	755 (57)
R-work	0.2745 (0.3451)	0.2400 (0.3671)	0.2144 (0.3257)	0.2141 (0.2900)
R-free	0.3149 (0.4997)	0.2575 (0.3731)	0.2426 (0.3734)	0.2386 (0.3405)
Number of non-hydrogen atoms	2503	2663	2543	2522
macromolecules	2330	2469	2431	2390
ligands	85	101	45	62
solvent	88	93	67	70
Protein residues	296	312	307	305
RMS(bonds)	0.005	0.002	0.002	0.004
RMS(angles)	0.89	0.42	0.44	0.64
Ramachandran favored (%)	96.85	95.81	97.36	95.02
Ramachandran allowed (%)	3.15	4.19	2.64	4.98
Ramachandran outliers (%)	0	0	0	0
Rotamer outliers (%)	0.4	0.37	0	0
Clashscore	9.9	3.8	6.01	4.42
Average B-factor	76.49	90.92	78.36	66.85
macromolecules	77.35	91.36	78.79	66.98
ligands	68.34	90.09	69.85	69.85
solvent	61.63	80.18	59.79	64.06

PDB Accession code	8UUH	8UUG	8UUF	8UOB	8UVM
Inhibitor	**Jun12199**	**Jun12303**	**Jun11941**	**Jun12682**	**Jun11313**
Data Statistics					
Wavelength	0.9201	0.9201	0.9201	0.9201	1.033
Resolution range	101.59 - 2.8 (2.95 - 2.8)	29.05 - 2.743 (2.89 - 2.743)	29.08 - 2.84 (2.99 - 2.84)	34.74 - 2.52 (2.62 - 2.52)	42.00 - 2.85 (2.952 - 2.85)
Space group	I 4_1 2 2	I 4_1 2 2	I 4_1 2 2	I 4_1 2 2	P 3 2 1
Unit cell dimensions a b c [Å]	114.713 114.713 218.719	114.2 114.2 218.557	114.285 114.285 219.48	115.825 115.825 219.317	190.997 190.997 112.926
Unit cell dimensions α β γ (°)	90 90 90	90 90 90	90 90 90	90 90 90	90 90 120
Unique reflections	18424 (2643)	19362 (2774)	17605 (2480)	25626 (2834)	54651 (2264)
Multiplicity	26.7 (27.3)	13.5 (13.8)	13.3 (13.6)	15.2 (15.4)	9.8 (4.8)
Completeness (%)	100 (100)	99.9 (99.6)	99.76 (98.2)	100 (100)	99.8 (96.7)
Mean I/sigma(I)	9.51 (1.2)	17.5 (3.2)	17.65 (3.8)	7.61 (0.72)	3.2 (0.4)
Wilson B-factor	64.65	60.06	63.01	57.81	59.43
R-merge	0.346 (3.758)	0.118 (0.883)	0.115 (0.746)	0.304 (4.946)	0.187(0.944)
R-meas	0.352 (3.829)	0.123 (0.947)	0.119 (0.775)	0.315 (5.11)	0.193(0.998)
R-pim	0.068 (0.730)	0.03315 (0.252)	0.033 (0.207)	0.081 (1.300)	0.043 (0.309)
CC1/2	0.997 (0.581)	0.999 (0.876)	0.999 (0.905)	0.995 (0.400)	0.996 (0.472)
Refinement Statistics					
Reflections used in refinement	18341 (1796)	19338 (1879)	17548 (1708)	25575 (2490)	54651 (2264)
Reflections used for R-free	951 (90)	939 (102)	848 (86)	1308 (110)	2793 (129)
R-work	0.2282 (0.3309)	0.2122 (0.2733)	0.2118 (0.2894)	0.2063 (0.3694)	0.2381 (0.3246)
R-free	0.2640 (0.3806)	0.2362 (0.2704)	0.2387 (0.3824)	0.2442 (0.4062)	0.2576 (0.3724)
Number of non-hydrogen atoms	2553	2580	2598	2699	10153
macromolecules	2427	2435	2452	2460	9791
ligands	64	56	47	52	177
solvent	62	89	99	187	185
Protein residues	307	311	312	311	1258
RMS(bonds)	0.002	0.002	0.002	0.003	0.002
RMS(angles)	0.46	0.52	0.47	0.58	0.43
Ramachandran favored (%)	95.68	95.47	97.1	97.09	95.03
Ramachandran allowed (%)	4.32	4.21	2.9	2.91	4.97
Ramachandran outliers (%)	0	0.32	0	0	0
Rotamer outliers (%)	0.77	0.38	0.75	0	0.19
Clashscore	3.1	4.54	3.71	4.08	4.5
Average B-factor	69.62	67.1	69.94	77.09	65.23
macromolecules	69.69	67.17	70.38	77.43	65.35
ligands	72.24	71.43	63.77	70.68	75.85
solvent	62.45	62.13	66.62	74.39	48.55

Statistics for the highest-resolution shell are shown in parentheses.

Rmerge=$\Sigma\Sigma|ni=1hkl$ Ii – $I|/\Sigma\Sigma Ini=1hkl$i

c Rpim= $\Sigma\sqrt{1n-1}hkl\ \Sigma|Ini=1$i - $I(hkl)\Sigma\Sigma Ini=1hkl$i

Table S2. *In vivo* oral snap PK of PL^{pro} inhibitors in C57BL/6J mice

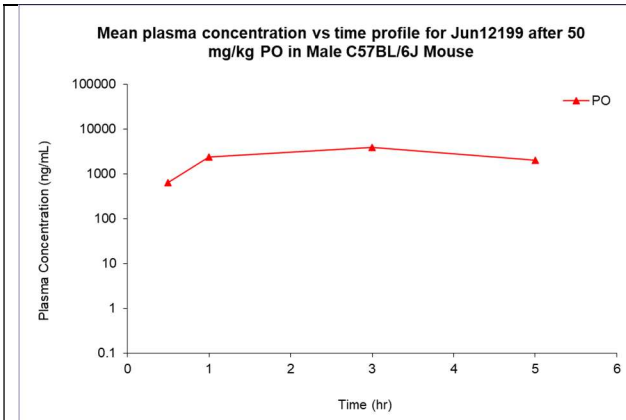

PK parameters	Unit	Mean
$T_{1/2}$	h	NA
T_{max}	h	3.00
C_{max}	ng/mL	3980
AUC_{last}	h*ng/mL	13355
AUC_{Inf}	h*ng/mL	NA
$AUC_{\_\%Extrap\_obs}$	%	NA
MRT_{Inf_obs}	h	NA
AUC_{last}/D	h*mg/mL	267
AUC_{inf}/D	h*mg/mL	NA
F	%	NA

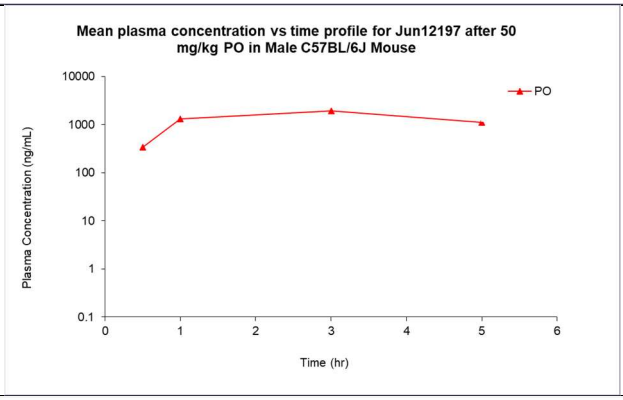

PK parameters	Unit	Mean
$T_{1/2}$	h	NA
T_{max}	h	3.00
C_{max}	ng/mL	1930
AUC_{last}	h*ng/mL	6787
AUC_{Inf}	h*ng/mL	NA
$AUC_{\_\%Extrap\_obs}$	%	NA
MRT_{Inf_obs}	h	NA
AUC_{last}/D	h*mg/mL	136
AUC_{inf}/D	h*mg/mL	NA
F	%	NA

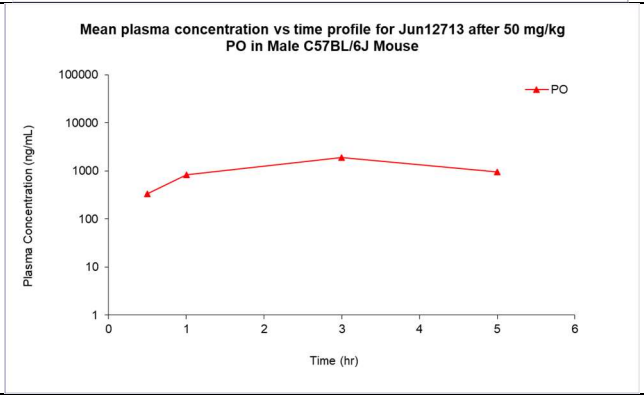

PK parameters	Unit	Mean
$T_{1/2}$	h	NA
T_{max}	h	3.00
C_{max}	ng/mL	1890
AUC_{last}	h*ng/mL	5940
AUC_{Inf}	h*ng/mL	NA
$AUC_{\_\%Extrap\_obs}$	%	NA
MRT_{Inf_obs}	h	NA
AUC_{last}/D	h*mg/mL	119
AUC_{inf}/D	h*mg/mL	NA
F	%	NA

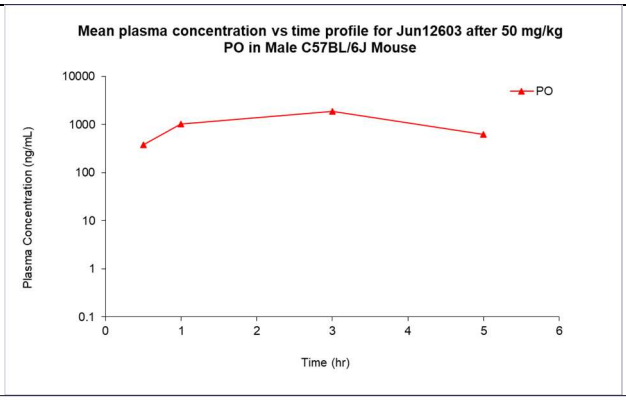

PK parameters	Unit	Mean
$T_{1/2}$	h	NA
T_{max}	h	3.00
C_{max}	ng/mL	1910
AUC_{last}	h*ng/mL	5935
AUC_{Inf}	h*ng/mL	NA
$AUC\_{}_{\%Extrap}\_{}obs$	%	NA
MRT_{Inf}_obs	h	NA
AUC_{last}/D	h*mg/mL	119
AUC_{inf}/D	h*mg/mL	NA
F	%	NA

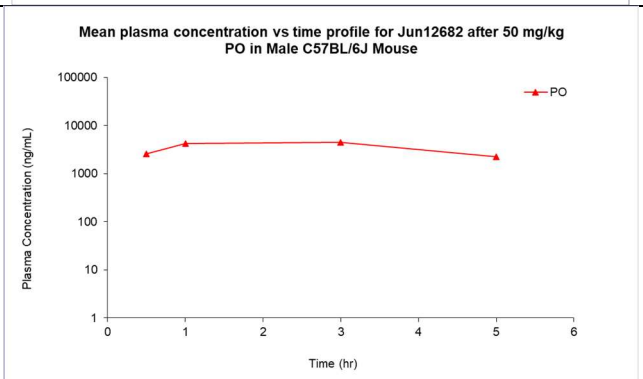

PK parameters	Unit	Mean
$T_{1/2}$	h	NA
T_{max}	h	3.00
C_{max}	ng/mL	4520
AUC_{last}	h*ng/mL	17895
AUC_{Inf}	h*ng/mL	NA
$AUC\_{}_{\%Extrap}\_{}obs$	%	NA
MRT_{Inf}_obs	h	NA
AUC_{last}/D	h*mg/mL	358
AUC_{inf}/D	h*mg/mL	NA
F	%	NA

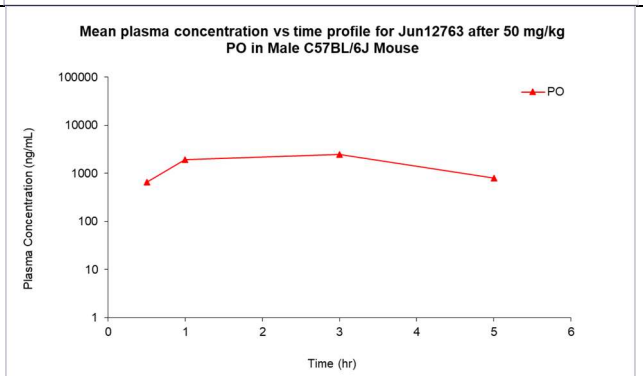

PK parameters	Unit	Mean
$T_{1/2}$	h	NA
T_{max}	h	3.00
C_{max}	ng/mL	2480
AUC_{last}	h*ng/mL	8541
AUC_{Inf}	h*ng/mL	NA
$AUC\_{}_{\%Extrap}\_{}obs$	%	NA
MRT_{Inf}_obs	h	NA
AUC_{last}/D	h*mg/mL	171
AUC_{inf}/D	h*mg/mL	NA
F	%	NA

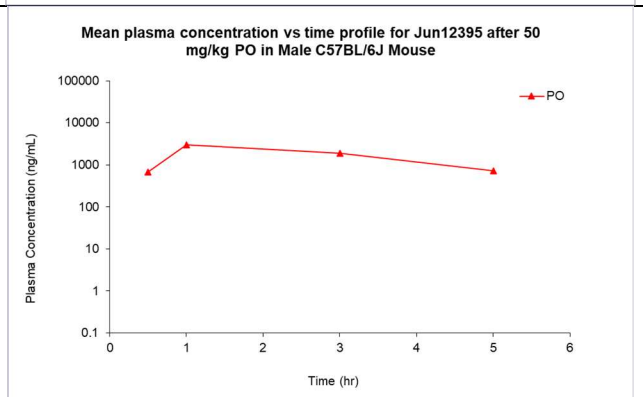

PK parameters	Unit	Mean
$T_{1/2}$	h	1.97
T_{max}	h	1.00
C_{max}	ng/mL	3000
AUC_{last}	h*ng/mL	8637
AUC_{Inf}	h*ng/mL	10722
$AUC\_{}_{\%Extrap}\_{}obs$	%	19.4
MRT_{Inf}_obs	h	3.30
AUC_{last}/D	h*mg/mL	173
AUC_{inf}/D	h*mg/mL	214
F	%	NA

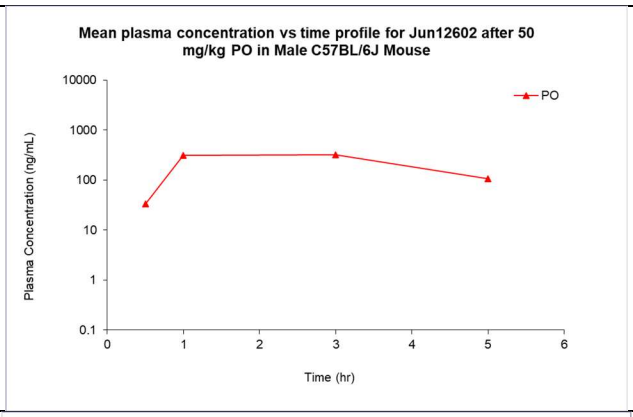

PK parameters	Unit	Mean
$T_{1/2}$	h	NA
T_{max}	h	3.00
C_{max}	ng/mL	323
AUC_{last}	h*ng/mL	1164
AUC_{Inf}	h*ng/mL	NA
$AUC_{\_\%Extrap\_obs}$	%	NA
MRT_{Inf_obs}	h	NA
AUC_{last}/D	h*mg/mL	23.3
AUC_{inf}/D	h*mg/mL	NA
F	%	NA

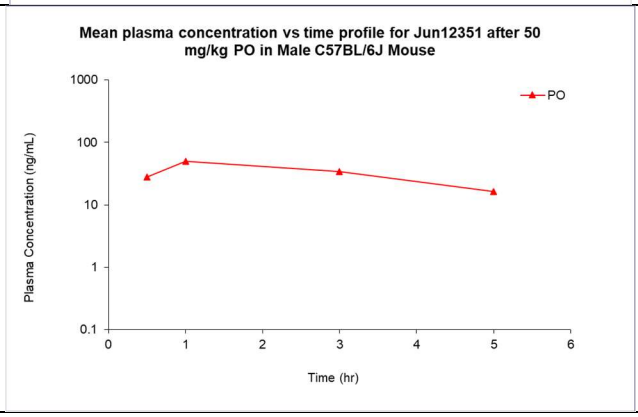

PK parameters	Unit	Mean
$T_{1/2}$	h	2.50
T_{max}	h	1.00
C_{max}	ng/mL	49.7
AUC_{last}	h*ng/mL	162
AUC_{Inf}	h*ng/mL	221
$AUC_{\_\%Extrap\_obs}$	%	26.8
MRT_{Inf_obs}	h	3.93
AUC_{last}/D	h*mg/mL	3.24
AUC_{inf}/D	h*mg/mL	4.42
F	%	NA

Table S3. *In vivo* oral PK of PL^{pro} inhibitor Jun12682 in C57BL/6J mice.

Summary of Jun12682 IV plasma PK parameters

PK parameters	Unit	Mouse 1	Mouse 2	Mouse 3	Mean	SD	CV(%)
Cl_obs	mL/min/kg	28.5	28.3	23.7	26.8	2.7	10.1
$T_{1/2}$	h	2.36	2.71	3.22	2.76	0.43	15.7
C_0	ng/mL	5890	6957	5898	6249	614	9.82
AUC_{last}	h*ng/mL	5840	5889	7011	6247	662	10.6
AUC_{Inf}	h*ng/mL	5843	5891	7028	6254	671	10.7
$AUC_{_\%Extrap_}$obs	%	0.0416	0.0395	0.245	0.109	0.118	109
MRT_{Inf}_obs	h	1.64	1.32	2.31	1.76	0.51	28.7
AUC_{last}/D	h*mg/mL	584	589	701	625	66	10.6
AUC_{inf}/D	h*mg/mL	584	589	703	625	67	10.7
V_{ss}_obs	L/kg	2.81	2.24	3.29	2.78	0.52	18.9

Summary of Jun12682 PO plasma PK parameters

PK parameters	Unit	Mouse 4	Mouse 5	Mouse 6	Mean	SD	CV(%)
$T_{1/2}$	h	2.17	1.80	2.04	2.01	0.19	9.38
T_{max}	h	2.00	2.00	1.00	1.67	0.58	34.6
C_{max}	ng/mL	5220	3100	5290	4537	1245	27.4
AUC_{last}	h*ng/mL	21521	18152	28590	22755	5327	23.4
AUC_{Inf}	h*ng/mL	21532	18155	28600	22762	5330	23.4
$AUC_{_\%Extrap_}$obs	%	0.0517	0.0152	0.0339	0.0336	0.0183	54.4
MRT_{Inf}_obs	h	4.15	4.11	4.05	4.10	0.05	1.17
AUC_{last}/D	h*mg/mL	430	363	572	455	107	23.4
AUC_{inf}/D	h*mg/mL	431	363	572	455	107	23.4
F	%	68.9	58.1	91.5	72.8	17.0	23.4

General Information of Chemical Synthesis

All chemicals were purchased from commercial vendors and used without further purification unless otherwise noted. ^{1}H and ^{13}C NMR spectra were recorded on a Bruker-400 or -500 NMR spectrometer. Chemical shifts are reported in parts per million referenced with respect to residual solvent (CD_3OD) 3.31 ppm, (DMSO-d_6) 2.50 ppm, and ($CDCl_3$) 7.26 ppm or from internal standard tetramethylsilane (TMS) 0.00 ppm. The following abbreviations were used in reporting spectra: s, singlet; d, doublet; t, triplet; q, quartet; m, multiplet; dd, doublet of doublets; ddd, doublet of doublet of doublets. All reactions were carried out under Ar atmosphere, unless otherwise stated. HPLC-grade solvents were used for all reactions. Flash column chromatography was performed using silica gel (230-400 mesh, Merck). Low-resolution mass spectra were obtained using an ESI technique on a 3200 Q Trap LC/MS/MS system (Applied Biosystems). The purity was assessed by using Shimadzu LC-MS with Waters XTerra MS C-18 column (part #186000538), 50 × 2.1 mm, at a flow rate of 0.3 mL/min; λ = 250 and 220 nm; mobile phase A, 0.1% formic acid in H_2O, and mobile phase B', 0.1% formic in 60% isopropanol, 30% CH_3CN and 9.9% H2O. All compounds submitted for testing were confirmed to be > 95.0% purity by LC-MS traces. All compounds were characterized by proton and carbon NMR and HRMS.

Synthesis of PL^{pro} inhibitors

Scheme 1. Synthesis of SARS-CoV-2 PL^{pro} inhibitors.

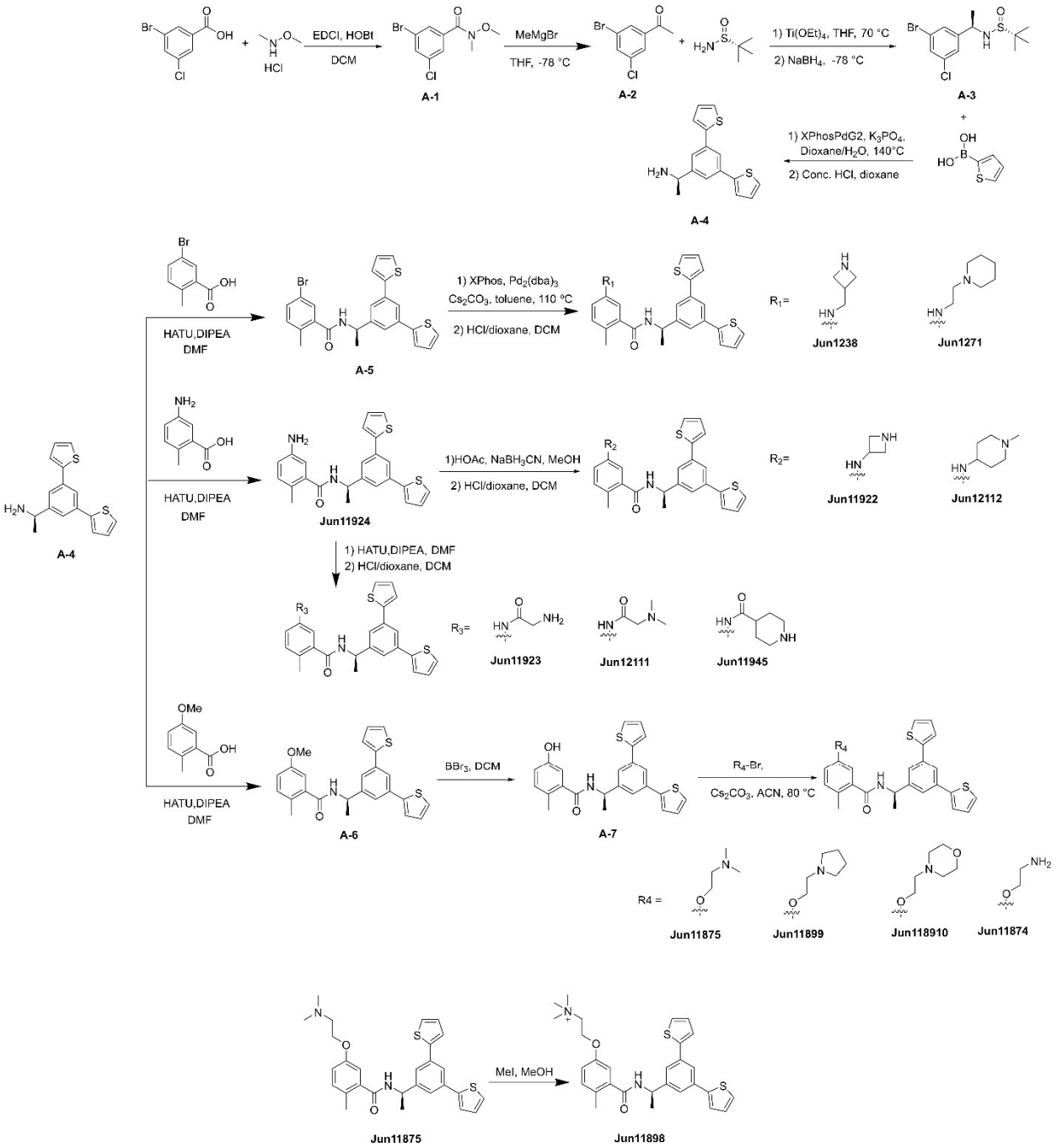

Synthetic Procedures for Scheme 1

3-bromo-5-chloro-N-methoxy-N-methylbenzamide (**A-1**). To a solution of 3-bromo-5-chlorobenzoic acid (1.0 equiv), *N*,*O*-dimethylhydroxylamine hydrochloride (1.2 equiv), HOBt (1.3 equiv) and EDCI (1.3 equiv) in DCM (0.1 M) was added dropwise of triethylamine (3 equiv) at 0 °C. The mixture was stirred at rt for 24 hours. After the reaction was completed, the organic layer was washed with water and brine, dried over Na_2SO_4, filtered, and concentrated under vacuum to give the product **A-1** for the next step without purification.

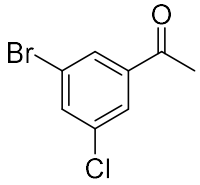

1-(3-bromo-5-chlorophenyl)ethan-1-one (**A-2**). To a solution of 3-bromo-5-chloro-*N*-methoxy-*N*-methylbenzamide (**A-1**, 1.0 equiv) in dry ether at -78 °C under N_2, the methylmagnesium bromide (3 M solution in diethyl ether, 3.0 equiv) was added slowly. After warming to room temperature and stirred for 2 hours, the reaction mixture was quenched with ice-cold saturated NH_4Cl and washed with water and brine, dried over Na_2SO_4, filtered, and concentrated under vacuum to give the crude residue, which was purified by silica gel column chromatography (Hexanes/EtOAc = 5:1) to provide the desired product **A-2** as a white solid. ***1-(3-bromo-5-chlorophenyl)ethan-1-one*** (**A-2**). White solid, 75% yield for two steps. ^{1}H NMR (400 MHz, $CDCl_3$) δ 7.95 (d, J = 1.7 Hz, 1H), 7.85 (s, 1H), 7.70 (s, 1H), 2.59 (s, 3H). ^{13}C NMR (101 MHz, $CDCl_3$) δ 195.22, 139.59, 135.79, 135.54, 129.68, 127.21, 123.26, 26.62. C_8H_6BrClO, MS calculated for m/z $[M+H]^+$: 232.9 (calculated), 233.1 (found).

(S)-N-((R)-1-(3-bromo-5-chlorophenyl)ethyl)-2-methylpropane-2-sulfinamide (**A-3**). To a solution of $Ti(OEt)_4$ (1.44 equiv) and 1-(3-bromo-5-chlorophenyl)ethan-1-one (1.00 equiv) in THF (0.1 M) under an Ar atmosphere was added (*R*)-2-methylpropane-2-sulfinamide (1.50 equiv) and the mixture was heated to 70 °C for overnight. Upon completion, as determined by TLC, the mixture was cooled to -78 °C, and $NaBH_4$ (3.00 equiv) was added carefully. The mixture was stirred at -78 °C for 3 h and then slowly warmed to room temperature. After another 3 h, MeOH was added dropwise until the gas was no longer evolved. The resulting suspension was filtered through a plug of Celite, and the filter cake was washed with EtOAc. The filtrate was washed with brine, and the brine layer was extracted with EtOAc. The combined organic phase was dried over Na_2SO_4, filtered, and concentrated under vacuum to give a residue that was purified by flash silica gel column chromatography (Hexanes/EtOAc = 3:1) to get the desired product **A-3** as a light yellow solid.

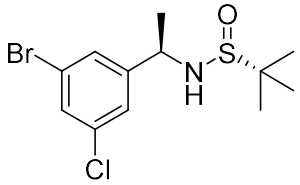

1-(3-bromo-5-chlorophenyl)ethan-1-one (**A-3**). White solid, 80% yield. ^{1}H NMR (400 MHz, $CDCl_3$) δ 7.44 (t, J = 1.9 Hz, 1H), 7.38 (d, J = 1.6 Hz, 1H), 7.27 (d, J = 1.8 Hz, 1H), 4.47 (m,

1H), 3.46 (s, 1H), 1.50 (d, J = 6.6 Hz, 3H), 1.24 (s, 9H). ^{13}C NMR (101 MHz, $CDCl_3$) δ 147.66, 135.42, 130.77, 128.16, 125.74, 123.02, 60.37, 55.74, 53.40, 22.79, 22.58, 21.03, 14.20. $C_{12}H_{17}BrClNOS$, MS calculated for m/z $[M+H]^+$: 338.0 (calculated), 338.0 (found).

(R)-1-(3,5-di(thiophen-2-yl)phenyl)ethan-1-amine **(A-4)**. To a solution of (*S*)-*N*-((*R*)-1-(3-bromo-5-chlorophenyl)ethyl)-2-methylpropane-2-sulfinamide (**A-3**) (1.0 equiv) in dioxane/H_2O (4:1) in a microwave reaction vial was added 2-thienylboronic acid (2.5 equiv) and tripotassium phosphate (1.8 equiv). The mixture was purged with nitrogen for 5 min, then XPhosPdG2 (0.1 equiv) was added. The resulting mixture was heated in the biotage microwave reactor at 140 °C for 90 min. LCMS indicated that the starting material was completely consumed. The reaction mixture was diluted with EtOAc and extracted with water and brine. The organic layers were dried over anhydrous Na_2SO_4, filtered, and concentrated under reduced pressure to give a residue for the next step without purification. The crude was dissolved in 1,4-dioxane (0.1 M) and then concentrated HCl was added. The reactions were stirred at room temperature. When the starting material was consumed entirely as monitored by LCMS, solvent was removed under vacuum to give a white solid **A-4**, which was used in the next step without purification.

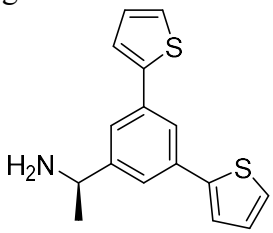

(R)-1-(3,5-di(thiophen-2-yl)phenyl)ethan-1-amine (**A-4**). White solid, 98% yield. ^{1}H NMR (400 MHz, $CDCl_3$) δ 7.85 (d, *J* = 1.8 Hz, 1H), 7.71 (d, *J* = 1.7 Hz, 2H), 7.53 (d, *J* = 3.6 Hz, 2H), 7.43 (d, *J* = 5.0 Hz, 2H), 7.19-6.90 (m, 2H), 4.55 (q, *J* = 6.8 Hz, 1H), 1.71 (d, *J* = 6.7 Hz, 3H). ^{13}C NMR (101 MHz, $CDCl_3$) δ 143.94, 141.37, 137.45, 129.37, 126.82, 125.45, 124.22, 123.89, 52.18, 49.64, 49.43, 49.21, 49.00, 48.79, 48.57, 48.36, 20.84. $C_{16}H_{16}NS_2$, MS calculated for m/z $[M+H]^+$: 286.1 (calculated), 286.0 (found).

(R)-5-bromo-N-(1-(3,5-di(thiophen-2-yl)phenyl)ethyl)-2-methylbenzamide (**A-5**). 5-bromo-2-methylbenzoic acid (1.1 equiv), HATU (1.1 equiv) and DIPEA (3.0 equiv) were dissolved in DMF (0.2 M) and stirred for 15 min. After that (*R*)-1-(3-bromo-5-chlorophenyl)ethan-1-amine (**A-4**) (1.0 equiv) was added and stirred at room temperature overnight. When the starting material was consumed entirely as monitored by LCMS, the mixture was diluted with EtOAc and was then washed with saturated aq. $NaHCO_3$, water, and brine. The organic layer was dried over Na_2SO_4, filtered, and concentrated under vacuum to give a residue that was purified by silica gel column chromatography (Hexanes/EtOAc = 4:1) to provide the desired product **A-5** as a slightly yellow solid.

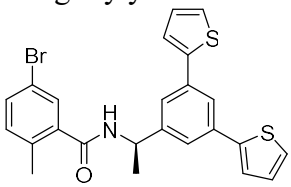

(R)-5-bromo-N-(1-(3,5-di(thiophen-2-yl)phenyl)ethyl)-2-methylbenzamide (**A-5**). White solid, 88% yield. ^{1}H NMR (400 MHz, $CDCl_3$) δ 7.75 (s, 1H), 7.51 (s, 3H), 7.46-7.41 (m, 1H), 7.37 (d, J = 3.6 Hz, 2H), 7.32 (d, J = 4.9 Hz, 2H), 7.22-6.85 (m, 3H), 6.09 (d, J = 8.0 Hz, 1H), 5.34 (td, J = 14.2, 13.8, 6.9 Hz, 1H), 2.37 (s, 3H), 1.65 (d, J = 7.0 Hz, 3H). ^{13}C NMR (101 MHz, DMSO-d_6) δ 167.30, 147.20, 143.34, 139.64, 135.14, 135.12, 133.09, 132.39, 129.95, 128.99, 126.52,

124.81, 122.90, 121.11, 118.70, 48.86, 22.86, 19.20. $C_{24}H_{21}BrNOS_2$, MS calculated for m/z $[M+H]^+$: 482.0 (calculated), 482.0 (found).

tert-butyl (R)-3-(((3-((1-(3,5-di(thiophen-2-yl)phenyl)ethyl)carbamoyl)-4-methylphenyl)amino)methyl)azetidine-1-carboxylate **(Jun1238).** To a solution of (*R*)-5-bromo-N-(1-(3,5-di(thiophen-2-yl)phenyl)ethyl)-2-methylbenzamide (**A-5**, 1.0 equiv) in dry toluene (8 mL) in a 15 mL sealed tube, tert-butyl 3-(aminomethyl)azetidine-1-carboxylate (1.5 equiv), XPhos (0.04 equiv), tris(dibenzylideneacetone)dipalladium (0.02 equiv) and Cs_2CO_3 (2.0 equiv) were added. The reaction mixture was degassed and purged with argon, and then the tube was sealed and heated to 110° C overnight. The mixture was diluted with EtOAc and was then washed with water and brine. The organic layer was dried over Na_2SO_4, filtered, and concentrated. The residue was purified by silica gel column chromatography (Hexanes/EtOAc = 1:1) to provide the desired intermediate. The intermediate was disolved in DCM and HCl (4M in dioxane, 10 equiv) was added. When the starting material was consumed entirely as monitored by LCMS, the mixture was diluted with DCM, adjusted to pH = 10, and then washed with water and brine. The organic layer was dried over Na_2SO_4, filtered, and concentrated under vacuum to give a residue which was purified by Prep-HPLC to give the final product **Jun1238** as a white solid.

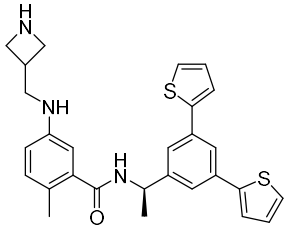

(R)-5-((azetidin-3-ylmethyl)amino)-N-(1-(3,5-di(thiophen-2-yl)phenyl)ethyl)-2-methylbenzamide (**Jun1238**). White solid, 58% yield for two steps. ^{1}H NMR (400 MHz, MeOD-d_4) δ 7.76 (d, J = 1.7 Hz, 1H), 7.64 (d, J = 1.7 Hz, 2H), 7.55 (d, J = 8.0 Hz, 2H), 7.49 (d, J = 3.6 Hz, 2H), 7.42 (dd, J = 12.0, 6.3 Hz, 4H), 7.11 (dd, J = 5.1, 3.5 Hz, 2H), 5.26 (q, J = 6.9 Hz, 1H), 4.14 (d, J = 10.1 Hz, 1H), 4.02 (t, J = 5.5 Hz, 1H), 3.80 (d, J = 6.9 Hz, 1H), 3.67-3.64 (m, 1H), 3.44 (q, J = 7.7, 6.9 Hz, 1H), 2.39 (s, 3H), 1.62 (d, J = 7.0 Hz, 3H). ^{13}C NMR (101 MHz, MeOD-d_4) δ 168.62, 145.60, 143.34, 138.56, 137.78, 135.48, 132.51, 132.47, 127.95, 125.02, 123.64, 123.54, 122.48, 121.44, 121.09, 60.80, 52.78, 49.33, 28.89, 21.03, 18.11. $C_{28}H_{29}N_3OS_2$, MS calculated for m/z $[M+H]^+$: 488.2 (calculated), 488.1 (found).

(R)-N-(1-(3,5-di(thiophen-2-yl)phenyl)ethyl)-2-methyl-5-((2-(piperidin-1-yl)ethyl)amino)benzamide (**Jun1271**). **Jun1271** was synthesized using the same coupling procedure as described for **Jun1238** with the starting material 2-(piperidin-1-yl)ethan-1-amine.

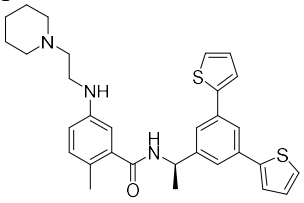

(R)-N-(1-(3,5-di(thiophen-2-yl)phenyl)ethyl)-2-methyl-5-((2-(piperidin-1-yl)ethyl)amino)benzamide (**Jun1271**). White solid, 62% yield. ^{1}H NMR (400 MHz, MeOD-d_4) δ 7.75 (d, J = 1.9 Hz, 1H), 7.61 (d, J = 1.7 Hz, 2H), 7.45 (d, J = 3.6 Hz, 2H), 7.38 (d, J = 5.1 Hz, 2H), 7.10 (dd, J = 5.1, 3.6 Hz, 2H), 7.01-6.95 (m, 1H), 6.65 (dd, J = 5.4, 2.9 Hz, 2H), 5.22 (q, J = 7.1 Hz, 1H), 3.40-3.33 (m, 2H), 2.96 (t, J = 6.5 Hz, 2H), 2.90 (t, J = 6.1 Hz, 4H), 2.23 (s, 3H), 1.70 (p, J = 5.8 Hz, 4H), 1.57 (d, J = 7.1 Hz, 3H), 1.52 (dt, J = 9.9, 5.3 Hz, 2H). ^{13}C NMR (101

MHz, MeOD-d_4) δ 171.41, 146.09, 145.81, 143.45, 137.22, 135.37, 131.19, 127.94, 124.98, 123.52, 123.49, 122.39, 121.23, 114.44, 110.93, 56.08, 53.50, 49.14, 38.78, 23.43, 22.05, 21.13, 17.43. $C_{31}H_{35}N_3OS_2$, MS calculated for m/z $[M+H]^+$: 529.2 (calculated), 529.2 (found).

(R)-5-amino-N-(1-(3,5-di(thiophen-2-yl)phenyl)ethyl)-2-methylbenzamide (**Jun11924**). 5-amino-2-methylbenzoic acid (1.1 equiv), HATU (1.1 equiv) and DIPEA (3 equiv) were dissolved in DMF (0.2 M) and stirred for 15 min. Then (*R*)-1-(3-bromo-5-chlorophenyl)ethan-1-amine (**A-4**) (1.0 equiv) was added and stirred at room temperature overnight. When the starting material was consumed entirely as monitored by LCMS, the mixture was diluted with EtOAc and was then washed with saturated aq. $NaHCO_3$, water, and brine. The organic layer was dried over Na_2SO_4, filtered, and concentrated under vacuum to give a residue that was purified by silica gel column chromatography (Hexanes/EtOAc = 2:1) to provide the desired product **Jun11924** as a slightly yellow solid.

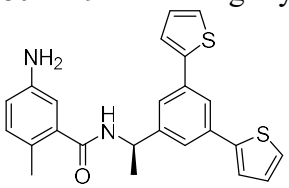

(R)-5-amino-N-(1-(3,5-di(thiophen-2-yl)phenyl)ethyl)-2-methylbenzamide (**Jun11924**). White solid, 70% yield. ^{1}H NMR (400 MHz, $CDCl_3$) δ 7.76 (d, J = 1.8 Hz, 1H), 7.51 (t, J = 1.9 Hz, 3H), 7.42 (dd, J = 8.2, 2.2 Hz, 1H), 7.40-7.35 (m, 2H), 7.32 (d, J = 5.0 Hz, 2H), 7.13-7.04 (m, 3H), 6.08 (d, J = 8.0 Hz, 1H), 5.35 (p, J = 7.1 Hz, 1H), 2.38 (s, 3H), 1.66 (d, J = 6.9 Hz, 3H). ^{13}C NMR (101 MHz, $CDCl_3$) δ 169.50, 144.90, 144.28, 143.73, 137.05, 135.48, 131.81, 128.15, 125.29, 125.14, 123.76, 122.99, 122.62, 116.72, 113.54, 48.91, 21.97, 18.83. $C_{24}H_{22}N_2OS_2$, MS calculated for m/z $[M+H]^+$: 419.1 (calculated), 419.1 (found).

(R)-5-(azetidin-3-ylamino)-N-(1-(3,5-di(thiophen-2-yl)phenyl)ethyl)-2-methylbenzamide **(Jun11922).** To a solution of (*R*)-5-amino-*N*-(1-(3,5-di(thiophen-2-yl)phenyl)ethyl)-2-methylbenzamide (**Jun11924**) (1.0 equiv) and tert-butyl 3-oxoazetidine-1-carboxylate (2.0 equiv) in dry MeOH (2 mL), HOAc (500 μL) was added and the solution was stirred for 3 hours at 50 ºC before $NaBH_3CN$ (3.0 equiv) was added. The mixture was poured into H_2O (10 mL) and extracted with EtOAc (20 mL). The organic phase was concentrated, and the residue was purified by flash silica gel column chromatography to provide the Boc-protected intermediate. The intermediate was dissolved in DCM (2 mL), and HCl (4M in dioxane, 10 equiv) was added. When the starting material was consumed entirely as monitored by LCMS, the mixture was diluted with DCM, adjusted to pH = 10, and then washed with water and brine. The organic layer was dried over Na_2SO_4, filtered, and concentrated under vacuum to give a residue which was purified by Prep-HPLC to give the final product **Jun11922** as a white solid.

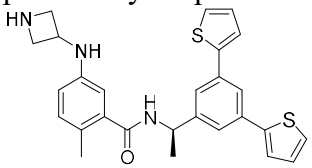

(R)-5-(azetidin-3-ylamino)-N-(1-(3,5-di(thiophen-2-yl)phenyl)ethyl)-2-methylbenzamide (**Jun11922**). White solid, 63% yield for two steps. ^{1}H NMR (400 MHz, MeOD-d_4) δ 7.66 (d, J = 1.7 Hz, 1H), 7.52 (d, J = 1.6 Hz, 2H), 7.37 (d, J = 3.6 Hz, 2H), 7.30 (d, J = 5.2 Hz, 3H), 7.13 (d, J = 8.0 Hz, 1H), 7.06 (s, 1H), 7.00 (dd, J = 5.1, 3.6 Hz, 2H), 4.58 (p, J = 7.3 Hz, 1H), 4.25 (q, J = 11.3, 9.1 Hz, 3H), 4.14-3.69 (m, 1H), 2.19 (s, 3H), 1.50 (d, J = 7.0 Hz, 3H). ^{13}C NMR (101 MHz, MeOD-d_4) δ 170.02, 145.58, 143.35, 137.51, 135.46, 132.09, 128.00, 125.10, 123.67,

122.42, 121.43, 119.48, 116.56, 58.58, 51.02, 49.62, 21.12, 17.83. $C_{27}H_{27}N_3OS_2$, MS calculated for m/z $[M+H]^+$: 474.2 (calculated), 474.1 (found).

(R)-N-(1-(3,5-di(thiophen-2-yl)phenyl)ethyl)-2-methyl-5-((1-methylpiperidin-4-yl)amino)benzamide (**Jun12112**). **Jun12112** was synthesized using the same reductive amination procedure as described for **Jun11922** with the starting material 1-methylpiperidin-4-one.

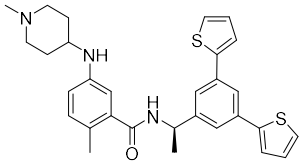

(R)-N-(1-(3,5-di(thiophen-2-yl)phenyl)ethyl)-2-methyl-5-((1-methylpiperidin-4-yl)amino)benzamide (**Jun12112**). White solid, 65% yield. ^{1}H NMR (400 MHz, $CDCl_3$) δ 7.73 (d, J = 1.7 Hz, 1H), 7.51 (d, J = 1.8 Hz, 2H), 7.36 (d, J = 3.6 Hz, 2H), 7.31 (d, J = 5.1 Hz, 2H), 7.09 (dd, J = 5.1, 3.5 Hz, 2H), 6.99 (dd, J = 8.2, 4.4 Hz, 1H), 6.66 (d, J = 2.5 Hz, 1H), 6.58 (dd, J = 8.3, 2.3 Hz, 1H), 6.21 (d, J = 8.1 Hz, 1H), 5.32 (q, J = 7.0 Hz, 1H), 3.32 (tt, J = 9.7, 4.4 Hz, 1H), 3.04 (t, J = 5.6 Hz, 1H), 2.93 (tt, J = 13.7, 6.3 Hz, 1H), 2.58 (d, J = 11.8 Hz, 3H), 2.51 (td, J = 12.1, 9.7, 3.7 Hz, 2H), 2.31 (s, 3H), 2.19-1.99 (m, 2H), 1.87 (d, J = 13.7 Hz, 2H), 1.62 (d, J = 6.9 Hz, 3H). ^{13}C NMR (101 MHz, $CDCl_3$) δ 169.48, 144.86, 144.75, 143.68, 143.62, 137.31, 135.52, 131.97, 128.16, 125.35, 125.31, 123.79, 123.76, 122.94, 122.64, 115.84, 112.30, 59.35, 57.54, 54.64, 49.04, 27.71, 22.04, 18.81. $C_{30}H_{33}N_3OS_2$, MS calculated for m/z $[M+H]^+$: 516.2 (calculated), 516.2 (found).

(R)-5-(2-aminoacetamido)-N-(1-(3,5-di(thiophen-2-yl)phenyl)ethyl)-2-methylbenzamide **(Jun11923).** (tert-butoxycarbonyl)glycine (1.1 equiv), HATU (1.1 equiv) and DIPEA (3 equiv) were dissolved in DMF (0.2 M) and stirred for 15 min. Then (*R*)-5-amino-*N*-(1-(3,5-di(thiophen-2-yl)phenyl)ethyl)-2-methylbenzamide (**Jun11924**) (1.0 equiv) was added and stirred at room temperature overnight. When the starting material was consumed entirely as monitored by LCMS, the mixture was diluted with EtOAc and was then washed with saturated aq. $NaHCO_3$, water, and brine. The organic layer was dried over Na_2SO_4, filtered, and concentrated under vacuum to give the Boc-protected intermediate. The intermediate was dissolved in DCM (2 mL), and HCl (4M in dioxane, 10 equiv) was added. When the starting material was consumed entirely as monitored by LCMS, the mixture was diluted with DCM, adjusted to pH = 10, and then washed with water and brine. The organic layer was dried over Na_2SO_4, filtered, and concentrated under vacuum to give a residue which was purified by Prep-HPLC to give the final product **Jun11923** as a white solid.

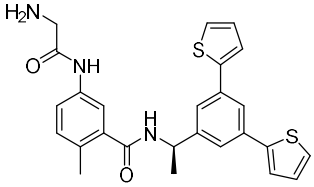

(R)-5-(2-aminoacetamido)-N-(1-(3,5-di(thiophen-2-yl)phenyl)ethyl)-2-methylbenzamide (**Jun11923**). White solid, 75% yield. ^{1}H NMR (400 MHz, MeOD-d_4) δ 7.79 (s, 1H), 7.65 (d, J = 9.7 Hz, 2H), 7.50 (s, 3H), 7.39 (d, J = 31.1 Hz, 3H), 7.23 (d, J = 8.3 Hz, 1H), 7.14 (s, 2H), 5.34-5.19 (m, 1H), 3.86 (s, 2H), 3.67 (s, 2H), 2.38 (d, J = 29.3 Hz, 3H), 1.62 (t, J = 7.4 Hz, 3H). ^{13}C NMR (101 MHz, MeOD-d_4) δ 145.71, 143.35, 135.36, 131.48, 127.82, 124.88, 123.44, 122.32, 121.29, 120.77, 120.28, 117.47, 52.02, 20.94, 17.57, 7.78. $C_{26}H_{25}N_3O_2S_2$, MS calculated for m/z $[M+H]^+$: 476.1 (calculated), 476.2 (found).

(R)-N-(1-(3,5-di(thiophen-2-yl)phenyl)ethyl)-5-(2-(dimethylamino)acetamido)-2-methylbenzamide (**Jun12111**). **Jun12111** was synthesized using the same amide coupling condition as described for **Jun11923** using the starting material dimethylglycine.

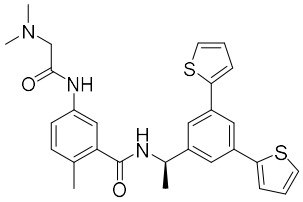

(R)-N-(1-(3,5-di(thiophen-2-yl)phenyl)ethyl)-5-(2-(dimethylamino)acetamido)-2-methylbenzamide (**Jun12111**). White solid, 77% yield. ^{1}H NMR (400 MHz, $CDCl_3$) δ 9.07 (s, 1H), 7.72 (d, J = 1.8 Hz, 1H), 7.58 (d, J = 2.3 Hz, 1H), 7.53 (d, J = 1.8 Hz, 2H), 7.36 (d, J = 3.6 Hz, 2H), 7.28 (d, J = 5.0 Hz, 2H), 7.12 (d, J = 8.3 Hz, 1H), 7.07 (dd, J = 5.1, 3.5 Hz, 2H), 6.62 (d, J = 8.0 Hz, 1H), 5.34 (m, 1H), 3.01-2.92 (m, 2H), 2.37 (s, 3H), 2.31 (s, 6H), 1.62 (d, J = 7.0 Hz, 3H). ^{13}C NMR (101 MHz, $CDCl_3$) δ 168.90, 168.81, 144.88, 143.73, 136.80, 135.48, 135.44, 131.64, 131.53, 128.09, 125.21, 123.74, 122.99, 122.62, 120.91, 117.97, 63.43, 49.06, 45.96, 38.59, 22.02, 19.30. $C_{28}H_{29}N_3O_2S_2$, MS calculated for m/z $[M+H]^+$: 504.2 (calculated), 504.1 (found).

(R)-N-(3-((1-(3,5-di(thiophen-2-yl)phenyl)ethyl)carbamoyl)-4-methylphenyl)piperidine-4-carboxamide (**Jun11945**). **Jun11945** was synthesized using the same procedures as described for **Jun11923** using the starting material 1-(tert-butoxycarbonyl)piperidine-4-carboxylic acid.

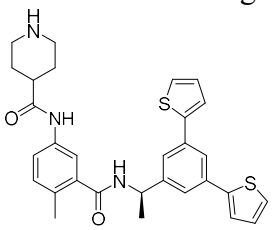

(R)-N-(3-((1-(3,5-di(thiophen-2-yl)phenyl)ethyl)carbamoyl)-4-methylphenyl)piperidine-4-carboxamide (**Jun11945**). White solid, 80% yield for two steps. ^{1}H NMR (400 MHz, MeOD-d_4) δ 7.78 (d, J = 1.8 Hz, 1H), 7.68 (d, J = 2.3 Hz, 1H), 7.64 (d, J = 1.6 Hz, 2H), 7.53-7.45 (m, 3H), 7.43 (d, J = 5.0 Hz, 2H), 7.22 (d, J = 8.3 Hz, 1H), 7.14 (dd, J = 5.2, 3.6 Hz, 2H), 5.27 (q, J = 7.2 Hz, 1H), 3.47 (dt, J = 13.3, 3.8 Hz, 2H), 3.09 (td, J = 12.5, 3.6 Hz, 2H), 2.75 (dq, J = 8.0, 5.4, 3.9 Hz, 1H), 2.34 (s, 3H), 2.18-1.83 (m, 4H), 1.61 (d, J = 7.2 Hz, 3H). ^{13}C NMR (101 MHz, MeOD-d_4) δ 172.85, 170.53, 145.85, 143.41, 136.83, 136.02, 135.42, 131.09, 130.82, 127.95, 124.99, 123.57, 122.32, 121.32, 118.71, 49.25, 42.93, 40.13, 37.72, 21.15, 17.87. $C_{30}H_{31}N_3O_2S_2$, MS calculated for m/z $[M+H]^+$: 530.2 (calculated), 530.1 (found).

(R)-5-bromo-N-(1-(3,5-di(thiophen-2-yl)phenyl)ethyl)-2-methylbenzamide (**A-6**). 5-methoxy-2-methylbenzoic acid (1.1 equiv), HATU (1.1 equiv) and DIPEA (3 equiv) were dissolved in DMF (0.2 M) and stirred for 15 min. After that (*R*)-1-(3-bromo-5-chlorophenyl)ethan-1-amine (**A-4**) was added and the solution was stirred at room temperature overnight. When the starting material was consumed entirely as monitored by LCMS, the mixture was diluted with EtOAc and was then washed with saturated aq. $NaHCO_3$, water, and brine. The organic layer was dried over Na_2SO_4, filtered, and concentrated under vacuum to give a residue which was purified by silica gel column chromatography (Hexanes/EtOAc = 4:1) to provide the desired product **A-6** as a slightly yellow solid.

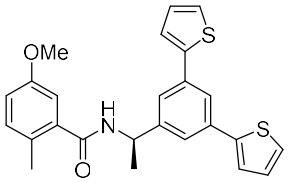

(R)-N-(1-(3,5-di(thiophen-2-yl)phenyl)ethyl)-5-methoxy-2-methylbenzamide (**A-6**). White solid, 83% yield. ^{1}H NMR (400 MHz, $CDCl_3$) δ 7.74 (t, J = 1.8 Hz, 1H), 7.51 (d, J = 1.7 Hz, 2H), 7.44-7.29 (m, 4H), 7.15-7.05 (m, 3H), 6.93 (d, J = 2.8 Hz, 1H), 6.84 (dd, J = 8.4, 2.8 Hz, 1H), 5.35 (m, 1H), 3.77 (s, 3H), 2.36 (s, 3H), 1.63 (d, J = 6.9 Hz, 3H). ^{13}C NMR (101 MHz, $CDCl_3$) δ 169.06, 157.54, 144.68, 143.70, 137.18, 135.57, 132.04, 128.10, 127.56, 125.29, 123.74, 122.95, 122.74, 115.50, 112.32, 55.47, 49.03, 21.98, 18.87. $C_{25}H_{24}NO_2S_2$, MS calculated for m/z $[M+H]^+$: 434.1 (calculated), 434.1 (found).

(R)-N-(1-(3,5-di(thiophen-2-yl)phenyl)ethyl)-5-hydroxy-2-methylbenzamide (**A-7**). (*R*)-5-bromo-*N*-(1-(3,5-di(thiophen-2-yl)phenyl)ethyl)-2-methylbenzamide (**A-6**) (1.0 equiv) was dissolved in DCM at 0 °C and BBr_3 (1 M solution in DCM, 3 equiv) was added slowly and the solution was stirred for 3 h. After the reaction was complete, the reaction was quenched with water and was then washed with DCM, water, and brine. The organic layer was dried over Na_2SO_4, filtered, and concentrated to give a residue that was purified by silica gel column chromatography (Hexanes/EtOAc =1:1) to provide the desired product **A-7** as a slightly yellow liquid.

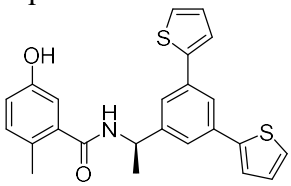

(R)-N-(1-(3,5-di(thiophen-2-yl)phenyl)ethyl)-5-hydroxy-2-methylbenzamide (**A-7**). White solid, 90% yield. ^{1}H NMR (400 MHz, $CDCl_3$) δ 7.74 (s, 1H), 7.66 (d, J = 1.8 Hz, 1H), 7.43 (d, J = 1.7 Hz, 2H), 7.28-7.26 (m, 2H), 7.24 (d, J = 1.3 Hz, 1H), 7.02 (dd, J = 5.1, 3.6 Hz, 2H), 6.84 (d, J = 8.3 Hz, 1H), 6.77 (d, J = 2.7 Hz, 1H), 6.64 (dd, J = 8.3, 2.7 Hz, 1H), 6.32 (d, J = 7.9 Hz, 1H), 5.23 (m, 1H), 2.22 (s, 3H), 1.53 (s, 3H). ^{13}C NMR (101 MHz, $CDCl_3$) δ 172.35, 156.25, 147.17, 144.81, 138.75, 136.69, 132.68, 129.17, 126.89, 126.21, 124.77, 123.69, 122.68, 117.69, 114.77, 50.41, 22.42, 18.76. $C_{24}H_{22}NO_2S_2$, MS calculated for m/z $[M+H]^+$: 420.1 (calculated), 420.1 (found).

(R)-N-(1-(3,5-di(thiophen-2-yl)phenyl)ethyl)-5-(2-(dimethylamino)ethoxy)-2-methylbenzamide (**Jun11875**). To a solution of *(R)-N-(1-(3,5-di(thiophen-2-yl)phenyl)ethyl)-5-hydroxy-2-methylbenzamide* (**A-7**) (1.0 equiv) and (2-bromoethyl)dimethylamine hydrobromide (1.1 equiv) in dry ACN, Cs_2CO_3 (2.0 equiv) was added. The reaction was stirred at 80 °C for overnight. After cooling down, the reaction was quenched with MeOH (1 mL). The mixture was diluted with EtOAc and was then washed with saturated aq. $NaHCO_3$, water, and brine. The organic layer was dried over Na_2SO_4, filtered, and concentrated to give a residue, which was purified by Prep-HPLC to afford the final product **Jun11875** as a white solid.

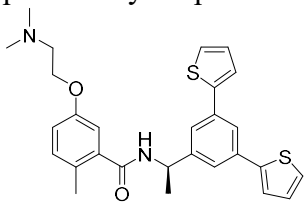

(R)-N-(1-(3,5-di(thiophen-2-yl)phenyl)ethyl)-5-(2-(dimethylamino)ethoxy)-2-methylbenzamide (**Jun11875**). White solid, 85% yield. ^{1}H NMR (400 MHz, MeOD-d_4) δ 7.78 (d, J = 1.8 Hz, 1H), 7.62 (d, J = 1.7 Hz, 2H), 7.44 (dd, J = 24.7, 4.4 Hz, 4H), 7.20-7.09 (m, 3H), 6.94 (d, J = 7.9 Hz, 2H), 5.25 (q, J = 7.0 Hz, 1H), 4.12 (t, J = 5.3 Hz, 2H), 2.89 (t, J = 5.3 Hz, 2H), 2.43 (s, 6H), 2.29 (s, 3H), 1.59 (d, J = 7.1 Hz, 3H). ^{13}C NMR (101 MHz, MeOD-d_4) δ 170.59, 156.16, 145.88, 143.42, 137.48, 135.38, 131.47, 127.85, 127.63, 124.90, 123.44, 122.33, 121.24, 115.71, 112.77, 64.15, 57.12, 49.10, 47.89, 47.84, 47.68, 47.63, 47.46, 47.42, 47.38, 47.17, 46.96, 43.71, 20.99, 17.39. $C_{28}H_{30}N_2O_2S_2$, MS calculated for m/z $[M+H]^+$: 491.2 (calculated), 491.1 (found).

(R)-N-(1-(3,5-di(thiophen-2-yl)phenyl)ethyl)-2-methyl-5-(2-(pyrrolidin-1-yl)ethoxy)benzamide (**Jun11899**). **Jun11899** was synthesized using the same alkylation procedures described for **Jun11875** with the starting material 1-(2-bromoethyl)pyrrolidine.

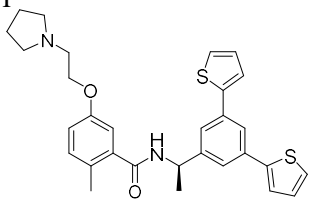

(R)-N-(1-(3,5-di(thiophen-2-yl)phenyl)ethyl)-2-methyl-5-(2-(pyrrolidin-1-yl)ethoxy)benzamide (**Jun11899**). White solid, 75% yield. ^{1}H NMR (400 MHz, MeOD-d_4) δ 7.66 (t, J = 1.7 Hz, 1H), 7.51 (d, J = 1.7 Hz, 2H), 7.36 (dd, J = 3.7, 1.1 Hz, 2H), 7.29 (dd, J = 5.1, 1.1 Hz, 2H), 7.10-6.92 (m, 3H), 6.90-6.74 (m, 2H), 5.13 (q, J = 7.0 Hz, 1H), 4.04 (t, J = 5.3 Hz, 2H), 3.00 (t, J = 5.3 Hz, 2H), 2.85-2.67 (m, 4H), 2.18 (s, 3H), 1.83-1.70 (m, 4H), 1.47 (d, J = 7.1 Hz, 3H). ^{13}C NMR (101 MHz, MeOD-d_4) δ 170.57, 156.25, 145.94, 143.45, 137.53, 135.40, 131.49, 127.88, 127.60, 124.93, 123.47, 122.35, 121.26, 115.69, 112.79, 65.29, 54.29, 54.19, 49.11, 47.41, 47.19, 46.98, 22.71, 21.03, 17.43. $C_{30}H_{32}N_2O_2S_2$, MS calculated for m/z $[M+H]^+$: 517.2 (calculated), 517.1 (found).

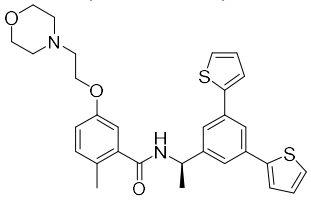

(R)-N-(1-(3,5-di(thiophen-2-yl)phenyl)ethyl)-2-methyl-5-(2-morpholino-ethoxy)benzamide (**Jun118910**). **Jun118910** was synthesized using the same alkylation procedures described for **Jun11875** with the starting material 4-(2-bromoethyl)morpholine.

(R)-N-(1-(3,5-di(thiophen-2-yl)phenyl)ethyl)-2-methyl-5-(2-morpholino-ethoxy)benzamide (**Jun118910**). White solid, 79% yield. ^{1}H NMR (400 MHz, MeOD-d_4) δ 7.68 (d, J = 1.8 Hz, 1H), 7.52 (d, J = 1.7 Hz, 2H), 7.39-7.35 (m, 2H), 7.31 (d, J = 5.0 Hz, 2H), 7.09-6.94 (m, 3H), 6.88-6.70 (m, 2H), 5.15 (m, 1H), 4.02 (t, J = 5.4 Hz, 2H), 3.59 (t, J = 4.7 Hz, 4H), 2.68 (t, J = 5.4 Hz, 2H), 2.47 (t, J = 4.8 Hz, 4H), 2.19 (s, 3H), 1.49 (d, J = 7.1 Hz, 3H). ^{13}C NMR (101 MHz, MeOD-d_4) δ 170.72, 156.58, 145.92, 143.48, 137.44, 135.40, 131.40, 130.95, 127.84, 127.25, 124.88, 123.42, 122.33, 121.26, 115.74, 112.68, 66.19, 65.24, 57.28, 53.71, 20.98, 17.35. $C_{30}H_{32}N_2O_3S_2$, MS calculated for m/z $[M+H]^+$: 533.2 (calculated), 533.1 (found).

(R)-5-(2-aminoethoxy)-N-(1-(3,5-di(thiophen-2-yl)phenyl)ethyl)-2-methylbenzamide (**Jun11874**). **Jun11874** was synthesized using the same alkylation procedures described for **Jun11875** with the starting material of tert-butyl (2-bromoethyl)carbamate. The Boc-protected intermediate was dissolved in DCM (2 mL), and HCl (4M in dioxane, 10 equiv) was added.

When the starting material was consumed entirely as monitored by LCMS, the mixture was diluted with DCM, adjusted to pH = 10, and then washed with water and brine. The organic layer was dried over Na_2SO_4, filtered, and concentrated under vacuum to give a residue which was purified by Prep-HPLC to give the final product **Jun11874** as a white solid.

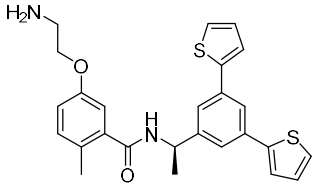

(R)-5-(2-aminoethoxy)-N-(1-(3,5-di(thiophen-2-yl)phenyl)ethyl)-2-methylbenzamide (**Jun11874**). White solid, 88% yield. ^{1}H NMR (400 MHz, MeOD-d_4) δ 7.78 (d, J = 1.8 Hz, 1H), 7.62 (d, J = 1.7 Hz, 2H), 7.48 (d, J = 3.6 Hz, 2H), 7.42 (d, J = 5.1 Hz, 2H), 7.20 (d, J = 8.3 Hz, 1H), 7.13 (dd, J = 5.1, 3.6 Hz, 2H), 7.04-6.85 (m, 2H), 5.28 (m, 1H), 4.21 (t, J = 5.0 Hz, 2H), 3.34 (d, J = 4.7 Hz, 2H), 2.31 (s, 3H), 1.60 (d, J = 7.1 Hz, 3H). ^{13}C NMR (101 MHz, MeOD-d_4) δ 170.51, 155.88, 145.84, 143.42, 137.65, 135.41, 131.57, 128.02, 127.91, 124.97, 123.50, 122.40, 121.30, 115.77, 112.87, 66.74, 64.09, 49.22, 47.44, 47.23, 47.01, 38.93, 21.02, 17.47. $C_{26}H_{26}N_2O_2S_2$, MS calculated for m/z $[M+H]^+$: 463.1 (calculated), 463.1 (found).

(R)-2-(3-((1-(3,5-di(thiophen-2-yl)phenyl)ethyl)carbamoyl)-4-methylphenoxy)-N,N,N-trimethylethan-1-aminium (**Jun11898**). To a solution of (*R*)-*N*-(1-(3,5-di(thiophen-2-yl)phenyl)ethyl)-5-(2-(dimethylamino)ethoxy)-2-methylbenzamide (**Jun11875**) (1.0 equiv) in dry MeOH, MeI (1.5 equiv) was added and the solution was stirred at room temperature for overnight. When the starting material was consumed entirely as monitored by LCMS, the mixture was concentrated under vacuum to give a residue, which was purified by Prep-HPLC to afford the final product **Jun11898** as a white solid.

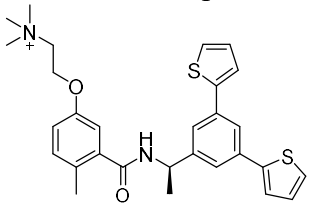

(R)-2-(3-((1-(3,5-di(thiophen-2-yl)phenyl)ethyl)carbamoyl)-4-methylphenoxy)-N,N,N-trimethylethan-1-aminium (**Jun11898**). White solid, 50% yield. ^{1}H NMR (400 MHz, MeOD-d_4) δ 7.67 (d, J = 1.8 Hz, 1H), 7.53 (d, J = 1.7 Hz, 2H), 7.38 (d, J = 3.6 Hz, 2H), 7.31 (d, J = 5.1 Hz, 2H), 7.08 (d, J = 8.2 Hz, 1H), 7.01 (dd, J = 5.1, 3.6 Hz, 2H), 6.88 (d, J = 8.1 Hz, 2H), 5.15 (q, J = 7.0 Hz, 1H), 4.36 (h, J = 2.4 Hz, 2H), 3.84-3.61 (m, 2H), 3.15 (s, 9H), 2.20 (s, 3H), 1.50 (d, J = 7.1 Hz, 3H). ^{13}C NMR (101 MHz, MeOD-d_4) δ 170.32, 155.28, 145.91, 143.42, 137.62, 135.41, 131.67, 128.42, 127.92, 124.99, 123.54, 122.41, 121.26, 115.78, 113.07, 65.15, 62.02, 53.49, 53.45, 49.23, 47.42, 47.20, 46.99, 21.07, 17.49. $C_{29}H_{33}N_2O_2S_2$, MS calculated for m/z $[M]^+$: 505.2(calculated), 505.1 (found).

Scheme 2. Synthesis of SARS-CoV-2 PL^{pro} inhibitors.

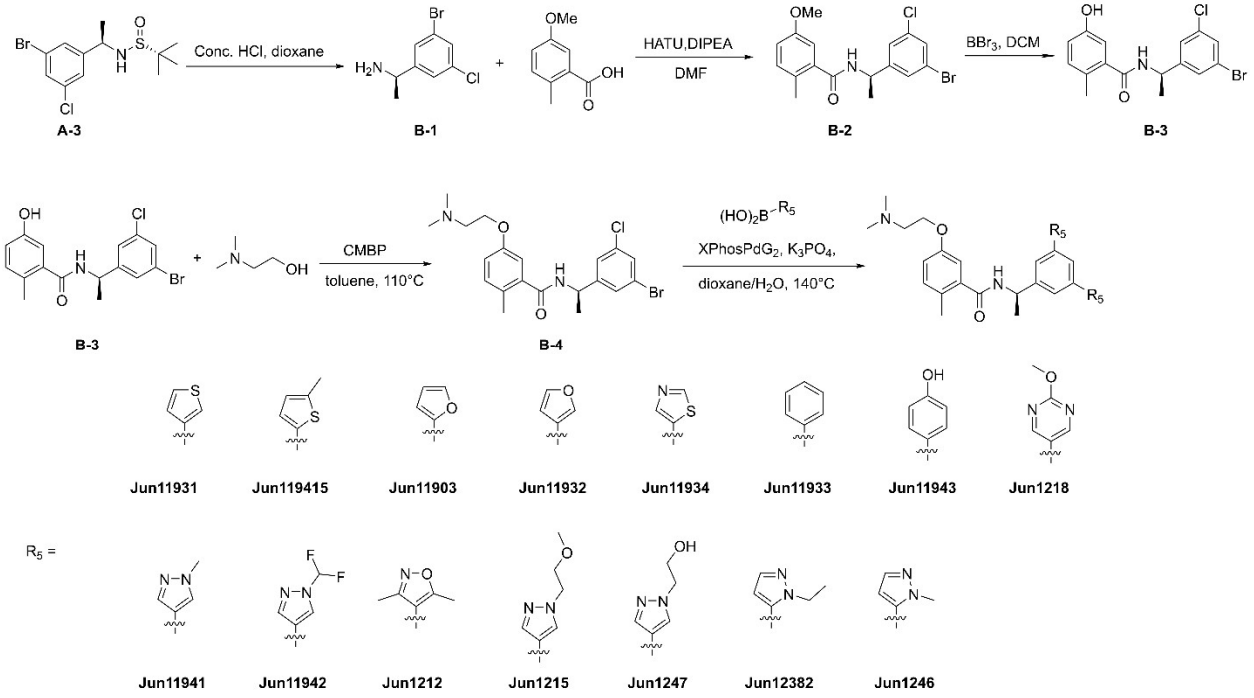

Synthetic Procedures for Scheme 2

(R)-1-(3-bromo-5-chlorophenyl)ethan-1-amine **(B-1)**. To a solution of compound **A-3** (1 equiv) in 1,4-dioxane (0.1 M), concentrated HCl was added. The reactions were stirred at room temperature for 10 min. When the starting material was consumed entirely as monitored by LCMS, the mixture was concentrated under vacuum to give the desired compound **B-1** as a white solid, which was used for the next step without further purification.

(R)-N-(1-(3-bromo-5-chlorophenyl)ethyl)-5-methoxy-2-methylbenzamide (**B-2**). 5-methoxy-2-methylbenzoic acid (1.1 equiv), HATU (1.1 equiv) and DIPEA (3 equiv) were dissolved in DMF (0.2 M) and stirred for 15 min. After that compound **B-1** was added and the solution was stirred at room temperature overnight. When the starting material was consumed entirely as monitored by LCMS, the mixture was diluted with EtOAc and was then washed with saturated aq. $NaHCO_3$, water, and brine. The organic layer was dried over Na_2SO_4, filtered, and concentrated under vacuum to give a residue that was purified by silica gel column chromatography (Hexanes/EtOAc = 3:1) to provide the desired product **B-2** as a slightly yellow solid.

1-(3-bromo-5-chlorophenyl)ethan-1-one (**B-2**). White solid, 86% yield. ^{1}H NMR (400 MHz, DMSO-d_6) δ 8.75 (d, J = 7.8 Hz, 1H), 7.59 (d, J = 1.8 Hz, 2H), 7.49 (d, J = 1.7 Hz, 1H), 7.15 (d, J = 8.3 Hz, 1H), 6.92 (dd, J = 8.3, 2.7 Hz, 1H), 6.89 (d, J = 2.8 Hz, 1H), 5.08 (m, 1H), 3.76 (s, 3H), 2.19 (s, 3H), 1.42 (d, J = 7.0 Hz, 3H). ^{13}C NMR (101 MHz, DMSO-d_6) δ 168.63, 157.40, 150.05, 138.01, 134.56, 131.96, 129.44, 128.33, 127.26, 125.86, 122.64, 115.20, 113.16, 55.69, 48.30, 38.70, 22.54, 18.73. $C_{17}H_{17}BrClNO_2$, MS calculated for m/z $[M+H]^+$: 382.0209 (calculated), 382.0 (found).

(R)-N-(1-(3-bromo-5-chlorophenyl)ethyl)-5-hydroxy-2-methylbenzamide (**B-3**). Compound **B-2** (1 equiv) was dissolved in DCM at 0 °C, and BBr_3 (1 M solution in DCM, 3 equiv) was added slowly and the solution was stirred for 3 h. When the starting material was consumed entirely as monitored by LCMS, the reaction was quenched with water and washed with DCM, water, and brine, respectively. The organic layer was dried over Na_2SO_4, filtered, and concentrated. The residue was purified by silica gel column chromatography (Hexanes/EtOAc = 1:1) to provide the desired product **B-3** as a colorless liquid.

1-(3-bromo-5-chlorophenyl)ethan-1-one (**B-3**). White solid, 89% yield. ^{1}H NMR (400 MHz, DMSO-d_6) δ 9.43 (s, 1H), 8.74 (d, J = 7.9 Hz, 1H), 7.58 (d, J = 5.0 Hz, 2H), 7.49 (d, J = 1.9 Hz, 1H), 7.02 (d, J = 8.1 Hz, 1H), 6.75 (dd, J = 10.7, 2.6 Hz, 2H), 5.09 (m, 1H), 2.16 (s, 3H), 1.41 (d, J = 7.2 Hz, 3H). ^{13}C NMR (101 MHz, DMSO-d_6) δ 168.93, 155.42, 150.10, 137.99, 134.57, 131.85, 129.41, 128.31, 125.83, 125.37, 122.63, 116.68, 114.34, 60.20, 48.22, 22.49, 21.17, 18.71, 14.51. $C_{16}H_{15}BrClNO_2$, MS calculated for m/z $[M+H]^+$: 368.0 (calculated), 368.1 (found).

(R)-N-(1-(3-bromo-5-chlorophenyl)ethyl)-5-(2-(dimethylamino)ethoxy)-2-methylbenzamide (**B-4**). To a solution of compound **B-3** (1 equiv) in dry toluene in a 15 mL sealed tube, 2-(dimethylamino)ethanol (1.5 equiv) and cyanomethylene trimethylphosphorane (CMMP) (2.0 equiv) were added. The reaction mixture was degassed and purged with argon, and then the tube was sealed and heated to 110° C overnight. When the starting material was consumed entirely as monitored by LCMS, the mixture was diluted with EtOAc and washed with water and brine. The organic layer was dried over Na_2SO_4, filtered, and concentrated. The residue was purified by silica gel column chromatography (DCM/MeOH = 20:1) to provide the desired product **B-4** as a white solid.

(R)-N-(1-(3-bromo-5-chlorophenyl)ethyl)-5-(2-(dimethylamino)ethoxy)-2-methylbenzamide (**B-4**). White solid, 94% yield. ^{1}H NMR (400 MHz, DMSO-d_6) δ 8.76 (d, J = 7.9 Hz, 1H), 7.70 (s, 1H), 7.62 (s, 2H), 7.14 (d, J = 8.2 Hz, 1H), 6.95-6.88 (m, 2H), 5.07 (m, 1H), 4.05 (t, J = 5.7 Hz, 2H), 2.64 (t, J = 5.7 Hz, 2H), 2.23 (s, 6H), 2.19 (s, 3H), 1.41 (d, J = 7.0 Hz, 3H). ^{13}C NMR (101 MHz, DMSO-d_6) δ 168.57, 156.59, 150.33, 137.90, 132.05, 131.99, 128.70, 127.41, 122.86, 115.78, 113.83, 66.34, 58.05, 48.26, 45.90, 22.56, 18.80. $C_{20}H_{24}BrClN_2O_2$, MS calculated for m/z $[M+H]^+$: 439.0788 (calculated), 439.0795 (found).

General procedures for the Suzuki coupling I. To a solution of compound **B-4** (1 equiv) in dioxane/H_2O (4:1) in a microwave reaction vial was added corresponding boronic acid or ester (2.5 equiv) and tripotassium phosphate (1.8 equiv). The mixture was purged with nitrogen for 5 min. Then XPhosPdG2 (0.1 equiv) was added, and the solution was heated in the biotage microwave reactor at 140 °C for 90 min. After the reaction was completed, the reaction mixture was diluted with EtOAc and washed with water and brine. The organic layer was separated, dried over anhydrous Na_2SO_4, filtered, and concentrated under vacuum to give a residue which was purified by Prep-HPLC to give the final product.

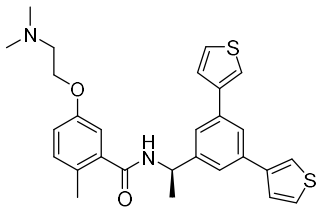

(R)-N-(1-(3,5-di(thiophen-3-yl)phenyl)ethyl)-5-(2-(dimethylamino)ethoxy)-2-methylbenzamide (**Jun11931**). White solid, 90% yield. ^{1}H NMR (400 MHz, DMSO-d_6) δ 8.76 (d, J = 8.3 Hz, 1H), 7.95 (d, J = 11.6 Hz, 3H), 7.68 (d, J = 13.8 Hz, 6H), 7.14 (d, J = 8.1 Hz, 1H), 6.91 (d, J = 7.8 Hz, 2H), 5.27-5.20 (m, 1H), 4.07 (t, J = 5.8 Hz, 2H), 2.69 (t, J = 5.7 Hz, 2H), 2.26 (s, 6H), 2.23 (s, 3H), 1.51 (d, J = 6.9 Hz, 3H). ^{13}C NMR (101 MHz, DMSO-d_6) 168.46, 156.53, 146.61, 141.98, 138.49, 136.21, 131.91, 127.48, 127.39, 126.83, 123.20, 122.74, 121.67, 115.82, 113.68, 66.15, 57.92, 48.89, 45.75, 23.32, 18.84. $C_{28}H_{30}N_2O_2S_2$, HRMS calculated for m/z $[M+H]^+$: 491.1827(calculated), 491.1832(found)

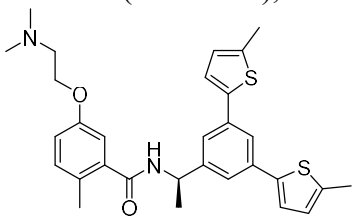

(R)-N-(1-(3,5-bis(5-methylthiophen-2-yl)phenyl)ethyl)-5-(2-(dimethylamino)ethoxy)-2-methylbenzamide (**Jun119415**). White solid, 86% yield. ^{1}H NMR (400 MHz, $CDCl_3$) δ 7.61 (d, J = 1.9 Hz, 1H), 7.43 (s, 2H), 7.15 (d, J = 3.6 Hz, 2H), 7.12 (s, 1H), 6.92 (d, J = 2.8 Hz, 1H), 6.82 (d, J = 5.6 Hz, 1H), 6.74 (d, J = 3.6 Hz, 2H), 6.28 (d, J = 8.0 Hz, 1H), 5.36-5.30 (m, 1H), 4.35-4.33 (m, 2H), 3.46-3.43 (m, 2H), 2.91 (s, 6H), 2.51 (s, 6H), 2.36 (s, 3H), 1.64 (d, J = 6.9 Hz, 3H). ^{13}C NMR (101 MHz, $CDCl_3$) δ 141.30, 139.99, 135.75, 132.33, 126.28, 123.50, 122.10, 115.84, 62.88, 56.42, 49.30, 43.68, 21.76, 18.92, 15.47. $C_{30}H_{34}N_2O_2S_2$, HRMS calculated for m/z $[M+H]^+$: 519.2140(calculated), 519.2144(found)

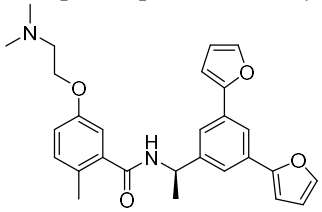

(R)-N-(1-(3,5-di(furan-2-yl)phenyl)ethyl)-5-(2-(dimethylamino)ethoxy)-2-methylbenzamide (**Jun11903**). White solid, 92% yield. ^{1}H NMR (400 MHz, DMSO-d_6) δ 8.82 (d, J = 8.0 Hz, 1H), 7.90 (d, J = 2.1 Hz, 1H), 7.79 (s, 2H), 7.68 (s, 2H), 7.15 (d, J = 7.6 Hz, 1H), 7.04 (s, 2H), 6.93 (d, J = 3.4 Hz, 2H), 6.64 (s, 2H), 5.21-5.14 (m, 1H), 4.09 (t, J = 5.8 Hz, 2H), 2.75 (t, J = 5.7 Hz, 2H), 2.30 (s, 6H), 2.21 (s, 3H), 1.49 (d, J = 6.9 Hz, 3H). ^{13}C NMR (101 MHz, DMSO-d_6) δ 168.50, 156.45, 153.23, 146.93, 143.55, 138.39, 131.92, 131.40, 128.70, 127.50, 122.86, 120.66, 117.24, 115.80, 113.74, 112.62, 106.81, 65.89, 57.79, 48.78, 45.57, 22.78, 18.79. $C_{28}H_{30}N_2O_4$, HRMS calculated for m/z $[M+H]^+$: 459.2284(calculated), 459.2291(found)

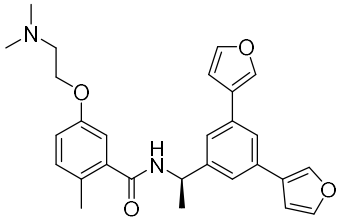

(R)-N-(1-(3,5-di(thiophen-3-yl)phenyl)ethyl)-5-(2-(dimethylamino)ethoxy)-2-methylbenzamide (**Jun11932**). White solid, 90% yield. ^{1}H NMR (400 MHz, DMSO-d_6) δ 8.71 (d, J = 8.5 Hz, 1H), 8.23 (s, 2H), 7.77 (d, J = 11.2 Hz, 3H), 7.55 (s, 2H), 7.14 (d, J = 7.4 Hz, 1H), 7.02 (s, 2H), 6.91 (d, J = 5.1 Hz, 2H), 5.21-5.14 (m, 1H), 4.06 (t, J = 5.7 Hz, 2H), 2.68 (t, J = 5.7 Hz, 2H), 2.25 (s, 6H), 2.21 (s, 3H), 1.49 (d, J = 6.9 Hz, 3H). ^{13}C NMR (101 MHz, DMSO-d_6) δ 168.45, 156.53,

146.51, 144.74, 139.93, 138.49, 132.90, 131.89, 127.35, 126.31, 122.41, 121.61, 115.78, 113.68, 109.24, 66.17, 57.94, 48.83, 45.76, 23.23, 18.80. $C_{28}H_{30}N_2O_4$, HRMS calculated for m/z $[M+H]^+$: 459.2284(calculated), 459.2297(found)

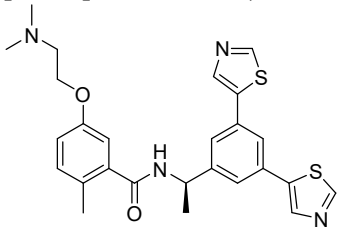

(R)-N-(1-(3,5-di(thiazol-5-yl)phenyl)ethyl)-5-(2-(dimethylamino)ethoxy)-2-methylbenzamide (**Jun11934**). White solid, 78% yield. ^{1}H NMR (400 MHz, DMSO-d_6) δ 8.90 (s, 2H), 8.59 (d, J = 8.1 Hz, 1H), 8.21 (s, 2H), 7.70 (s, 1H), 7.43 (s, 2H), 6.91 (d, J = 8.5 Hz, 1H), 6.69 (d, J = 6.7 Hz, 2H), 4.99-4.91 (m, 1H), 3.85 (d, J = 5.9 Hz, 2H), 2.25 (s, 2H), 2.07 (s, 6H), 1.97 (s, 3H), 1.25 (d, J = 7.0 Hz, 3H). ^{13}C NMR (101 MHz, DMSO-d_6) δ 168.57, 156.46, 154.55, 147.91, 140.66, 138.42, 138.34, 132.29, 131.95, 127.45, 124.98, 123.00, 115.91, 113.68, 65.84, 57.71, 48.64, 45.52, 23.00, 18.83. $C_{26}H_{28}N_4O_2S_2$, HRMS calculated for m/z $[M+H]^+$: 493.1732(calculated), 493.1740(found)

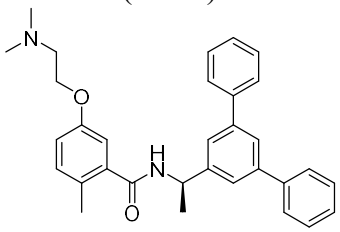

(R)-N-(1-([1,1':3',1''-terphenyl]-5'-yl)ethyl)-5-(2-(dimethylamino)ethoxy)-2-methylbenzamide (**Jun11933**). White solid, 88% yield. ^{1}H NMR (400 MHz, DMSO-d_6) δ 8.82 (d, J = 8.3 Hz, 1H), 7.77 (d, J = 7.6 Hz, 5H), 7.71 (s, 2H), 7.50 (t, J = 7.5 Hz, 4H), 7.41 (d, J = 7.3 Hz, 2H), 7.14 (d, J = 8.2 Hz, 1H), 6.92 (d, J = 7.7 Hz, 2H), 5.32-5.25 (m, 1H), 4.06 (t, J = 5.7 Hz, 2H), 2.69 (t, J = 5.6 Hz, 2H), 2.26 (s, 6H), 2.23 (s, 3H), 1.54 (d, J = 7.0 Hz, 3H). ^{13}C NMR (101 MHz, DMSO-d_6) δ 168.48, 156.52, 146.77, 141.44, 140.75, 138.47, 131.92, 129.39, 128.06, 127.39, 124.22, 124.02, 115.80, 113.68, 66.08, 57.91, 48.92, 45.72, 23.23, 18.84. $C_{32}H_{34}N_2O_2$, HRMS calculated for m/z $[M+H]^+$: 479.2698(calculated), 479.2709(found)

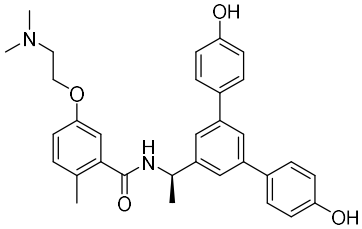

(R)-N-(1-(4,4''-dihydroxy-[1,1':3',1''-terphenyl]-5'-yl)ethyl)-5-(2-(dimethylamino)ethoxy)-2-methylbenzamide (**Jun11943**). White solid, 88% yield. ^{1}H NMR (400 MHz, DMSO-d_6) δ 9.59 (s, 2H), 8.77 (d, J = 8.3 Hz, 1H), 7.59-7.52 (m, 7H), 7.14 (d, J = 8.3 Hz, 1H), 6.92-6.86 (m, 6H), 5.25-5.18 (m, 1H), 4.06 (d, J = 5.9 Hz, 2H), 2.68 (t, J = 5.6 Hz, 2H), 2.26 (s, 6H), 2.22 (s, 3H), 1.50 (d, J = 7.0 Hz, 3H). ^{13}C NMR (101 MHz, DMSO-d_6) δ 168.41, 157.66, 156.51, 146.37, 141.27, 138.51, 131.90, 131.65, 128.35, 127.38, 122.61, 122.51, 116.15, 115.79, 113.65, 66.13, 57.92, 48.93, 46.03, 45.73, 23.22, 18.83. $C_{32}H_{34}N_2O_4$, HRMS calculated for m/z $[M+H]^+$: 511.2597(calculated), 511.2605(found)

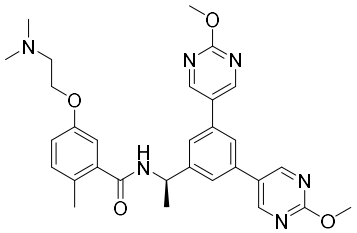

(R)-N-(1-(3,5-bis(2-methoxypyrimidin-5-yl)phenyl)ethyl)-5-(2-(dimethylamino)ethoxy)-2-methylbenzamide (**Jun1218)**. White solid, 84% yield. ^{1}H NMR (400 MHz, DMSO-d_6) δ 8.99 (s, 4H), 8.96 (s, 1H), 8.71 (d, J = 8.2 Hz, 1H), 7.93 (s, 1H), 7.76 (s, 2H), 7.14 (d, J = 8.4 Hz, 1H), 6.93 (s, 1H), 5.27-5.20 (m, 1H), 4.25 (t, J = 5.0 Hz, 2H), 3.92 (s, 6H), 3.44 (q, J = 4.7 Hz, 2H), 2.80 (s, 6H), 2.17 (s, 3H), 1.46 (d, J = 7.1 Hz, 3H). ^{13}C NMR (101 MHz, DMSO-d_6) δ 168.40, 165.20, 158.85, 158.51, 158.00, 157.95, 155.70, 147.24, 138.67, 135.32, 131.97, 128.15, 127.58, 127.50, 124.16, 123.18, 118.26, 115.98, 114.09, 62.87, 55.90, 55.25, 55.22, 48.98, 43.27, 23.50, 18.82. $C_{30}H_{34}N_6O_4$, HRMS calculated for m/z $[M+H]^+$: 543.2720(calculated), 543.2727(found)

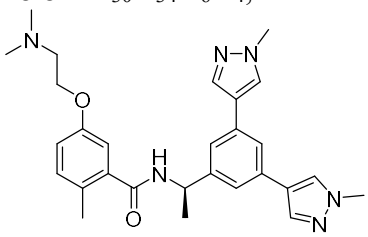

(R)-N-(1-(3,5-bis(1-methyl-1H-pyrazol-4-yl)phenyl)ethyl)-5-(2 (dimethylamino)ethoxy)-2-methylbenzamide (**Jun11941**). White solid, 79% yield. ^{1}H NMR (400 MHz, DMSO-d_6) δ 8.68 (d, J = 8.3 Hz, 1H), 8.15 (s, 2H), 7.89 (s, 2H), 7.66 (s, 1H), 7.43 (s, 2H), 7.14 (d, J = 8.1 Hz, 1H), 6.92 (d, J = 7.9 Hz, 2H), 5.18-5.11 (m, 1H), 4.08 (t, J = 5.8 Hz, 2H), 3.88 (s, 6H), 2.72 (t, J = 5.7 Hz, 2H), 2.28 (s, 6H), 2.22 (s, 3H), 1.48 (d, J = 7.1 Hz, 3H). ^{13}C NMR (101 MHz, DMSO-d_6) δ 168.40, 156.49, 146.33, 138.55, 136.51, 133.50, 131.88, 128.30, 127.40, 122.51, 120.92, 120.49, 115.74, 113.73, 66.01, 57.84, 48.83, 45.64, 39.14, 23.14, 23.00, 18.82. $C_{28}H_{34}N_6O_2$, HRMS calculated for m/z $[M+H]^+$: 487.2821(calculated), 487.2830(found)

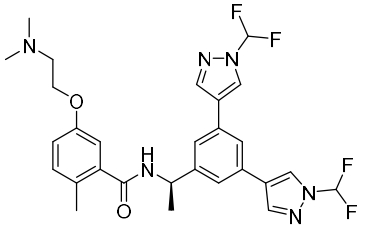

(R)-N-(1-(3,5-bis(1-(difluoromethyl)-1H-pyrazol-4-yl)phenyl)ethyl)-5-(2-(dimethylamino)ethoxy)-2-methylbenzamide (**Jun11942**). White solid, 86% yield. ^{1}H NMR (400 MHz, $CDCl_3$) δ 8.11 (s, 2H), 7.96 (s, 2H), 7.54 (s, 1H), 7.46 (s, 2H), 7.38 (s, 1H), 7.27 (s, 1H), 7.12-7.08 (m, 1H), 6.98 (d, J = 2.7 Hz, 1H), 6.87 (dd, J = 8.4, 2.8 Hz, 1H), 6.15 (d, J = 7.8 Hz, 1H), 5.39-5.31 (m, 1H), 4.03 (t, J = 5.6 Hz, 2H), 2.71 (t, J = 5.6 Hz, 2H), 2.36 (s, 3H), 2.32 (s, 6H), 1.64 (d, J = 6.9 Hz, 3H). ^{13}C NMR (101 MHz, $CDCl_3$) δ 168.94, 156.78, 145.16, 139.66, 139.64, 139.62, 136.85, 132.42, 132.12, 127.99, 125.37, 123.11, 123.09, 122.85, 115.71, 113.63, 113.58, 111.09, 108.60, 66.08, 58.27, 49.11, 45.80, 21.97, 18.89. $C_{28}H_{30}F_4N_6O_2$, HRMS calculated for m/z $[M+H]^+$: 559.2446(calculated), 559.2451(found)

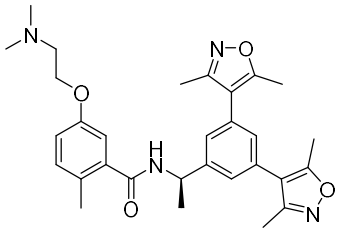

(R)-N-(1-(3,5-bis(3,5-dimethylisoxazol-4-yl)phenyl)ethyl)-5-(2-(dimethylamino)ethoxy)-2-methylbenzamide (**Jun1212**). White solid, 77% yield. ^{1}H NMR (400 MHz, DMSO-d_6) δ 8.74 (d, J = 8.2 Hz, 1H), 7.35 (s, 2H), 7.21 (s, 1H), 7.12 (d, J = 8.3 Hz, 1H), 6.93-6.88 (m, 2H), 5.22-5.14 (m, 1H), 4.23 (t, J = 5.1 Hz, 2H), 3.44 (s, 2H), 2.79 (s, 6H), 2.40 (s, 6H), 2.23 (s, 6H), 2.14 (s, 3H), 1.44 (d, J = 7.0 Hz, 3H). ^{13}C NMR (101 MHz, DMSO-d_6) δ 168.32, 165.86, 158.63, 155.67, 146.49, 138.53, 132.00, 130.93, 128.21, 127.85, 126.11, 116.12, 115.92, 114.03, 62.88, 55.89, 48.65, 43.27, 22.98, 18.81, 11.95, 11.04. $C_{30}H_{36}N_4O_4$, HRMS calculated for m/z $[M+H]^+$: 517.2815(calculated), 517.2821(found)

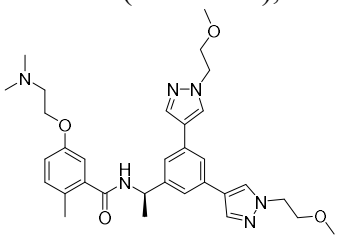

(R)-N-(1-(3,5-bis(1-(2-methoxyethyl)-1H-pyrazol-4-yl)phenyl)ethyl)-5-(2-(dimethylamino)ethoxy)-2-methylbenzamide (**Jun1215**). White solid, 74% yield. ^{1}H NMR (400 MHz, DMSO-d_6) δ 8.69 (d, J = 8.3 Hz, 1H), 8.18 (s, 2H), 7.93 (s, 2H), 7.68 (s, 1H), 7.44 (s, 2H), 7.14 (d, J = 8.1 Hz, 1H), 6.91 (d, J = 8.0 Hz, 2H), 5.18-5.11 (m, 1H), 4.29 (t, J = 5.3 Hz, 4H), 4.07 (t, J = 5.7 Hz, 2H), 3.72 (t, J = 5.3 Hz, 4H), 3.25 (s, 6H), 2.70 (t, J = 5.7 Hz, 2H), 2.27 (s, 6H), 2.22 (s, 3H), 1.48 (d, J = 7.0 Hz, 3H). ^{13}C NMR (101 MHz, DMSO-d_6) δ 168.40, 156.50, 146.33, 138.56, 136.68, 133.48, 131.88, 128.12, 127.37, 122.26, 120.92, 120.41, 115.71, 113.71, 73.99, 70.97, 66.04, 58.47, 57.86, 51.85, 48.84, 46.03, 45.67, 25.42, 23.19, 18.82, 9.50. $C_{32}H_{42}N_6O_4$, HRMS calculated for m/z $[M+H]^+$: 575.3346(calculated), 575.3352(found)

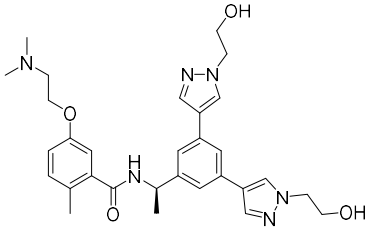

(R)-N-(1-(3,5-bis(1-(2-hydroxyethyl)-1H-pyrazol-4-yl)phenyl)ethyl)-5-(2-(dimethylamino)ethoxy)-2-methylbenzamide (**Jun1247**). White solid, 72% yield. ^{1}H NMR (400 MHz, DMSO-d_6) δ 8.72 (d, J = 8.3 Hz, 1H), 8.19 (s, 2H), 7.93 (s, 2H), 7.69 (s, 1H), 7.45 (s, 2H), 7.19 (d, J = 8.4 Hz, 1H), 6.97 (d, J = 10.8 Hz, 2H), 5.20-5.12 (m, 1H), 4.30 (q, J = 5.9 Hz, 4H), 4.18 (t, J = 5.6 Hz, 2H), 3.78 (t, J = 5.6 Hz, 2H), 3.73 (t, J = 5.3 Hz, 2H), 3.50 (q, J = 4.6 Hz, 2H), 2.86 (s, 6H), 2.24 (s, 3H), 1.49 (d, J = 7.1 Hz, 3H). ^{13}C NMR (101 MHz, DMSO-d_6) δ 168.40, 158.76, 158.42, 155.67, 146.54, 142.67, 138.55, 138.45, 132.00, 131.22, 128.18, 126.94, 126.57, 115.98, 114.04, 106.63, 62.85, 55.93, 48.70, 43.29, 38.09, 23.03, 18.82. $C_{30}H_{38}N_6O_4$, HRMS calculated for m/z $[M+H]^+$: 547.3033(calculated), 547.3040(found)

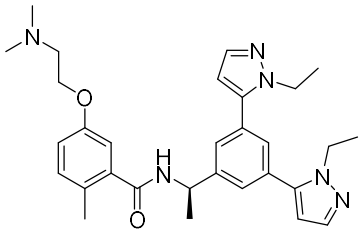

(R)-N-(1-(3,5-bis(1-ethyl-1H-pyrazol-5-yl)phenyl)ethyl)-5-(2-(dimethylamino)ethoxy)-2-methylbenzamide (**Jun12382**). White solid, 74% yield. ^{1}H NMR (400 MHz, DMSO-d_6) δ 8.84 (d, J = 8.1 Hz, 1H), 7.55 (d, J = 9.1 Hz, 4H), 7.43 (d, J = 1.8 Hz, 1H), 7.19 (d, J = 8.2 Hz, 1H), 6.98 (d, J = 8.7 Hz, 2H), 6.44 (s, 2H), 5.30-5.23 (m, J = 7.2 Hz, 1H), 4.31 (t, J = 4.9 Hz, 2H), 4.19 (q, J = 7.1 Hz, 4H), 3.51 (q, J = 4.6 Hz, 2H), 2.87 (s, 6H), 2.20 (s, 3H), 1.53 (d, J = 7.0 Hz, 3H), 1.33 (t, J = 7.2 Hz, 6H). ^{13}C NMR (101 MHz, DMSO-d_6) δ 168.42, 155.69, 146.62, 142.26, 138.69, 138.49, 131.98, 131.46, 128.18, 127.16, 126.80, 115.88, 114.10, 106.66, 62.90, 55.89, 48.64, 44.62, 43.26, 22.70, 18.77, 15.93. $C_{30}H_{38}N_6O_2$, HRMS calculated for m/z $[M+H]^+$: 515.3134 (calculated), 515.3140 (found)

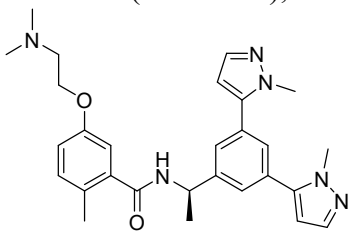

(R)-N-(1-(3,5-bis(1-methyl-1H-pyrazol-5-yl)phenyl)ethyl)-5-(2-(dimethylamino)ethoxy)-2-methylbenzamide (**Jun1246**). White solid, 78% yield. ^{1}H NMR (400 MHz, DMSO-d_6) δ 8.78 (s, 4H), 8.76 (s, 2H), 7.77 (s, 1H), 7.63 (s, 2H), 7.44 (s, 1H), 7.20 (d, J = 8.2 Hz, 1H), 6.98 (s, 2H), 5.28-5.21 (m, 1H), 4.32 (d, J = 4.9 Hz, 2H), 4.05 (s, 12H), 3.51 (t, J = 6.4 Hz, 2H), 2.86 (d, J = 3.2 Hz, 6H), 2.69 (s, 2H), 2.24 (s, 4H), 1.50 (d, J = 6.9 Hz, 3H). ^{13}C NMR (101 MHz, DMSO-d_6) δ 168.40, 158.76, 158.42, 155.67, 146.54, 142.67, 138.55, 138.45, 132.00, 131.22, 128.18, 126.94, 126.57, 115.98, 114.04, 106.63, 62.85, 55.93, 48.70, 43.29, 38.09, 23.03, 18.82. $C_{28}H_{34}N_6O_2$, HRMS calculated for m/z $[M+H]^+$: 487.2821 (calculated), 487.2828 (found)

Scheme 3. Synthesis of SARS-CoV-2 PL^{pro} inhibitors

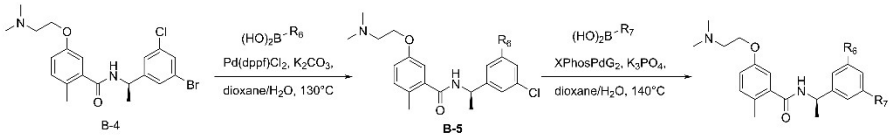

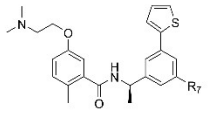

R_7 =

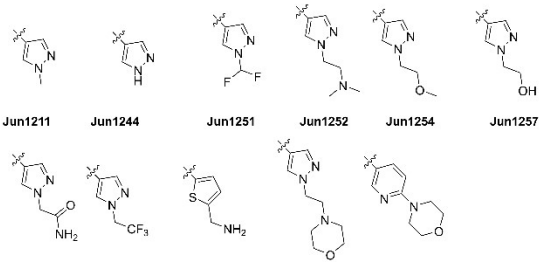

Jun1211 Jun1244 Jun1251 Jun1252 Jun1254 Jun1257

Jun121210 Jun12149 Jun12129 Jun121910 Jun12511

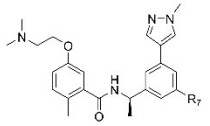

R_7 =

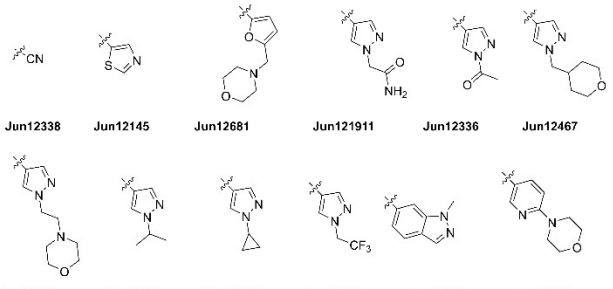

Jun12338 Jun12145 Jun12681 Jun121911 Jun12336 Jun12467

Jun12351 Jun12199 Jun12197 Jun12603 Jun12446 Jun12278

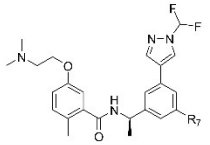

R_7 =

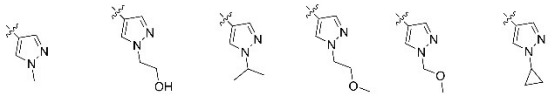

Jun12162 Jun12208 Jun12235 Jun12281 Jun12303 Jun12284

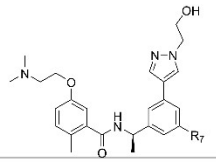

R_7 =

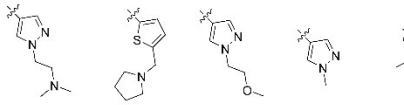

Jun12165 Jun12168 Jun12163 Jun12164 Jun12198

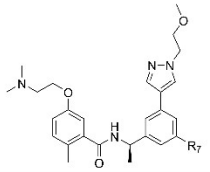

R_7 =

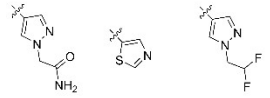

Jun12242 Jun12147 Jun12759

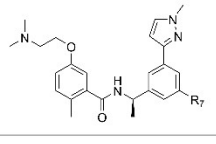

R_7 =

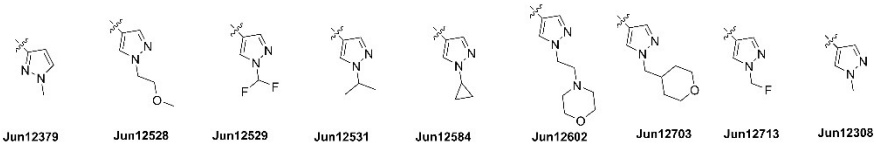

Jun12379 Jun12528 Jun12529 Jun12531 Jun12584 Jun12602 Jun12703 Jun12713 Jun12308

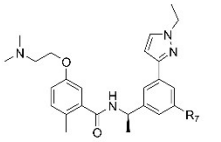

R_7 =

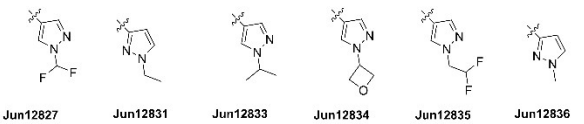

Jun12827 Jun12831 Jun12833 Jun12834 Jun12835 Jun12836

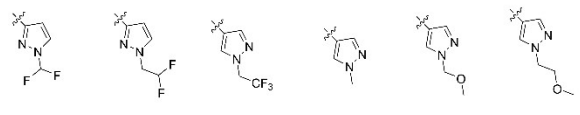

Jun12837 Jun1314 Jun12839 Jun12682 Jun12924 Jun12763

Synthetic Procedure for Scheme 3

General procedures for the Suzuki coupling II. To a solution of compound **B-4** (1 equiv) in dioxane/H_2O (4:1) in a microwave reaction vial was added corresponding boronic acid or ester (1.2 equiv) and potassium carbonate (1.8 equiv). The mixture was purged with nitrogen for 5 min. Then Pd(dppf)Cl_2 (0.1 equiv) was added, and the solution was heated in the biotage microwave reactor at 130 °C for 90 min. The reaction mixture was diluted with EtOAc and extracted with aqueous $NaHCO_3$ solution and brine. The organic layer was separated, dried over anhydrous Na_2SO_4, filtered, and concentrated under vacuum to get intermediate **B-5**. To a solution of intermediate **B-5** (1 equiv) in dioxane/H_2O (4:1) in a microwave reaction vial was added corresponding boronic acid or ester (1.2 equiv) and tripotassium phosphate (1.8 equiv). The mixture was purged with nitrogen for 5 min. Then XPhosPdG2 (0.1 equiv) was added, and the solution was heated in the biotage microwave reactor at 140 °C for 90 min. After the reaction was completed, the reaction mixture was diluted with EtOAc and washed with water and brine. The organic layer was separated, dried over anhydrous Na_2SO_4, filtered, and concentrated under vacuum to give a residue which was purified by Prep-HPLC to give the final product.

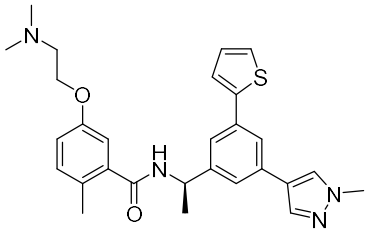

(R)-5-(2-(dimethylamino)ethoxy)-2-methyl-N-(1-(3-(1-methyl-1H-pyrazol-4-yl)-5-(thiophen-2-yl)phenyl)ethyl)benzamide (**Jun1211**). White solid, 68% yield for two steps. ^{1}H NMR (400 MHz, DMSO-d_6) δ 8.73 (d, J = 8.1 Hz, 1H), 8.17 (s, 1H), 7.87 (s, 1H), 7.67 (s, 1H), 7.51 (t, J = 4.7 Hz, 2H), 7.47 (s, 1H), 7.43 (s, 1H), 7.4-7.09 (m, 2H), 6.90 (s, 1H), 5.13-5.06 (m, 1H), 4.24 (t, J = 5.0 Hz, 2H), 3.82 (s, 3H), 3.45-3.42 (m, 2H), 2.86 (s, 1H), 2.79 (s, 6H), 2.17 (s, 2H), 1.42 (d, J = 7.0 Hz, 3H). ^{13}C NMR (101 MHz, DMSO-d_6) δ 168.36, 158.79, 158.46, 155.68, 146.75, 143.95, 138.77, 136.65, 134.82, 133.87, 131.95, 128.87, 128.63, 128.17, 126.16, 124.37, 122.68, 122.02, 121.28, 120.73, 115.92, 114.02, 62.87, 55.91, 48.79, 43.27, 39.16, 22.99, 18.84. $C_{28}H_{32}N_4O_2S$, HRMS calculated for m/z $[M+H]^+$: 489.2324 (calculated), 489.2330 (found)

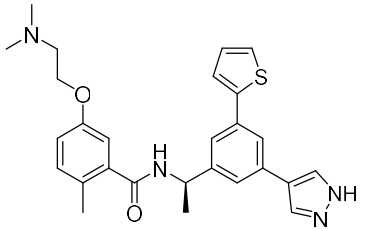

(R)-N-(1-(3,5-bis(2-methoxypyrimidin-5-yl)phenyl)ethyl)-5-(2-(dimethylamino)ethoxy)-2-methylbenzamide (**Jun1244**). White solid, 66% yield for two steps. ^{1}H NMR (400 MHz, $CDCl_3$) δ 8.65 (d, J = 2.3 Hz, 4H), 7.49 (s, 2H), 7.43 (s, 1H), 7.32 (s, 1H), 7.12 (d, J = 8.3 Hz, 1H), 6.99 (d, J = 2.8 Hz, 1H), 6.83 (dd, J = 8.4, 2.8 Hz, 1H), 6.63 (d, J = 7.7 Hz, 1H), 5.41-5.34 (m, 1H), 4.38 (dt, J = 6.8, 3.7 Hz, 2H), 3.47 (q, J = 4.8 Hz, 2H), 2.93 (s, 6H), 2.36 (s, 3H), 1.65 (d, J = 6.9 Hz, 3H). ^{13}C NMR (101 MHz, $CDCl_3$) δ 168.70, 160.11, 155.61, 155.54, 155.07, 145.86, 137.02, 136.60, 132.39, 129.68, 122.78, 122.67, 122.29, 121.71, 116.05, 113.46, 62.99, 56.57, 49.42, 43.77, 43.39, 37.75, 37.55, 22.17, 19.03. $C_{27}H_{30}N_4O_2S$, HRMS calculated for m/z $[M+H]^+$: 475.2168 (calculated), 475.2173 (found)

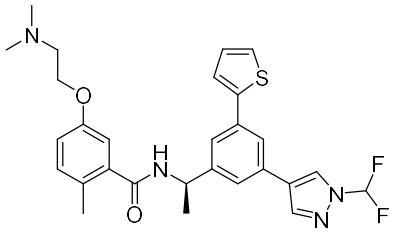

(R)-N-(1-(3-(1-(difluoromethyl)-1H-pyrazol-4-yl)-5-(thiophen-2-yl)phenyl)ethyl)-5-(2-(dimethylamino)ethoxy)-2-methylbenzamide (**Jun1251**). White solid, 68% yield for two steps. ^{1}H NMR (400 MHz, $CDCl_3$) δ 8.14 (s, 1H), 7.98 (s, 1H), 7.63 (s, 1H), 7.57 (s, 1H), 7.50 (s, 1H), 7.37 (d, J = 3.6 Hz, 1H), 7.32 (d, J = 5.0 Hz, 1H), 7.12-7.08 (m, 2H), 6.97 (d, J = 2.8 Hz, 1H), 6.82 (d, J = 8.4 Hz, 1H), 6.51 (d, J = 7.9 Hz, 1H), 5.38-5.31 (m, 1H), 4.37-4.34 (m, 2H), 3.44-3.42 (m, 2H), 2.91 (s, 6H), 2.36 (s, 3H), 1.66 (d, J = 6.9 Hz, 3H). ^{13}C NMR (101 MHz, $CDCl_3$) δ 168.67, 155.03, 145.16, 143.66, 139.73, 137.25, 135.66, 132.35, 132.19, 129.66, 128.13, 125.48, 125.31, 123.75, 123.20, 123.08, 122.66, 115.95, 113.53, 111.08, 62.94, 56.63, 49.32, 43.82, 21.98, 18.94. $C_{28}H_{30}F_2N_4O_2S$, HRMS calculated for m/z $[M+H]^+$: 525.2136 (calculated), 525.2141 (found)

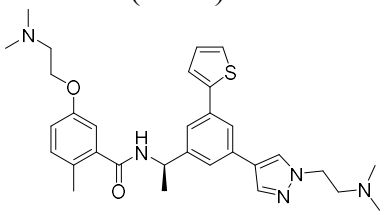

(R)-5-(2-(dimethylamino)ethoxy)-N-(1-(3-(1-(2-(dimethylamino)ethyl)-1H-pyrazol-4-yl)-5-(thiophen-2-yl)phenyl)ethyl)-2-methylbenzamide (**Jun1252**). White solid, 65% yield for two steps. ^{1}H NMR (400 MHz, DMSO-d_6) δ 8.82 (d, J = 8.1 Hz, 1H), 8.40 (s, 1H), 8.09 (s, 1H), 7.76 (s, 1H), 7.57 (dd, J = 13.5, 6.1 Hz, 4H), 7.19 (q, J = 6.0, 4.7 Hz, 2H), 6.98 (d, J = 8.3 Hz, 2H), 5.21-5.13 (m, 1H), 4.58 (t, J = 6.3 Hz, 2H), 4.32 (t, J = 5.0 Hz, 2H), 3.63 (t, J = 6.3 Hz, 2H), 3.51 (s, 2H), 2.86 (s, 6H), 2.83 (s, 6H), 2.23 (s, 3H), 1.49 (d, J = 7.0 Hz, 3H). ^{13}C NMR (101 MHz, DMSO-d_6) δ 168.39, 158.74, 158.43, 155.70, 146.91, 143.86, 138.74, 137.72, 134.91, 133.40, 131.96, 128.89, 128.77, 128.14, 126.26, 124.39, 122.95, 122.52, 121.41, 120.81, 115.91, 114.03, 62.90, 56.11, 55.88, 48.84, 46.66, 43.26, 43.15, 23.00, 18.84. $C_{31}H_{39}N_5O_2S$, HRMS calculated for m/z $[M+H]^+$: 546.2903 (calculated), 546.2910(found)

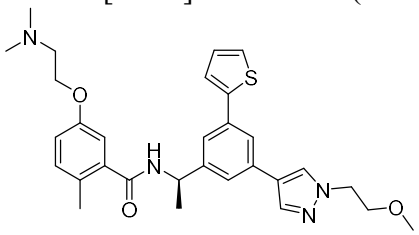

(R)-5-(2-(dimethylamino)ethoxy)-N-(1-(3-(1-(2-methoxyethyl)-1H-pyrazol-4-yl)-5-(thiophen-2-yl)phenyl)ethyl)-2-methylbenzamide (**Jun1254**). White solid, 75% yield for two steps. ^{1}H NMR (400 MHz, DMSO-d_6) δ 8.88 (d, J = 8.2 Hz, 1H), 8.33 (s, 1H), 8.05 (s, 1H), 7.84 (s, 1H), 7.69 – 7.62 (m, 3H), 7.58 (s, 1H), 7.30 – 7.24 (m, 2H), 7.06 (d, J = 8.1 Hz, 2H), 5.29-5.21 (m, 1H), 4.39 (dt, J = 10.1, 5.0 Hz, 4H), 3.88 (s, 2H), 3.81 (t, J = 5.2 Hz, 3H), 3.59 (s, 2H), 2.94 (s, 6H), 2.32 (s, 3H), 1.57 (d, J = 7.0 Hz, 3H). ^{13}C NMR (101 MHz, DMSO-d_6) δ 168.35, 155.68, 146.74, 143.95, 138.79, 136.80, 134.82, 133.86, 131.95, 128.86, 128.42, 128.16, 126.15, 124.41, 122.70,

121.79, 121.30, 120.71, 115.92, 114.02, 70.91, 62.88, 58.46, 55.89, 51.83, 48.80, 43.27, 23.02, 18.84. $C_{30}H_{36}N_4O_3S$, HRMS calculated for m/z $[M+H]^+$: 533.2586 (calculated), 533.2594(found)

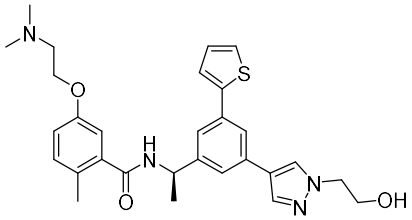

(R)-5-(2-(dimethylamino)ethoxy)-N-(1-(3-(1-(2-hydroxyethyl)-1H-pyrazol-4-yl)-5-(thiophen-2-yl)phenyl)ethyl)-2-methylbenzamide (**Jun1257**). White solid, 72% yield for two steps. ^{1}H NMR (400 MHz, DMSO-d_6) δ 9.73 (s, 1H), 8.79 (d, J = 8.2 Hz, 1H), 8.25 (s, 1H), 7.97 (s, 1H), 7.76 (s, 1H), 7.60-7.55 (m, 3H), 7.49 (s, 1H), 7.21-7.17 (m, 2H), 6.98 (d, J = 10.2 Hz, 2H), 5.21-5.13 (m, 1H), 4.31 (t, J = 5.0 Hz, 2H), 4.19 (t, J = 5.7 Hz, 2H), 3.79 (t, J = 5.6 Hz, 2H), 3.51 (s, 2H), 2.86 (s, 6H), 2.25 (s, 3H), 1.49 (d, J = 7.1 Hz, 3H). ^{13}C NMR (101 MHz, DMSO-d_6) δ 168.98, 168.35, 155.68, 146.76, 143.93, 138.78, 137.07, 134.81, 133.82, 131.95, 129.47, 128.88, 128.18, 126.16, 124.41, 122.66, 122.03, 121.39, 120.72, 115.96, 113.99, 62.86, 55.91, 54.48, 48.78, 43.28, 23.00, 18.84. $C_{29}H_{34}N_4O_3S$, HRMS calculated for m/z $[M+H]^+$: 519.2430 (calculated), 519.2436 (found)

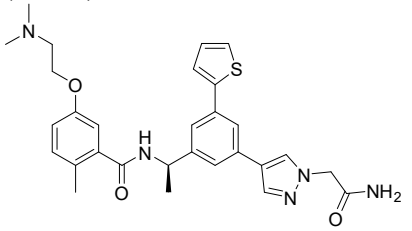

(R)-N-(1-(3-(1-(2-amino-2-oxoethyl)-1H-pyrazol-4-yl)-5-(thiophen-2-yl)phenyl)ethyl)-5-(2-(dimethylamino)ethoxy)-2-methylbenzamide (**Jun121210**). White solid, 52% yield for two steps. ^{1}H NMR (400 MHz, DMSO-d_6) δ 9.82 (s, 1H), 8.80 (d, J = 8.1 Hz, 1H), 8.24 (s, 1H), 7.98 (s, 1H), 7.77 (s, 1H), 7.59 (dd, J = 12.2, 3.7 Hz, 4H), 7.51 (s, 1H), 7.31 (s, 1H), 7.21-7.16 (m, 2H), 6.97 (s, 1H), 5.22-5.15 (m, 1H), 4.81 (s, 2H), 4.31 (t, J = 5.0 Hz, 2H), 3.51 (d, J = 5.0 Hz, 2H), 2.86 (s, 6H), 2.25 (s, 3H), 1.50 (d, J = 7.0 Hz, 3H). ^{13}C NMR (101 MHz, DMSO-d_6) δ 168.98, 168.35, 155.68, 146.76, 143.93, 138.78, 137.07, 134.81, 133.82, 131.95, 129.47, 128.88, 128.18, 126.16, 124.41, 122.66, 122.03, 121.39, 120.72, 115.96, 113.99, 62.86, 55.91, 54.48, 48.78, 43.28, 23.00, 18.84. $C_{29}H_{33}N_5O_3S$, HRMS calculated for m/z $[M+H]^+$: 532.2382 (calculated), 532.2388 (found)

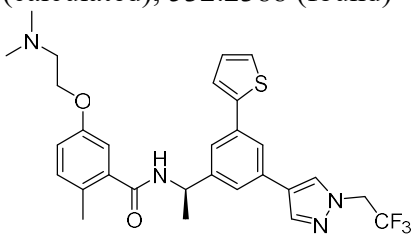

(R)-5-(2-(dimethylamino)ethoxy)-2-methyl-N-(1-(3-(thiophen-2-yl)-5-(1-(2,2,2-trifluoroethyl)-1H-pyrazol-4-yl)phenyl)ethyl)benzamide (**Jun12149**). White solid, 62% yield for two steps. ^{1}H NMR (400 MHz, DMSO-d_6) δ 8.74 (d, J = 8.1 Hz, 1H), 8.33 (s, 1H), 8.07 (s, 1H), 7.73 (d, J = 2.0 Hz, 1H), 7.55 (d, J = 3.6 Hz, 1H), 7.51 (d, J = 5.4 Hz, 2H), 7.49-7.46 (m, 1H), 7.12 (q, J = 6.2, 4.5 Hz, 2H), 6.91 (d, J = 7.4 Hz, 2H), 5.16-5.09 (m, 3H), 4.25 (t, J = 4.9 Hz, 2H), 3.44 (q, J = 4.4 Hz, 2H), 2.79 (s, 6H), 2.17 (s, 3H), 1.43 (d, J = 6.9 Hz, 3H). ^{13}C NMR (101 MHz, DMSO-

d_6) δ 168.37, 158.81, 158.48, 155.69, 146.87, 143.79, 138.77, 138.63, 134.93, 133.03, 131.95, 129.73, 128.88, 128.16, 126.26, 124.54, 123.18, 122.98, 121.83, 121.01, 115.93, 114.03, 62.88, 55.91, 52.33, 51.99, 48.79, 43.27, 22.97, 18.82. $C_{29}H_{31}F_3N_4O_2S$, HRMS calculated for m/z $[M+H]^+$: 557.2198(calculated), 557.2205(found)

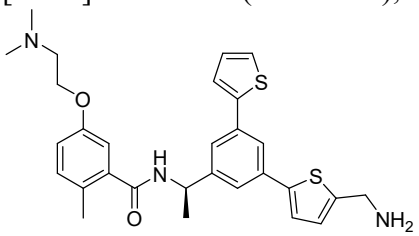

(R)-N-(1-(3-(5-(aminomethyl)thiophen-2-yl)-5-(thiophen-2-yl)phenyl)ethyl)-5-(2-(dimethylamino)ethoxy)-2-methylbenzamide (**Jun12129**). White solid, 66% yield for two steps. ^{1}H NMR (400 MHz, DMSO-d_6) δ 8.89 (d, J = 7.9 Hz, 1H), 8.47 (s, 3H), 7.77 (s, 1H), 7.65 (s, 1H), 7.62-7.57 (m, 4H), 7.28 (d, J = 3.7 Hz, 1H), 7.20 (d, J = 4.4 Hz, 2H), 6.98 (s, 1H), 5.23-5.16 (m, 1H), 4.34-4.30 (m, 4H), 3.52 (s, 2H), 2.87 (s, 6H), 2.24 (s, 3H), 1.51 (d, J = 6.9 Hz, 3H). ^{13}C NMR (101 MHz, DMSO-d_6) δ 168.47, 159.06, 158.74, 155.71, 147.46, 144.40, 143.22, 138.63, 135.64, 135.20, 134.66, 131.96, 130.79, 129.04, 128.16, 126.66, 124.83, 124.73, 123.20, 122.95, 120.99, 115.96, 114.01, 62.91, 55.85, 48.76, 43.23, 37.52, 22.83, 18.86. $C_{29}H_{33}N_3O_2S_2$, HRMS calculated for m/z $[M+H]^+$: 520.2092 (calculated), 520.2099 (found)

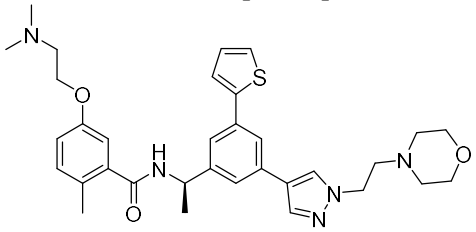

(R)-5-(2-(dimethylamino)ethoxy)-2-methyl-N-(1-(3-(1-(2-morpholinoethyl)-1H-pyrazol-4-yl)-5-(thiophen-2-yl)phenyl)ethyl)benzamide (**Jun121910**). White solid, 78% yield for two steps. ^{1}H NMR (400 MHz, DMSO-d_6) δ 8.81 (d, J = 8.1 Hz, 1H), 8.38 (s, 1H), 8.09 (s, 1H), 7.76 (s, 1H), 7.61-7.53 (m, 4H), 7.23-7.16 (m, 2H), 6.98 (d, J = 7.7 Hz, 2H), 5.21-5.14 (m, 1H), 4.62 (t, J = 6.4 Hz, 2H), 4.32 (t, J = 5.0 Hz, 2H), 3.69 (t, J = 6.5 Hz, 2H), 3.52 (d, J = 5.3 Hz, 2H), 2.87 (s, 6H), 2.24 (s, 3H), 1.50 (d, J = 7.0 Hz, 3H). ^{13}C NMR (101 MHz, DMSO-d_6) δ 168.39, 159.00, 158.66, 155.70, 146.90, 143.87, 138.75, 137.71, 134.92, 133.41, 131.95, 128.88, 128.68, 128.17, 126.24, 124.38, 122.96, 122.53, 121.44, 120.84, 118.43, 115.92, 114.05, 63.79, 62.92, 55.91, 55.46, 51.94, 48.85, 46.21, 43.28, 22.96, 18.83. $C_{33}H_{41}N_5O_3S$, HRMS calculated for m/z $[M+H]^+$: 588.3008 (calculated), 588.3015 (found)

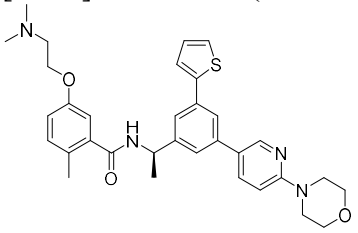

(R)-5-(2-(dimethylamino)ethoxy)-2-methyl-N-(1-(3-(6-morpholinopyridin-3-yl)-5-(thiophen-2-yl)phenyl)ethyl)benzamide (**Jun12511**). White solid, 74% yield for two steps. ^{1}H NMR (400 MHz, $CDCl_3$) δ 8.45 (s, 1H), 8.11 (dd, J = 9.3, 2.2 Hz, 1H), 7.67 (s, 1H), 7.58 (s, 1H), 7.51 (s, 1H), 7.38 (d, J = 3.6 Hz, 1H), 7.33 (d, J = 5.0 Hz, 1H), 7.13-7.10 (m, 2H), 7.03 (d, J = 9.3 Hz, 1H), 6.97 (d, J = 2.7 Hz, 1H), 6.82 (dd, J = 8.3, 2.7 Hz, 1H), 6.75 (d, J = 7.6 Hz, 1H), 5.37-5.33

(m, 1H), 4.35 (q, J = 6.8, 5.9 Hz, 2H), 3.90 (t, J = 4.8 Hz, 4H), 3.73 (t, J = 5.0 Hz, 4H), 3.47 (q, J = 4.2 Hz, 2H), 2.92 (s, 6H), 2.36 (s, 3H), 1.65 (d, J = 7.0 Hz, 3H). ^{13}C NMR (101 MHz, DMSO-d_6) δ 168.43, 155.69, 146.93, 143.20, 142.81, 138.61, 138.43, 134.82, 131.98, 131.57, 129.04, 128.18, 126.66, 125.83, 124.94, 124.10, 123.64, 115.96, 114.03, 106.50, 62.89, 55.89, 48.73, 43.26, 38.00, 22.94, 18.84. $C_{33}H_{38}N_4O_3S$, HRMS calculated for m/z $[M+H]^+$: 571.2743 (calculated), 571.2750 (found)

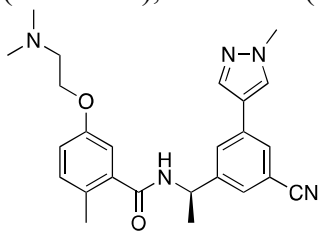

(R)-N-(1-(3-cyano-5-(1-methyl-1H-pyrazol-4-yl)phenyl)ethyl)-5-(2-(dimethylamino)ethoxy)-2-methylbenzamide (**Jun12338**). White solid, 60% yield for two steps. ^{1}H NMR (400 MHz, $CDCl_3$) δ 8.79 (d, J = 7.9 Hz, 1H), 8.27 (s, 1H), 7.98 (s, 1H), 7.96 (s, 2H), 7.64 (s, 1H), 7.20 (d, J = 8.4 Hz, 1H), 6.99 (d, J = 6.1 Hz, 2H), 5.21-5.13 (m, 1H), 4.32 (t, J = 4.9 Hz, 2H), 3.88 (s, 3H), 3.52 (q, J = 4.8 Hz, 2H), 2.87 (d, J = 3.7 Hz, 6H), 2.22 (s, 3H), 1.47 (d, J = 7.0 Hz, 3H). ^{13}C NMR (101 MHz, DMSO-d_6) δ 168.47, 159.01, 158.66, 155.70, 147.47, 138.39, 136.86, 134.59, 131.99, 129.09, 128.21, 127.96, 127.24, 127.07, 120.58, 119.40, 115.98, 114.11, 112.38, 62.87, 55.90, 48.59, 43.26, 39.24, 22.70, 18.77. $C_{25}H_{29}N_5O_2$, HRMS calculated for m/z $[M+H]^+$: 432.2399 (calculated), 432.2406(found)

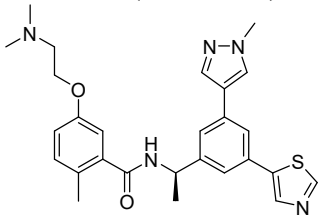

(R)-5-(2-(dimethylamino)ethoxy)-2-methyl-N-(1-(3-(1-methyl-1H-pyrazol-4-yl)-5-(thiazol-5-yl)phenyl)ethyl)benzamide (**Jun12145**). White solid, 55% yield for two steps. ^{1}H NMR (400 MHz, DMSO-d_6) δ 9.11 (s, 1H), 8.78 (d, J = 8.2 Hz, 1H), 8.38 (s, 1H), 8.25 (s, 1H), 7.96 (s, 1H), 7.81 (d, J = 1.8 Hz, 1H), 7.61 (s, 1H), 7.51 (d, J = 1.8 Hz, 1H), 7.20 (d, J = 8.1 Hz, 1H), 6.98 (d, J = 8.3 Hz, 2H), 5.22-5.14 (m, 1H), 4.32 (t, J = 4.9 Hz, 2H), 3.89 (s, 3H), 3.52 (s, 2H), 2.86 (s, 6H), 2.24 (s, 3H), 1.49 (d, J = 7.0 Hz, 3H). ^{13}C NMR (101 MHz, DMSO-d_6) δ 168.38, 158.86, 158.52, 155.70, 154.07, 147.00, 140.03, 139.20, 138.74, 136.72, 134.10, 131.96, 131.80, 128.72, 128.16, 123.40, 122.53, 121.81, 121.73, 115.95, 114.03, 62.89, 55.93, 48.78, 43.29, 39.18, 23.03, 18.81. $C_{27}H_{31}N_5O_2S$, HRMS calculated for m/z $[M+H]^+$: 490.2277(calculated), 490.2283(found)

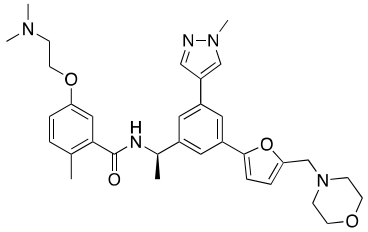

(R)-5-(2-(dimethylamino)ethoxy)-2-methyl-N-(1-(3-(1-methyl-1H-pyrazol-4-yl)-5-(5-(morpholinomethyl)furan-2-yl)phenyl)ethyl)benzamide (**Jun12681**). White solid, 65% yield for two steps. ^{1}H NMR (400 MHz, DMSO-d_6) δ 8.80 (d, J = 8.1 Hz, 1H), 8.22 (s, 1H), 7.92 (s, 1H), 7.74 (s, 1H), 7.60 (s, 2H), 7.49 (s, 1H), 7.34 (d, J = 3.7 Hz, 1H), 7.19 (d, J = 8.2 Hz, 1H), 6.98 (d,

J = 6.3 Hz, 2H), 5.21-5.14 (p, 1H), 4.62 (s, 2H), 4.32 (t, J = 5.0 Hz, 2H), 3.89 (s, 3H), 2.87 (s, 6H), 2.23 (s, 3H), 1.50 (d, J = 7.0 Hz, 3H). ^{13}C NMR (101 MHz, DMSO-d_6) δ 168.39, 159.15, 158.81, 155.70, 146.99, 146.90, 138.69, 136.60, 134.14, 134.03, 131.93, 128.62, 128.15, 124.64, 123.21, 121.91, 121.54, 120.80, 115.90, 114.04, 63.84, 62.88, 55.85, 53.62, 50.92, 48.82, 43.22, 39.17, 22.85, 18.83. $C_{33}H_{41}N_5O_4$, HRMS calculated for m/z $[M+H]^+$: 572.3637(calculated), 572.3644 (found)

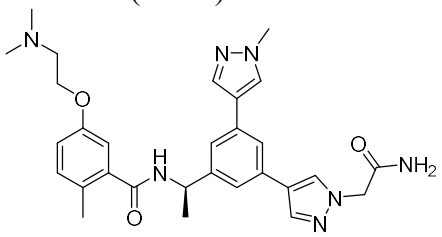

(R)-N-(1-(3-(1-(2-amino-2-oxoethyl)-1H-pyrazol-4-yl)-5-(1-methyl-1H-pyrazol-4-yl)phenyl)ethyl)-5-(2-(dimethylamino)ethoxy)-2-methylbenzamide (**Jun121911**). White solid, 45% yield for two steps. ^{1}H NMR (400 MHz, DMSO-d_6) δ 8.71 (d, J = 8.3 Hz, 1H), 8.17 (d, J = 5.9 Hz, 2H), 7.92 (d, J = 10.1 Hz, 2H), 7.69 (s, 1H), 7.58 (s, 1H), 7.45 (d, J = 9.5 Hz, 2H), 7.30 (s, 1H), 7.19 (d, J = 8.3 Hz, 1H), 6.97 (d, J = 10.6 Hz, 2H), 5.20-5.13 (m, 1H), 4.80 (s, 2H), 4.30 (t, J = 4.8 Hz, 2H), 3.88 (s, 3H), 3.50 (q, J = 5.0 Hz, 2H), 2.86 (s, 6H), 2.24 (s, 3H), 1.49 (d, J = 6.9 Hz, 3H). ^{13}C NMR (101 MHz, DMSO-d_6) δ 169.00, 168.27, 155.67, 146.20, 138.85, 136.92, 136.53, 133.52, 133.47, 131.92, 129.16, 128.38, 128.17, 122.48, 114.01, 62.83, 55.92, 54.48, 48.86, 43.27, 39.14, 23.12, 18.81. $C_{29}H_{35}N_7O_3$, HRMS calculated for m/z $[M+H]^+$: 530.2880 (calculated), 530.2886 (found)

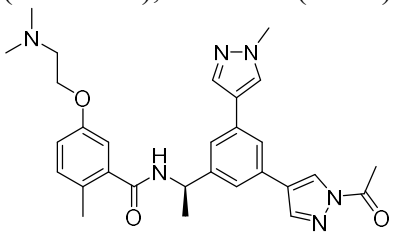

(R)-N-(1-(3-(1-acetyl-1H-pyrazol-4-yl)-5-(1-methyl-1H-pyrazol-4-yl)phenyl)ethyl)-5-(2-(dimethylamino)ethoxy)-2-methylbenzamide (**Jun12336**). White solid, 40% yield for two steps. ^{1}H NMR (400 MHz, DMSO-d_6) δ 8.94 (s, 1H), 8.42 (s, 1H), 8.21 (s, 1H), 8.08 (s, 1H), 7.95 (s, 1H), 7.90 (d, J = 8.2 Hz, 2H), 7.65 (s, 1H), 7.55 (s, 1H), 7.20 (d, J = 8.2 Hz, 1H), 6.98 (d, J = 8.2 Hz, 2H), 5.22-5.14 (m, 1H), 4.32-4.29 (m, 3H), 3.89 (s, 6H), 3.50 (q, J = 5.0 Hz, 3H), 2.86 (d, J = 4.4 Hz, 9H), 2.69 (s, 3H), 2.24 (d, J = 3.3 Hz, 4H), 1.49 (d, J = 4.2 Hz, 3H). ^{13}C NMR (101 MHz, DMSO-d_6) δ 168.31, 158.88, 158.52, 155.69, 146.44, 142.61, 138.87, 138.82, 136.65, 133.79, 131.95, 131.32, 128.54, 128.15, 126.37, 125.01, 122.52, 122.22, 121.70, 117.62, 114.02, 62.83, 55.94, 48.88, 43.29, 23.30, 23.18, 21.93, 18.78. $C_{29}H_{34}N_6O_3$, HRMS calculated for m/z $[M+H]^+$: 515.2770 (calculated), 515.2778 (found)

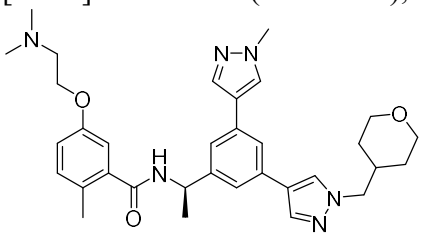

(R)-5-(2-(dimethylamino)ethoxy)-2-methyl-N-(1-(3-(1-methyl-1H-pyrazol-4-yl)-5-(1-((tetrahydro-2H-pyran-4-yl)methyl)-1H-pyrazol-4-yl)phenyl)ethyl)benzamide (**Jun12467**).

White solid, 60% yield for two steps. ^{1}H NMR (400 MHz, DMSO-d_6) δ 8.71 (d, J = 8.2 Hz, 1H), 8.18 (d, J = 13.1 Hz, 2H), 7.91 (d, J = 11.3 Hz, 2H), 7.68 (d, J = 1.9 Hz, 1H), 7.44 (s, 2H), 7.19 (d, J = 8.2 Hz, 1H), 6.97 (d, J = 8.1 Hz, 2H), 5.19-5.12 (m, 1H), 4.31 (t, J = 4.9 Hz, 2H), 4.04 (d, J = 7.0 Hz, 2H), 3.88 (s, 3H), 3.84 (dd, J = 11.2, 4.0 Hz, 2H), 3.51 (q, J = 4.8 Hz, 2H), 3.27 (t, J = 11.5 Hz, 2H), 2.87 (s, 6H), 2.24 (s, 3H), 1.49 (d, J = 7.0 Hz, 3H), 1.43 (dd, J = 12.9, 3.7 Hz, 2H), 1.26 (qd, J = 12.2, 4.5 Hz, 2H). ^{13}C NMR (101 MHz, DMSO-d_6) δ 1 168.28, 159.01, 158.65, 155.68, 146.19, 138.84, 136.63, 136.51, 133.51, 131.92, 128.33, 128.15, 128.12, 122.49, 122.12, 121.02, 120.94, 120.53, 115.85, 114.05, 67.00, 62.85, 57.41, 55.90, 48.92, 43.25, 39.13, 36.19, 30.47, 23.09, 18.80. $C_{33}H_{42}N_6O_3$, HRMS calculated for m/z $[M+H]^+$: 571.3397(calculated), 571.3405(found)

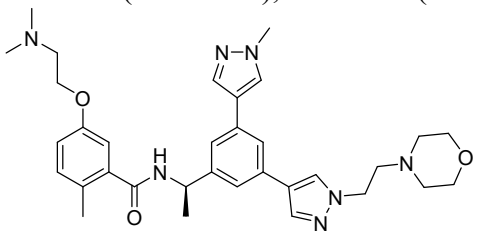

(R)-5-(2-(dimethylamino)ethoxy)-2-methyl-N-(1-(3-(1-methyl-1H-pyrazol-4-yl)-5-(1-(2-morpholinoethyl)-1H-pyrazol-4-yl)phenyl)ethyl)benzamide (**Jun12351**). White solid, 82% yield for two steps. ^{1}H NMR (400 MHz, DMSO-d_6) δ 8.70 (d, J = 8.2 Hz, 1H), 8.30 (s, 1H), 8.13 (s, 1H), 8.04 (s, 1H), 7.87 (s, 1H), 7.68 (d, J = 1.7 Hz, 1H), 7.45 (d, J = 11.8 Hz, 2H), 7.19 (d, J = 8.3 Hz, 1H), 6.98 (dd, J = 11.7, 3.5 Hz, 2H), 5.19-5.11 (m, J = 7.1 Hz, 1H), 4.58 (t, J = 6.5 Hz, 2H), 4.30 (t, J = 5.0 Hz, 2H), 3.89 (s, 4H), 3.65 (s, 2H), 3.50 (d, J = 5.0 Hz, 2H), 2.85 (s, 6H), 2.22 (s, 3H), 1.48 (d, J = 7.0 Hz, 3H).. ^{13}C NMR (101 MHz, DMSO-d_6) δ 168.31, 155.69, 146.33, 138.79, 137.60, 136.49, 133.61, 133.04, 131.93, 128.41, 128.32, 128.14, 122.97, 122.44, 121.25, 121.12, 120.60, 115.85, 114.06, 63.79, 62.87, 55.88, 55.44, 51.92, 48.93, 46.19, 43.25, 39.16, 23.07, 18.81. $C_{33}H_{43}N_7O_3$, MS calculated for m/z $[M+H]^+$: 586.3506 (calculated), 586.3512 (found).

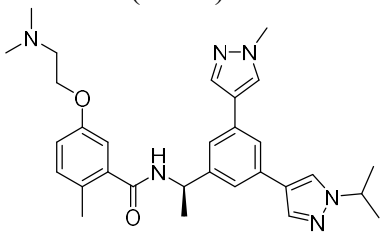

(R)-5-(2-(dimethylamino)ethoxy)-N-(1-(3-(1-isopropyl-1H-pyrazol-4-yl)-5-(1-methyl-1H-pyrazol-4-yl)phenyl)ethyl)-2-methylbenzamide (**Jun12199**). White solid, 77% yield for two steps. ^{1}H NMR (400 MHz, DMSO-d_6) δ 8.69 (d, J = 8.3 Hz, 1H), 8.25 (s, 1H), 8.16 (s, 1H), 7.89 (s, 2H), 7.68 (s, 1H), 7.44 (d, J = 9.3 Hz, 2H), 7.20 (d, J = 8.2 Hz, 1H), 6.97 (d, J = 8.6 Hz, 2H), 5.20-5.12 (m, 1H), 4.55-4.49 (m 1H), 4.31 (t, J = 5.0 Hz, 2H), 3.89 (s, 3H), 3.51 (q, J = 4.6 Hz, 2H), 2.86 (s, 6H), 2.24 (s, 3H), 1.48 (t, J = 7.2 Hz, 9H). ^{13}C NMR (101 MHz, DMSO-d_6) δ 168.27, 155.69, 146.11, 138.88, 136.52, 136.00, 133.72, 133.48, 131.92, 128.31, 128.17, 125.13, 122.54, 121.99, 121.00, 120.87, 120.53, 115.87, 114.09, 62.87, 55.94, 53.61, 48.92, 43.29, 39.13, 23.16, 23.12, 18.80. $C_{30}H_{38}N_6O_2$, HRMS calculated for m/z $[M+H]^+$: 515.3134(calculated), 515.3144(found)

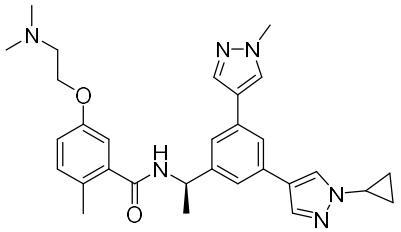

(R)-N-(1-(3-(1-cyclopropyl-1H-pyrazol-4-yl)-5-(1-methyl-1H-pyrazol-4-yl)phenyl)ethyl)-5-(2-(dimethylamino)ethoxy)-2-methylbenzamide (**Jun12197**). White solid, 73% yield for two steps. ^{1}H NMR (400 MHz, DMSO-d_6) δ 8.68 (d, J = 8.3 Hz, 1H), 8.26 (s, 1H), 8.15 (s, 1H), 7.88 (d, J = 3.6 Hz, 2H), 7.68 (s, 1H), 7.43 (d, J = 6.2 Hz, 2H), 7.20 (d, J = 8.3 Hz, 1H), 6.97 (d, J = 11.6 Hz, 2H), 5.19-5.11 (m, 1H), 4.31 (t, J = 4.9 Hz, 2H), 3.88 (s, 3H), 3.75 (tt, J = 7.4, 3.9 Hz, 1H), 3.50 (q, J = 5.0 Hz, 2H), 2.86 (s, 6H), 2.24 (s, 3H), 1.48 (d, J = 7.1 Hz, 3H), 1.08 (q, J = 4.3 Hz, 2H), 1.00 (q, J = 7.3, 6.0 Hz, 2H). ^{13}C NMR (101 MHz, DMSO-d_6) δ 168.26, 155.68, 146.12, 138.88, 136.53, 133.50, 133.40, 131.92, 128.32, 128.17, 127.44, 122.50, 122.22, 121.00, 120.58, 115.88, 114.09, 62.86, 55.96, 48.89, 43.31, 39.14, 33.24, 23.13, 18.80, 6.73, 6.71. $C_{30}H_{36}N_6O_2$, HRMS calculated for m/z $[M+H]^+$: 513.2978(calculated), 513.2983 (found)

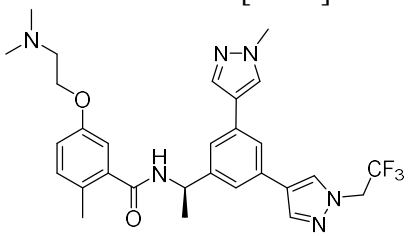

(R)-5-(2-(dimethylamino)ethoxy)-2-methyl-N-(1-(3-(1-methyl-1H-pyrazol-4-yl)-5-(1-(2,2,2-trifluoroethyl)-1H-pyrazol-4-yl)phenyl)ethyl)benzamide (**Jun12603**). White solid, 69% yield for two steps. ^{1}H NMR (400 MHz, DMSO-d_6) δ 8.72 (d, J = 8.3 Hz, 1H), 8.32 (s, 1H), 8.19 (s, 1H), 8.09 (s, 1H), 7.92 (s, 1H), 7.72 (s, 1H), 7.48 (s, 2H), 7.19 (d, J = 8.1 Hz, 1H), 6.98 (d, J = 7.4 Hz, 2H), 5.18 (m, 3H), 4.31 (t, J = 4.9 Hz, 2H), 3.89 (s, 3H), 3.51 (q, J = 4.8 Hz, 2H), 2.87 (s, 6H), 2.24 (s, 3H), 1.50 (d, J = 6.9 Hz, 3H). ^{13}C NMR (101 MHz, DMSO-d_6) δ 168.31, 155.69, 146.33, 138.82, 138.51, 136.57, 133.65, 132.69, 131.92, 129.39, 128.43, 128.15, 123.64, 122.39, 121.51, 121.23, 120.78, 115.87, 114.04, 62.85, 55.90, 48.89, 43.25, 39.13, 23.07, 18.78. $C_{29}H_{33}F_3N_6O_2$, MS calculated for m/z $[M+H]^+$: 555.2695 (calculated), 555.2700 (found).

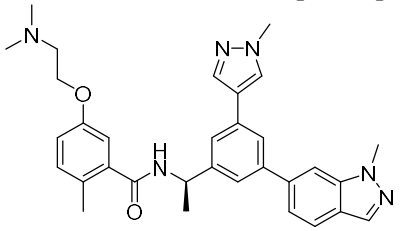

(R)-5-(2-(dimethylamino)ethoxy)-2-methyl-N-(1-(3-(1-methyl-1H-indazol-6-yl)-5-(1-methyl-1H-pyrazol-4-yl)phenyl)ethyl)benzamide (**Jun12446**). White solid, 72% yield for two steps. ^{1}H NMR (400 MHz, DMSO-d_6) δ 8.79 (d, J = 8.2 Hz, 1H), 8.25 (s, 1H), 8.08 (s, 1H), 7.96 (d, J = 3.5 Hz, 2H), 7.86-7.84 (m, 2H), 7.64 (d, J = 7.6 Hz, 2H), 7.52 (d, J = 8.5 Hz, 1H), 7.20 (d, J = 8.3 Hz, 1H), 6.98 (d, J = 7.0 Hz, 2H), 5.28-5.21 (m, 1H), 4.30 (t, J = 5.0 Hz, 2H), 4.13 (s, 3H), 3.90 (s, 3H), 3.50 (q, J = 4.5 Hz, 2H), 2.85 (s, 6H), 2.25 (s, 3H), 1.54 (d, J = 7.0 Hz, 3H), 1.16 (t, J = 7.3 Hz, 3H). ^{13}C NMR (101 MHz, DMSO-d_6) δ 168.33, 155.69, 146.39, 141.61, 140.73, 138.84, 136.69, 133.71, 132.71, 131.94, 128.57, 128.15, 123.30, 123.22, 122.78, 122.55, 122.42, 121.54, 120.60, 115.88, 114.07, 107.88, 62.84, 55.91, 49.00, 43.27, 41.81, 39.17, 35.89, 23.23,

18.85, 11.46. $C_{32}H_{36}N_6O_2$, MS calculated for m/z $[M+H]^+$: 537.2978 (calculated), 537.2985 (found).

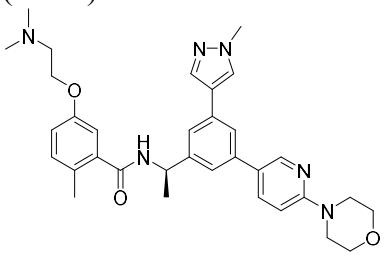

(R)-5-(2-(dimethylamino)ethoxy)-2-methyl-N-(1-(3-(1-methyl-1H-pyrazol-4-yl)-5-(6-morpholinopyridin-3-yl)phenyl)ethyl)benzamide (**Jun12278**). White solid, 81% yield for two steps. ^{1}H NMR (400 MHz, DMSO-d_6) δ 8.74 (d, J = 8.3 Hz, 1H), 8.51 (s, 1H), 8.22 (s, 1H), 8.08 (d, J = 9.0 Hz, 1H), 7.94 (s, 1H), 7.73 (d, J = 1.7 Hz, 1H), 7.57 (s, 1H), 7.52 (s, 1H), 7.20 (d, J = 8.1 Hz, 1H), 7.11 (d, J = 9.1 Hz, 1H), 6.98 (d, J = 8.4 Hz, 2H), 5.25-5.17 (m, 1H), 4.31 (t, J = 5.0 Hz, 2H), 3.89 (s, 3H), 3.75 (t, J = 4.8 Hz, 4H), 3.57 (t, J = 4.9 Hz, 4H), 3.51 (s, 2H), 2.86 (s, 6H), 2.24 (s, 3H), 1.50 (d, J = 6.9 Hz, 3H). ^{13}C NMR (101 MHz, DMSO-d_6) δ 168.32, 158.98, 158.62, 155.69, 146.52, 138.82, 137.75, 136.67, 133.82, 131.93, 128.55, 128.15, 125.83, 122.37, 122.12, 121.66, 121.31, 117.75, 115.89, 114.07, 66.24, 62.87, 55.93, 48.96, 45.84, 43.28, 39.15, 23.23, 18.81. $C_{33}H_{40}N_6O_3$, HRMS calculated for m/z $[M+H]^+$: 569.3240 (calculated), 569.3248(found)

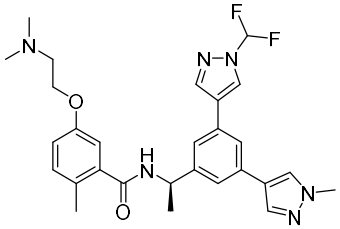

(R)-N-(1-(3-(1-(difluoromethyl)-1H-pyrazol-4-yl)-5-(1-methyl-1H-pyrazol-4-yl)phenyl)ethyl)-5-(2-(dimethylamino)ethoxy)-2-methylbenzamide (**Jun12162**). White solid, 77% yield for two steps. ^{1}H NMR (400 MHz, DMSO-d_6) δ 8.75 (s, 1H), 8.69 (d, J = 8.0 Hz, 1H), 8.31 (s, 1H), 8.18 (s, 1H), 7.92 (s, 1H), 7.85-7.81 (m, 1H), 7.55 (d, J = 13.8 Hz, 2H), 7.19 (d, J = 8.3 Hz, 1H), 6.97 (d, J = 7.0 Hz, 2H), 5.21-5.14 (m, 1H), 4.31 (t, J = 4.9 Hz, 2H), 3.89 (s, 3H), 3.50 (s, 2H), 2.86 (s, 6H), 2.23 (s, 3H), 1.49 (d, J = 7.1 Hz, 3H). ^{13}C NMR (101 MHz, DMSO-d_6) δ 168.31, 158.82, 158.49, 155.69, 146.37, 140.44, 138.80, 136.59, 133.74, 131.93, 131.75, 128.44, 128.16, 125.66, 125.10, 122.29, 122.03, 121.64, 121.20, 115.90, 114.06, 111.13, 62.86, 55.92, 48.90, 43.27, 39.17, 23.13, 18.79. $C_{28}H_{32}F_2N_6O_2$, HRMS calculated for m/z $[M+H]^+$: 523.2633(calculated), 523.2639(found)

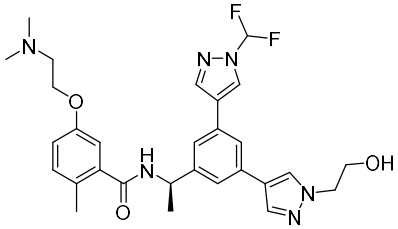

(R)-N-(1-(3-(1-(difluoromethyl)-1H-pyrazol-4-yl)-5-(1-(2-hydroxyethyl)-1H-pyrazol-4-yl)phenyl)ethyl)-5-(2-(dimethylamino)ethoxy)-2-methylbenzamide (**Jun12208**). White solid, 73% yield for two steps. ^{1}H NMR (400 MHz, DMSO-d_6) δ 8.77 (s, 1H), 8.71 (d, J = 8.6 Hz, 1H), 8.32 (s, 1H), 8.20 (s, 1H), 7.95 (s, 1H), 7.86 (d, J = 11.2 Hz, 2H), 7.56 (d, J = 5.6 Hz, 2H), 7.20 (d, J = 8.1 Hz, 1H), 6.98 (d, J = 7.0 Hz, 2H), 5.22-5.15 (m, 2H), 4.31 (t, J = 4.9 Hz, 2H), 4.18 (t,

J = 5.5 Hz, 2H), 3.78 (t, J = 5.5 Hz, 2H), 3.50 (q, J = 4.8 Hz, 2H), 2.86 (s, 6H), 2.24 (s, 3H), 1.50 (d, J = 7.0 Hz, 3H). ^{13}C NMR (101 MHz, DMSO-d_6) δ 168.30, 155.69, 146.36, 140.45, 138.82, 136.60, 133.85, 131.93, 131.73, 128.24, 128.15, 125.67, 125.11, 121.96, 121.90, 121.60, 121.13, 115.91, 114.04, 62.85, 60.49, 55.91, 54.85, 48.90, 43.26, 23.17, 18.80. $C_{29}H_{34}F_2N_6O_3$, HRMS calculated for m/z $[M+H]^+$: 553.2739(calculated), 553.2745(found)

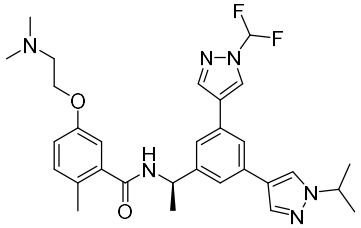

(R)-N-(1-(3-(1-(difluoromethyl)-1H-pyrazol-4-yl)-5-(1-isopropyl-1H-pyrazol-4-yl)phenyl)ethyl)-5-(2-(dimethylamino)ethoxy)-2-methylbenzamide (**Jun12235**). White solid, 78% yield for two steps. ^{1}H NMR (400 MHz, DMSO-d_6) δ 8.75 (s, 1H), 8.70 (d, J = 8.5 Hz, 1H), 8.30 (d, J = 13.1 Hz, 2H), 7.93 (s, 1H), 7.84 (s, 1H), 7.56 (s, 2H), 7.20 (d, J = 8.2 Hz, 1H), 6.98 (d, J = 6.9 Hz, 2H), 5.22-5.15 (m, 1H), 4.56-4.51 (m, 1H), 4.31 (t, J = 4.9 Hz, 2H), 3.50 (q, J = 4.9 Hz, 2H), 2.86 (s, 6H), 2.24 (s, 3H), 1.50 (d, J = 7.1 Hz, 3H), 1.47 (d, J = 6.8 Hz, 6H). ^{13}C NMR (101 MHz, DMSO-d_6) δ 168.30, 155.69, 146.31, 140.44, 138.82, 136.08, 133.93, 131.93, 131.70, 128.15, 125.62, 125.24, 125.14, 122.06, 121.77, 121.54, 121.16, 117.80, 115.88, 114.89, 114.06, 111.14, 62.84, 55.92, 53.65, 48.92, 43.26, 23.16, 18.79. $C_{30}H_{36}F_2N_6O_2$, HRMS calculated for m/z $[M+H]^+$: 551.2946(calculated), 551.2950(found)

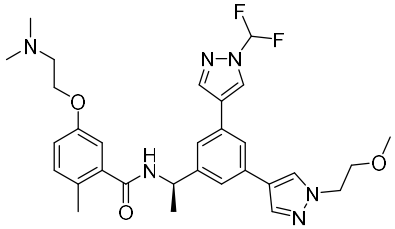

(R)-N-(1-(3-(1-(difluoromethyl)-1H-pyrazol-4-yl)-5-(1-(2-methoxyethyl)-1H-pyrazol-4-yl)phenyl)ethyl)-5-(2-(dimethylamino)ethoxy)-2-methylbenzamide (**Jun12281**). White solid, 81% yield for two steps. ^{1}H NMR (400 MHz, DMSO-d_6) δ 8.85 (s, 1H), 8.79 (d, *J* = 7.8 Hz, 1H), 8.40 (s, 1H), 8.28 (s, 1H), 8.04 (s, 1H), 7.92 (s, 1H), 7.64 (d, *J* = 10.2 Hz, 2H), 7.27 (d, *J* = 8.2 Hz, 1H), 7.05 (d, *J* = 7.2 Hz, 2H), 5.29-5.23 (m, 1H), 4.72 (s, 4H), 4.38 (q, *J* = 5.0 Hz, 3H), 3.80 (t, *J* = 5.2 Hz, 2H), 3.59 (t, *J* = 4.8 Hz, 2H), 2.94 (s, 6H), 2.32 (s, 3H), 1.58 (d, *J* = 7.1 Hz, 3H). ^{13}C NMR (101 MHz, DMSO-d_6) δ 168.32, 155.70, 146.40, 140.46, 138.80, 136.76, 133.74, 131.92, 131.75, 128.25, 128.15, 125.69, 125.11, 122.06, 121.66, 121.16, 115.89, 114.05, 70.96, 62.86, 58.47, 55.87, 51.90, 48.92, 43.23, 23.16, 18.79. $C_{30}H_{36}F_2N_6O_3$, HRMS calculated for m/z $[M+H]^+$: 567.2895(calculated), 567.2901(found)

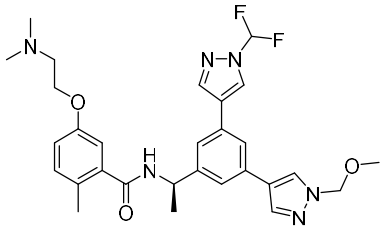

(R)-N-(1-(3-(1-(difluoromethyl)-1H-pyrazol-4-yl)-5-(1-(methoxymethyl)-1H-pyrazol-4-yl)phenyl)ethyl)-5-(2-(dimethylamino)ethoxy)-2-methylbenzamide (**Jun12303**). White solid, 65% yield for two steps. ^{1}H NMR (400 MHz, DMSO-d_6) δ 8.70 (s, 1H), 8.63 (d, J = 8.0 Hz, 1H),

8.34 (s, 1H), 8.25 (s, 1H), 8.00 (s, 1H), 7.82 (d, J = 8.8 Hz, 2H), 7.53 (s, 2H), 7.12 (d, J = 8.8 Hz, 1H), 6.91 (d, J = 4.9 Hz, 2H), 5.35 (s, 2H), 5.12 (m, 1H), 4.24 (t, J = 4.9 Hz, 2H), 3.43 (d, J = 4.8 Hz, 2H), 3.21 (s, 3H), 2.79 (s, 6H), 2.16 (s, 3H), 1.43 (d, J = 6.9 Hz, 3H). ^{13}C NMR (101 MHz, DMSO-d_6) δ 168.32, 155.69, 146.43, 140.44, 138.79, 137.87, 133.31, 131.93, 131.82, 128.49, 128.15, 125.69, 125.05, 123.19, 122.27, 121.98, 121.42, 118.35, 115.91, 114.05, 111.14, 81.88, 62.85, 56.61, 55.91, 48.92, 43.26, 23.16, 18.79. $C_{29}H_{34}F_2N_6O_3$, MS calculated for m/z $[M+H]^+$: 553.2739 (calculated), 553.2745 (found).

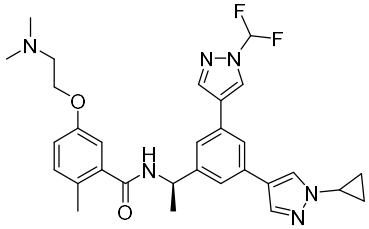

(R)-N-(1-(3-(1-cyclopropyl-1H-pyrazol-4-yl)-5-(1-(difluoromethyl)-1H-pyrazol-4-yl)phenyl)ethyl)-5-(2-(dimethylamino)ethoxy)-2-methylbenzamide (**Jun12284**). White solid, 75% yield for two steps. ^{1}H NMR (400 MHz, $CDCl_3$) δ 8.17 (s, 1H), 8.01 (d, J = 2.9 Hz, 2H), 7.84 (s, 1H), 7.53 (s, 2H), 7.50 (s, 1H), 7.14 (d, J = 8.4 Hz, 1H), 7.06 (s, 1H), 6.89-6.81 (m, 2H), 5.38-5.31 (m, 1H), 4.69-4.63 (m, 1H), 4.40 (s, 2H), 3.47 (s, 2H), 2.96 (s, 6H), 2.36 (s, 3H), 1.68 (d, J = 7.0 Hz, 3H), 1.60 (d, J = 6.7 Hz, 4H). ^{13}C NMR (101 MHz, DMSO-d_6) δ 168.33, 155.69, 146.37, 140.43, 138.77, 136.61, 133.61, 131.93, 131.72, 128.15, 127.59, 125.63, 125.11, 122.07, 122.00, 121.64, 121.20, 115.89, 114.05, 62.84, 55.89, 48.93, 43.24, 33.24, 23.17, 18.78, 6.74, 6.72. $C_{30}H_{34}F_2N_6O_2$, HRMS calculated for m/z $[M+H]^+$: 549.2789(calculated), 549.2794(found)

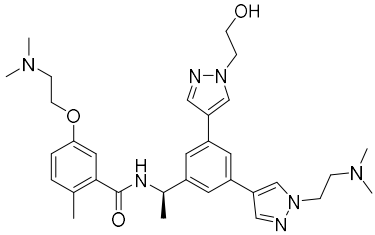

(R)-5-(2-(dimethylamino)ethoxy)-N-(1-(3-(1-(2-(dimethylamino)ethyl)-1H-pyrazol-4-yl)-5-(1-(2-hydroxyethyl)-1H-pyrazol-4-yl)phenyl)ethyl)-2-methylbenzamide (**Jun12165**). White solid, 66% yield for two steps. ^{1}H NMR (400 MHz, DMSO-d_6) δ 8.73 (d, J = 8.2 Hz, 1H), 8.33 (s, 1H), 8.16 (s, 1H), 8.06 (s, 1H), 7.91 (s, 1H), 7.70 (s, 1H), 7.46 (d, J = 17.9 Hz, 2H), 7.19 (d, J = 8.1 Hz, 1H), 6.97 (d, J = 8.4 Hz, 2H), 5.19-5.12 (m, 1H), 4.58 (t, J = 6.2 Hz, 2H), 4.31 (t, J = 4.9 Hz, 2H), 4.18 (t, J = 5.5 Hz, 2H), 3.78 (t, J = 5.5 Hz, 2H), 3.63 (t, J = 6.3 Hz, 2H), 3.51 (t, J = 5.1 Hz, 2H), 2.85 (d, J = 11.1 Hz, 12H), 2.23 (s, 3H), 1.49 (d, J = 6.9 Hz, 3H). ^{13}C NMR (101 MHz, DMSO-d_6) δ 168.30, 158.94, 158.61, 155.69, 146.34, 138.81, 137.62, 136.49, 133.73, 133.02, 131.92, 128.49, 128.14, 128.10, 122.99, 122.05, 121.23, 121.08, 120.53, 118.54, 115.87, 115.59, 114.04, 62.87, 60.49, 56.11, 55.89, 54.82, 48.93, 46.63, 43.25, 43.14, 23.10, 18.81. $C_{32}H_{43}N_7O_3$, HRMS calculated for m/z $[M+H]^+$: 574.3506(calculated), 574.3511(found)

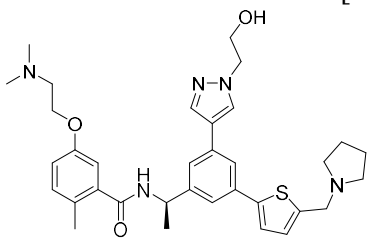

(R)-5-(2-(dimethylamino)ethoxy)-N-(1-(3-(1-(2-hydroxyethyl)-1H-pyrazol-4-yl)-5-(5-(pyrrolidin-1-ylmethyl)thiophen-2-yl)phenyl)ethyl)-2-methylbenzamide (**Jun12168**). White solid, 60% yield for two steps. ^{1}H NMR (400 MHz, DMSO-d_6) δ 10.03 (s, 1H), 8.80 (d, J = 8.1 Hz, 1H), 8.23 (s, 1H), 7.95 (s, 1H), 7.75 (s, 1H), 7.61 (s, 1H), 7.59 (d, J = 3.6 Hz, 1H), 7.48 (s, 1H), 7.35 (d, J = 3.7 Hz, 1H), 7.19 (d, J = 8.1 Hz, 1H), 6.98 (d, J = 7.6 Hz, 2H), 5.21-5.14 (m, 1H), 4.63 (s, 2H), 4.32 (t, J = 4.9 Hz, 2H), 4.19 (t, J = 5.5 Hz, 2H), 3.78 (t, J = 5.5 Hz, 2H), 3.51 (t, J = 5.5 Hz, 3H), 3.46 (s, 1H), 2.86 (s, 6H), 2.23 (s, 3H), 2.03 (d, J = 9.9 Hz, 2H), 1.91-1.88 (m, 2H), 1.50 (d, J = 7.1 Hz, 3H). ^{13}C NMR (101 MHz, DMSO-d_6) δ 168.38, 155.70, 146.88, 146.43, 138.73, 136.61, 134.14, 132.98, 131.94, 128.40, 128.14, 124.57, 123.10, 121.54, 121.50, 115.92, 114.04, 62.88, 60.46, 55.88, 54.83, 53.14, 51.34, 48.82, 43.25, 23.07, 18.84. $C_{34}H_{43}N_5O_3S$, HRMS calculated for m/z $[M+H]^+$: 602.3165(calculated), 602.3171 (found)

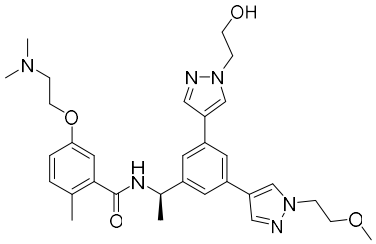

(R)-5-(2-(dimethylamino)ethoxy)-N-(1-(3-(1-(2-hydroxyethyl)-1H-pyrazol-4-yl)-5-(1-(2-methoxyethyl)-1H-pyrazol-4-yl)phenyl)ethyl)-2-methylbenzamide (**Jun12163**). White solid, 76% yield for two steps. ^{1}H NMR (400 MHz, DMSO-d_6) δ 9.83 (s, 1H), 8.72 (d, J = 8.3 Hz, 1H), 8.19 (s, 2H), 7.93 (d, J = 2.4 Hz, 2H), 7.69 (s, 1H), 7.44 (d, J = 3.4 Hz, 2H), 7.19 (d, J = 8.3 Hz, 1H), 6.98 (d, J = 11.1 Hz, 2H), 5.20-5.12 (m, 1H), 4.30 (q, J = 5.8 Hz, 4H), 4.18 (t, J = 5.4 Hz, 2H), 3.78 (t, J = 5.5 Hz, 2H), 3.73 (t, J = 5.2 Hz, 2H), 3.50 (d, J = 5.0 Hz, 2H), 3.25 (s, 3H), 2.86 (s, 6H), 2.24 (s, 3H), 1.49 (d, J = 7.0 Hz, 3H). ^{13}C NMR (101 MHz, DMSO-d_6) δ 168.27, 158.86, 158.52, 155.68, 146.17, 138.87, 136.68, 136.54, 133.62, 133.49, 131.92, 128.14, 122.27, 122.11, 120.93, 120.44, 115.88, 114.04, 70.96, 62.85, 60.50, 58.47, 55.92, 54.80, 51.84, 48.90, 43.27, 23.15, 18.81. $C_{31}H_{40}N_6O_4$, HRMS calculated for m/z $[M+H]^+$: 561.3189(calculated), 561.3195 (found)

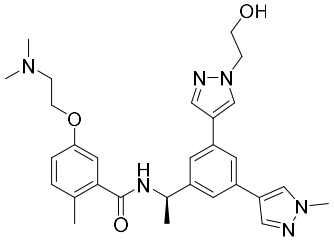

(R)-5-(2-(dimethylamino)ethoxy)-N-(1-(3-(1-(2-hydroxyethyl)-1H-pyrazol-4-yl)-5-(1-methyl-1H-pyrazol-4-yl)phenyl)ethyl)-2-methylbenzamide (**Jun12164**). White solid, 74% yield for two steps. ^{1}H NMR (400 MHz, DMSO-d_6) δ 9.82 (s, 1H), 8.71 (d, J = 8.3 Hz, 1H), 8.17 (s, 2H), 7.91 (d, J = 7.1 Hz, 2H), 7.68 (s, 1H), 7.44 (d, J = 6.7 Hz, 2H), 7.19 (d, J = 8.2 Hz, 1H), 6.99-6.96 (m, 2H), 5.19-5.12 (m, 1H), 4.31 (t, J = 4.9 Hz, 2H), 4.18 (t, J = 5.5 Hz, 2H), 3.88 (s, 3H), 3.78 (t, J = 5.5 Hz, 2H), 3.50 (d, J = 4.9 Hz, 2H), 2.86 (s, 6H), 2.24 (s, 3H), 1.48 (d, J = 7.0 Hz, 3H). ^{13}C NMR (101 MHz, DMSO-d_6) δ 168.27, 158.83, 158.49, 155.68, 146.17, 138.86, 136.52, 133.62, 133.50, 131.92, 128.35, 128.16, 128.11, 122.50, 122.11, 120.92, 120.47, 115.88, 114.04, 62.85, 60.50, 55.92, 54.80, 48.89, 43.27, 39.14, 23.13, 18.81. $C_{29}H_{36}N_6O_3$, HRMS calculated for m/z $[M+H]^+$: 517.2927(calculated), 517.2933(found)

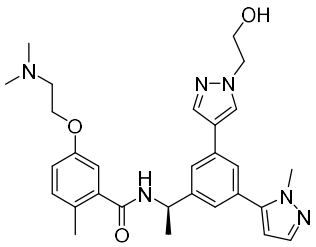

(R)-5-(2-(dimethylamino)ethoxy)-N-(1-(3-(1-(2-hydroxyethyl)-1H-pyrazol-4-yl)-5-(1-methyl-1H-pyrazol-5-yl)phenyl)ethyl)-2-methylbenzamide (**Jun12198**). White solid, 77% yield for two steps. ^{1}H NMR (400 MHz, DMSO-d_6) δ 8.77 (d, J = 8.1 Hz, 1H), 8.24 (s, 1H), 7.96 (s, 1H), 7.67 (s, 1H), 7.61 (s, 1H), 7.50 (s, 1H), 7.36 (s, 1H), 7.19 (d, J = 8.3 Hz, 1H), 6.97 (d, J = 10.8 Hz, 2H), 6.43 (d, J = 2.1 Hz, 1H), 5.25-5.18 (m, 1H), 4.30 (t, J = 4.8 Hz, 2H), 4.17 (t, J = 5.5 Hz, 2H), 3.89 (s, 3H), 3.78 (t, J = 5.5 Hz, 2H), 3.51 (q, J = 4.8 Hz, 2H), 2.86 (s, 6H), 2.23 (s, 3H), 1.50 (d, J = 7.1 Hz, 3H). ^{13}C NMR (101 MHz, DMSO-d_6) δ 168.34, 155.68, 146.36, 143.28, 138.72, 138.34, 136.71, 133.75, 131.95, 131.30, 128.42, 128.19, 124.09, 123.76, 123.31, 121.58, 115.94, 114.05, 106.27, 62.88, 60.46, 55.94, 54.80, 48.80, 43.30, 37.98, 23.05, 18.80. $C_{29}H_{36}N_6O_3$, HRMS calculated for m/z $[M+H]^+$: 517.2927(calculated), 517.2934 (found)

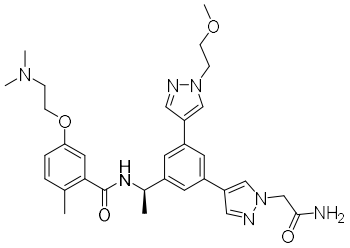

(R)-N-(1-(3-(1-(2-amino-2-oxoethyl)-1H-pyrazol-4-yl)-5-(1-(2-methoxyethyl)-1H-pyrazol-4-yl)phenyl)ethyl)-5-(2-(dimethylamino)ethoxy)-2-methylbenzamide (**Jun12242**). White solid, 58% yield for two steps. ^{1}H NMR (400 MHz, DMSO-d_6) δ 8.72 (d, J = 8.2 Hz, 1H), 8.18 (d, J = 8.1 Hz, 2H), 7.94 (s, 2H), 7.70 (s, 1H), 7.58 (s, 1H), 7.45 (d, J = 6.3 Hz, 2H), 7.31 (s, 1H), 7.19 (d, J = 8.3 Hz, 1H), 6.97 (d, J = 8.4 Hz, 2H), 5.19-5.13 (m, 1H), 4.80 (s, 2H), 4.30 (q, J = 5.4 Hz, 4H), 3.72 (t, J = 5.2 Hz, 2H), 3.50 (q, J = 4.9 Hz, 2H), 3.25 (s, 3H), 2.85 (s, 6H), 2.24 (s, 3H), 1.49 (d, J = 7.0 Hz, 3H). ^{13}C NMR (101 MHz, DMSO-d_6) 169.01, 168.27, 155.67, 146.20, 138.85, 136.94, 136.69, 133.50, 133.47, 131.92, 129.19, 128.16, 122.48, 122.24, 121.07, 120.92, 120.47, 117.94, 115.91, 114.00, 70.95, 62.82, 58.46, 55.91, 54.48, 51.85, 48.88, 43.26, 23.13, 18.81. $C_{31}H_{39}N_7O_4$, HRMS calculated for m/z $[M+H]^+$: 574.3142(calculated), 571.3146(found)

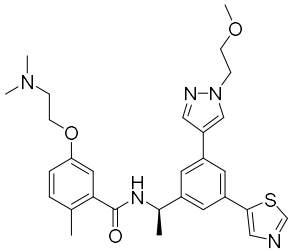

(R)-5-(2-(dimethylamino)ethoxy)-N-(1-(3-(1-(2-methoxyethyl)-1H-pyrazol-4-yl)-5-(thiazol-5-yl)phenyl)ethyl)-2-methylbenzamide (**Jun12147**). White solid, 54% yield for two steps. ^{1}H NMR (400 MHz, DMSO-d_6) δ 9.19 (s, 1H), 8.86 (d, J = 8.1 Hz, 1H), 8.47 (s, 1H), 8.35 (s, 1H), 8.07 (s, 1H), 7.89 (s, 1H), 7.70 (s, 1H), 7.59 (s, 1H), 7.28 (d, J = 8.1 Hz, 1H), 7.05 (s, 1H), 5.30-5.22 (m, 1H), 4.38 (q, J = 5.2 Hz, 4H), 3.90 (s, 3H), 3.81 (t, J = 5.2 Hz, 3H), 3.58 (q, J = 4.6 Hz, 2H), 2.93 (s, 6H), 2.32 (s, 3H), 1.57 (d, J = 7.0 Hz, 3H). ^{13}C NMR (101 MHz, DMSO-d_6) δ

168.36, 155.69, 154.06, 146.97, 140.06, 139.18, 138.77, 136.87, 134.09, 131.95, 131.80, 128.51, 128.15, 123.41, 122.54, 121.71, 121.58, 115.95, 114.02, 70.90, 62.86, 58.46, 55.94, 51.86, 48.77, 43.29, 23.04, 18.81. $C_{29}H_{35}N_5O_3S$, HRMS calculated for m/z $[M+H]^+$: 534.2539(calculated), 534.2545(found)

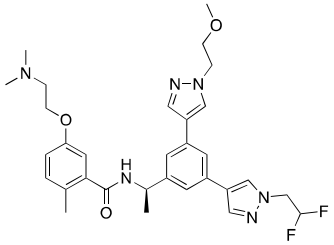

(R)-N-(1-(3-(1-(2,2-difluoroethyl)-1H-pyrazol-4-yl)-5-(1-(2-methoxyethyl)-1H-pyrazol-4-yl)phenyl)ethyl)-5-(2-(dimethylamino)ethoxy)-2-methylbenzamide (**Jun12759**). White solid, 77% yield for two steps. ^{1}H NMR (400 MHz, DMSO-d_6) δ 8.79 (d, J = 8.3 Hz, 1H), 8.34 (s, 1H), 8.27 (s, 1H), 8.11 (s, 1H), 8.01 (s, 1H), 7.79 (s, 1H), 7.54 (s, 2H), 7.27 (d, J = 8.2 Hz, 1H), 7.05 (d, J = 9.4 Hz, 2H), 5.28-5.21 (m, 1H), 4.75 (t, J = 13.4 Hz, 2H), 4.38 (q, J = 5.4 Hz, 4H), 3.94 (s, 3H), 3.81 (t, J = 5.2 Hz, 2H), 3.58 (q, J = 4.6 Hz, 2H), 2.93 (s, 6H), 2.32 (s, 3H), 1.57 (d, J = 7.0 Hz, 3H). ^{13}C NMR (101 MHz, DMSO-d_6) δ 168.30, 158.87, 158.53, 155.68, 146.26, 138.85, 137.81, 136.70, 133.59, 133.02, 131.92, 129.07, 128.18, 128.15, 123.13, 122.18, 121.31, 121.14, 120.64, 115.88, 114.47, 114.04, 70.95, 62.84, 58.46, 55.93, 51.85, 48.90, 43.27, 23.09, 18.79. $C_{31}H_{38}F_2N_6O_3$, HRMS calculated for m/z $[M+H]^+$: 581.3052(calculated), 581.3060(found)

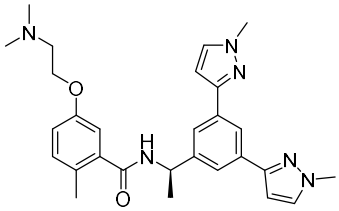

(R)-N-(1-(3,5-bis(1-methyl-1H-pyrazol-3-yl)phenyl)ethyl)-5-(2-(dimethylamino)ethoxy)-2-methylbenzamide (**Jun12379**). White solid, 78% yield. ^{1}H NMR (400 MHz, DMSO-d_6) δ 8.84 (d, J = 8.2 Hz, 1H), 8.06 (s, 1H), 7.76 (s, 4H), 7.19 (d, J = 8.1 Hz, 1H), 6.97 (d, J = 8.1 Hz, 2H), 6.73 (d, J = 1.9 Hz, 2H), 5.22-5.15 (m, 1H), 4.31 (t, J = 5.1 Hz, 2H), 3.90 (s, 6H), 3.88 (s, 1H), 3.51 (s, 2H), 2.86 (s, 6H), 2.24 (s, 3H), 1.50 (d, J = 7.0 Hz, 3H). ^{13}C NMR (101 MHz, DMSO-d_6) δ 168.29, 159.01, 158.66, 155.65, 150.50, 150.46, 146.01, 138.80, 138.76, 134.24, 132.78, 131.91, 128.28, 122.32, 120.54, 115.84, 114.94, 114.09, 103.00, 62.84, 55.89, 48.91, 43.25, 39.11, 39.08, 22.87, 18.83. $C_{28}H_{34}N_6O_2$, HRMS calculated for m/z $[M+H]^+$: 487.2821(calculated), 487.2830 (found)

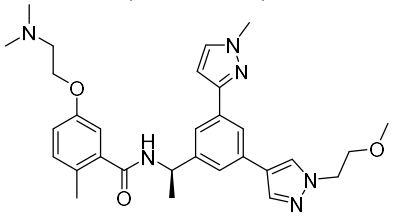

(R)-5-(2-(dimethylamino)ethoxy)-N-(1-(3-(1-(2-methoxyethyl)-1H-pyrazol-4-yl)-5-(1-methyl-1H-pyrazol-3-yl)phenyl)ethyl)-2-methylbenzamide (**Jun12528**). White solid, 68% yield for two steps. ^{1}H NMR (400 MHz, DMSO-d_6) δ 8.80 (d, J = 8.3 Hz, 1H), 8.21 (s, 1H), 7.93 (s, 1H), 7.83 (s, 1H), 7.76 (s, 1H), 7.70 (s, 1H), 7.53 (s, 1H), 7.19 (d, J = 8.1 Hz, 1H), 6.98 (d, J = 7.6 Hz, 2H), 6.76 (s, 1H), 5.21-5.14 (m, 1H), 4.31 (q, J = 5.8 Hz, 4H), 3.90 (s, 3H), 3.73 (t, J = 5.3 Hz, 2H),

3.54-3.47 (m, 2H), 3.25 (s, 3H), 2.86 (s, 6H), 2.24 (s, 3H), 1.50 (d, J = 7.0 Hz, 3H). ^{13}C NMR (101 MHz, DMSO-d_6) δ 168.28, 155.67, 150.52, 146.15, 138.83, 136.61, 134.49, 133.29, 132.72, 131.91, 128.22, 128.17, 122.43, 122.20, 120.90, 120.50, 115.84, 114.07, 103.11, 70.94, 62.85, 58.44, 55.88, 51.78, 48.90, 43.24, 39.10, 22.99, 18.82. $C_{30}H_{38}N_6O_3$, HRMS calculated for m/z $[M+H]^+$: 531.3083(calculated), 531.3087 (found)

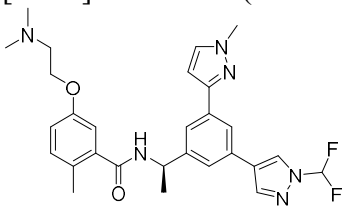

(R)-N-(1-(3-(1-(difluoromethyl)-1H-pyrazol-4-yl)-5-(1-methyl-1H-pyrazol-3-yl)phenyl)ethyl)-5-(2-(dimethylamino)ethoxy)-2-methylbenzamide (**Jun12529**). White solid, 77% yield for two steps. ^{1}H NMR (400 MHz, DMSO-d_6) δ 8.73 (d, J = 5.6 Hz, 2H), 8.25 (s, 1H), 7.88 (s, 1H), 7.79 (s, 1H), 7.74 (s, 1H), 7.70 (s, 1H), 7.59 (s, 1H), 7.12 (d, J = 9.0 Hz, 1H), 6.91 (d, J = 6.2 Hz, 2H), 6.72 (d, J = 2.2 Hz, 1H), 5.16-5.09 (m, 1H), 4.24 (t, J = 5.0 Hz, 2H), 3.83 (s, 3H), 3.44 (q, J = 4.0 Hz, 2H), 2.79 (s, 6H), 2.17 (s, 3H), 1.44 (d, J = 7.0 Hz, 3H).^{13}C NMR (101 MHz, DMSO-d_6) δ 168.33, 155.67, 150.31, 146.36, 140.49, 138.77, 134.70, 132.78, 131.92, 131.57, 128.25, 125.91, 124.97, 123.17, 121.89, 121.26, 115.87, 114.09, 103.26, 62.86, 55.88, 48.90, 43.24, 39.12, 22.98, 18.82. $C_{28}H_{32}F_2N_6O_2$, HRMS calculated for m/z $[M+H]^+$: 523.2633(calculated), 523.2641 (found)

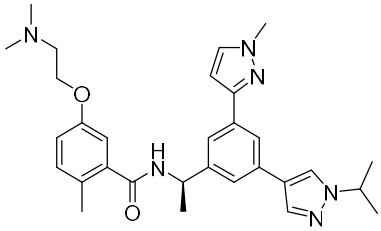

(R)-5-(2-(dimethylamino)ethoxy)-N-(1-(3-(1-isopropyl-1H-pyrazol-4-yl)-5-(1-methyl-1H-pyrazol-3-yl)phenyl)ethyl)-2-methylbenzamide (**Jun12531**). White solid, 76% yield for two steps. ^{1}H NMR (400 MHz, DMSO-d_6) δ 8.72 (d, J = 8.2 Hz, 1H), 8.21 (s, 1H), 7.82 (s, 1H), 7.77 (s, 1H), 7.68 (s, 1H), 7.62 (s, 1H), 7.47 (s, 1H), 7.12 (d, J = 8.2 Hz, 1H), 6.90 (d, J = 7.3 Hz, 2H), 6.68 (d, J = 2.2 Hz, 1H), 5.14-5.06 (m, 1H), 4.49-4.42 (m, 1H), 4.24 (t, J = 5.0 Hz, 2H), 3.82 (s, 3H), 2.79 (s, 6H), 2.17 (s, 3H), 1.42 (d, J = 6.9 Hz, 3H), 1.40 (d, J = 6.7 Hz, 6H). ^{13}C NMR (101 MHz, DMSO-d_6) δ 168.28, 155.67, 150.57, 146.09, 138.82, 135.95, 134.46, 133.50, 132.70, 131.91, 128.23, 125.23, 122.46, 121.94, 120.79, 120.52, 115.84, 114.09, 103.11, 62.86, 55.88, 53.62, 48.93, 43.24, 39.10, 23.15, 23.00, 18.83. $C_{30}H_{38}N_6O_2$, HRMS calculated for m/z $[M+H]^+$: 515.3134(calculated), 515.3141 (found)

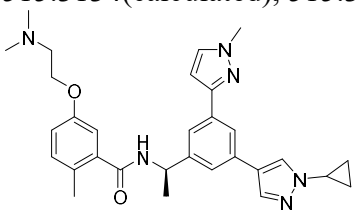

(R)-N-(1-(3-(1-cyclopropyl-1H-pyrazol-4-yl)-5-(1-methyl-1H-pyrazol-3-yl)phenyl)ethyl)-5-(2-(dimethylamino)ethoxy)-2-methylbenzamide (**Jun12584**). White solid, 74% yield for two steps. ^{1}H NMR (400 MHz, DMSO-d_6) δ 8.78 (d, J = 8.2 Hz, 1H), 8.30 (s, 1H), 7.89 (s, 1H), 7.83 (s, 1H), 7.75 (s, 1H), 7.70 (s, 1H), 7.54 (s, 1H), 7.19 (d, J = 8.1 Hz, 1H), 6.98 (d, J = 7.8 Hz, 2H),

6.75 (s, 1H), 5.21-5.13 (m, 1H), 4.31 (t, J = 5.0 Hz, 2H), 3.89 (s, 3H), 3.76 (tt, J = 7.6, 3.9 Hz, 1H), 3.51 (q, J = 4.7 Hz, 2H), 2.87 (s, 6H), 2.24 (s, 3H), 1.49 (d, J = 7.0 Hz, 3H), 1.12-1.08 (m, 2H), 1.00 (q, J = 7.2 Hz, 2H). ^{13}C NMR (101 MHz, DMSO-d_6) δ 168.29, 155.66, 150.53, 146.10, 138.82, 136.50, 134.48, 133.19, 132.70, 131.91, 128.24, 127.47, 122.50, 122.16, 120.88, 120.60, 115.84, 114.09, 103.13, 62.85, 55.90, 48.91, 43.25, 39.09, 33.27, 23.00, 18.82, 6.73, 6.71, 6.63. $C_{30}H_{36}N_6O_2$, HRMS calculated for m/z $[M+H]^+$: 513.2978(calculated), 513.2984(found)

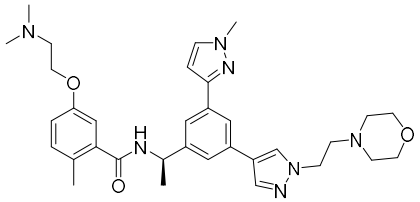

(R)-5-(2-(dimethylamino)ethoxy)-2-methyl-N-(1-(3-(1-methyl-1H-pyrazol-3-yl)-5-(1-(2-morpholinoethyl)-1H-pyrazol-4-yl)phenyl)ethyl)benzamide (**Jun12602**). White solid, 81% yield for two steps. ^{1}H NMR (400 MHz, $CDCl_3$) δ 8.01 (s, 1H), 7.89 (s, 2H), 7.76 (s, 1H), 7.49 (s, 1H), 7.44 (d, J = 6.7 Hz, 2H), 7.13 (d, J = 8.3 Hz, 1H), 7.03 (d, J = 2.7 Hz, 1H), 6.85 – 6.80 (m, 2H), 5.34-5.27 (m , 1H), 4.75 (t, J = 5.9 Hz, 2H), 4.39 (d, J = 9.2 Hz, 2H), 4.00 (s, 3H), 3.95 (t, J = 4.9 Hz, 5H), 3.69 (t, J = 5.6 Hz, 3H), 3.48 (q, J = 8.7, 7.3 Hz, 2H), 3.12 (s, 3H), 2.95 (s, 6H), 2.37 (s, 3H), 1.65 (d, J = 7.0 Hz, 3H). ^{13}C NMR (101 MHz, DMSO-d_6) δ 168.32, 159.14, 158.81, 155.67, 150.44, 146.30, 138.77, 137.52, 134.57, 132.83, 132.77, 131.92, 128.47, 128.22, 122.94, 122.65, 121.06, 120.56, 118.31, 115.83, 115.38, 114.08, 103.04, 63.74, 62.88, 55.85, 55.40, 51.87, 48.94, 46.15, 43.22, 39.10, 22.96, 18.82. $C_{33}H_{43}N_7O_3$, MS calculated for m/z $[M+H]^+$: 586.3506 (calculated), 586.3510 (found).

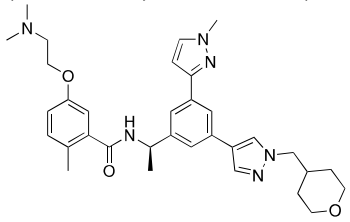

(R)-5-(2-(dimethylamino)ethoxy)-2-methyl-N-(1-(3-(1-methyl-1H-pyrazol-3-yl)-5-(1-((tetrahydro-2H-pyran-4-yl)methyl)-1H-pyrazol-4-yl)phenyl)ethyl)benzamide (**Jun12703**). White solid, 70% yield for two steps. ^{1}H NMR (400 MHz, DMSO-d_6) δ 8.74 (d, J = 8.2 Hz, 1H), 8.31 (s, 1H), 8.25 (s, 1H), 7.96 (d, J = 12.5 Hz, 1H), 7.75 (s, 1H), 7.50 (d, J = 9.0 Hz, 1H), 7.26 (d, J = 8.3 Hz, 1H), 7.07-6.99 (m, 2H), 5.25-5.18 (m, 1H), 4.58 (p, J = 6.7 Hz, 1H), 4.37 (t, J = 5.0 Hz, 1H), 4.10 (d, J = 7.1 Hz, 1H), 3.90 (dd, J = 11.6, 3.1 Hz, 1H), 3.56 (d, J = 5.0 Hz, 1H), 2.92 (d, J = 4.0 Hz, 3H), 2.30 (s, 2H), 2.15 (ddd, J = 11.2, 7.5, 3.9 Hz, 1H), 1.53 (q, J = 6.8, 6.3 Hz, 7H), 1.48 (d, J = 3.6 Hz, 1H), 1.33 (qd, J = 12.0, 4.4 Hz, 1H). ^{13}C NMR (101 MHz, DMSO-d_6) δ 168.32, 155.65, 150.51, 146.14, 138.79, 136.58, 134.48, 133.28, 132.73, 131.92, 128.23, 122.47, 122.05, 120.88, 120.52, 117.93, 115.85, 114.08, 103.10, 67.00, 62.83, 57.35, 55.91, 48.94, 43.26, 39.09, 36.15, 30.44, 22.94, 18.80. $C_{33}H_{42}N_6O_3$, MS calculated for m/z $[M+H]^+$: 571.3397 (calculated), 571.3404(found).

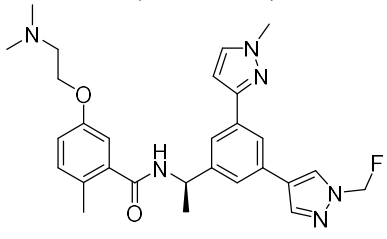

(R)-5-(2-(dimethylamino)ethoxy)-N-(1-(3-(1-(fluoromethyl)-1H-pyrazol-4-yl)-5-(1-methyl-1H-pyrazol-3-yl)phenyl)ethyl)-2-methylbenzamide (**Jun12713**). White solid, 79% yield for two steps. ^{1}H NMR (400 MHz, DMSO-d_6) δ 8.82 (d, J = 8.2 Hz, 1H), 8.33 (t, J = 1.9 Hz, 1H), 8.24 (s, 1H), 7.93 (d, J = 3.6 Hz, 2H), 7.79 (s, 1H), 7.64 (s, 1H), 7.19 (d, J = 8.2 Hz, 1H), 7.12-7.08 (m, 1H), 6.98 (d, J = 7.4 Hz, 2H), 5.23-5.16 (m, 1H), 4.31 (t, J = 5.0 Hz, 2H), 3.90 (s, 3H), 3.51 (q, J = 4.7 Hz, 2H), 2.87 (s, 6H), 2.23 (s, 3H), 1.51 (d, J = 7.0 Hz, 3H). ^{13}C NMR (101 MHz, DMSO-d_6) δ 168.34, 155.65, 150.35, 146.31, 139.98, 138.75, 134.62, 132.78, 132.25, 131.93, 129.66, 128.24, 124.43, 122.88, 121.60, 120.96, 115.87, 114.06, 103.17, 62.83, 55.90, 48.89, 43.25, 39.10, 22.92, 18.80. $C_{28}H_{33}FN_6O_2$, MS calculated for m/z $[M+H]^+$: 505.2727 (calculated), 505.2733 (found).

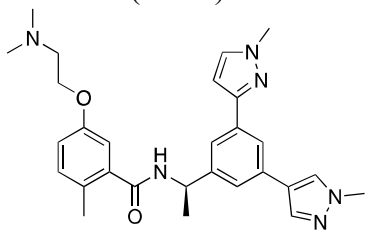

(R)-5-(2-(dimethylamino)ethoxy)-2-methyl-N-(1-(3-(1-methyl-1H-pyrazol-3-yl)-5-(1-methyl-1H-pyrazol-4-yl)phenyl)ethyl)benzamide (**Jun12308**). White solid, 82% yield for two steps. ^{1}H NMR (400 MHz, DMSO-d_6) δ 8.77 (d, J = 8.3 Hz, 1H), 8.19 (s, 1H), 7.88 (s, 1H), 7.81 (d, J = 1.7 Hz, 1H), 7.75 (d, J = 2.2 Hz, 1H), 7.68 (d, J = 1.9 Hz, 1H), 7.51 (d, J = 1.9 Hz, 1H), 7.19 (d, J = 8.2 Hz, 1H), 7.00-6.94 (m, 2H), 6.73 (d, J = 2.3 Hz, 1H), 5.20-5.13 (m, 1H), 4.30 (t, J = 5.0 Hz, 2H), 3.89 (d, J = 3.1 Hz, 6H), 3.50 (q, J = 4.9 Hz, 2H), 2.85 (d, J = 4.3 Hz, 6H), 2.23 (s, 3H), 1.49 (d, J = 7.0 Hz, 3H). ^{13}C NMR (101 MHz, DMSO-d_6) δ 168.28, 155.66, 150.51, 146.09, 138.85, 136.46, 134.49, 133.31, 132.72, 131.92, 128.40, 128.25, 122.42, 120.90, 120.55, 115.87, 114.10, 103.09, 62.85, 55.97, 48.88, 43.31, 39.11, 22.95, 18.82. $C_{28}H_{34}N_6O_2$, HRMS calculated for m/z $[M+H]^+$: 487.2821(calculated), 487.2826 (found)

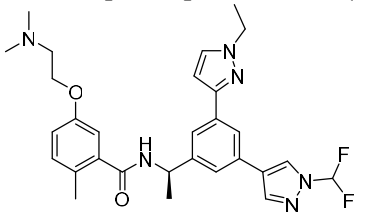

(R)-N-(1-(3-(1-(difluoromethyl)-1H-pyrazol-4-yl)-5-(1-ethyl-1H-pyrazol-3-yl)phenyl)ethyl)-5-(2-(dimethylamino)ethoxy)-2-methylbenzamide (**Jun12827**). White solid, 83% yield for two steps. ^{1}H NMR (400 MHz, DMSO-d_6) δ 8.78 (d, J = 8.1 Hz, 2H), 8.32 (s, 1H), 7.95 (s, 1H), 7.86 (s, 1H), 7.80 (s, 2H), 7.65 (s, 1H), 7.19 (d, J = 8.2 Hz, 1H), 6.98 (d, J = 7.6 Hz, 2H), 6.79 (d, J = 2.2 Hz, 1H), 5.23-5.15 (m, 1H), 4.31 (t, J = 5.1 Hz, 2H), 4.19 (q, J = 7.2 Hz, 2H), 3.50 (q, J = 4.8 Hz, 2H), 2.86 (s, 6H), 2.24 (s, 3H), 1.51 (d, J = 7.0 Hz, 3H), 1.42 (t, J = 7.3 Hz, 3H). ^{13}C NMR (101 MHz, DMSO-d_6) δ 168.33, 155.67, 150.13, 146.29, 140.50, 138.81, 134.81, 131.92, 131.56, 131.21, 128.24, 125.90, 124.99, 123.13, 121.89, 121.31, 115.87, 114.10, 103.12, 62.85, 55.91, 48.90, 46.83, 43.26, 22.96, 18.82, 16.01. $C_{29}H_{34}F_2N_6O_2$, MS calculated for m/z $[M+H]^+$: 537.2789 (calculated), 537.2795 (found).

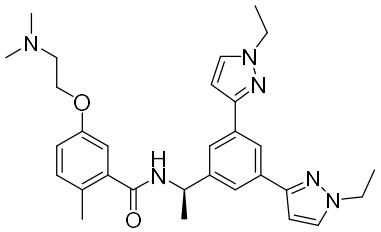

(R)-N-(1-(3,5-bis(1-ethyl-1H-pyrazol-3-yl)phenyl)ethyl)-5-(2-(dimethylamino)ethoxy)-2-methylbenzamide (**Jun12831**). White solid, 82% yield. ^{1}H NMR (400 MHz, DMSO-d_6) δ 8.82 (d, J = 8.2 Hz, 1H), 8.04 (s, 1H), 7.80 (d, J = 2.3 Hz, 2H), 7.75 (s, 2H), 7.19 (d, J = 8.2 Hz, 1H), 7.00 – 6.94 (m, 2H), 6.73 (d, J = 2.3 Hz, 2H), 5.22-5.14 (m, J = 7.1 Hz, 1H), 4.30 (t, J = 5.1 Hz, 2H), 4.19 (q, J = 7.2 Hz, 4H), 3.50 (q, J = 4.8 Hz, 2H), 2.85 (d, J = 3.9 Hz, 6H), 2.24 (s, 3H), 1.50 (d, J = 7.0 Hz, 3H), 1.42 (t, J = 7.2 Hz, 6H). ^{13}C NMR (101 MHz, DMSO-d_6) δ 168.32, 155.65, 150.31, 145.95, 138.82, 134.34, 131.90, 131.21, 128.26, 122.32, 120.58, 115.82, 114.10, 102.87, 62.84, 55.89, 48.94, 46.82, 43.24, 22.87, 18.83, 16.04. $C_{30}H_{38}N_6O_2$, MS calculated for m/z $[M+H]^+$: 515.3134 (calculated), 515.3141 (found).

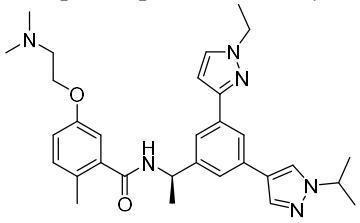

(R)-5-(2-(dimethylamino)ethoxy)-N-(1-(3-(1-ethyl-1H-pyrazol-3-yl)-5-(1-isopropyl-1H-pyrazol-4-yl)phenyl)ethyl)-2-methylbenzamide (**Jun12833**). White solid, 71% yield for two steps. ^{1}H NMR (400 MHz, DMSO-d_6) δ 8.78 (d, J = 8.2 Hz, 1H), 8.28 (s, 1H), 7.90 (s, 1H), 7.84 (s, 1H), 7.80 (s, 1H), 7.69 (s, 1H), 7.54 (s, 1H), 7.19 (d, J = 8.2 Hz, 1H), 6.98 (d, J = 7.8 Hz, 2H), 6.75 (s, 1H), 5.21-5.13 (m, 1H), 4.56-4.49 (m, 1H), 4.31 (t, J = 5.1 Hz, 2H), 4.18 (q, J = 7.3 Hz, 2H), 3.51 (s, 2H), 2.86 (s, 6H), 2.24 (s, 3H), 1.50 (d, J = 6.9 Hz, 3H), 1.47 (d, J = 6.7 Hz, 6H), 1.42 (t, J = 7.2 Hz, 3H). ^{13}C NMR (101 MHz, DMSO-d_6) δ 168.30, 155.66, 150.39, 146.04, 138.84, 135.96, 134.57, 133.49, 131.91, 131.11, 128.22, 125.23, 122.42, 121.95, 120.80, 120.57, 115.82, 114.10, 102.99, 62.85, 55.89, 53.62, 48.94, 46.80, 43.25, 23.15, 22.98, 18.82, 16.03. $C_{31}H_{40}N_6O_2$, MS calculated for m/z $[M+H]^+$: 529.3291(calculated), 529.3297 (found).

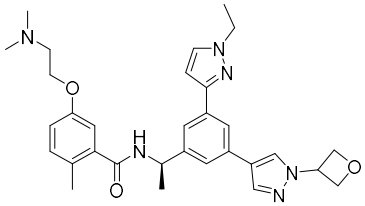

(R)-5-(2-(dimethylamino)ethoxy)-N-(1-(3-(1-ethyl-1H-pyrazol-3-yl)-5-(1-(oxetan-3-yl)-1H-pyrazol-4-yl)phenyl)ethyl)-2-methylbenzamide (**Jun12834**). White solid, 78% yield for two steps. ^{1}H NMR (400 MHz, DMSO-d_6) δ 8.61 (d, J = 8.2 Hz, 1H), 8.28 (s, 1H), 7.89 (s, 1H), 7.69 (s, 1H), 7.62 (s, 1H), 7.54 (s, 1H), 7.39 (s, 1H), 7.01 (d, J = 8.3 Hz, 1H), 6.80 (d, J = 7.9 Hz, 2H), 6.58 (s, 1H), 5.47-5.40 (m, 1H), 5.04-4.96 (m, 1H), 4.77 (d, J = 3.6 Hz, 2H), 4.13 (d, J = 5.3 Hz, 2H), 4.01 (q, J = 7.2 Hz, 2H), 2.68 (s, 6H), 2.07 (s, 3H), 1.32 (d, J = 7.0 Hz, 3H), 1.24 (t, J = 7.2 Hz, 3H). ^{13}C NMR (101 MHz, DMSO-d_6) δ 168.32, 155.66, 150.31, 146.14, 138.82, 137.46, 134.65, 132.98, 131.91, 131.15, 128.23, 127.21, 122.81, 122.55, 121.08, 120.73, 115.84, 114.09, 102.99, 77.10, 62.85, 55.89, 55.15, 48.91, 46.81, 43.25, 22.96, 18.82, 16.02. $C_{31}H_{38}N_6O_3$, MS calculated for m/z $[M+H]^+$: 543.3084 (calculated), 543.3091 (found).

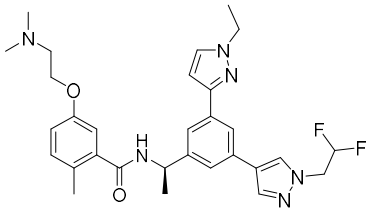

(R)-N-(1-(3-(1-(2,2-difluoroethyl)-1H-pyrazol-4-yl)-5-(1-ethyl-1H-pyrazol-3-yl)phenyl)ethyl)-5-(2-(dimethylamino)ethoxy)-2-methylbenzamide (**Jun12835**). White solid, 75% yield for two steps. ^{1}H NMR (400 MHz, DMSO-d_6) δ 8.79 (d, J = 8.2 Hz, 1H), 8.29 (s, 1H), 8.03 (s, 1H), 7.85 (s, 1H), 7.80 (s, 1H), 7.72 (s, 1H), 7.55 (s, 1H), 7.19 (d, J = 8.2 Hz, 1H), 6.98 (d, J = 8.2 Hz, 2H), 6.76 (d, J = 2.1 Hz, 1H), 5.47 (s, 1H), 5.22-5.14 (m, 1H), 4.67 (td, J = 15.2, 3.8 Hz, 2H), 4.31 (d, J = 5.2 Hz, 2H), 4.19 (q, J = 7.2 Hz, 2H), 3.50 (d, J = 5.0 Hz, 2H), 2.86 (s, 6H), 2.24 (s, 3H), 1.50 (d, J = 7.0 Hz, 3H), 1.42 (t, J = 7.2 Hz, 3H). ^{13}C NMR (101 MHz, DMSO-d_6) δ 168.32, 155.67, 150.26, 146.20, 138.82, 137.75, 134.67, 132.79, 131.91, 131.18, 129.12, 128.22, 123.07, 122.54, 121.24, 120.69, 115.84, 114.49, 114.08, 102.99, 62.85, 55.89, 48.91, 46.82, 43.24, 22.94, 18.81, 16.02. $C_{30}H_{36}F_2N_6O_2$, MS calculated for m/z $[M+H]^+$: 551.2946(calculated), 551.2952 (found).

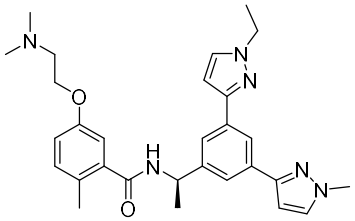

(R)-5-(2-(dimethylamino)ethoxy)-N-(1-(3-(1-ethyl-1H-pyrazol-3-yl)-5-(1-methyl-1H-pyrazol-3-yl)phenyl)ethyl)-2-methylbenzamide (**Jun13836**). White solid, 70% yield for two steps. ^{1}H NMR (400 MHz, DMSO-d_6) δ 8.83 (d, J = 8.2 Hz, 1H), 8.05 (s, 1H), 7.80 (d, J = 2.3 Hz, 1H), 7.76 (s, 3H), 7.19 (d, J = 8.1 Hz, 1H), 6.97 (d, J = 8.7 Hz, 2H), 6.73 (s, 2H), 5.22-5.15 (m, 1H), 4.31 (t, J = 5.0 Hz, 2H), 4.19 (q, J = 7.3 Hz, 2H), 3.90 (s, 3H), 3.50 (q, J = 4.9 Hz, 2H), 2.86 (s, 6H), 2.24 (s, 3H), 1.50 (d, J = 7.0 Hz, 3H), 1.42 (t, J = 7.2 Hz, 3H). ^{13}C NMR (101 MHz, DMSO-d_6) δ 168.29, 155.65, 150.48, 150.29, 145.98, 138.82, 134.34, 134.22, 132.77, 131.90, 131.22, 128.27, 122.34, 122.30, 120.55, 115.83, 114.10, 103.01, 102.85, 62.84, 55.90, 48.92, 46.82, 43.25, 39.10, 22.87, 18.82, 16.03. $C_{29}H_{36}N_6O_2$, MS calculated for m/z $[M+H]^+$: 501.2978 (calculated), 501.2989 (found).

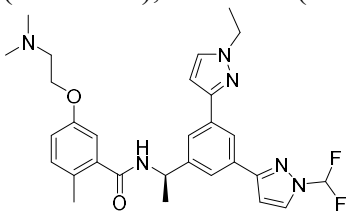

(R)-N-(1-(3-(1-(difluoromethyl)-1H-pyrazol-3-yl)-5-(1-ethyl-1H-pyrazol-3-yl)phenyl)ethyl)-5-(2-(dimethylamino)ethoxy)-2-methylbenzamide (**Jun12837**). White solid, 68% yield for two steps. ^{1}H NMR (400 MHz, DMSO-d_6) δ 8.86 (d, J = 8.1 Hz, 1H), 8.33 (s, 1H), 8.14 (s, 1H), 7.88 (s, 2H), 7.86 (s, 1H), 7.82 (s, 1H), 7.19 (d, J = 8.2 Hz, 1H), 7.10 (d, J = 2.7 Hz, 1H), 6.98 (d, J = 9.5 Hz, 2H), 6.77 (s, 1H), 5.25-5.17 (m, 1H), 4.30 (d, J = 5.3 Hz, 2H), 4.20 (q, J = 7.3 Hz, 2H), 3.50 (s, 2H), 2.85 (s, 6H), 2.23 (s, 3H), 1.51 (d, J = 7.0 Hz, 3H), 1.43 (t, J = 7.2 Hz, 3H). ^{13}C NMR (101 MHz, DMSO-d_6) δ 168.34, 155.66, 149.98, 146.34, 138.77, 134.64, 132.58, 131.93, 131.34, 128.26, 123.66, 122.95, 121.27, 115.88, 114.07, 106.09, 103.01, 62.83, 55.90, 48.91,

46.86, 43.26, 22.85, 18.81, 16.05. $C_{29}H_{34}F_2N_6O_2$, MS calculated for m/z $[M+H]^+$: 537.2789 (calculated), 537.2796 (found).

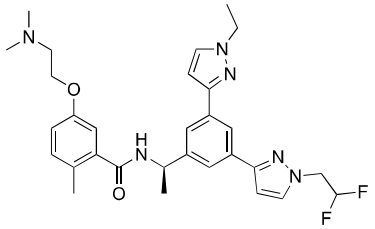

(R)-N-(1-(3-(1-(2,2-difluoroethyl)-1H-pyrazol-3-yl)-5-(1-ethyl-1H-pyrazol-3-yl)phenyl)ethyl)-5-(2-(dimethylamino)ethoxy)-2-methylbenzamide (**Jun1314**). White solid, 66% yield for two steps. ^{1}H NMR (400 MHz, DMSO-d_6) δ 8.77 (d, J = 8.2 Hz, 1H), 8.28 (s, 1H), 8.02 (s, 1H), 7.84 (s, 1H), 7.80 (d, J = 2.3 Hz, 1H), 7.71 (s, 1H), 7.54 (s, 1H), 7.19 (d, J = 8.2 Hz, 1H), 7.00 – 6.93 (m, 2H), 6.75 (d, J = 2.3 Hz, 1H), 5.21-5.14 (m, 1H), 4.67 (td, J = 15.2, 3.8 Hz, 2H), 4.30 (t, J = 5.0 Hz, 2H), 4.18 (q, J = 7.3 Hz, 3H), 3.50 (q, J = 5.0 Hz, 2H), 2.85 (d, J = 4.1 Hz, 6H), 2.24 (s, 3H), 1.49 (d, J = 7.0 Hz, 3H), 1.42 (t, J = 7.2 Hz, 3H). ^{13}C NMR (101 MHz, DMSO-d_6) δ 168.40, 168.33, 155.66, 151.58, 150.22, 146.07, 138.80, 134.44, 133.72, 131.91, 131.25, 128.26, 122.71, 122.57, 120.76, 115.84, 114.09, 103.92, 102.89, 62.86, 55.88, 48.94, 46.84, 43.24, 22.86, 18.82, 16.04. $C_{30}H_{36}F_2N_6O_2$, MS calculated for m/z $[M+H]^+$: 551.2946 (calculated), 551.2951 (found).

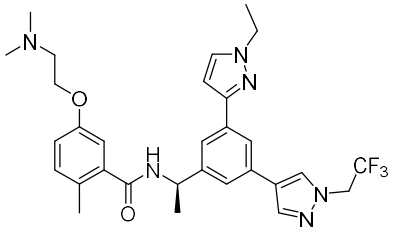

(R)-5-(2-(dimethylamino)ethoxy)-N-(1-(3-(1-ethyl-1H-pyrazol-3-yl)-5-(1-(2,2,2-trifluoroethyl)-1H-pyrazol-4-yl)phenyl)ethyl)-2-methylbenzamide (**Jun12839**). White solid, 72% yield for two steps. ^{1}H NMR (400 MHz, $CDCl_3$) δ 7.97 (s, 1H), 7.91 (s, 1H), 7.85 (s, 1H), 7.75 (s, 1H), 7.56 (s, 1H), 7.51 (d, J = 2.4 Hz, 1H), 7.13 (d, J = 8.4 Hz, 1H), 6.98 (d, J = 2.7 Hz, 1H), 6.83 (dd, J = 8.4, 2.6 Hz, 1H), 6.66 (d, J = 6.6 Hz, 2H), 5.41-5.34 (m, J = 7.1 Hz, 1H), 4.78 (q, J = 8.3 Hz, 2H), 4.41-4.36 (m, 2H), 4.32 (q, J = 7.3 Hz, 2H), 3.45 (d, J = 4.7 Hz, 2H), 2.92 (d, J = 2.5 Hz, 6H), 2.36 (s, 3H), 1.68 (d, J = 6.8 Hz, 3H), 1.57 (t, J = 7.3 Hz, 3H). ^{13}C NMR (101 MHz, DMSO-d_6) δ 168.34, 155.67, 150.21, 146.25, 138.80, 138.49, 134.71, 132.46, 131.91, 131.19, 129.51, 128.21, 123.55, 122.66, 121.43, 120.80, 115.84, 114.07, 103.03, 62.84, 55.88, 48.91, 46.82, 43.24, 22.93, 18.80, 16.01. $C_{30}H_{35}F_3N_6O_2$, MS calculated for m/z $[M+H]^+$: 569.2852 (calculated), 569.2860 (found).

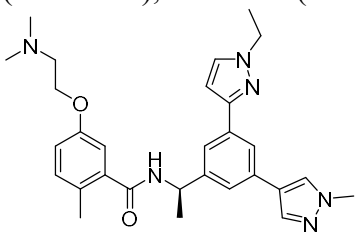

(R)-5-(2-(dimethylamino)ethoxy)-N-(1-(3-(1-ethyl-1H-pyrazol-3-yl)-5-(1-methyl-1H-pyrazol-4-yl)phenyl)ethyl)-2-methylbenzamide (**Jun12682**). White solid, 74% yield for two steps. ^{1}H NMR (400 MHz, DMSO-d_6) δ 8.71 (d, J = 8.2 Hz, 1H), 8.12 (s, 1H), 7.82 (s, 1H), 7.77-7.71 (m, 2H), 7.62 (s, 1H), 7.45 (s, 1H), 7.12 (d, J = 8.2 Hz, 1H), 6.90 (d, J = 7.3 Hz, 2H), 6.67 (d, J = 2.2 Hz, 1H), 5.13-5.06 (m, 1H), 4.24 (t, J = 5.0 Hz, 2H), 4.11 (q, J = 7.2 Hz, 2H), 3.81 (s, 3H), 3.43

(s, 2H), 2.79 (s, 6H), 2.17 (s, 3H), 1.42 (d, J = 7.0 Hz, 3H), 1.35 (t, J = 7.3 Hz, 3H). ^{13}C NMR (101 MHz, DMSO-d_6) δ 168.31, 155.67, 150.34, 146.11, 138.83, 136.48, 134.61, 133.30, 131.91, 131.15, 128.40, 128.23, 122.44, 122.38, 120.90, 120.58, 115.84, 114.10, 102.96, 62.86, 55.89, 48.91, 46.81, 43.25, 39.11, 22.96, 18.83, 16.02. $C_{29}H_{36}N_6O_2$, MS calculated for m/z $[M+H]^+$: 501.2978 (calculated), 501.2985 (found).

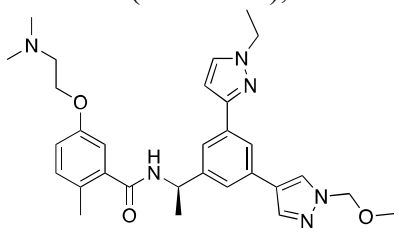

(R)-5-(2-(dimethylamino)ethoxy)-N-(1-(3-(1-ethyl-1H-pyrazol-3-yl)-5-(1-(methoxymethyl)-1H-pyrazol-3-yl)phenyl)ethyl)-2-methylbenzamide (**Jun12924**). White solid, 79% yield for two steps. ^{1}H NMR (400 MHz, DMSO-d_6) δ 8.78 (d, J = 8.2 Hz, 1H), 8.42 (s, 1H), 8.04 (s, 1H), 7.88 (d, J = 2.0 Hz, 1H), 7.80 (d, J = 2.3 Hz, 1H), 7.73 (s, 1H), 7.58 (s, 1H), 7.19 (d, J = 9.0 Hz, 1H), 6.98 (d, J = 7.0 Hz, 2H), 6.76 (d, J = 2.4 Hz, 1H), 5.42 (s, 2H), 5.22-5.15 (m, 1H), 4.31 (t, J = 5.0 Hz, 2H), 4.18 (q, J = 7.3 Hz, 2H), 3.51 (q, J = 4.6 Hz, 2H), 3.28 (s, 3H), 2.86 (d, J = 3.4 Hz, 6H), 2.24 (s, 3H), 1.51 (d, J = 7.0 Hz, 3H), 1.42 (t, J = 7.2 Hz, 3H). ^{13}C NMR (101 MHz, DMSO-d_6) δ 168.32, 155.67, 150.29, 146.17, 138.83, 137.85, 134.68, 132.87, 131.91, 131.15, 128.52, 128.24, 123.29, 122.63, 121.22, 120.81, 115.85, 114.10, 103.01, 81.79, 62.87, 56.59, 55.91, 48.92, 46.81, 43.26, 22.96, 18.81, 16.00. $C_{30}H_{38}N_6O_3$, MS calculated for m/z $[M+H]^+$: 531.3084 (calculated), 531.3091 (found).

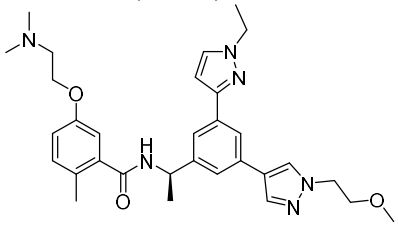

(R)-5-(2-(dimethylamino)ethoxy)-N-(1-(3-(1-ethyl-1H-pyrazol-3-yl)-5-(1-(2-methoxyethyl)-1H-pyrazol-4-yl)phenyl)ethyl)-2-methylbenzamide (**Jun12763**). White solid, 74% yield for two steps. ^{1}H NMR (400 MHz, DMSO-d_6) δ 8.72 (d, J = 8.3 Hz, 1H), 8.14 (s, 1H), 7.87-7.84 (m, 1H), 7.76 (t, J = 1.6 Hz, 1H), 7.73 (d, J = 2.3 Hz, 1H), 7.62 (d, J = 1.6 Hz, 1H), 7.46 (d, J = 1.7 Hz, 1H), 7.12 (d, J = 8.2 Hz, 1H), 6.90 (d, J = 7.4 Hz, 2H), 6.68 (d, J = 2.3 Hz, 1H), 5.10 (m, 1H), 4.23 (q, J = 5.5 Hz, 4H), 4.11 (q, J = 7.2 Hz, 2H), 3.66 (t, J = 5.3 Hz, 2H), 3.42 (d, J = 6.3 Hz, 2H), 3.18 (s, 3H), 2.84-2.75 (m, 6H), 2.17 (s, 3H), 1.42 (d, J = 7.0 Hz, 3H), 1.35 (t, J = 7.3 Hz, 3H). ^{13}C NMR (101 MHz, DMSO-d_6) δ 168.30, 155.67, 150.34, 146.11, 138.84, 136.63, 134.60, 133.28, 131.91, 131.14, 128.21, 128.18, 122.39, 122.21, 120.92, 120.55, 115.83, 114.08, 102.98, 70.95, 62.85, 58.44, 55.88, 51.78, 48.92, 46.81, 43.24, 22.98, 18.82, 16.03. $C_{31}H_{40}N_6O_3$, MS calculated for m/z $[M+H]^+$: 545.3240 (calculated), 545.3245 (found).

HNMR and CNMR spectra of A-2

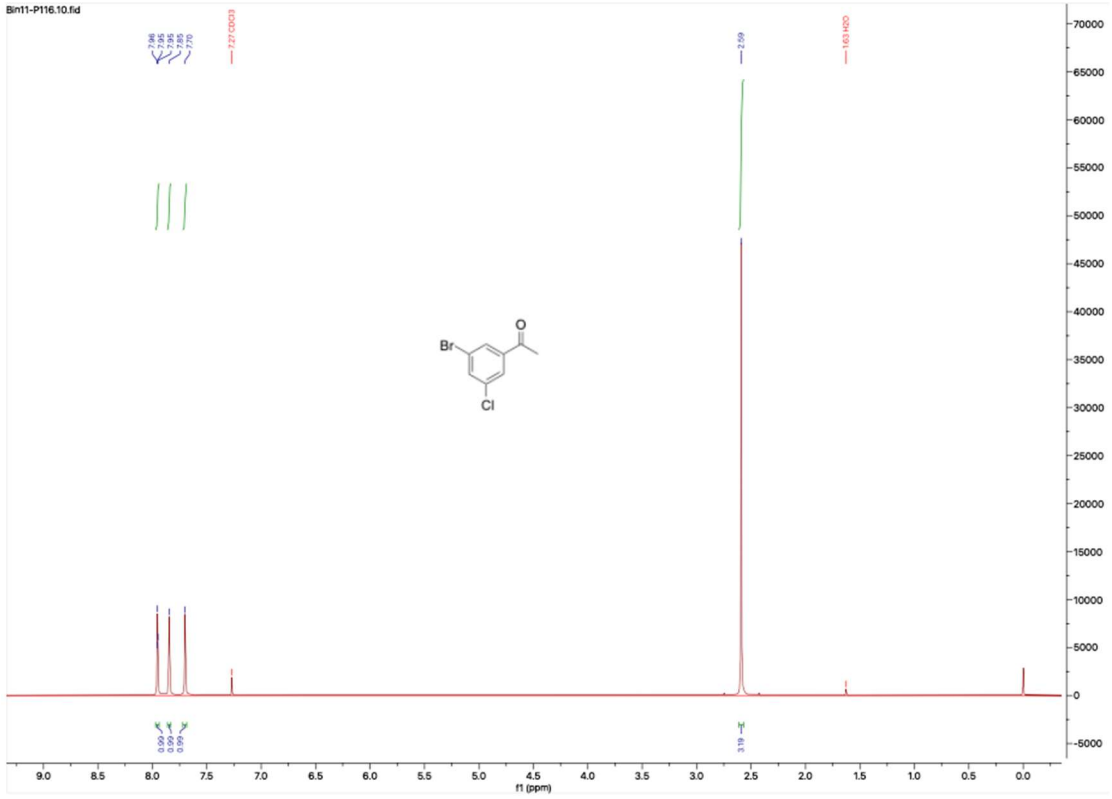

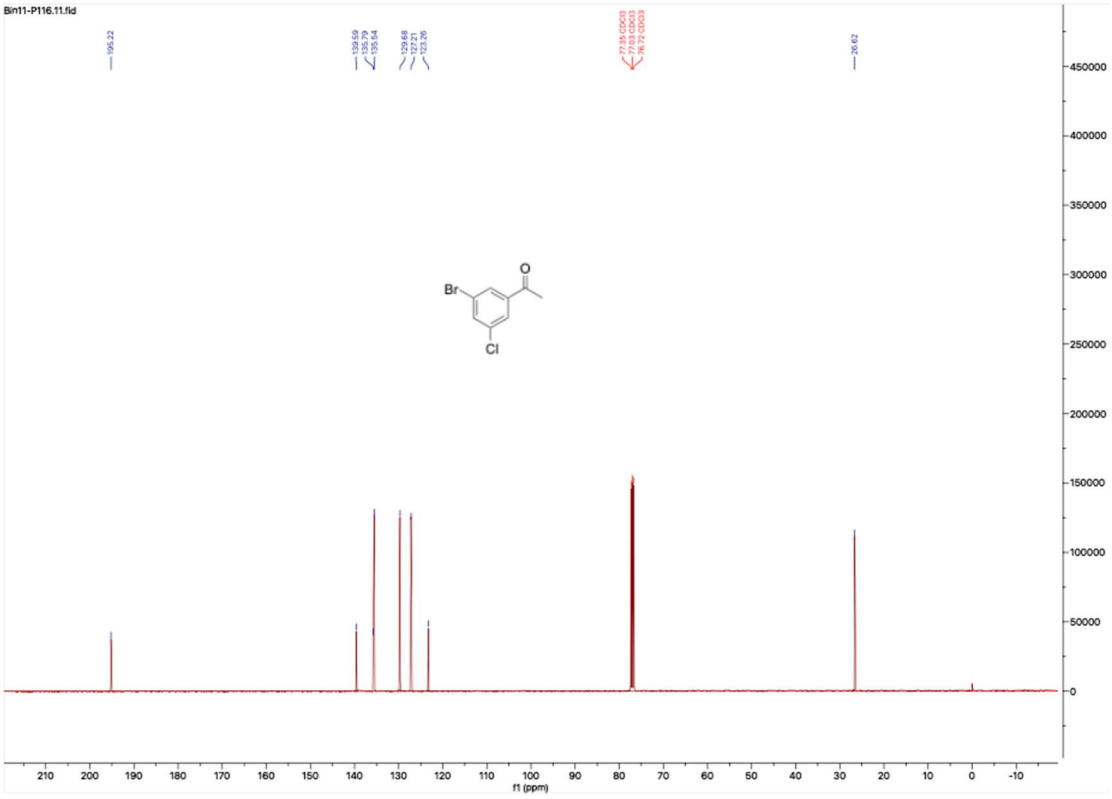

HNMR and CNMR spectra of A-3

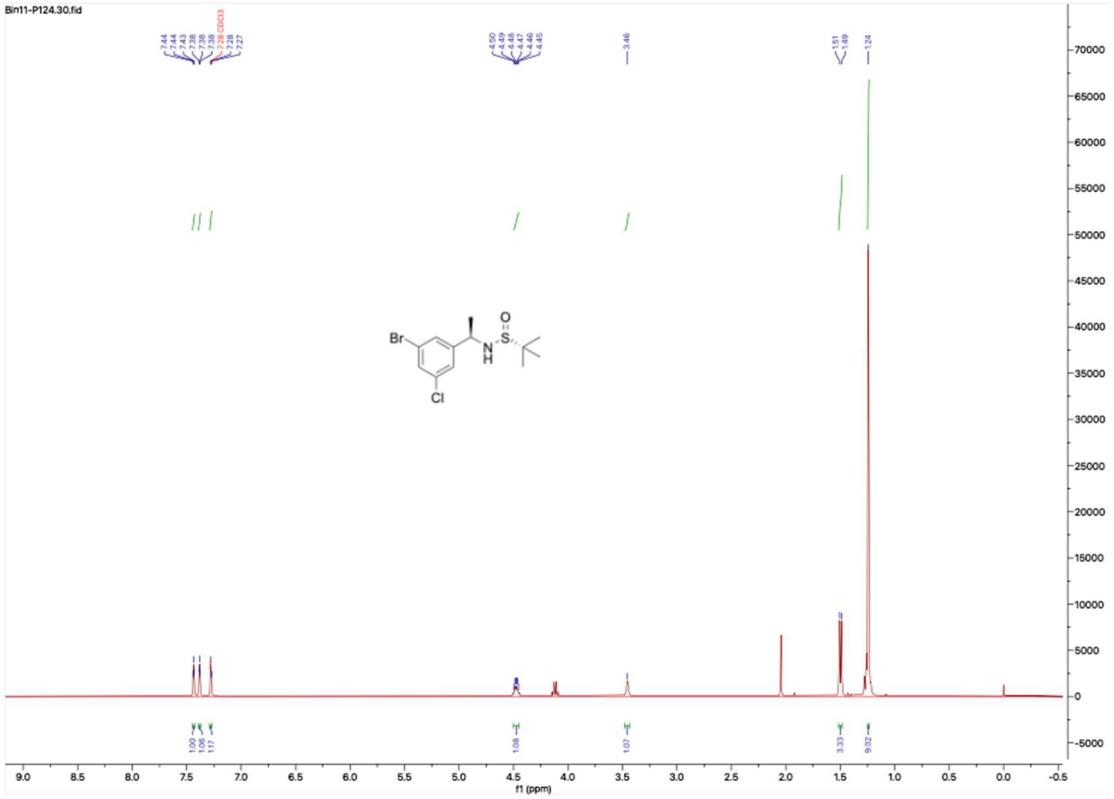

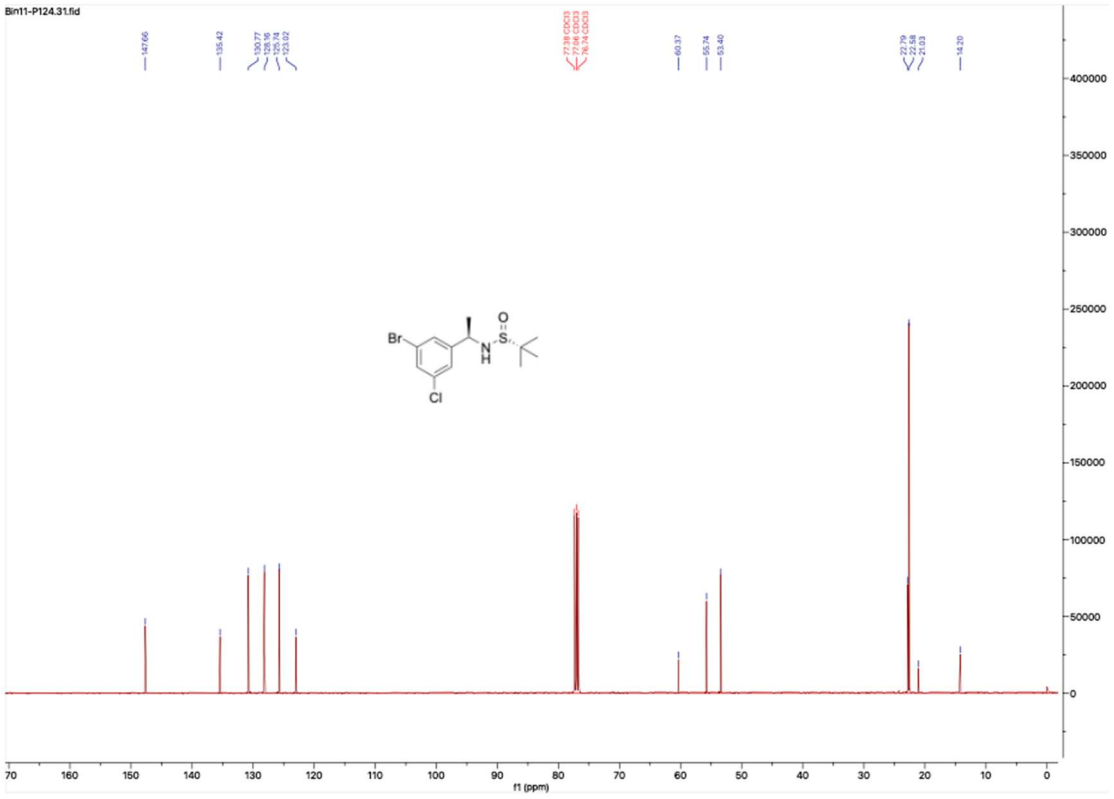

HNMR and CNMR spectra of A-4

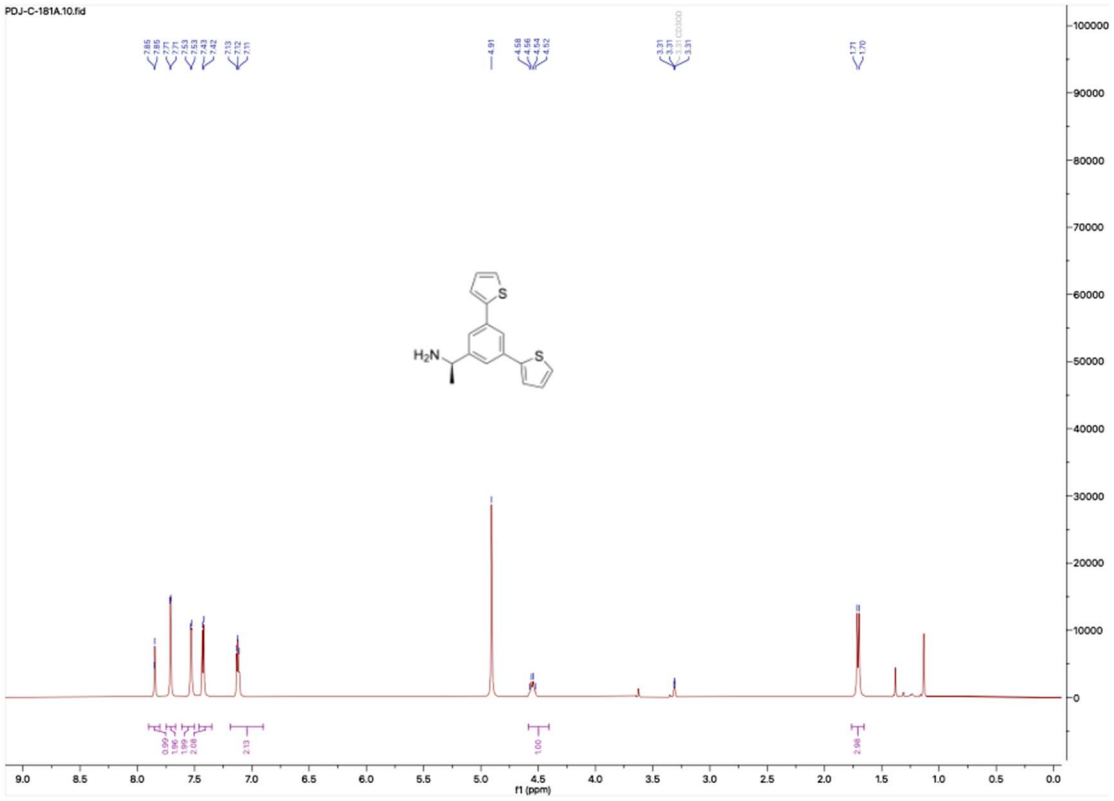

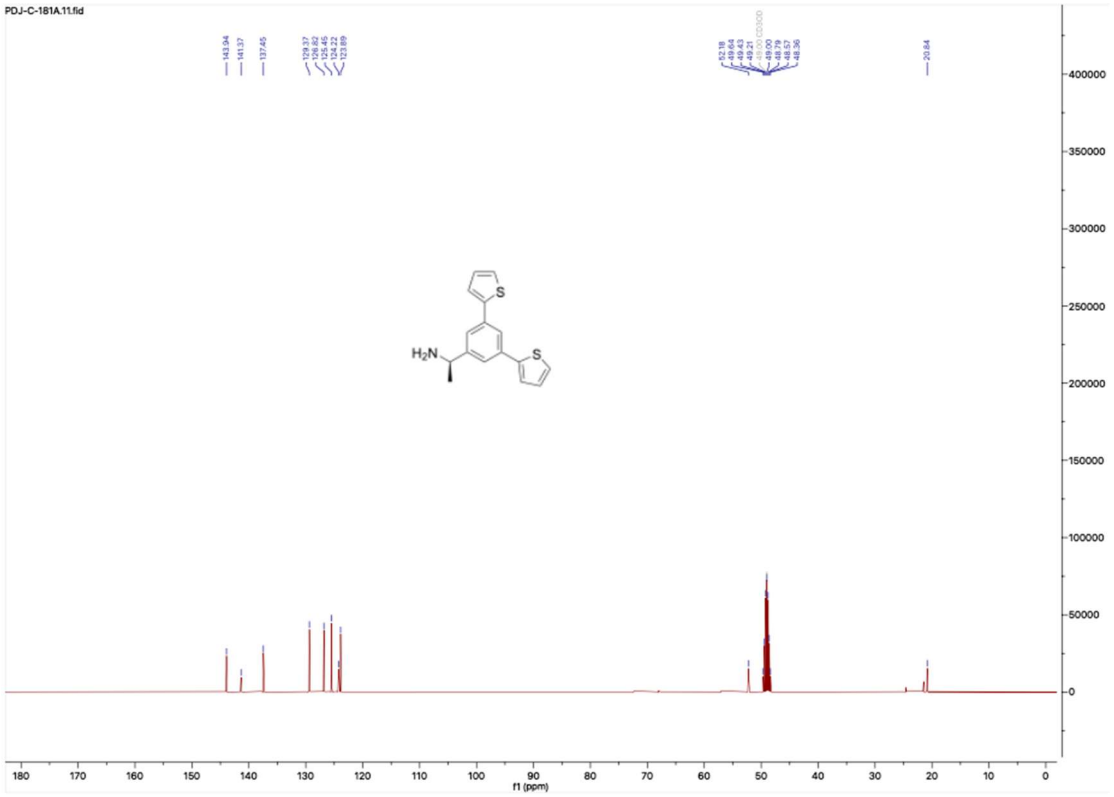

HNMR and CNMR spectra of A-5

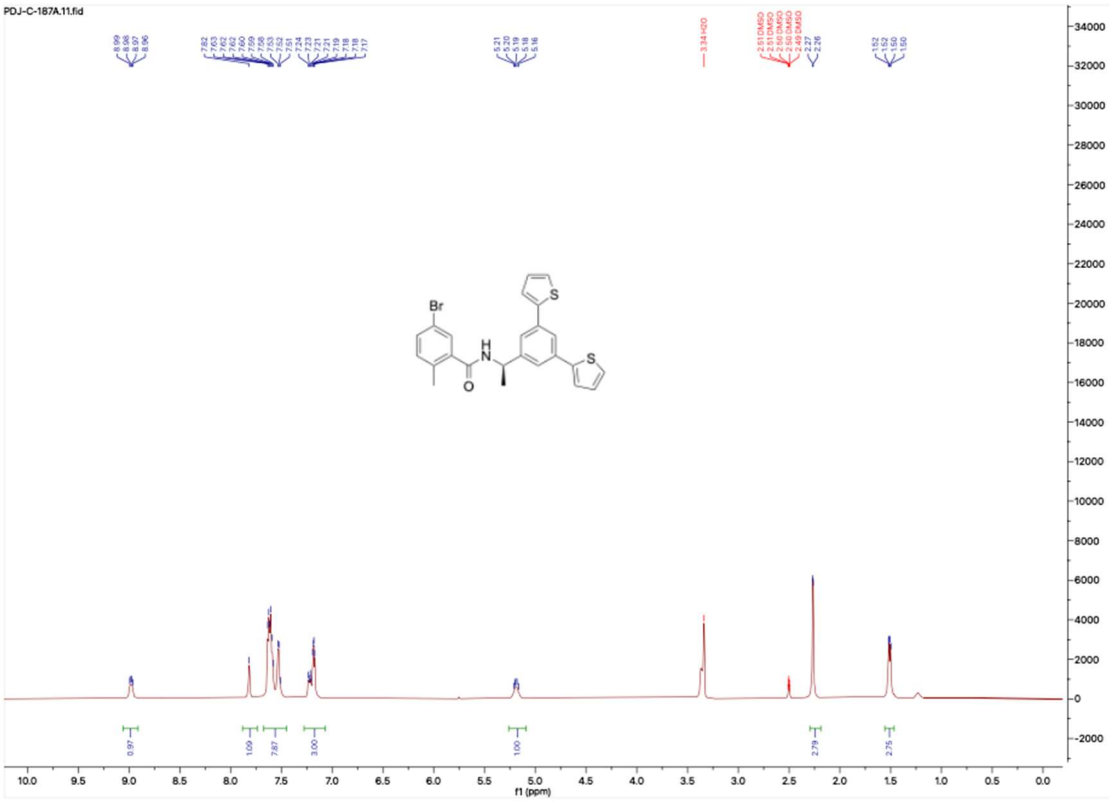

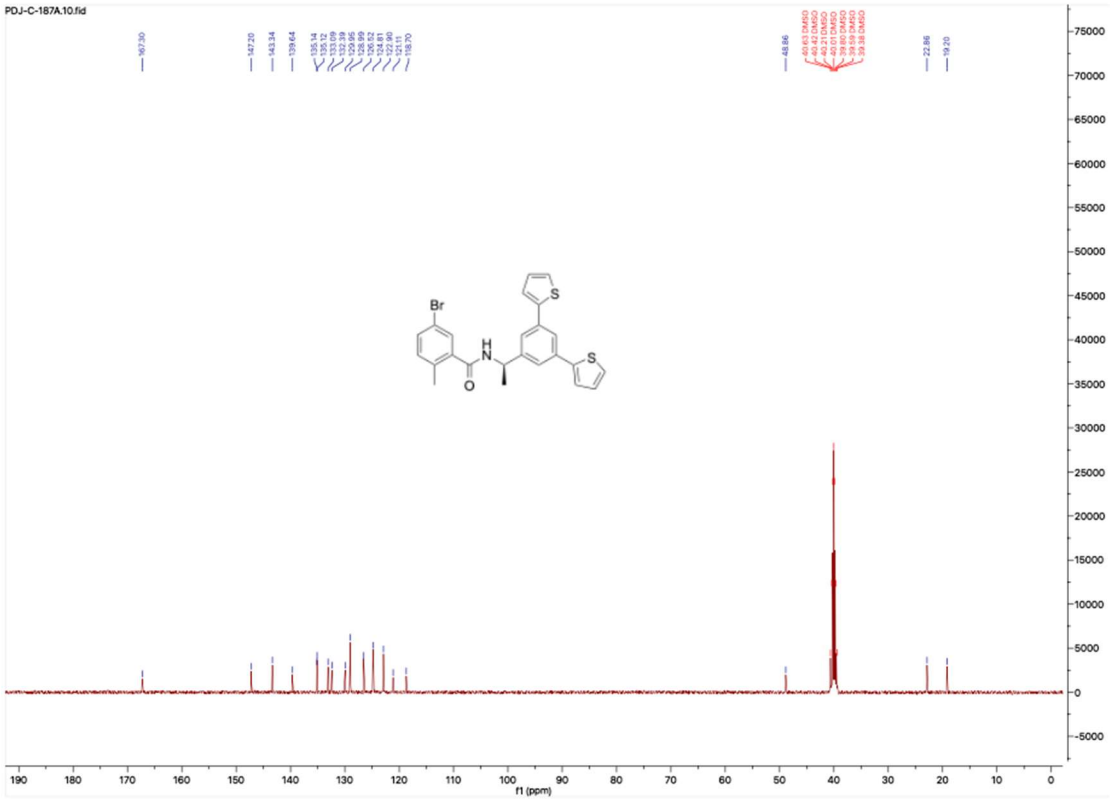

HNMR and CNMR spectra of Jun1238

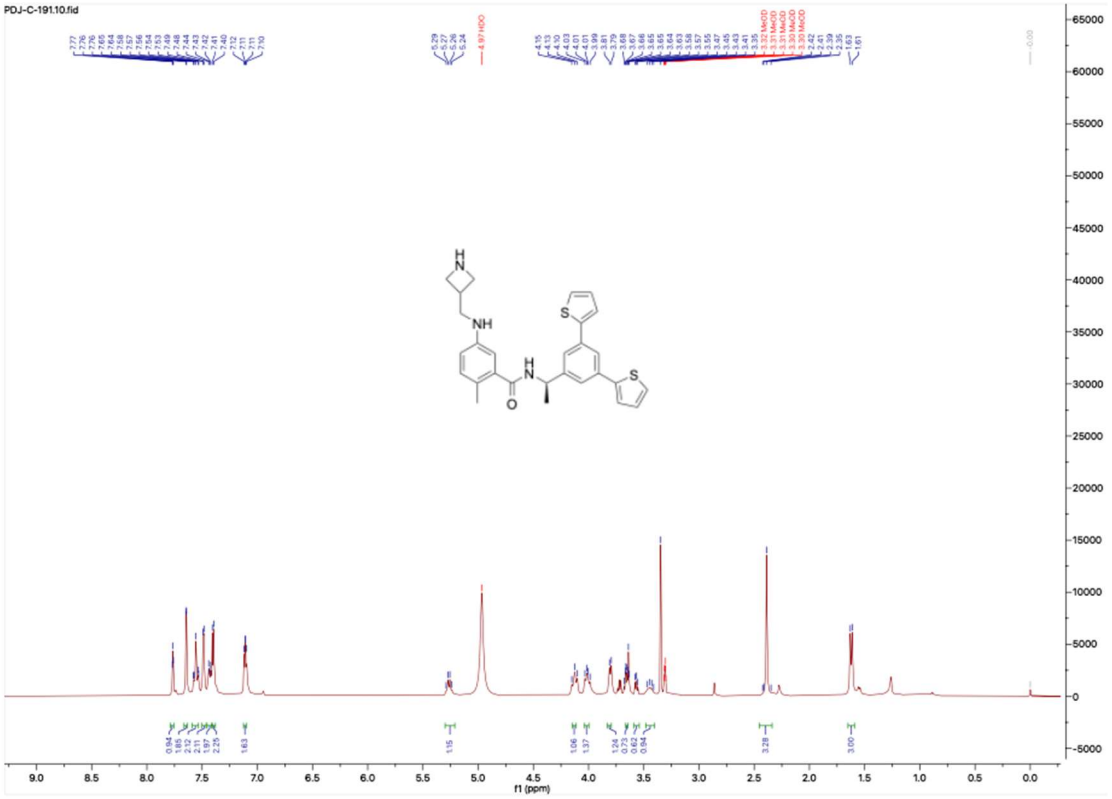

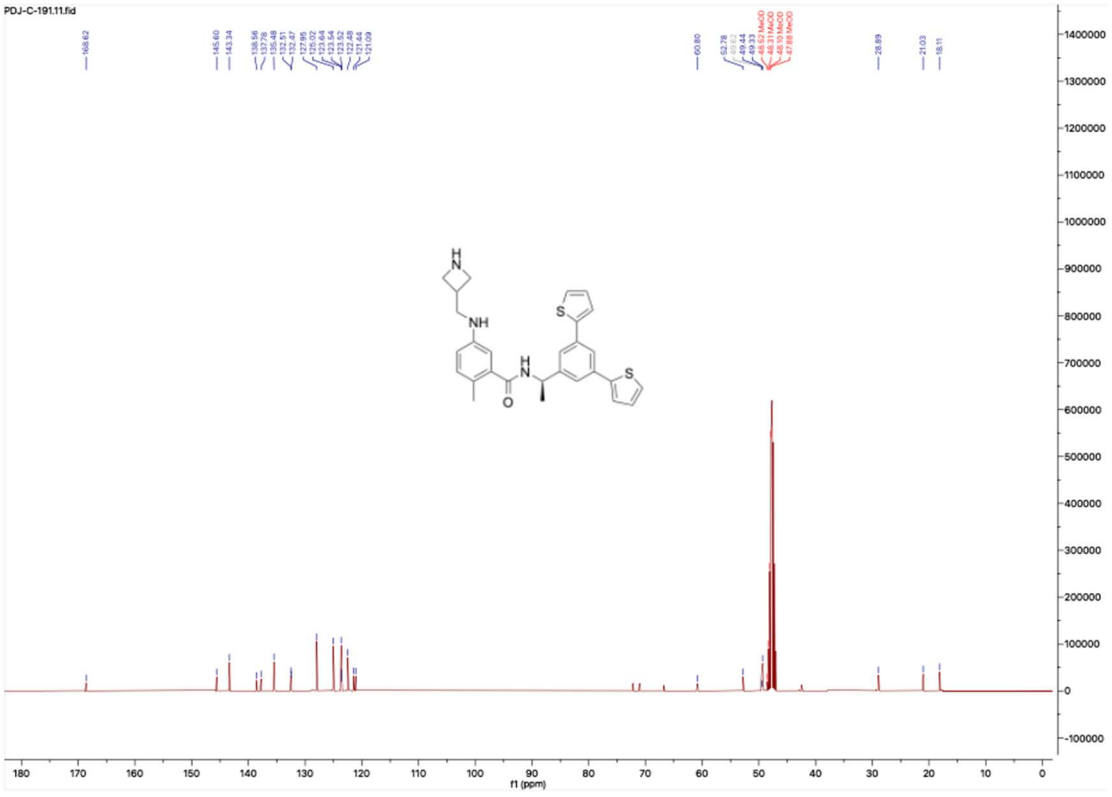

HNMR and CNMR spectra of Jun1271

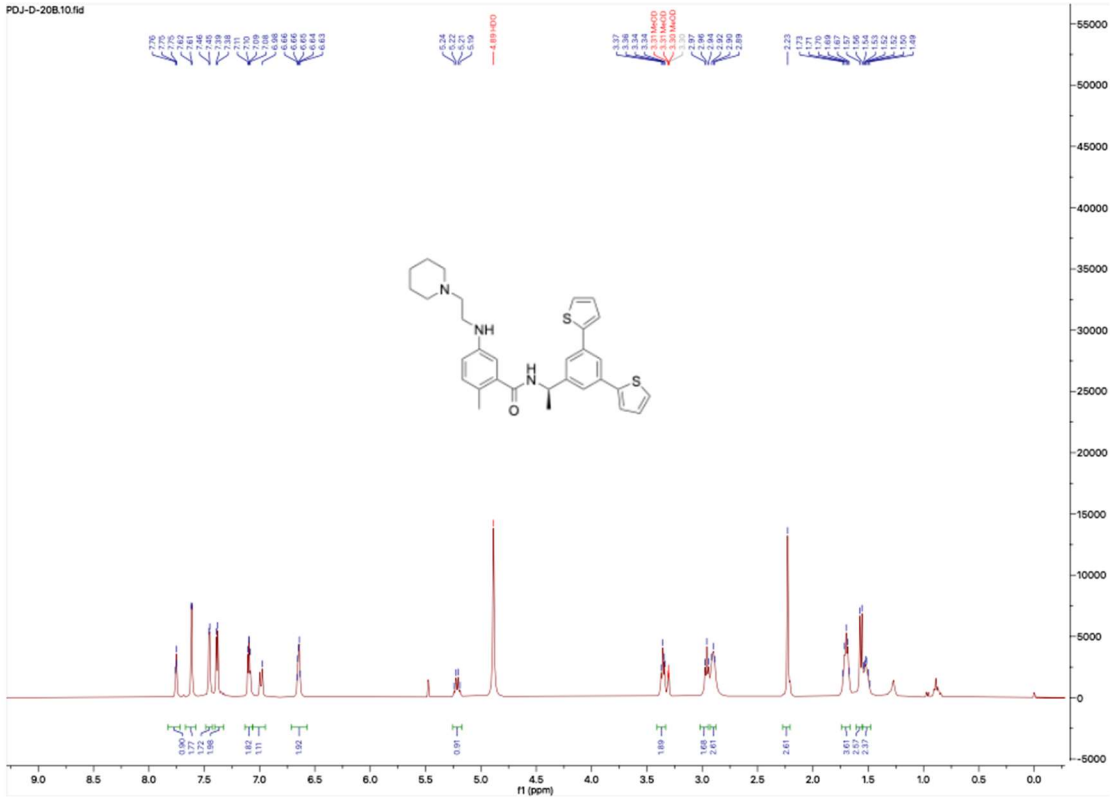

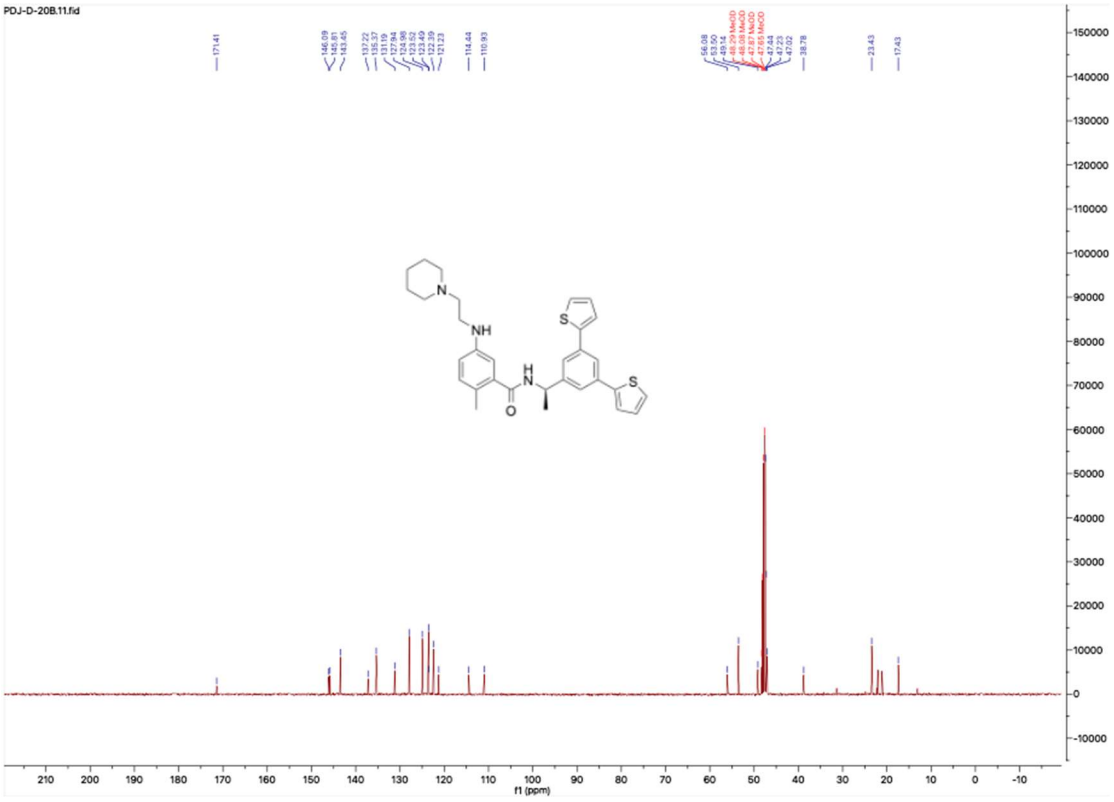

HNMR and CNMR spectra of Jun11924

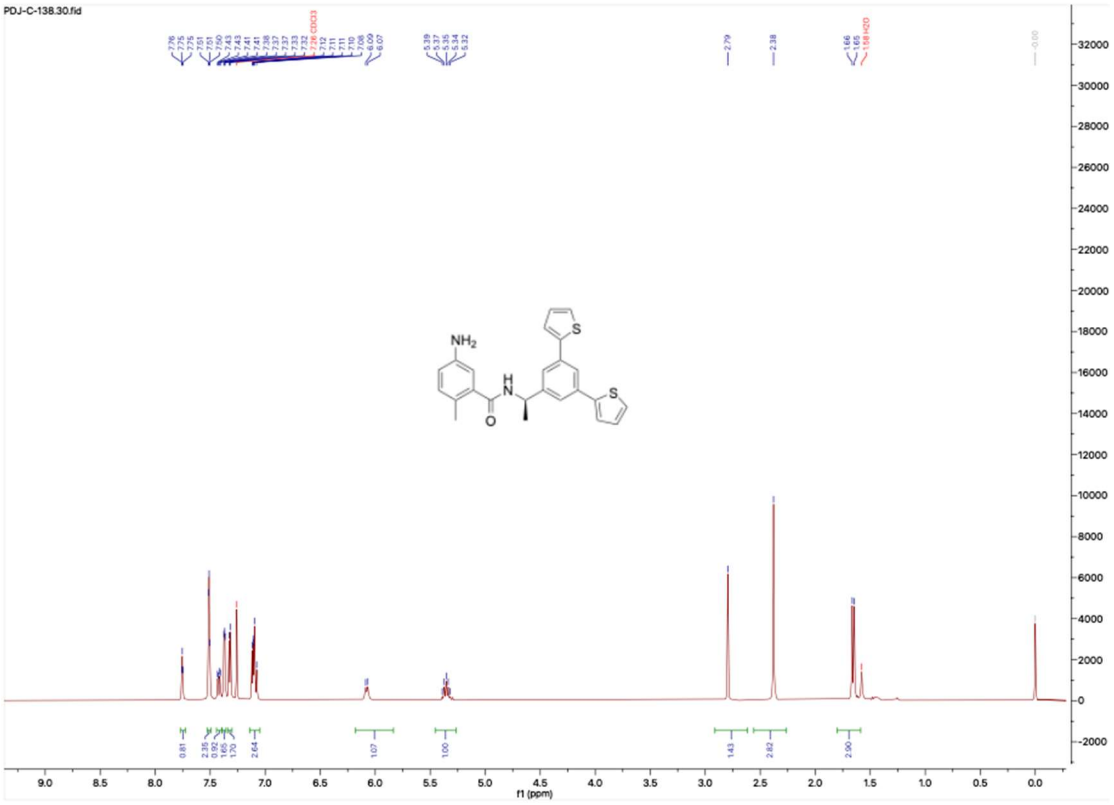

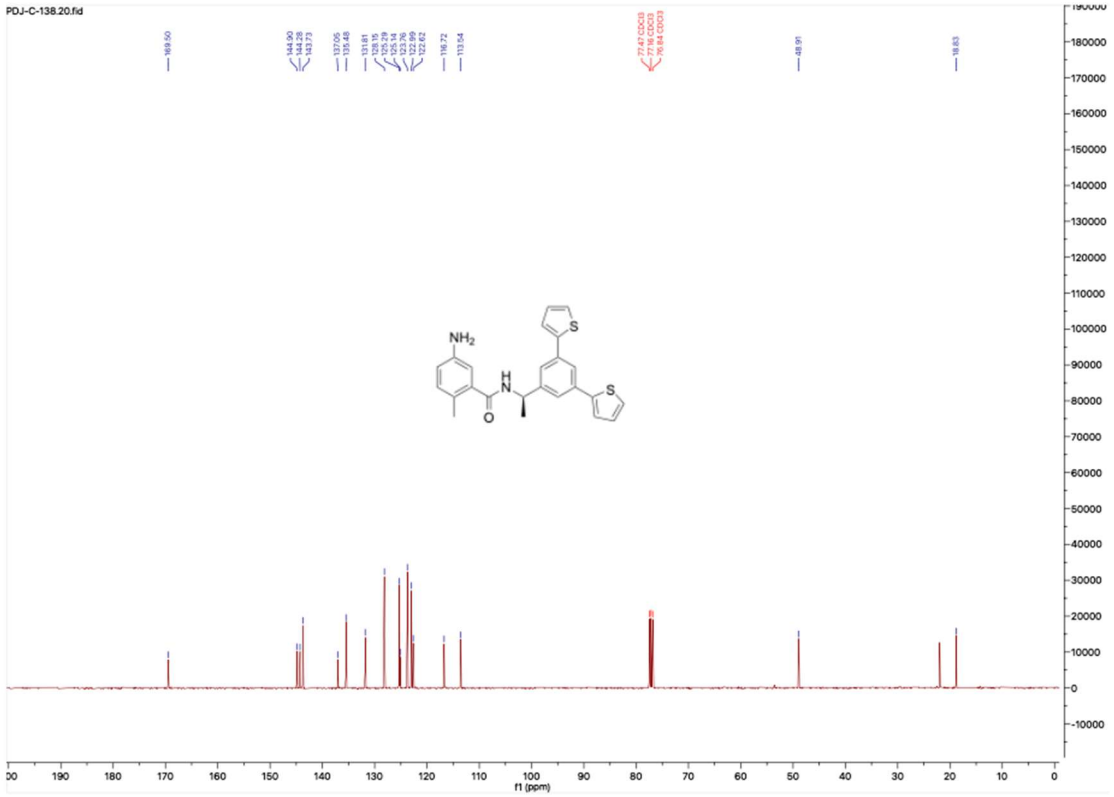

HNMR and CNMR spectra of Jun11922

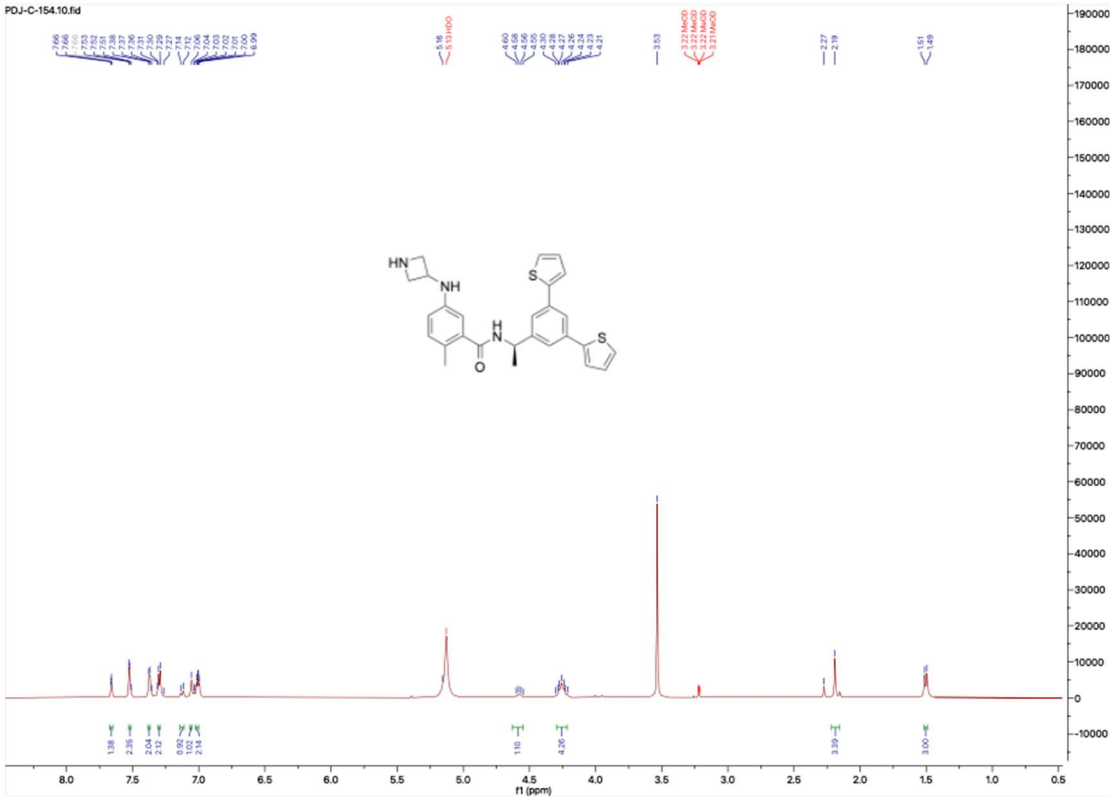

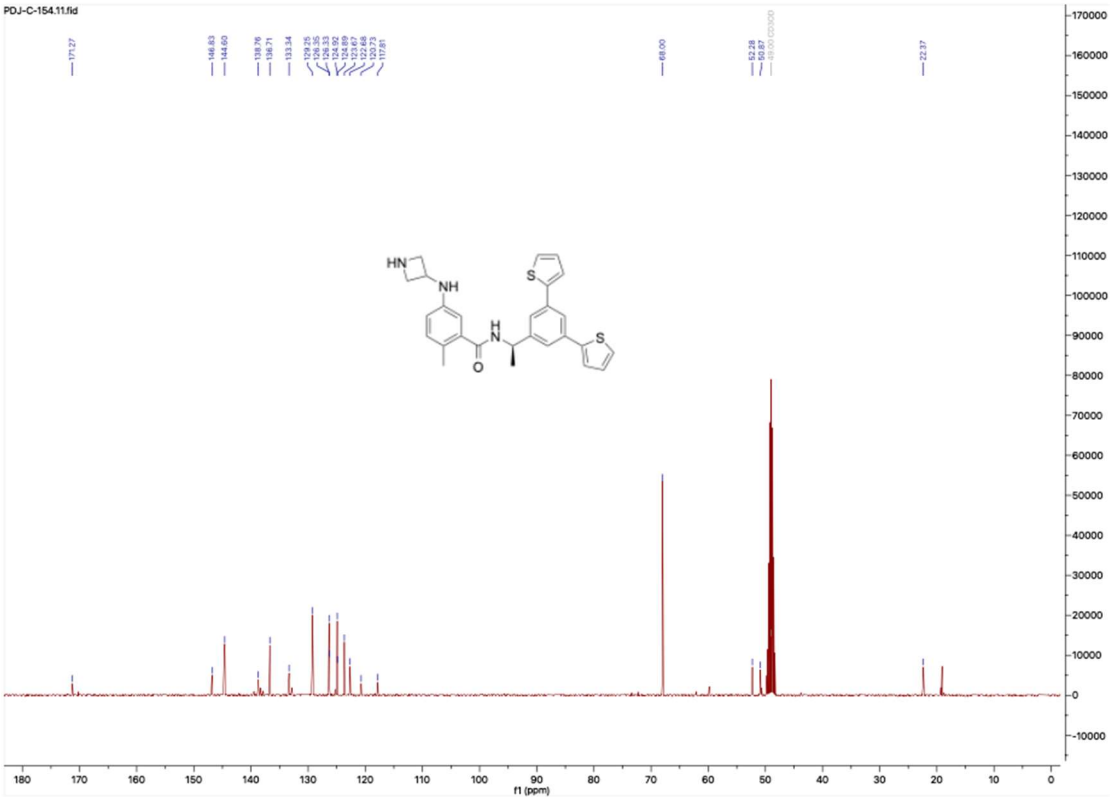

HNMR and CNMR spectra of Jun12112

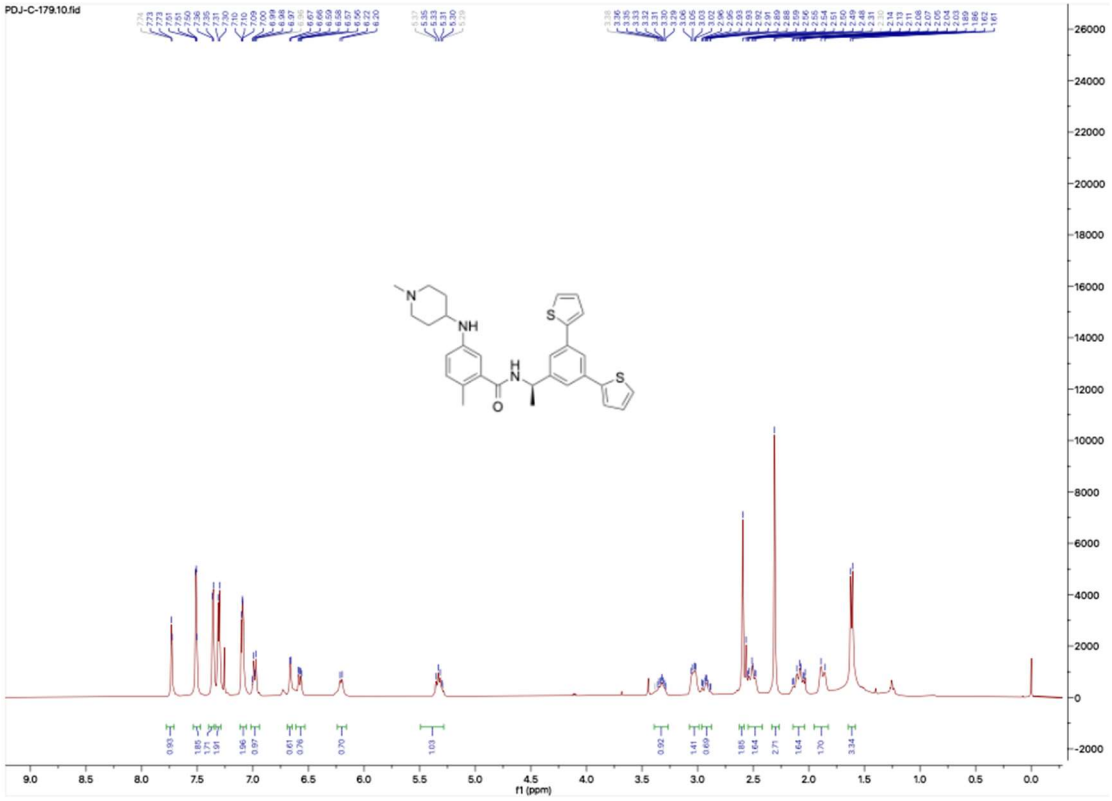

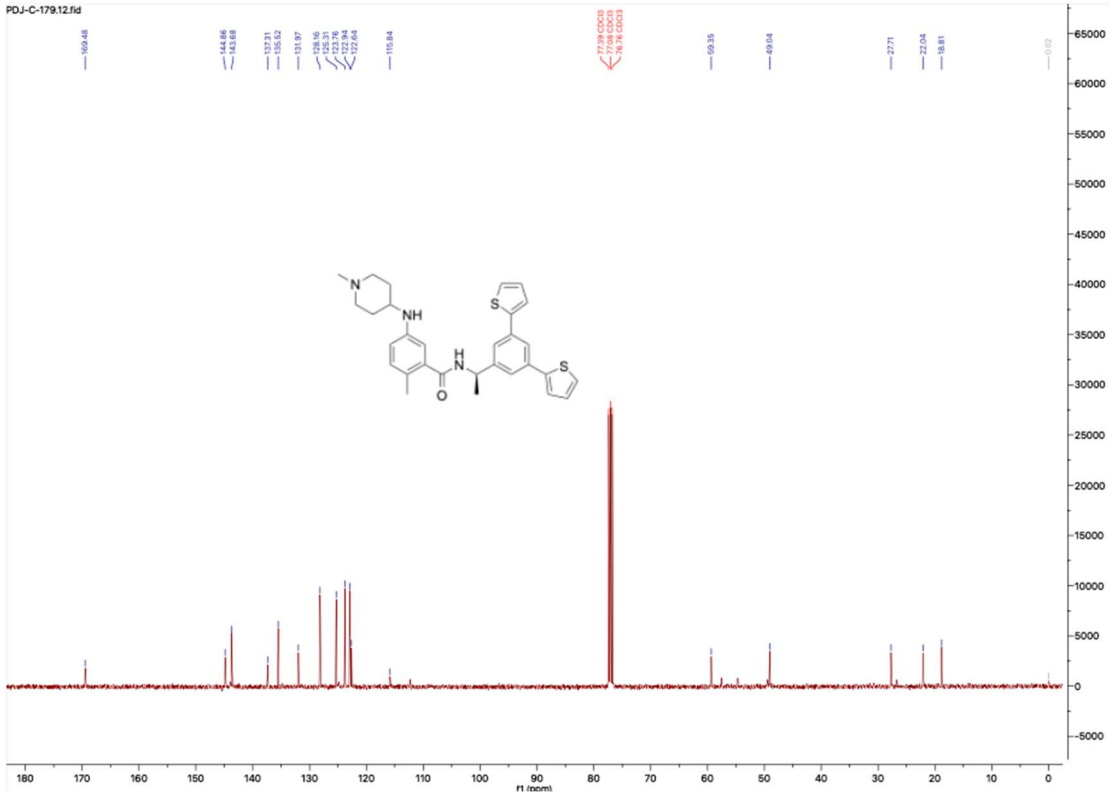

HNMR and CNMR spectra of Jun11923

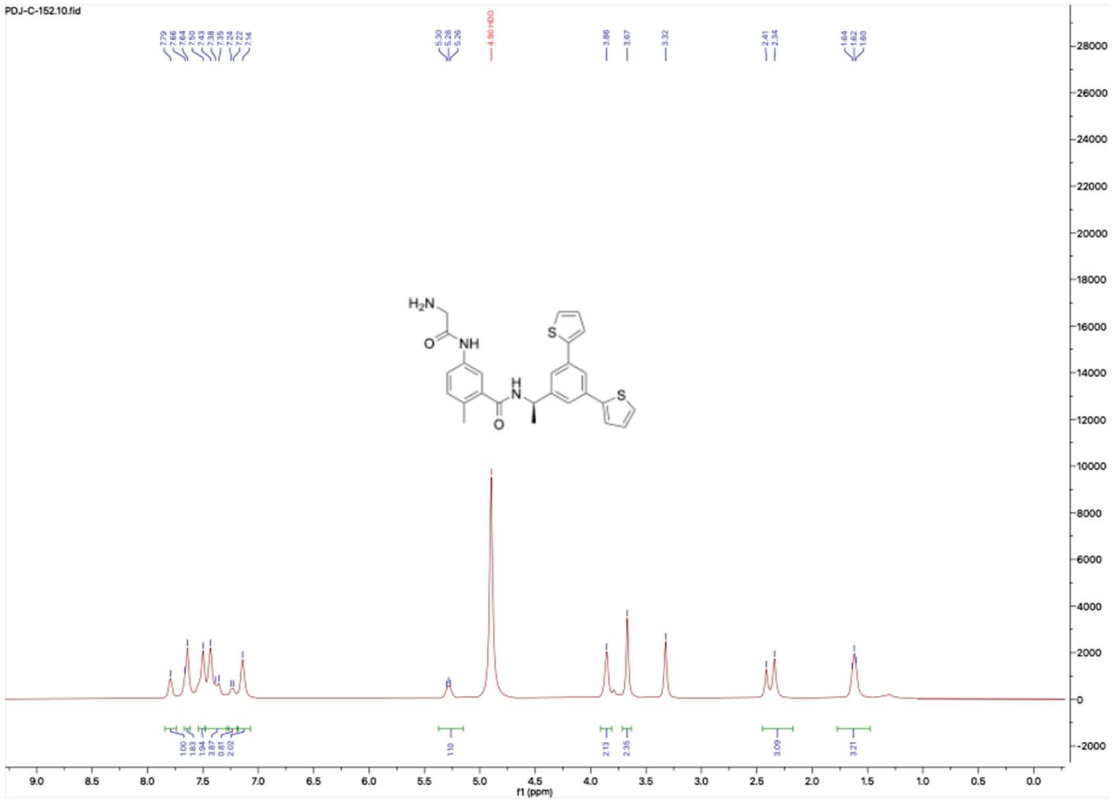

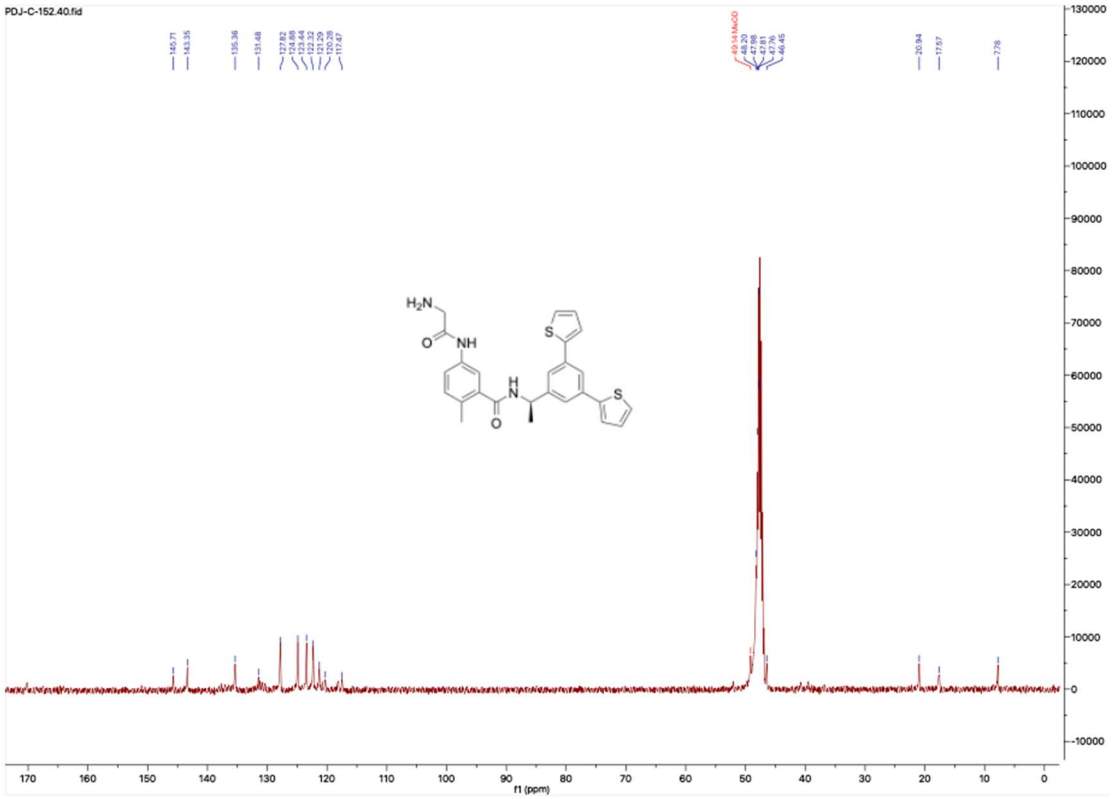

HNMR and CNMR spectra of Jun12111

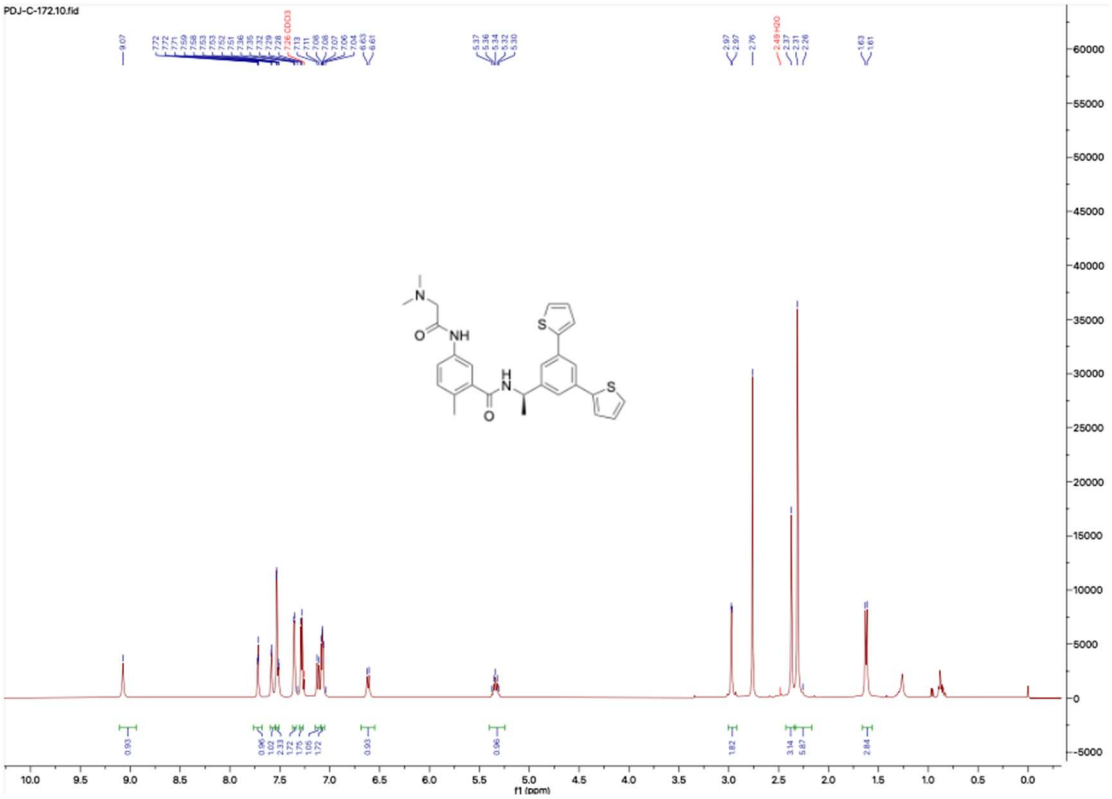

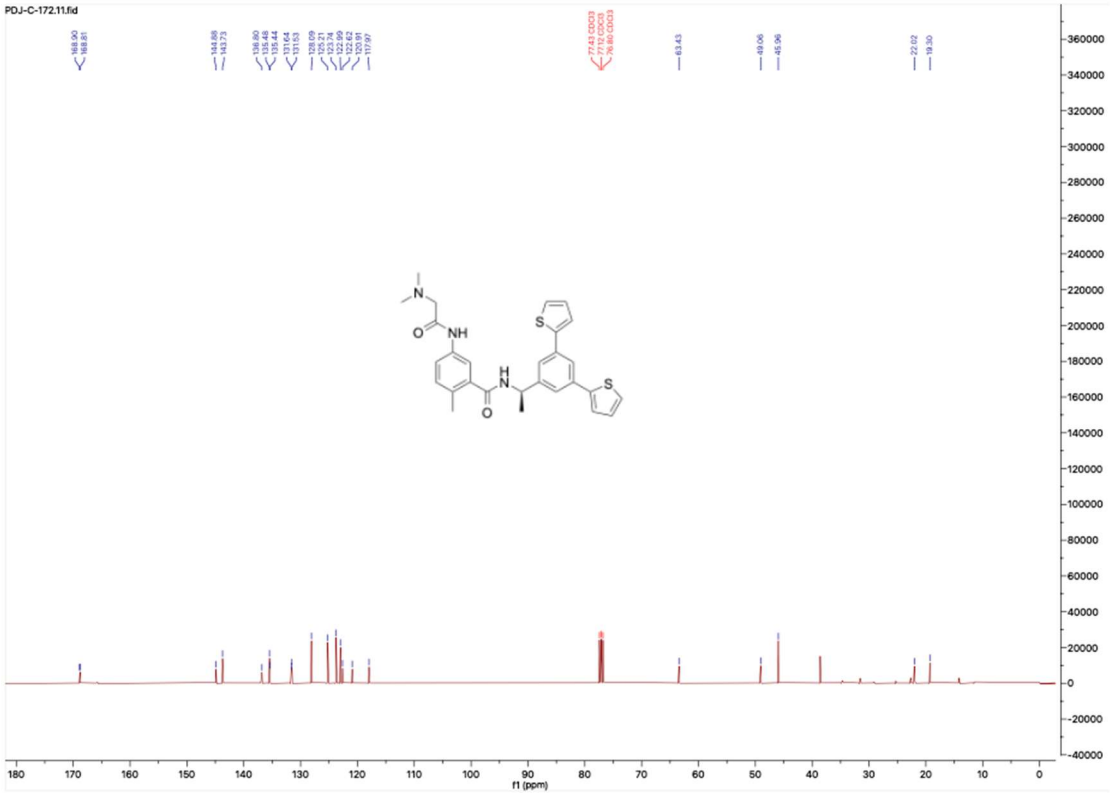

HNMR and CNMR spectra of Jun11945

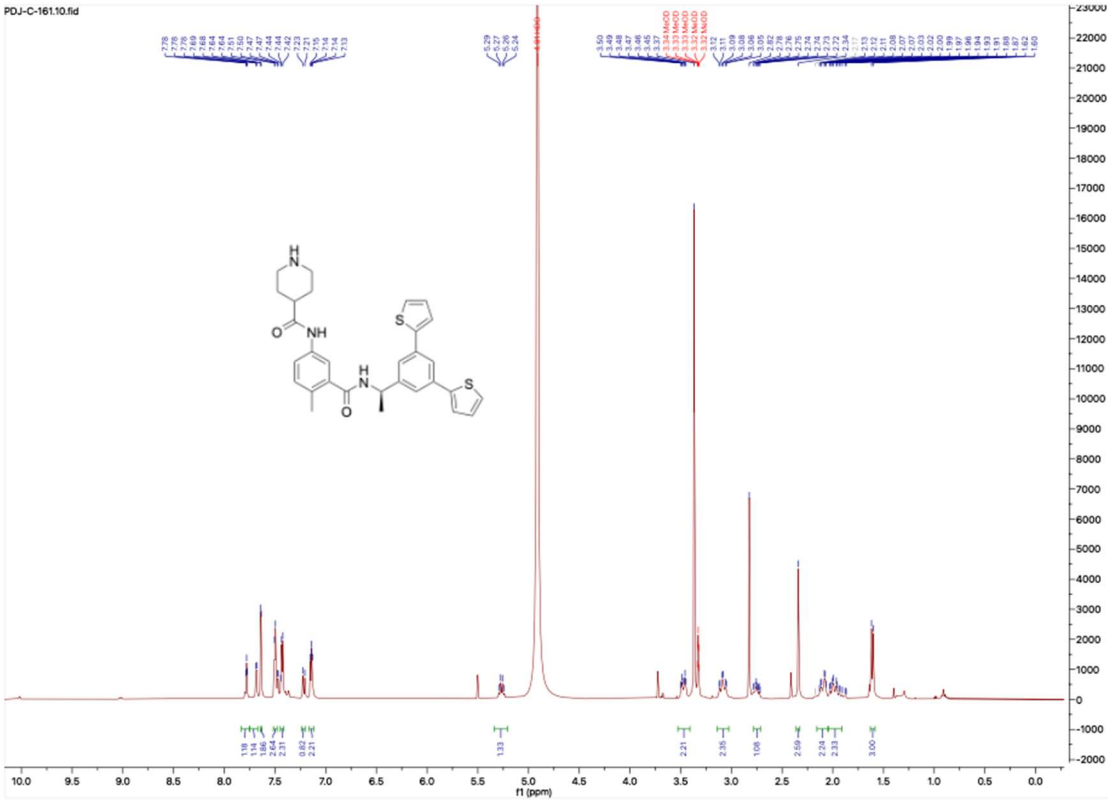

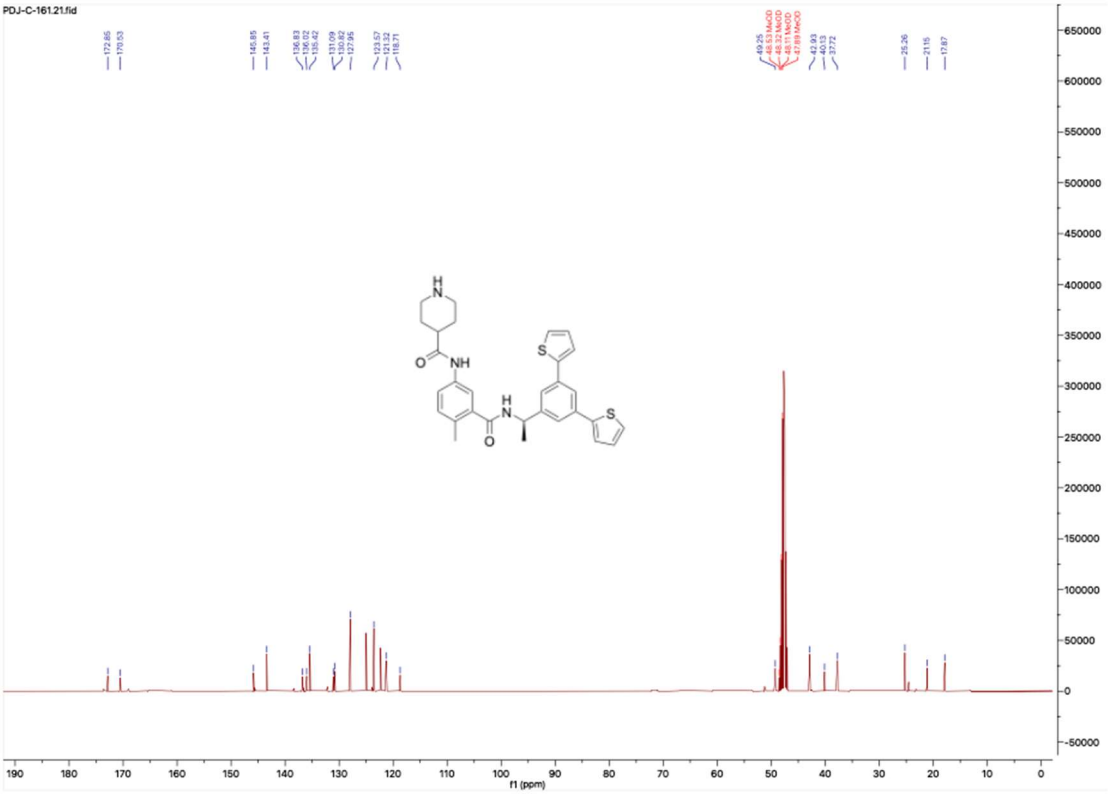

HNMR and CNMR spectra of A-6

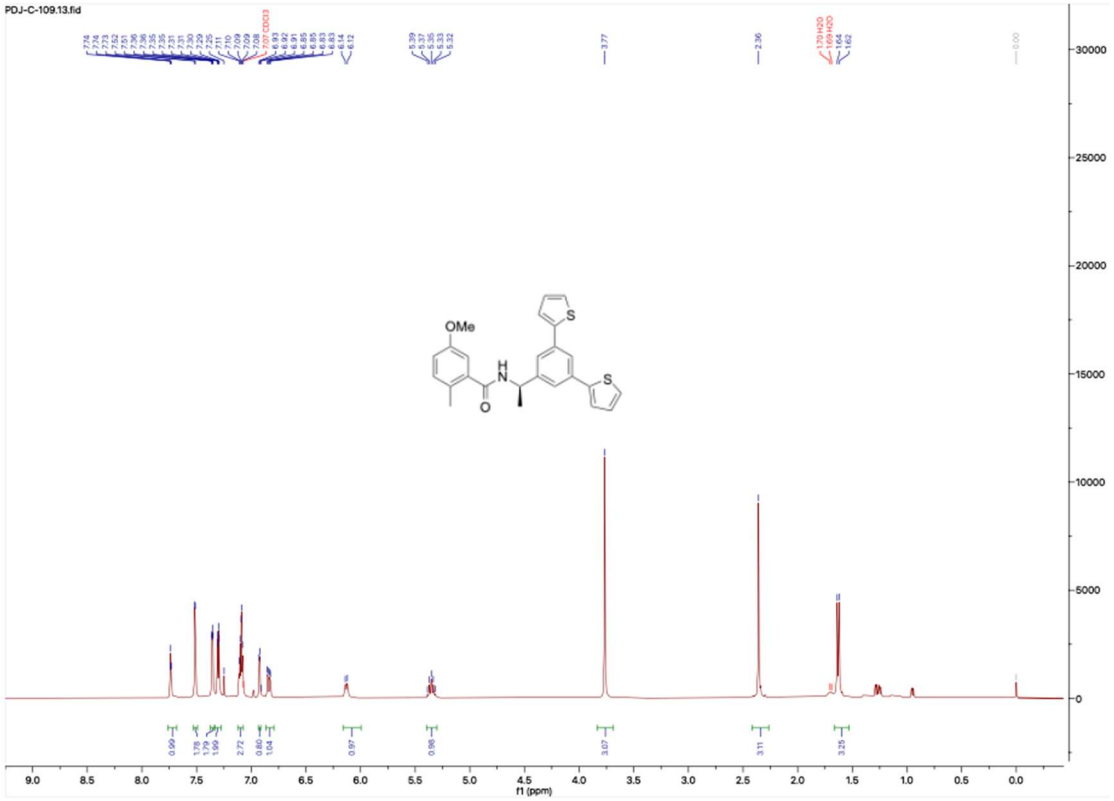

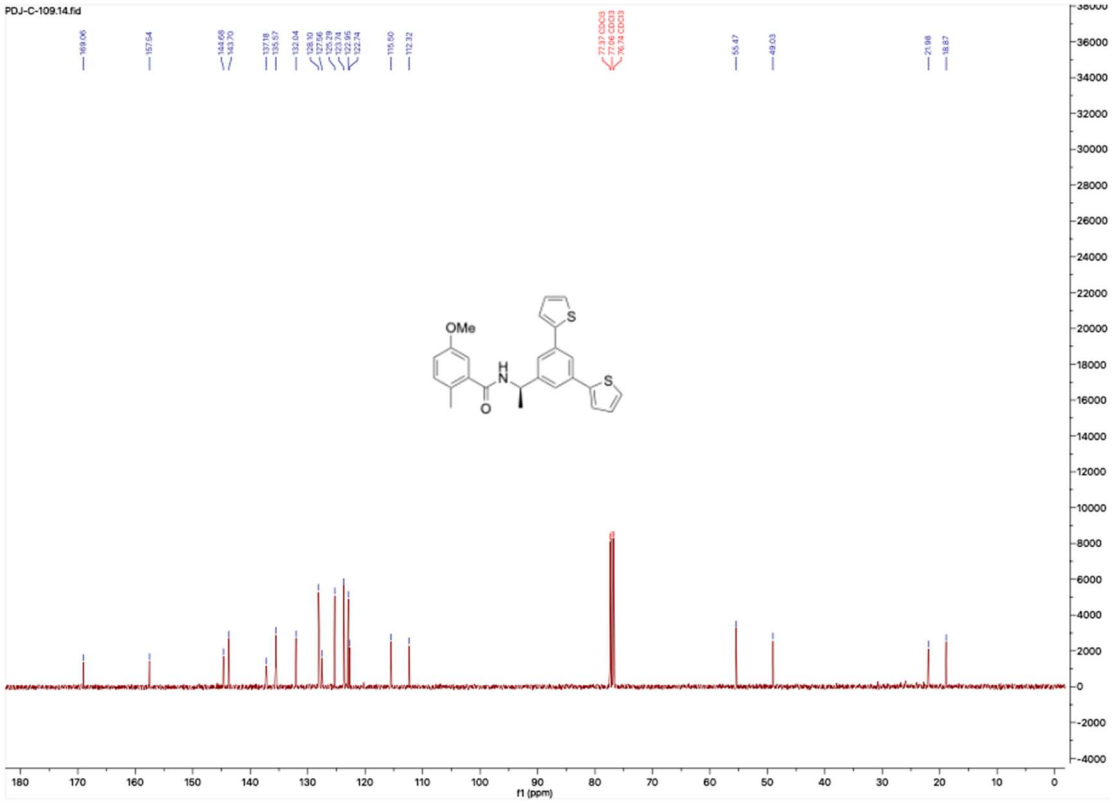

HNMR and CNMR spectra of A-7

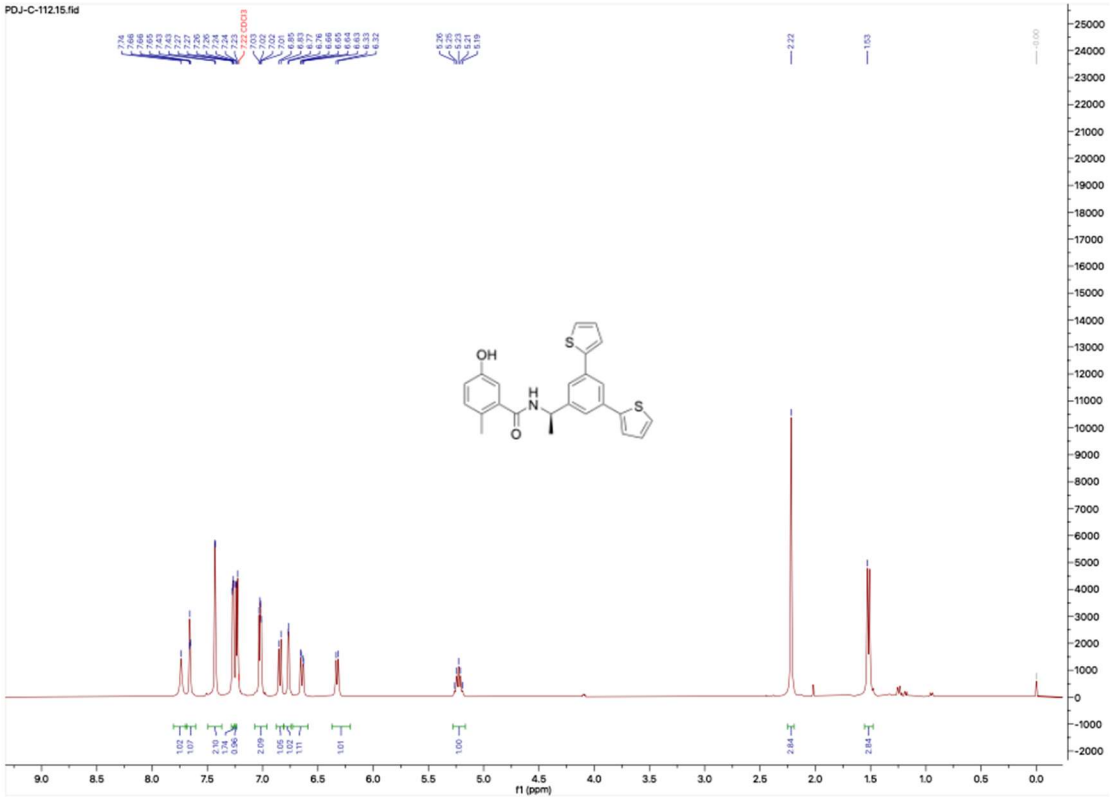

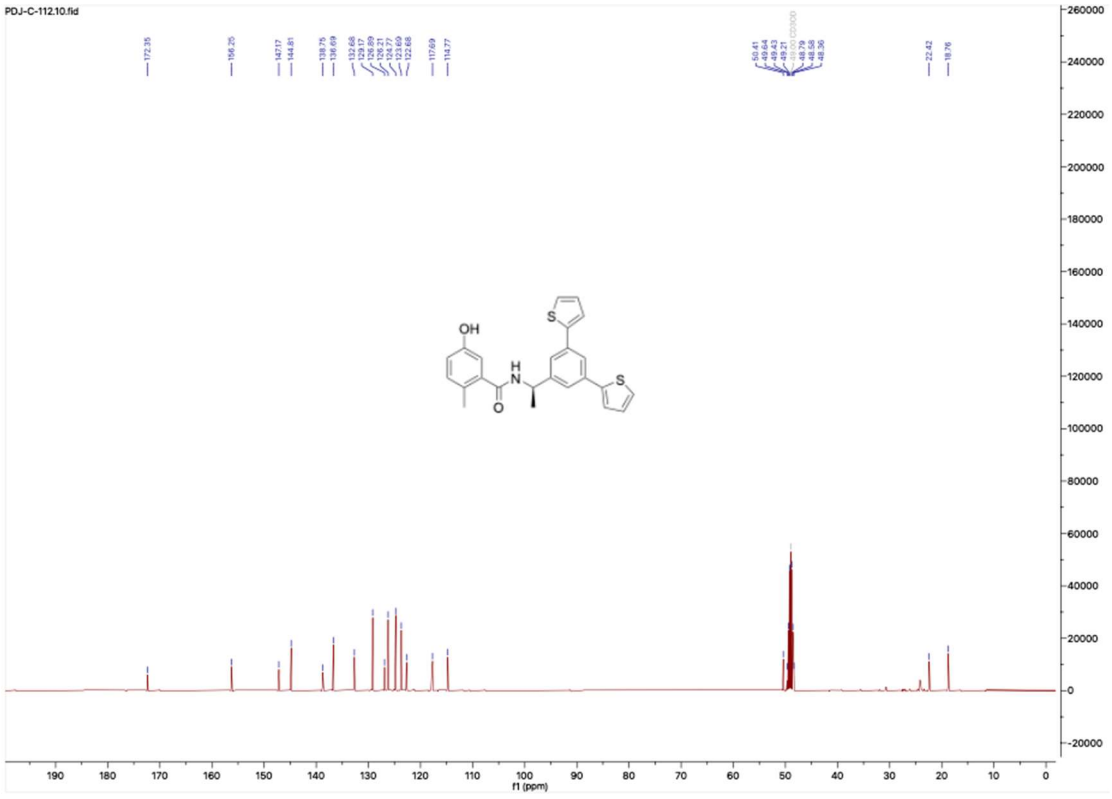

HNMR and CNMR spectra of Jun11874

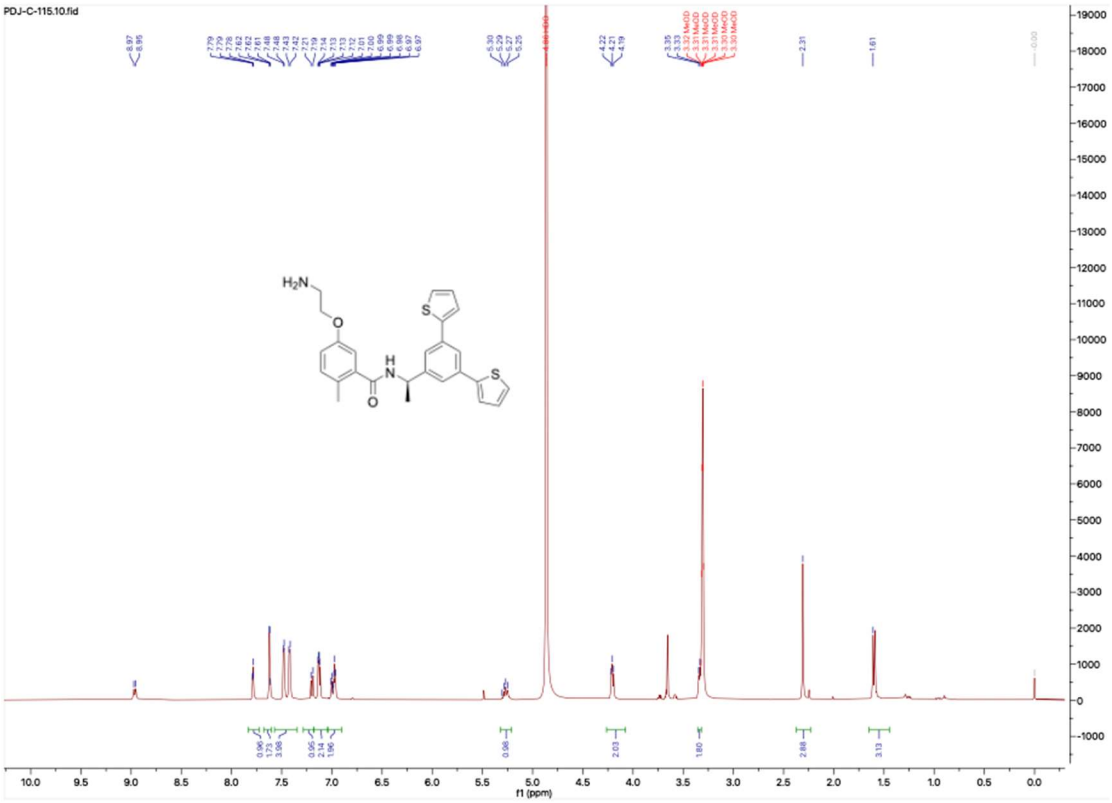

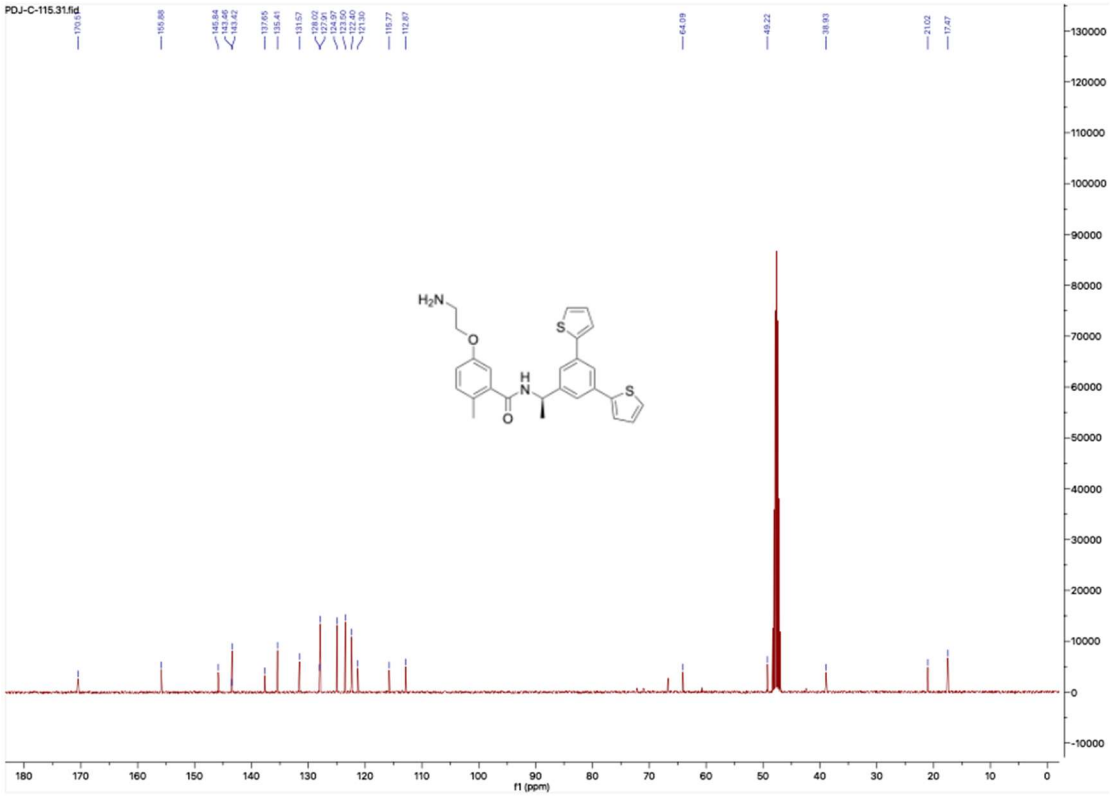

HNMR and CNMR spectra of Jun11875

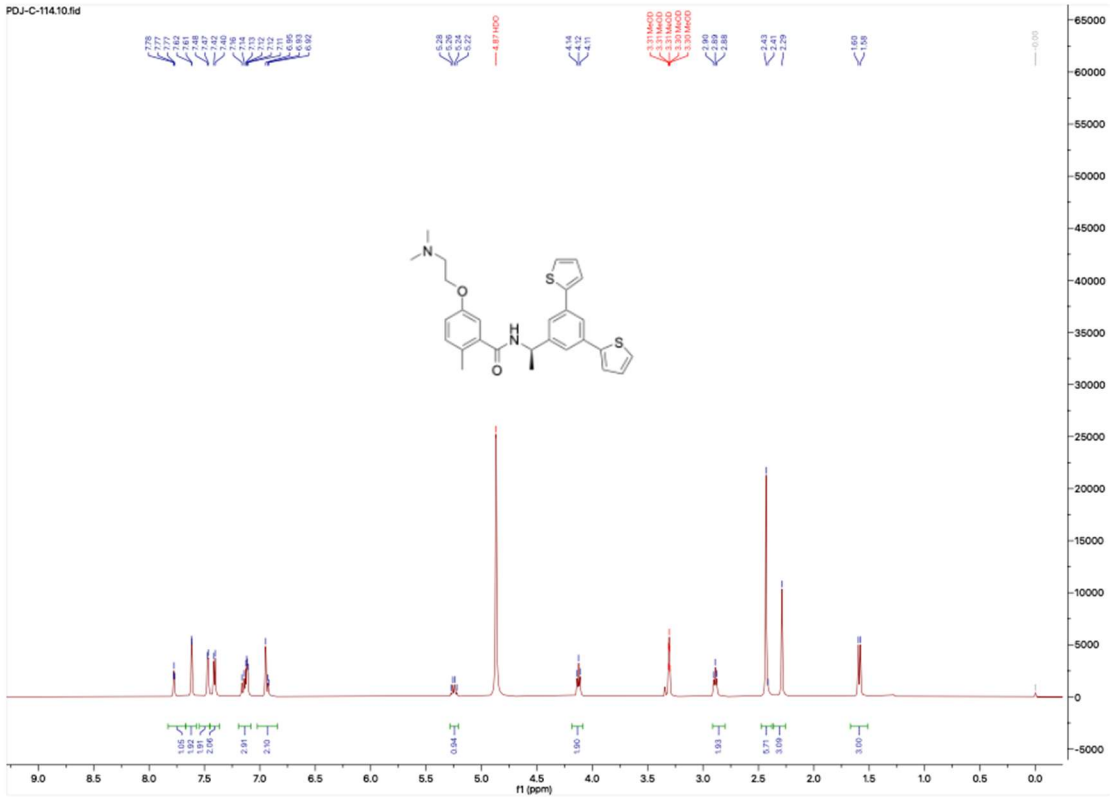

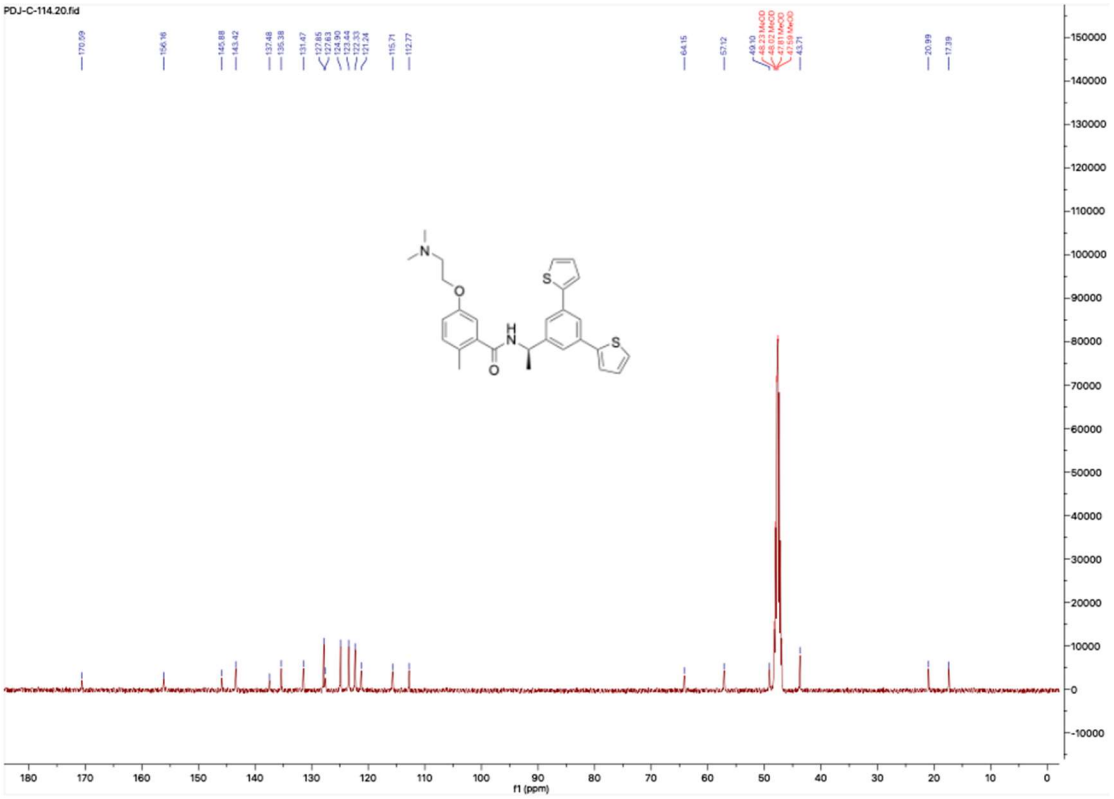

HNMR and CNMR spectra of Jun11898

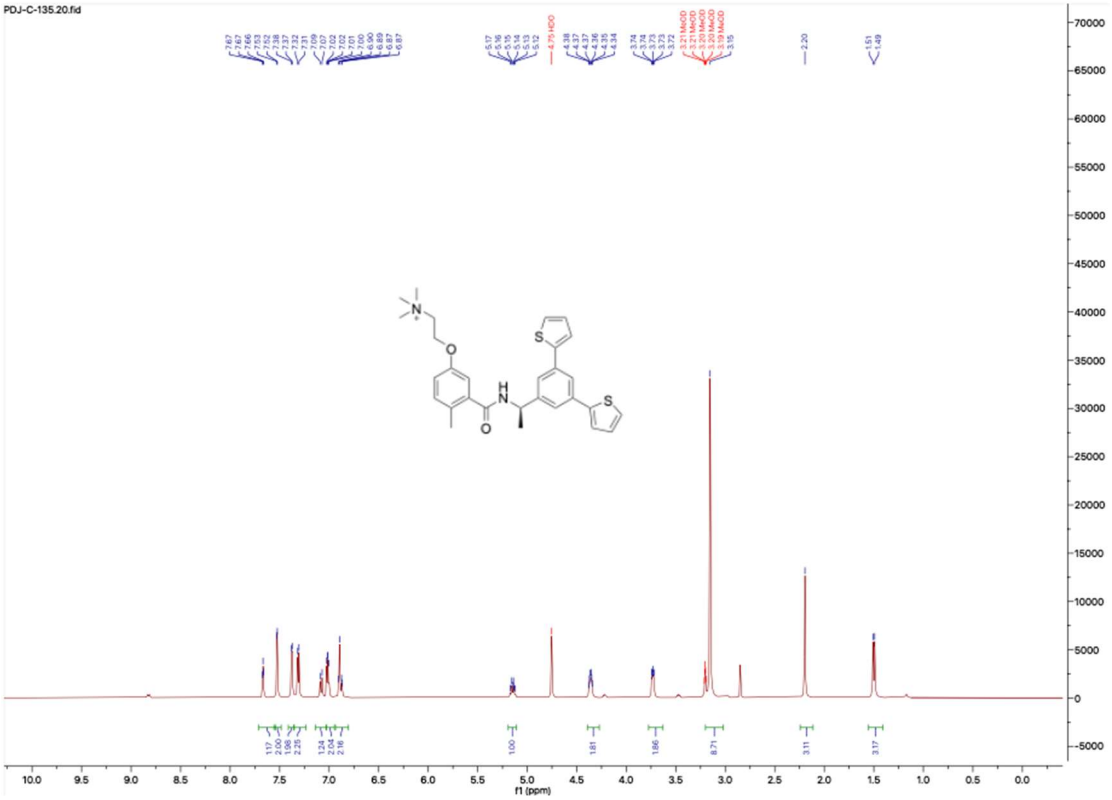

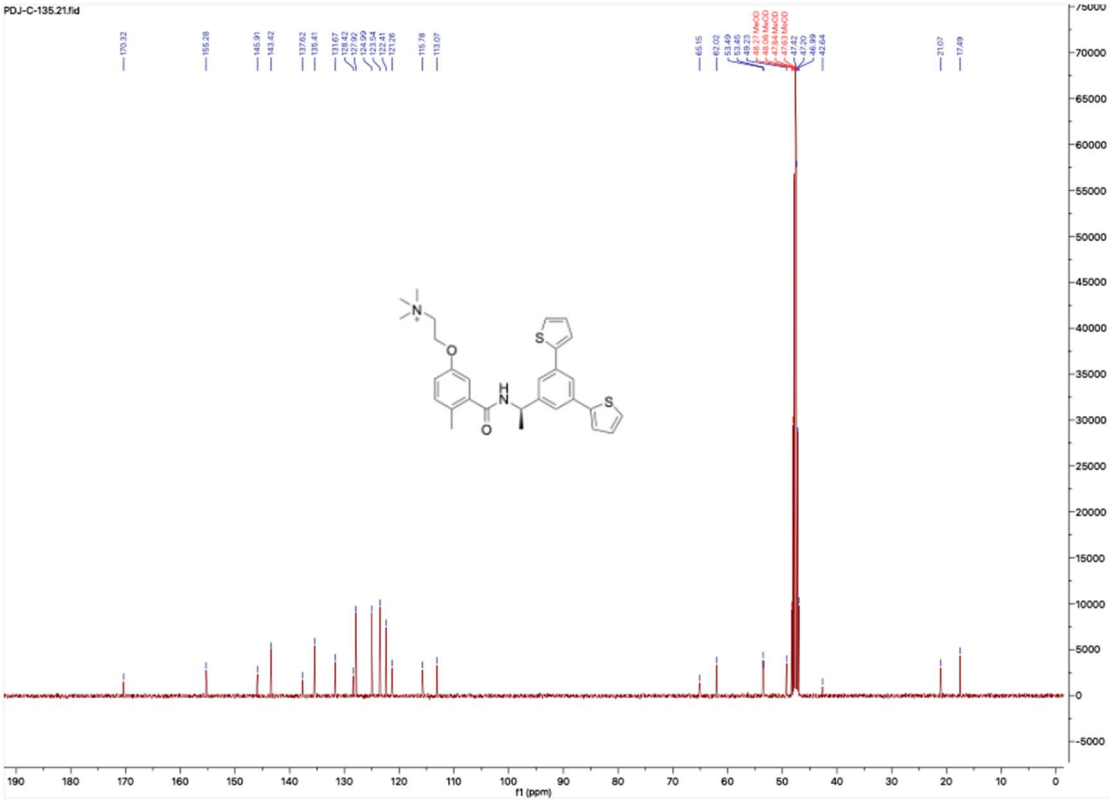

HNMR and CNMR spectra of Jun11899

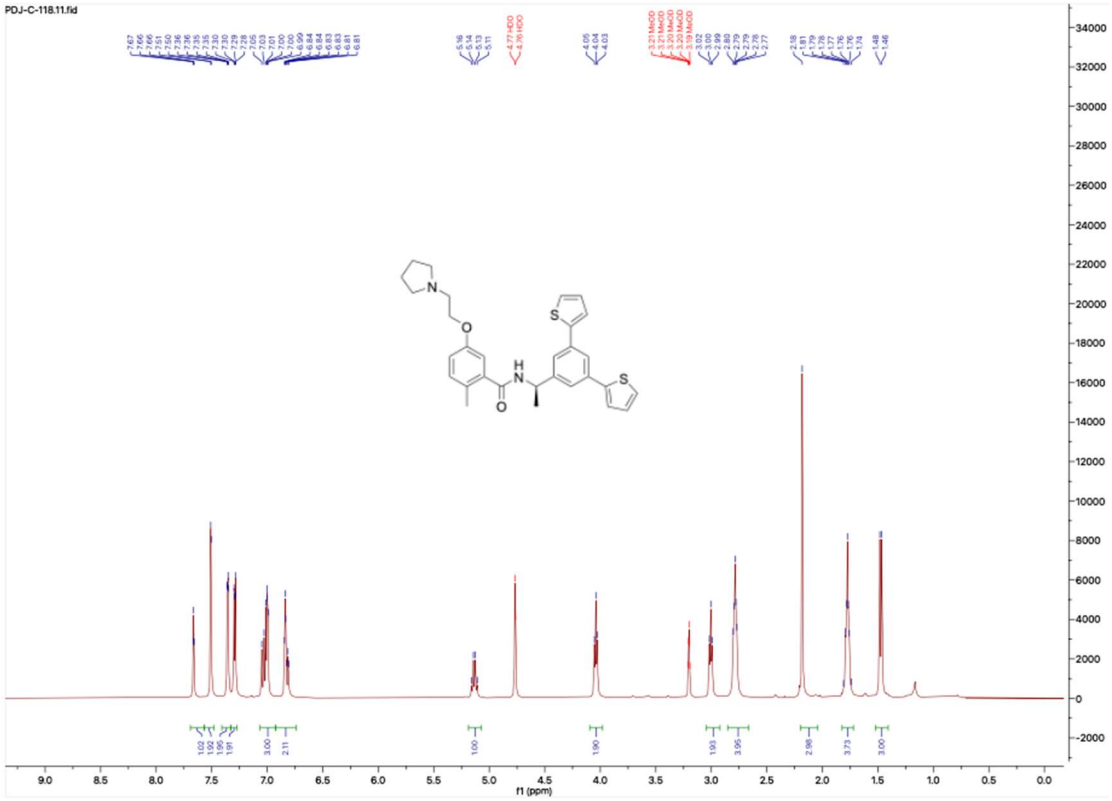

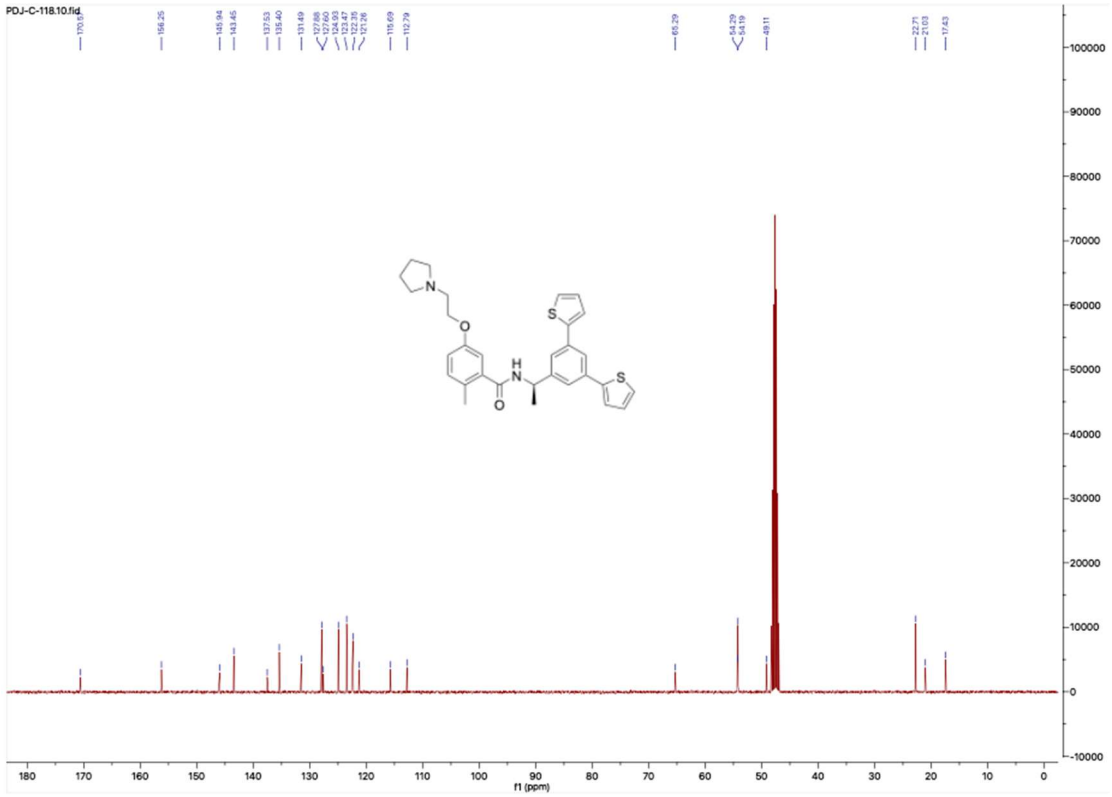

HNMR and CNMR spectra of Jun118910

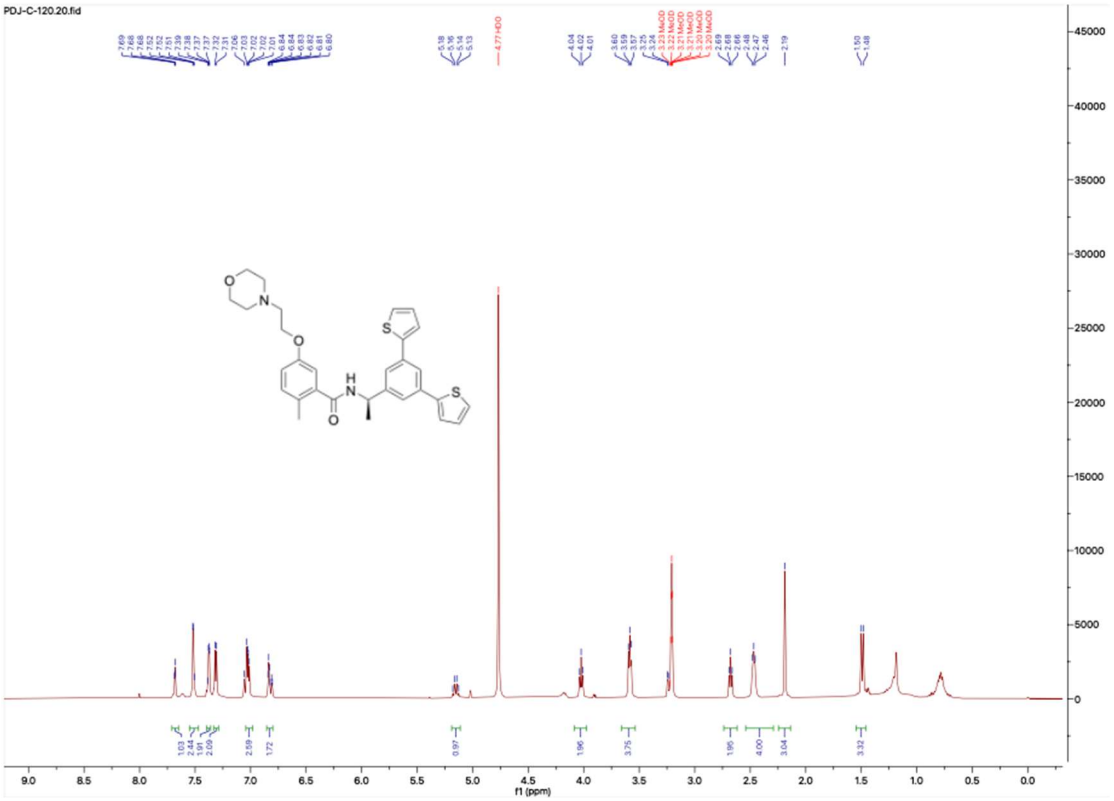

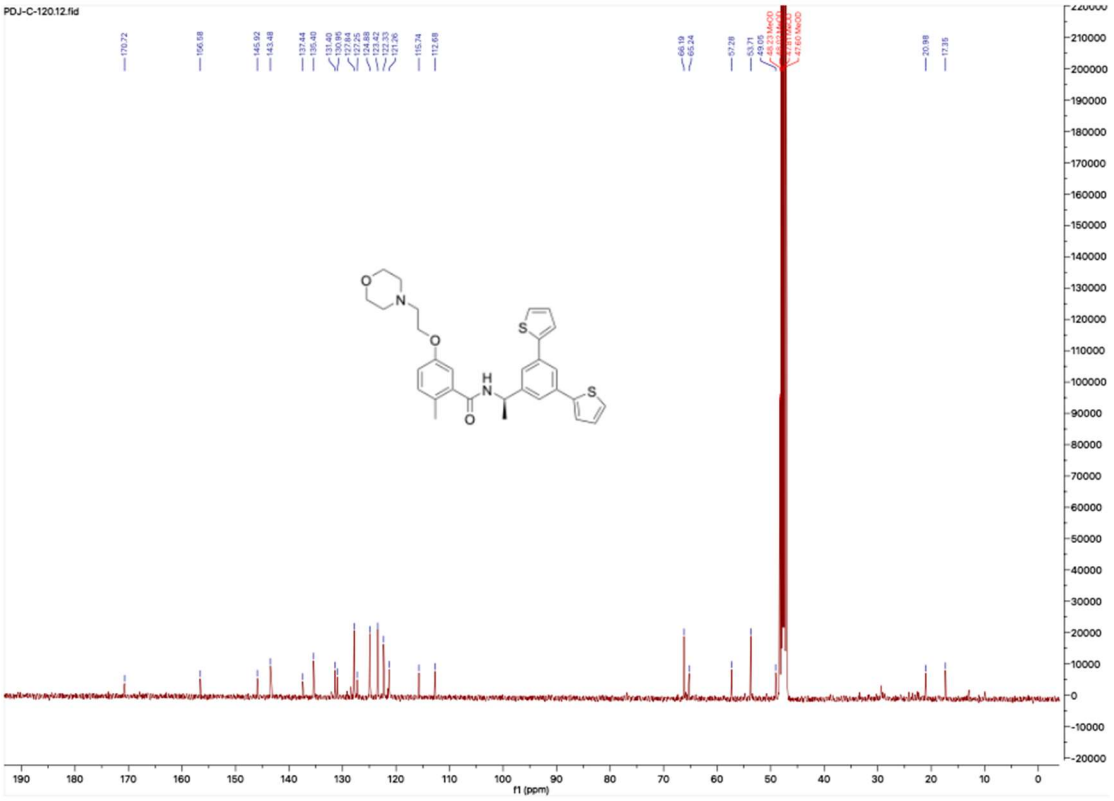

HNMR and CNMR spectra of B-2

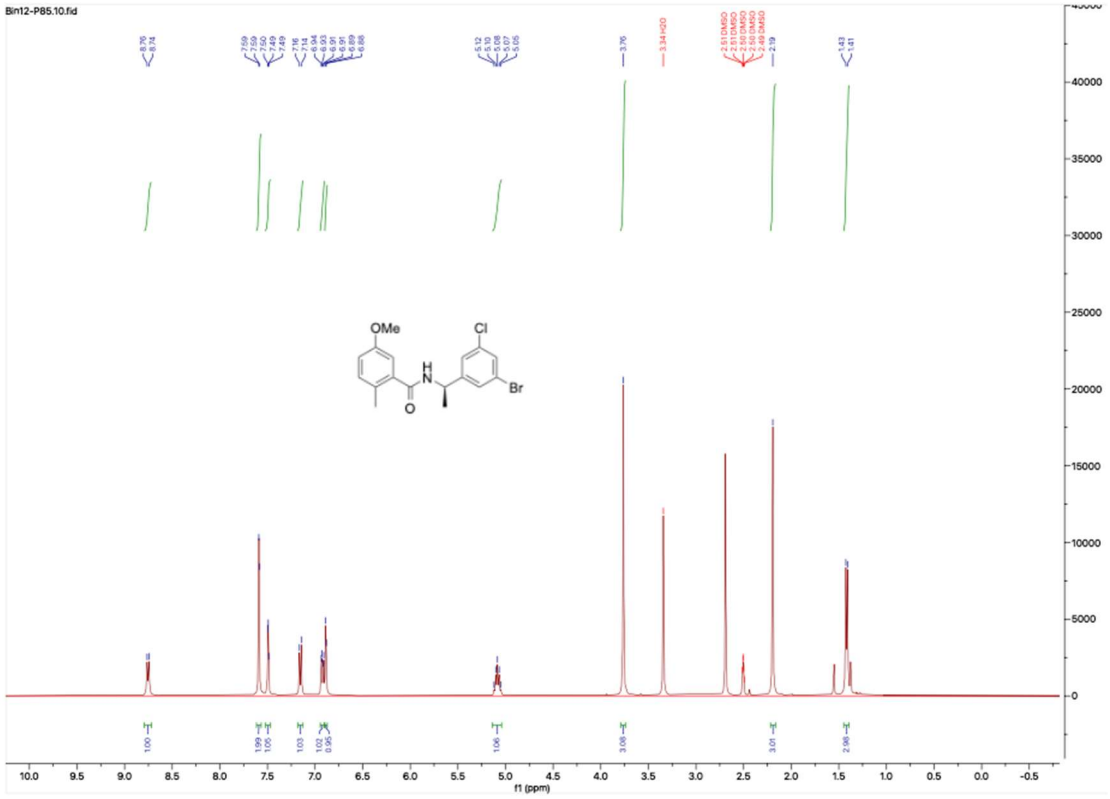

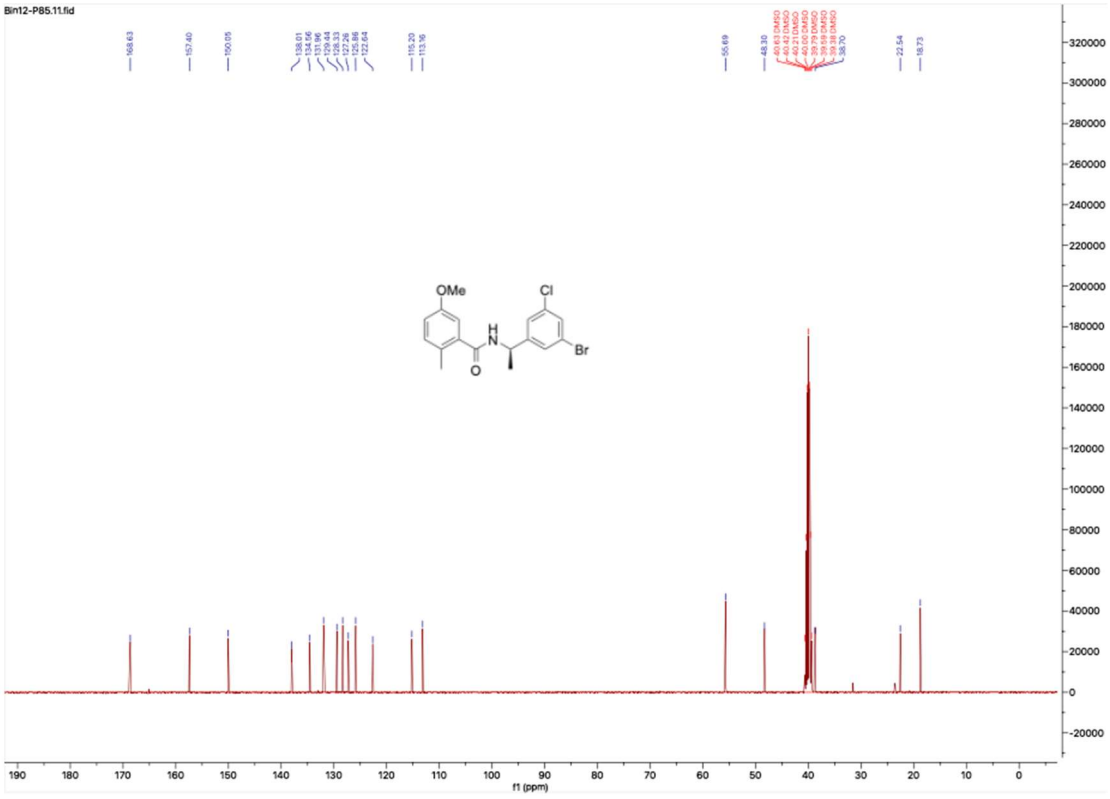

HNMR and CNMR spectra of B-3

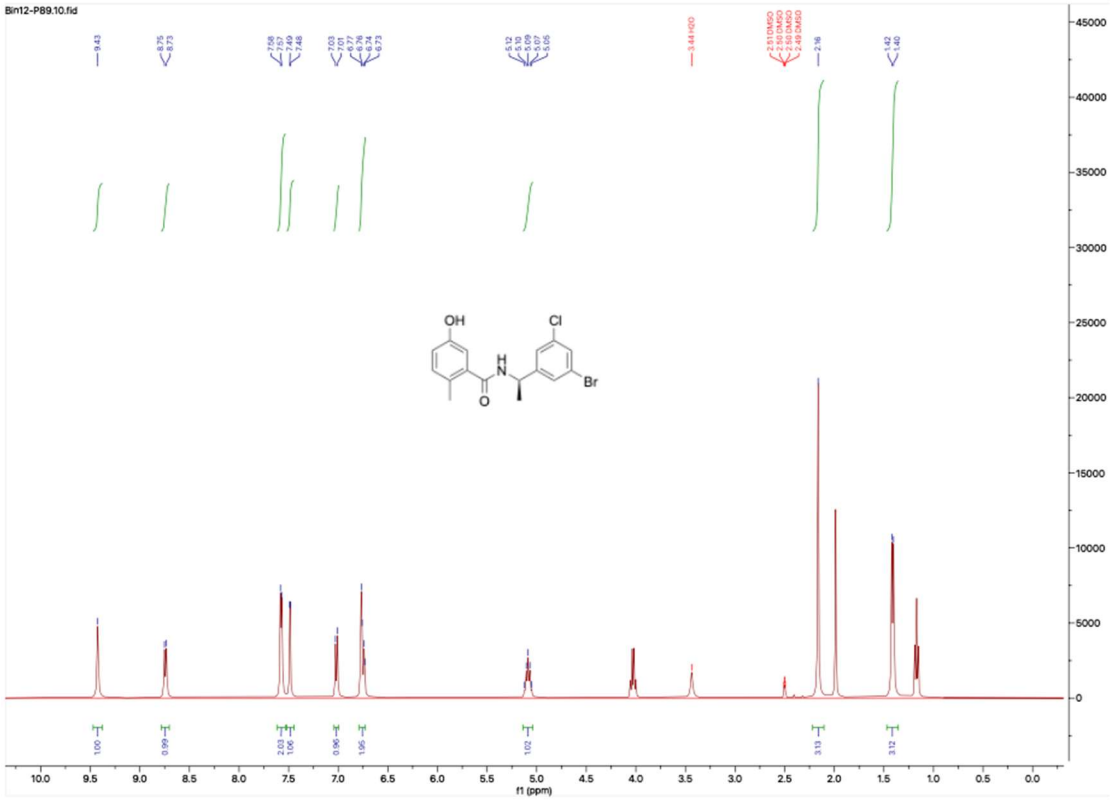

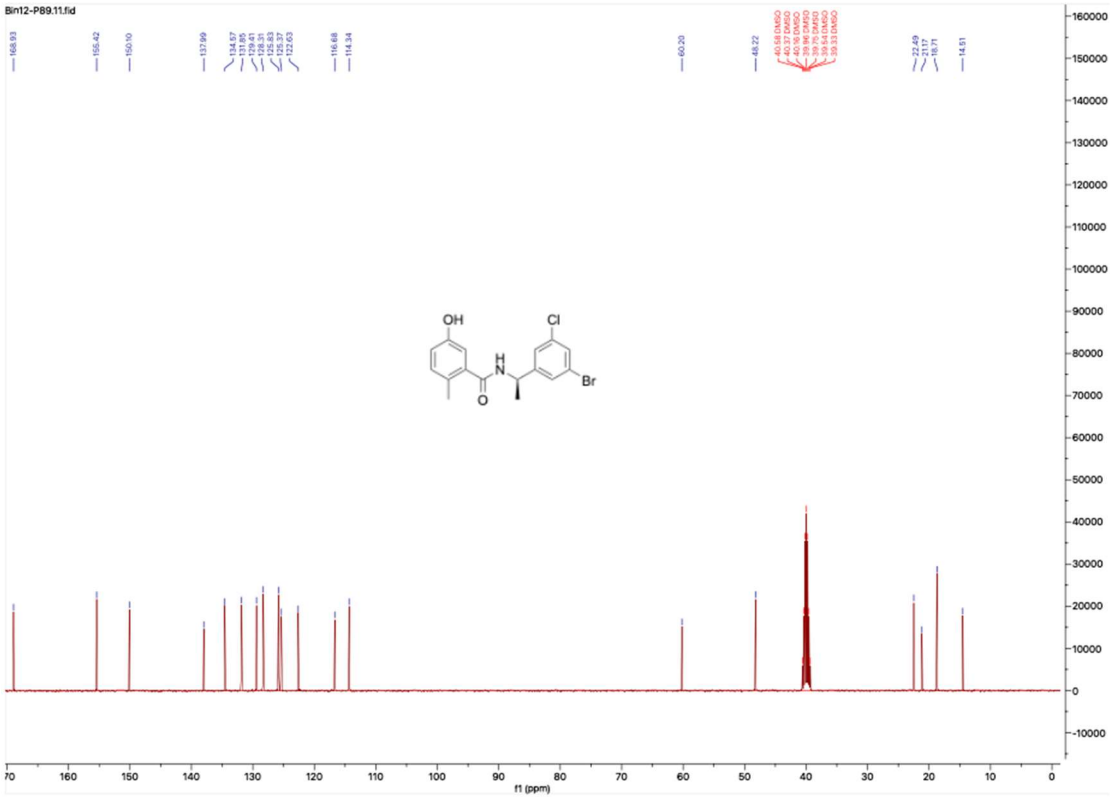

HNMR and CNMR spectra of B-4

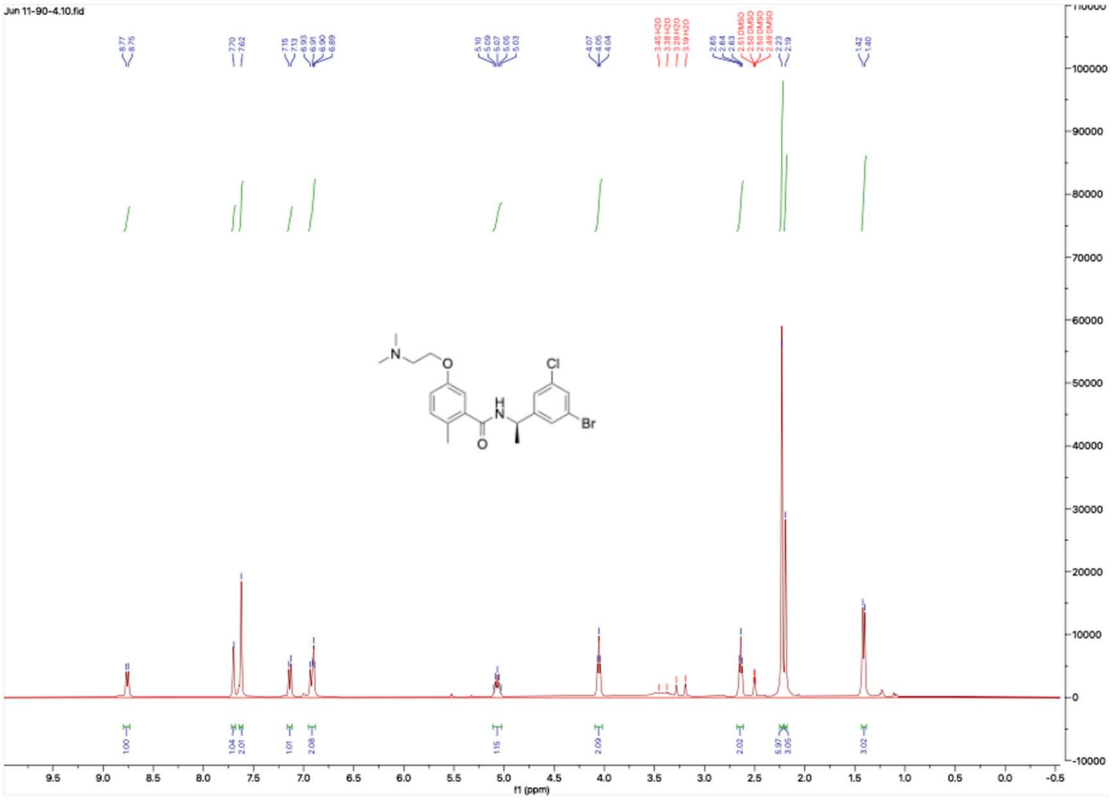

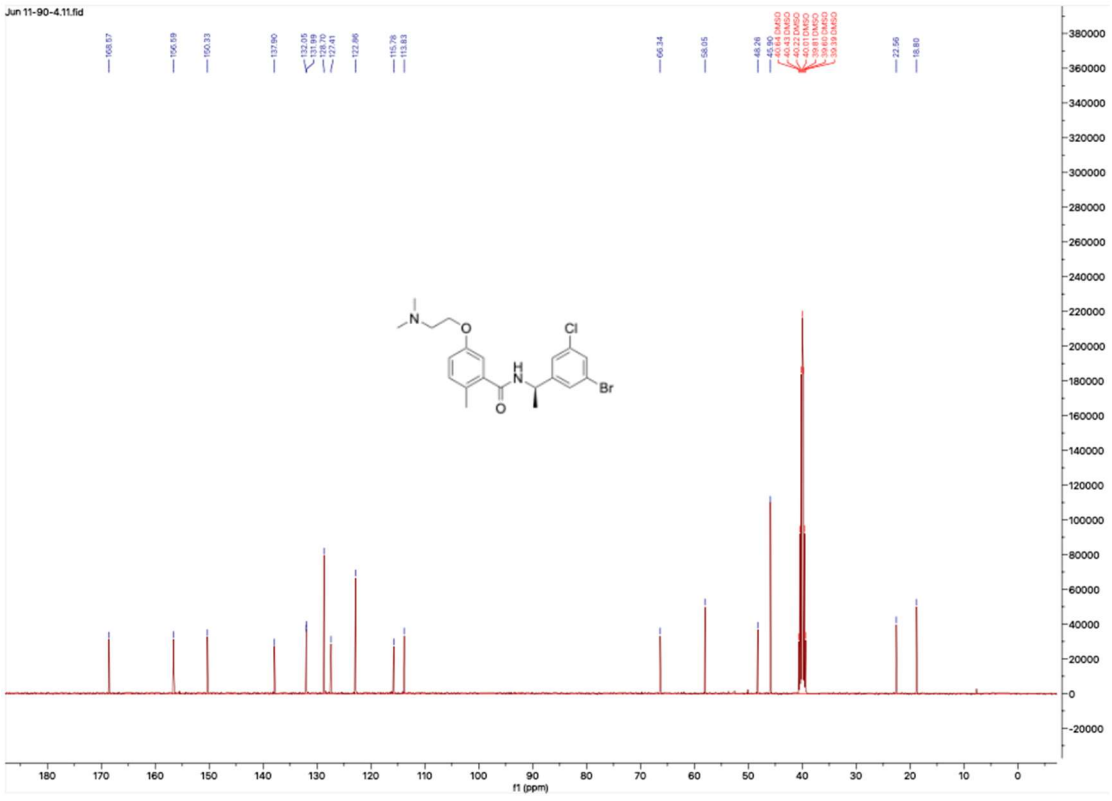

HNMR and CNMR spectra of Jun11931

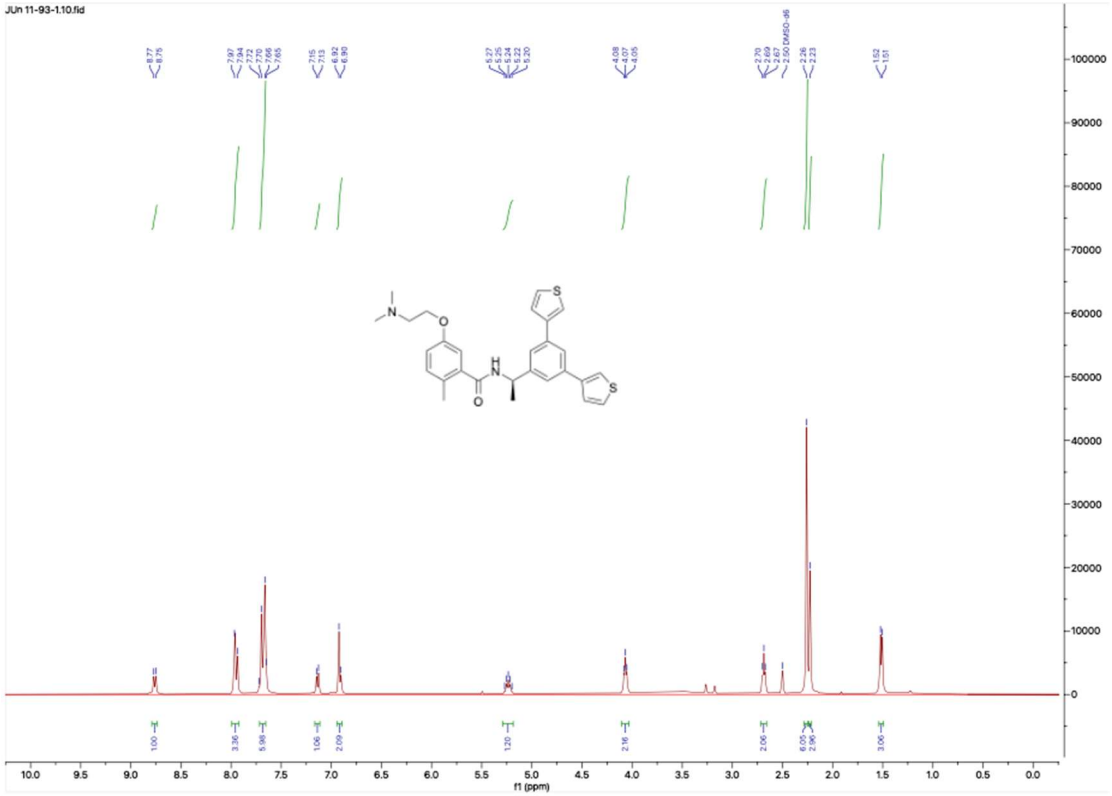

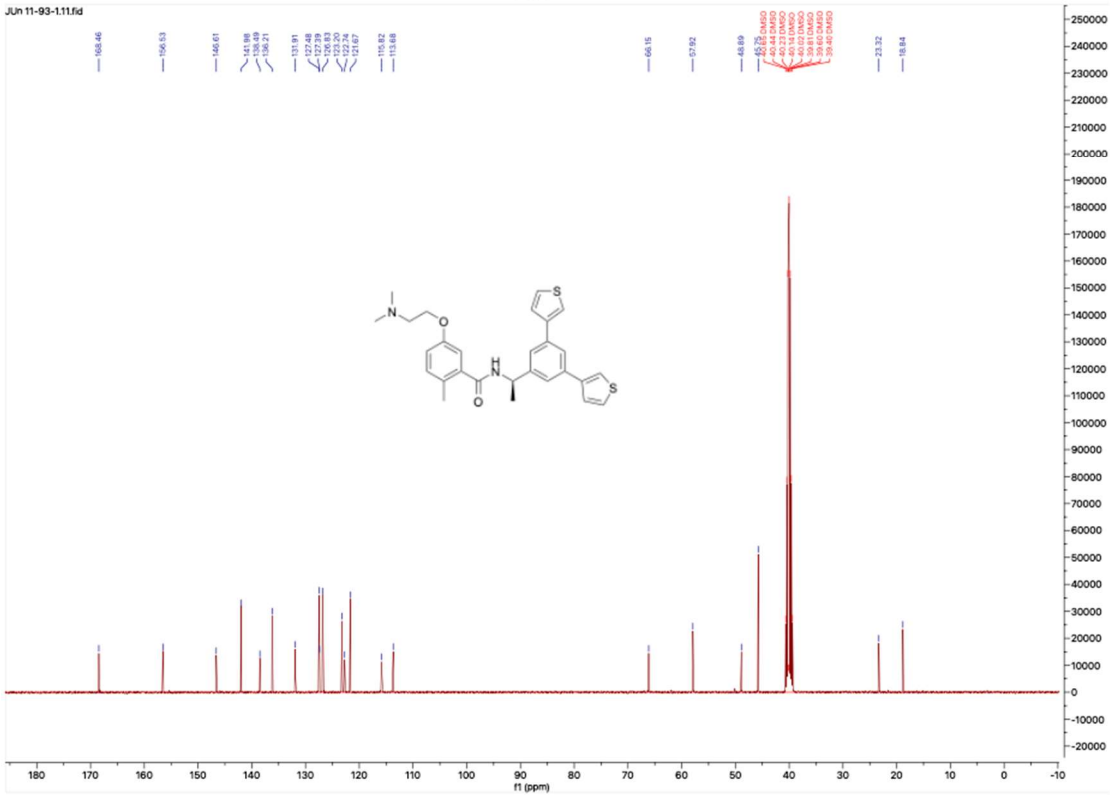

HNMR and CNMR spectra of Jun119415

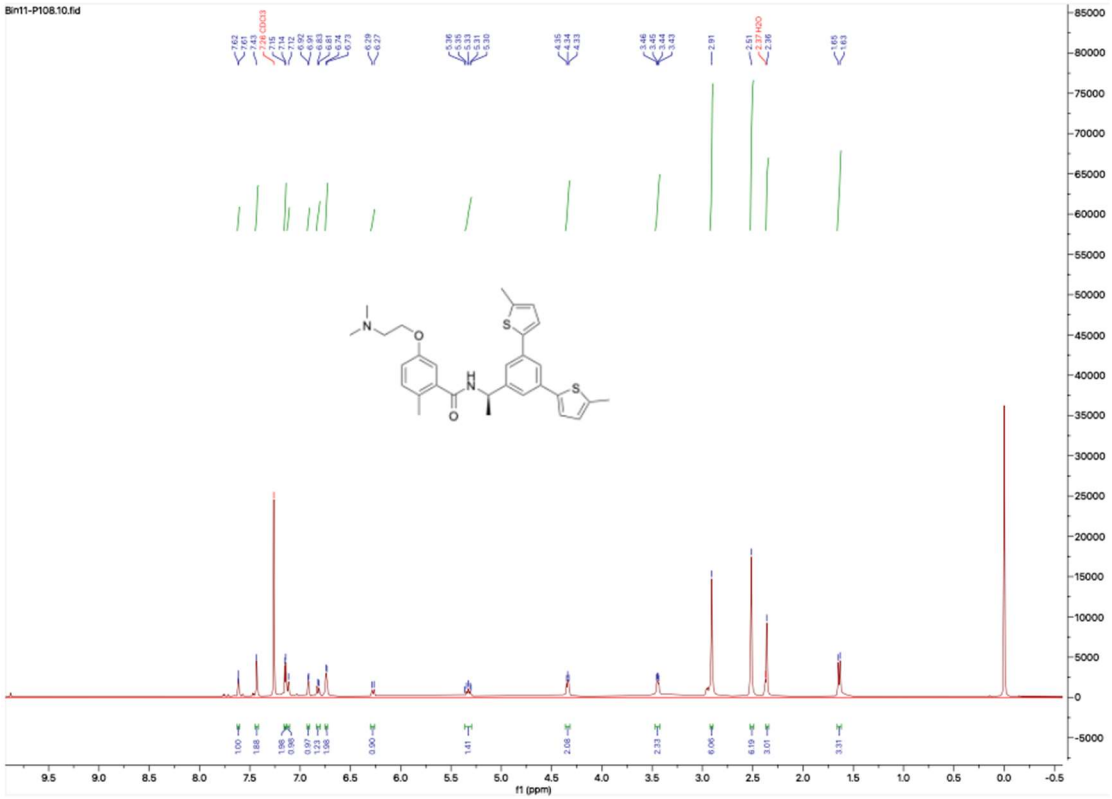

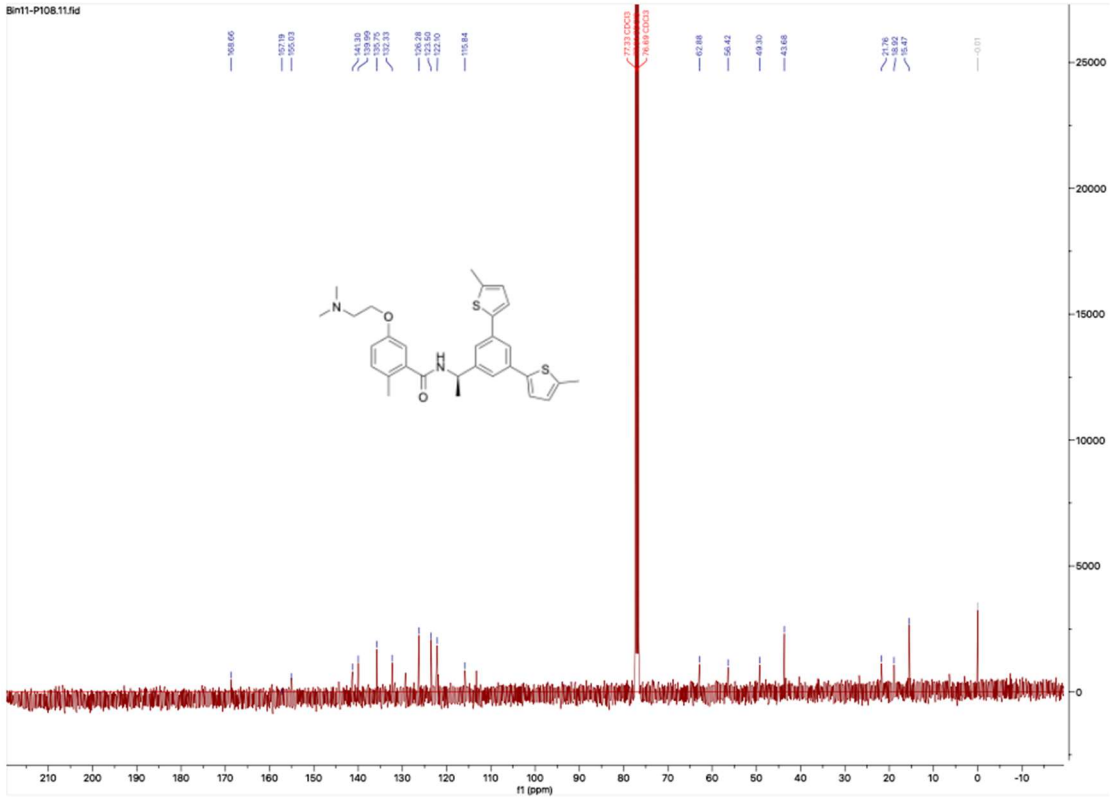

HNMR and CNMR spectra of Jun11903

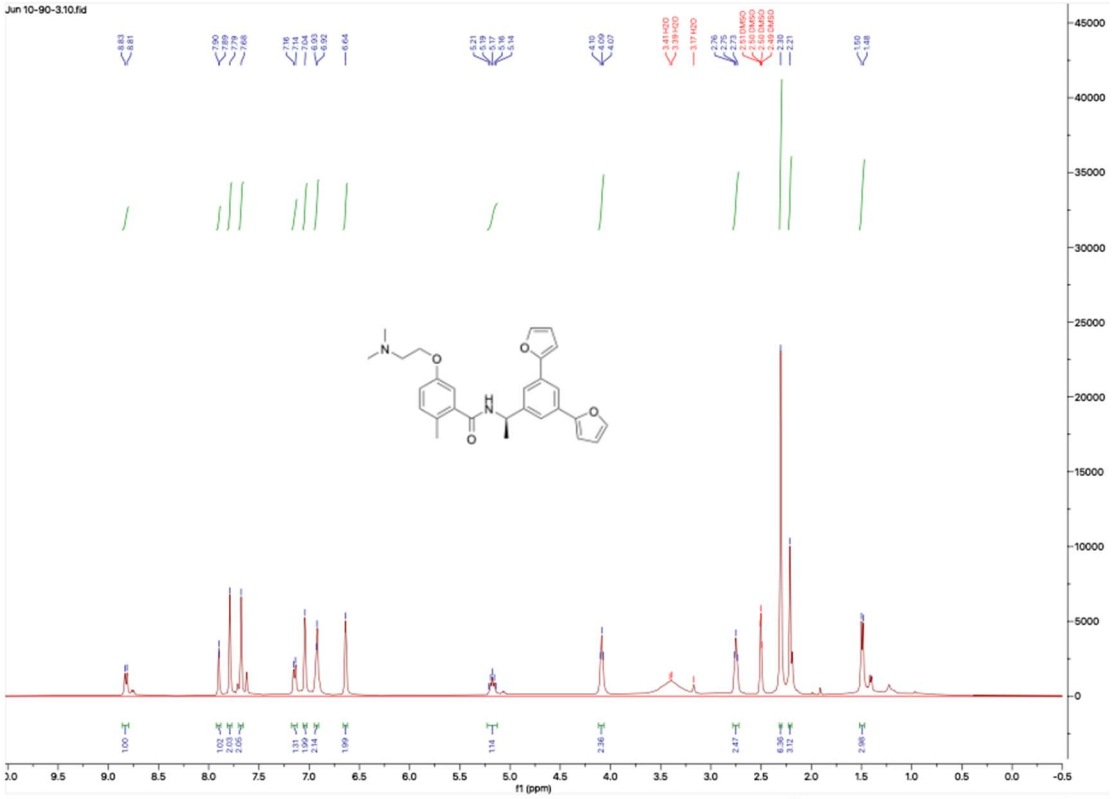

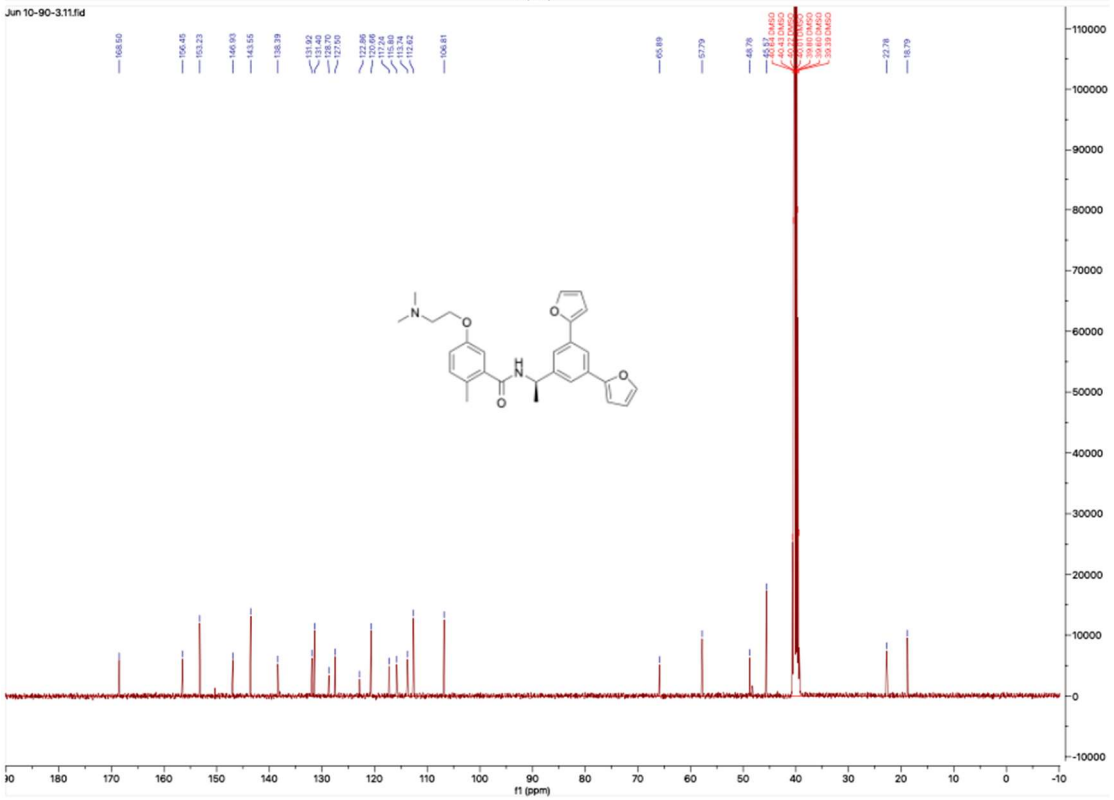

HNMR and CNMR spectra of Jun11932

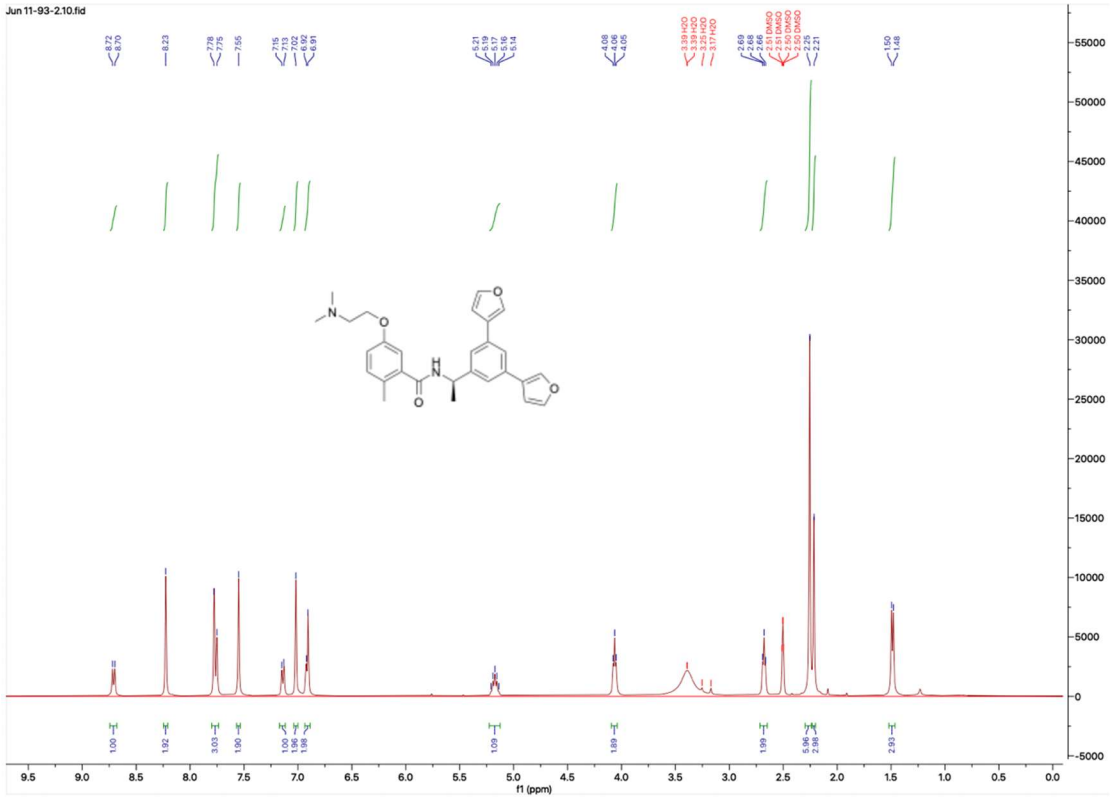

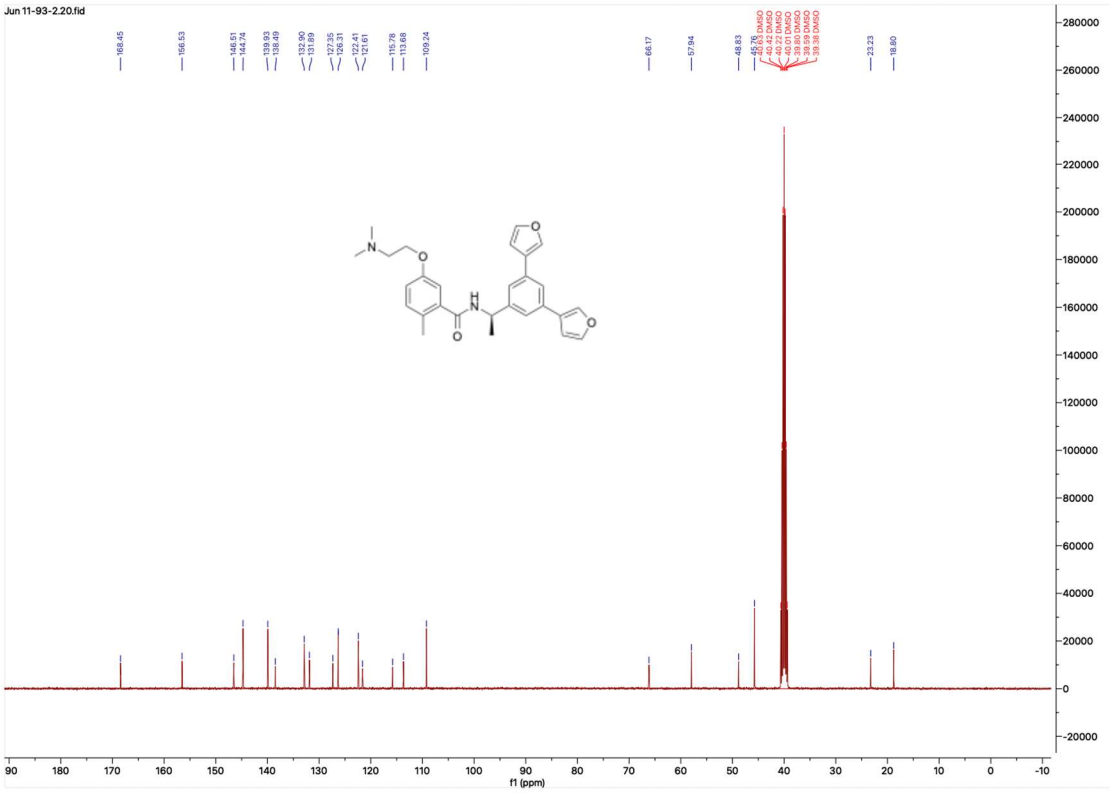

HNMR and CNMR spectra of Jun11934

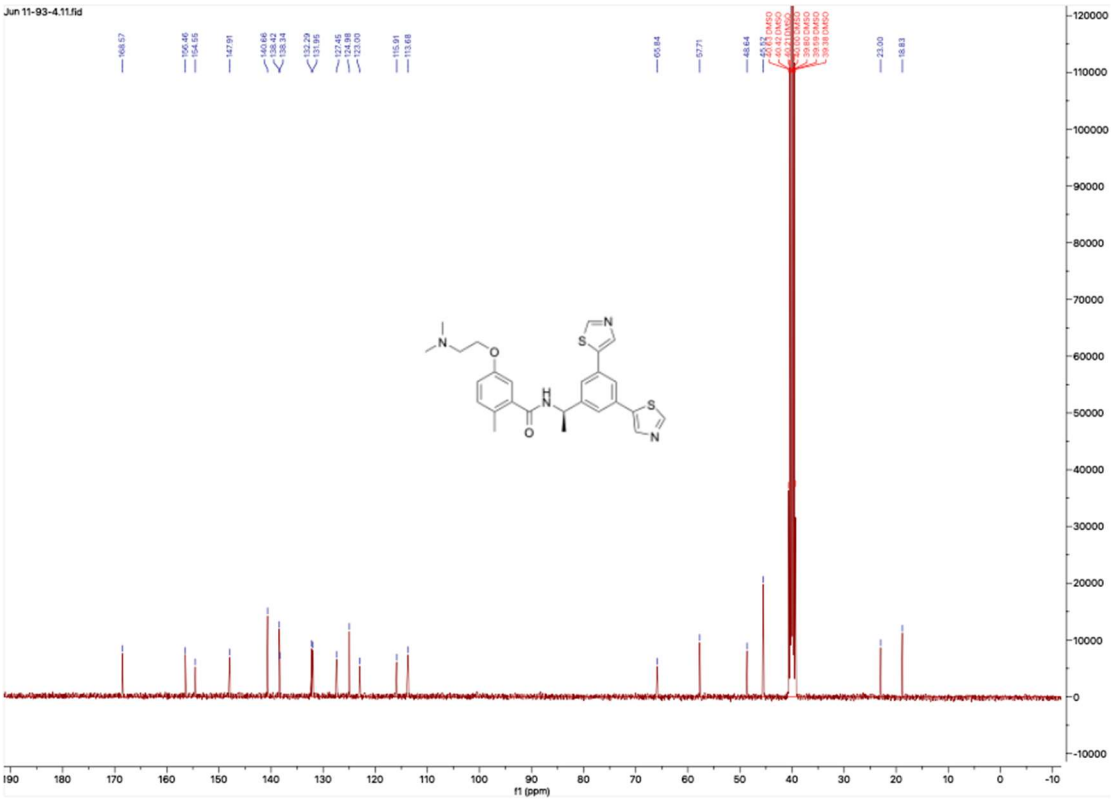

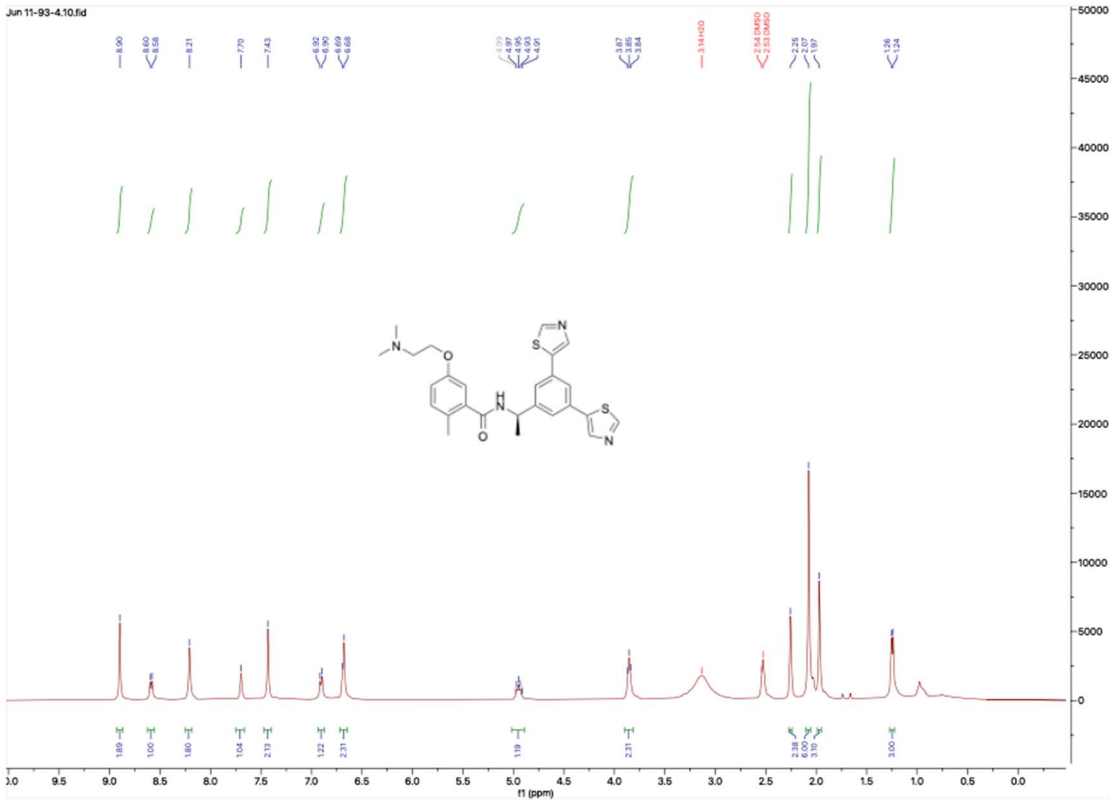

HNMR and CNMR spectra of Jun11933

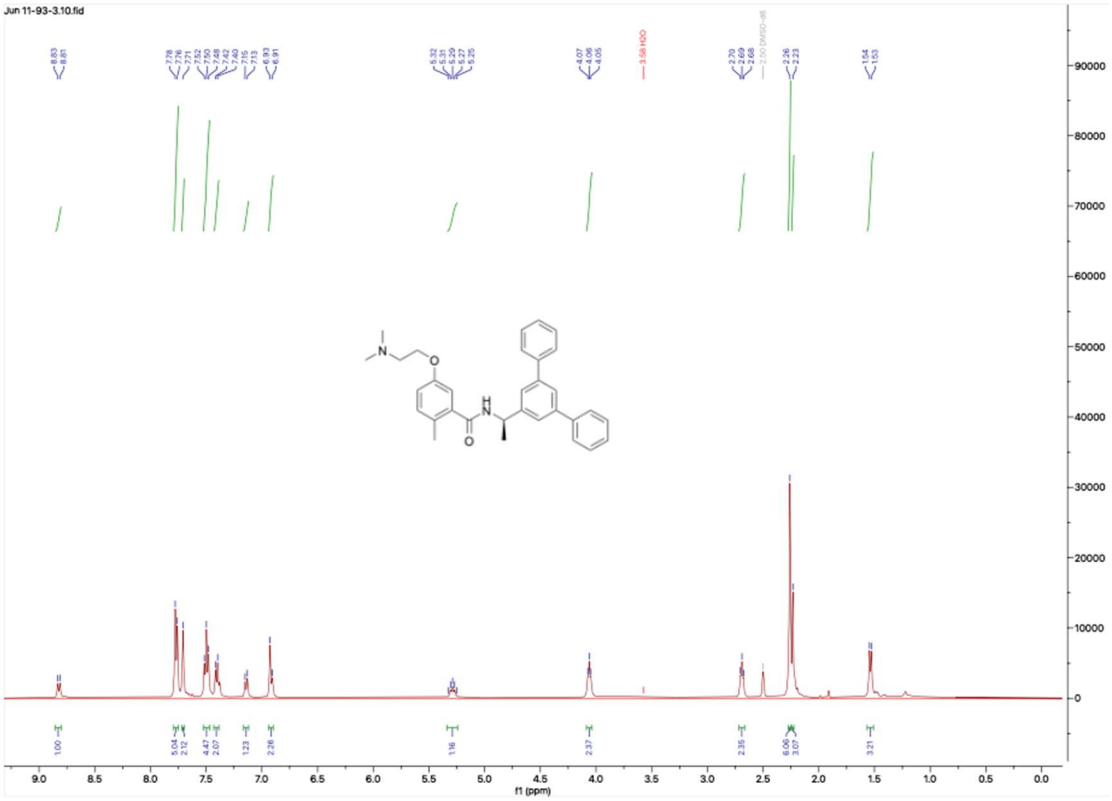

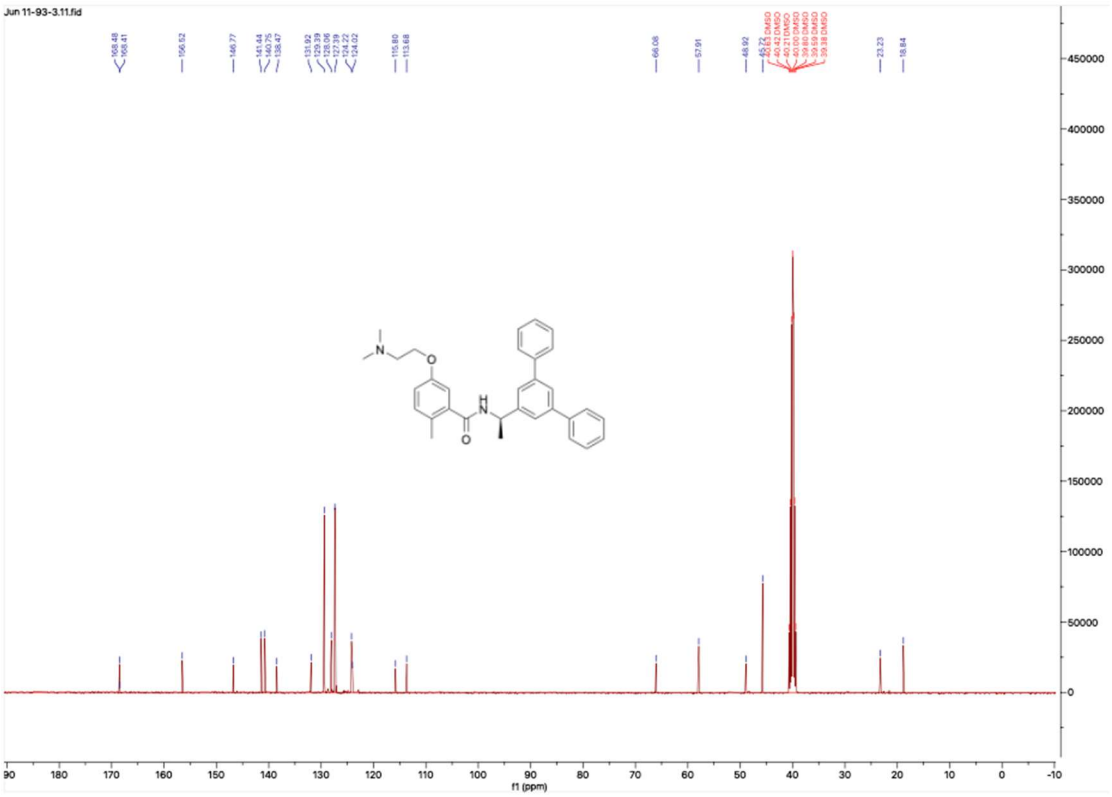

HNMR and CNMR spectra of Jun11943

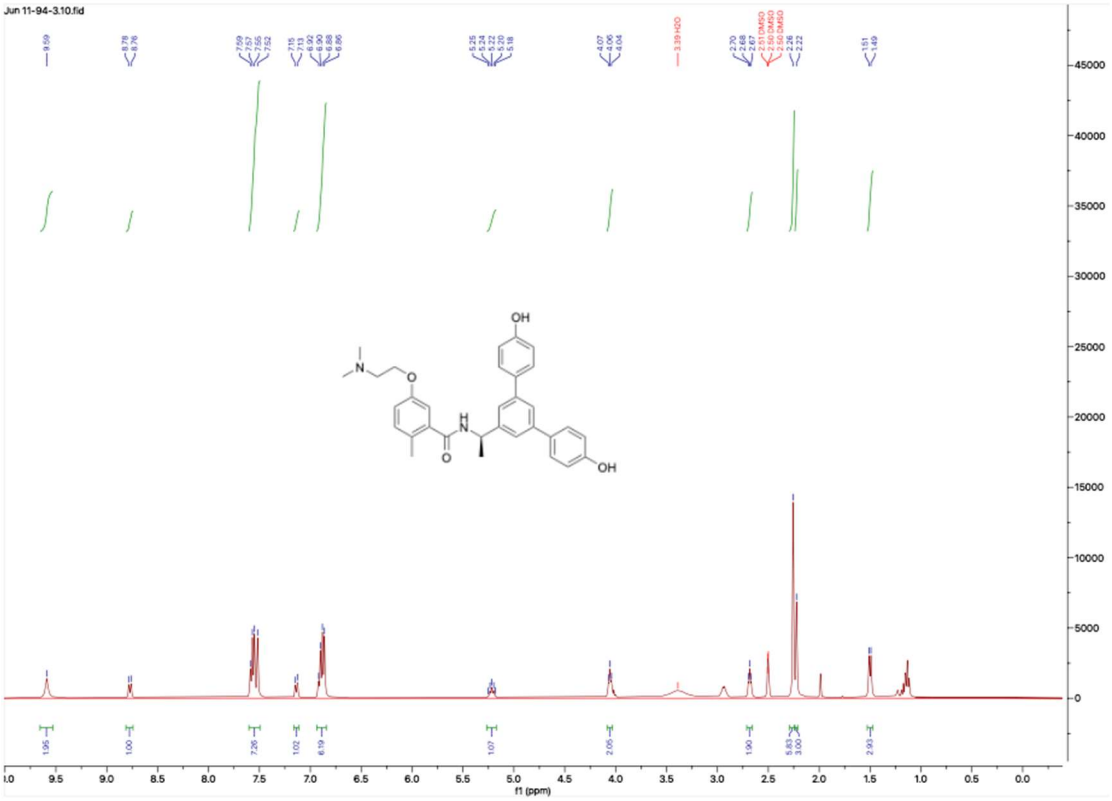

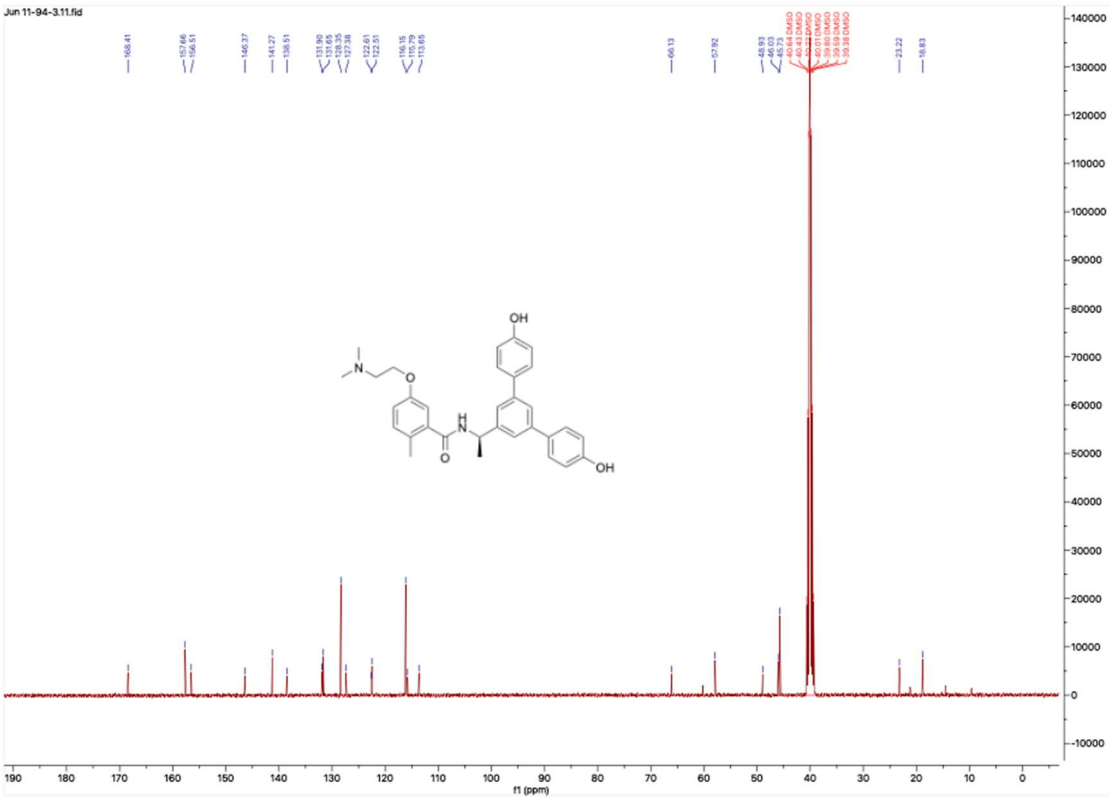

HNMR and CNMR spectra of Jun1218

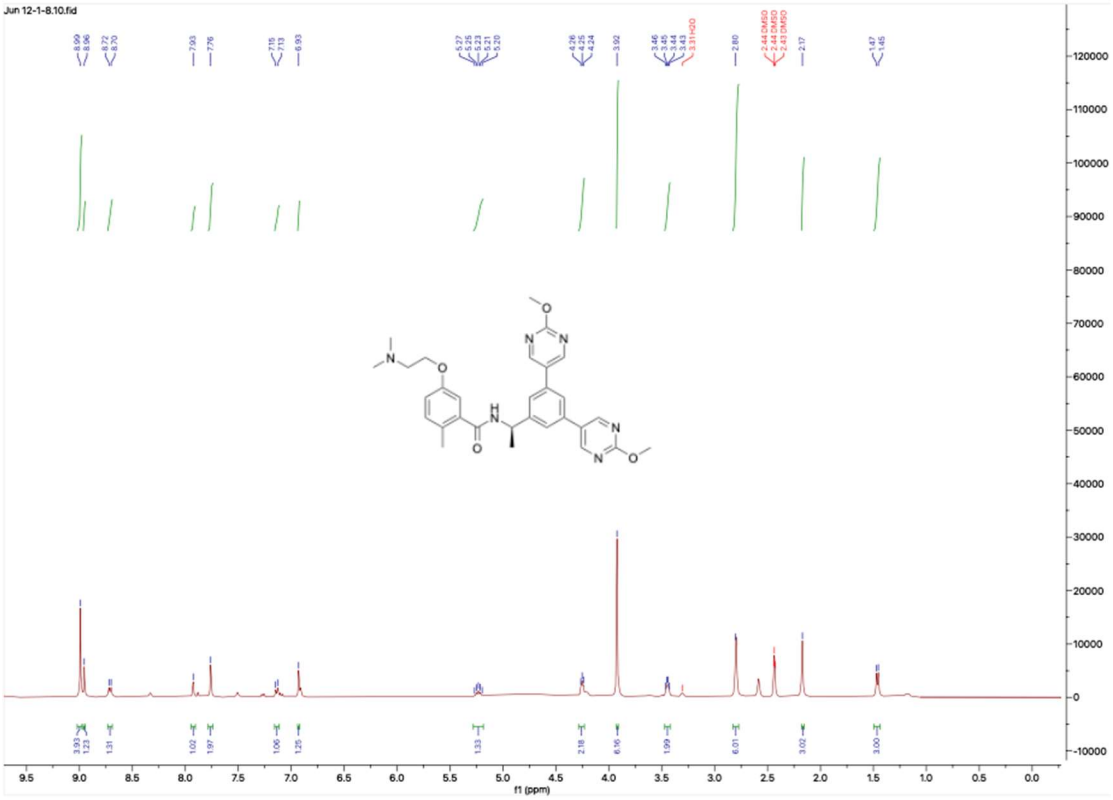

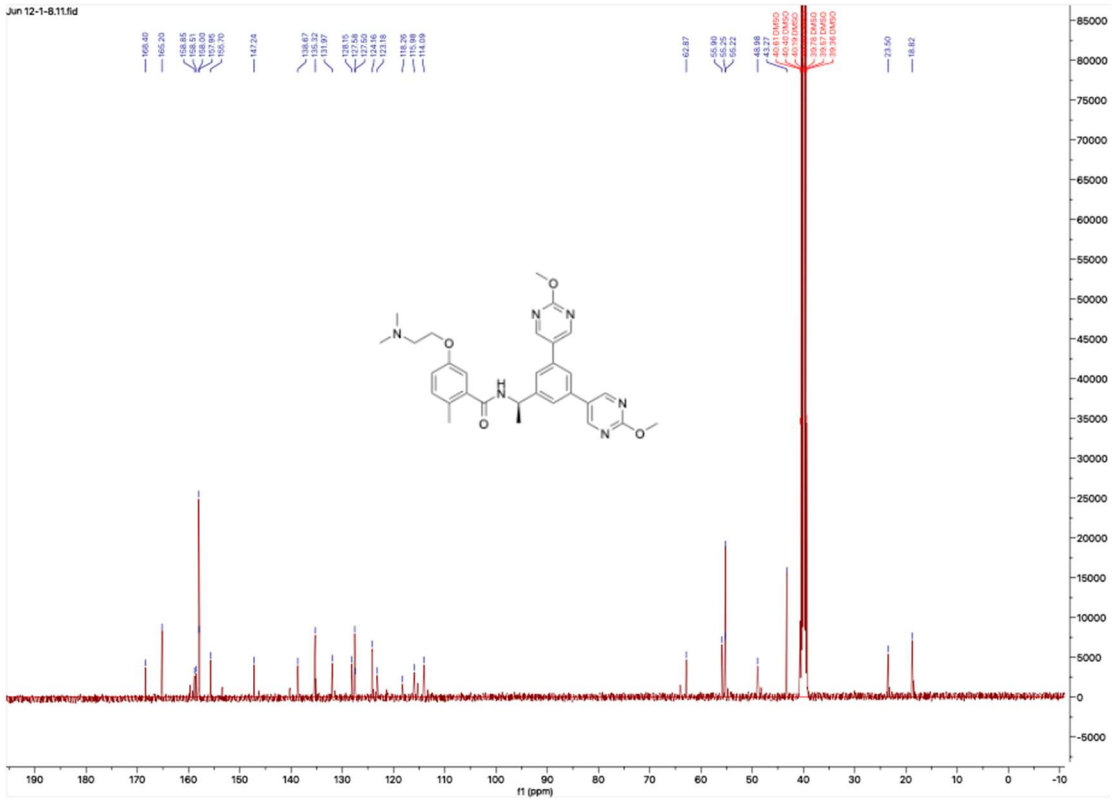

HNMR and CNMR spectra of Jun11941

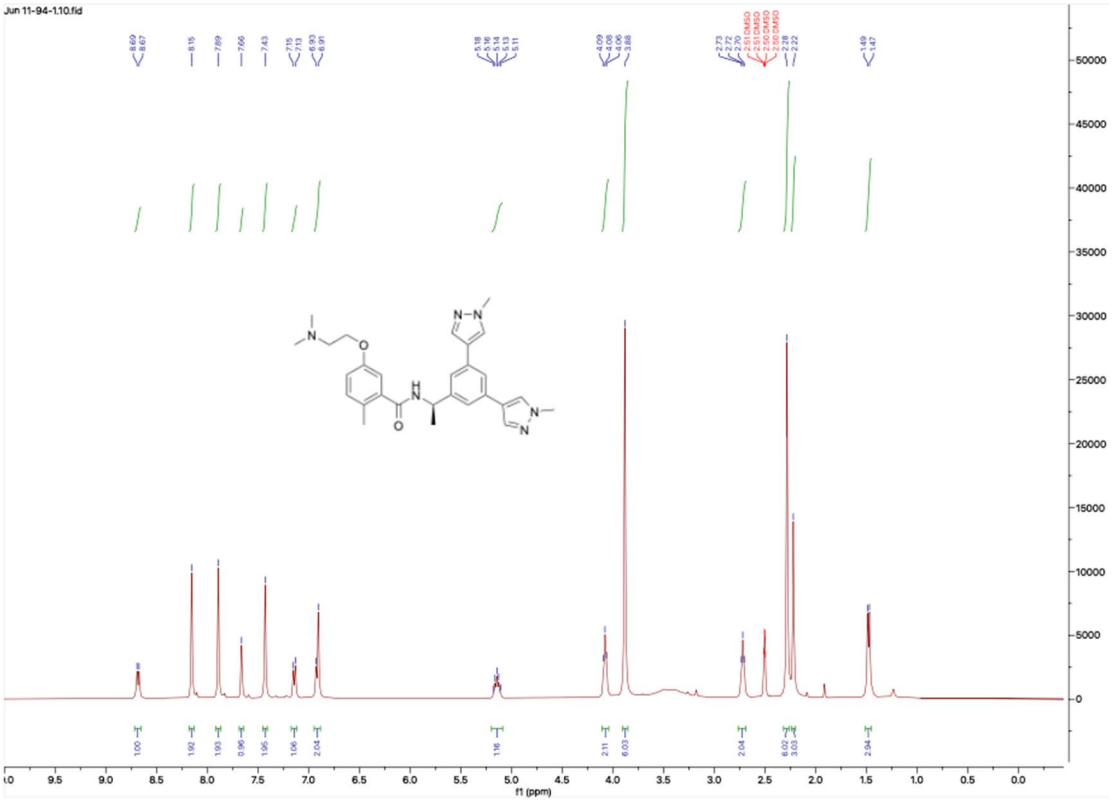

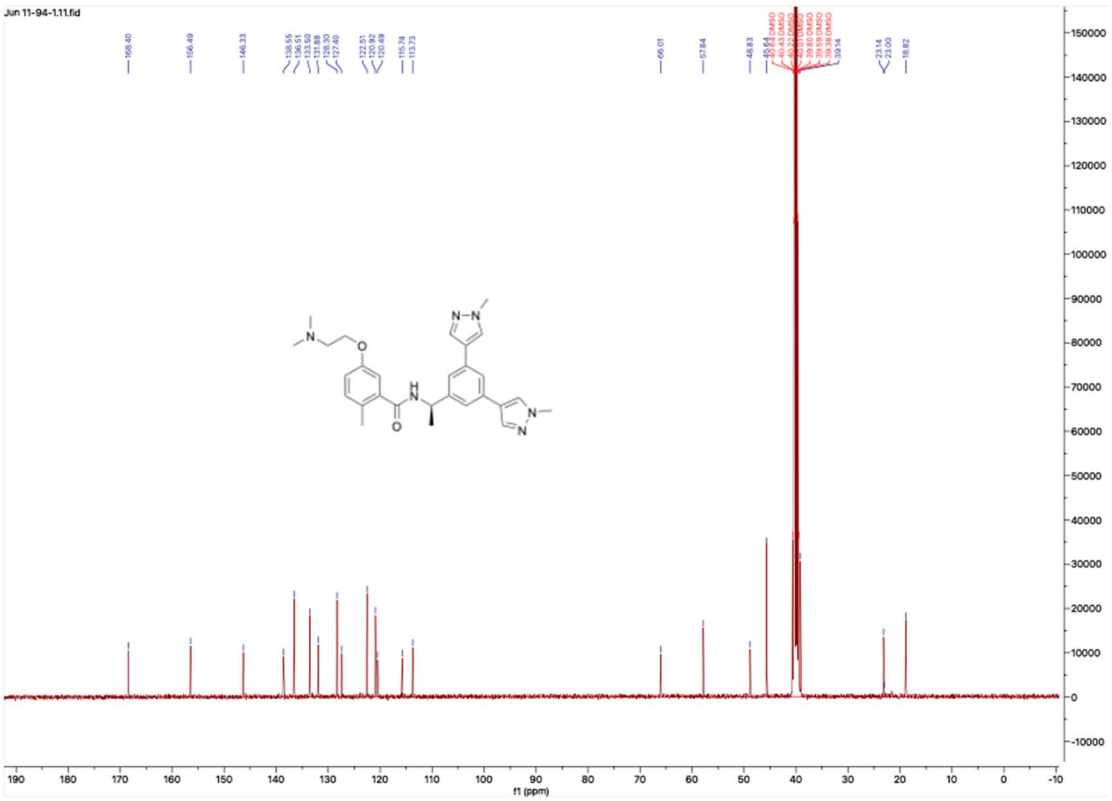

HNMR and CNMR spectra of Jun11942

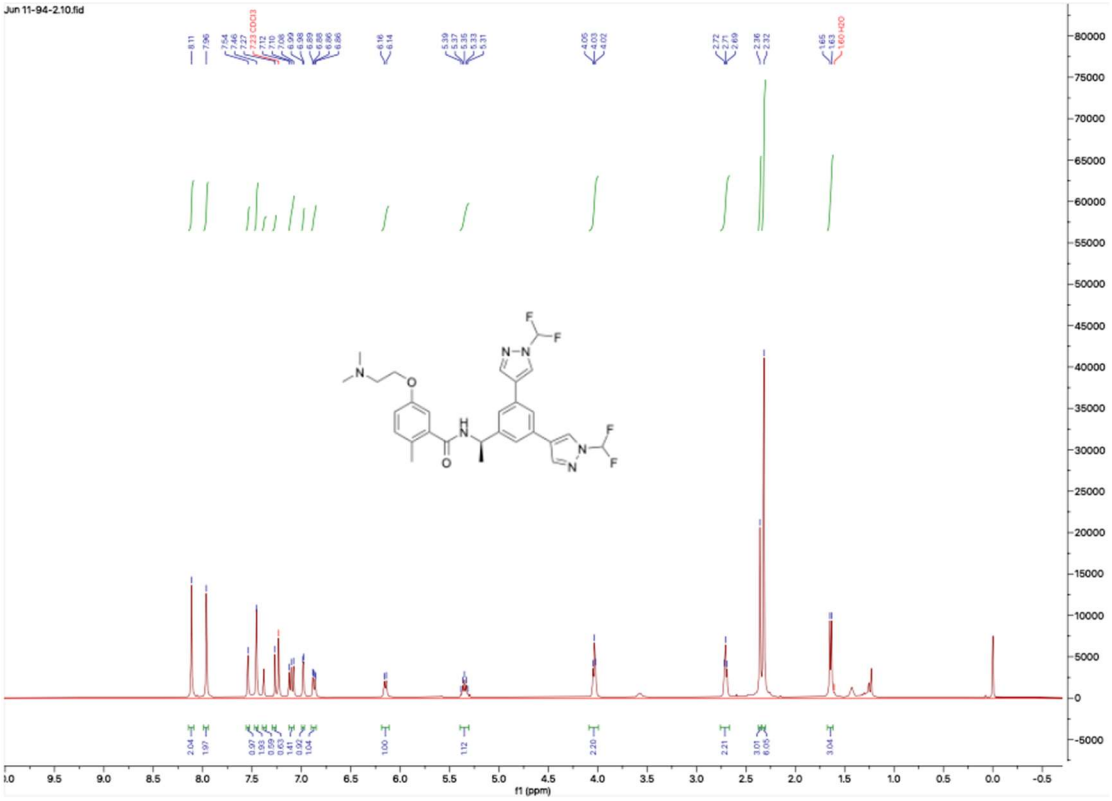

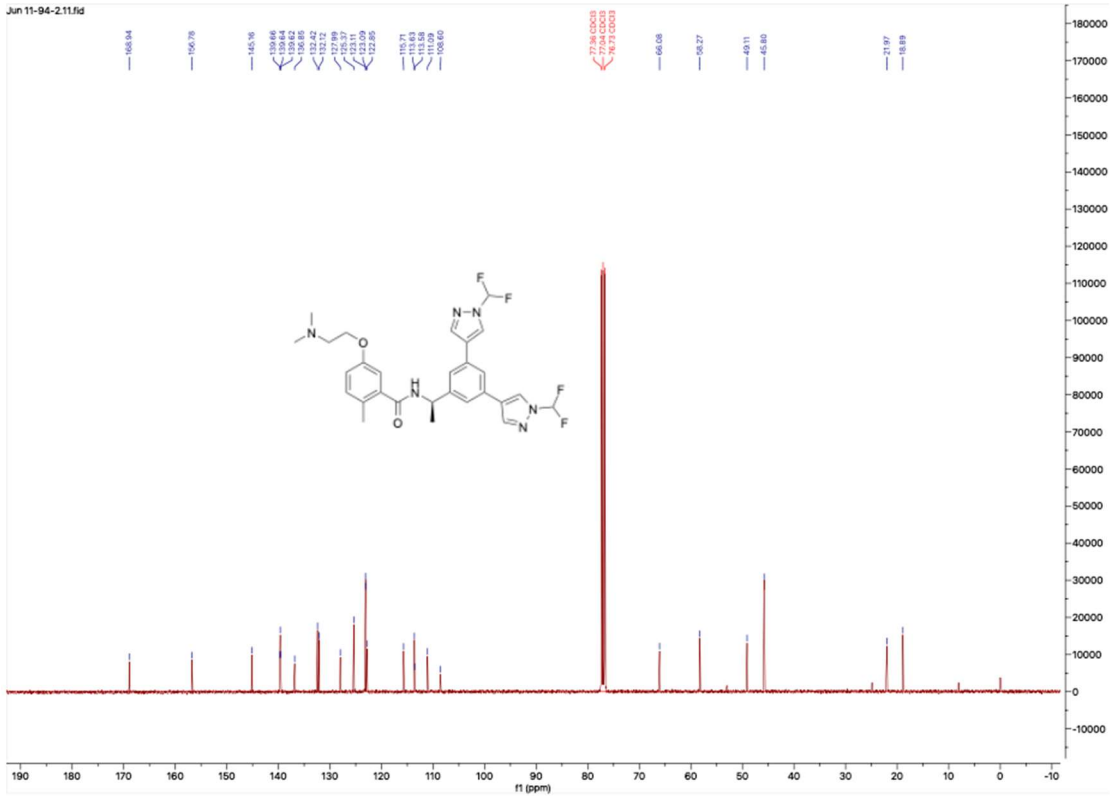

HNMR and CNMR spectra of Jun1212

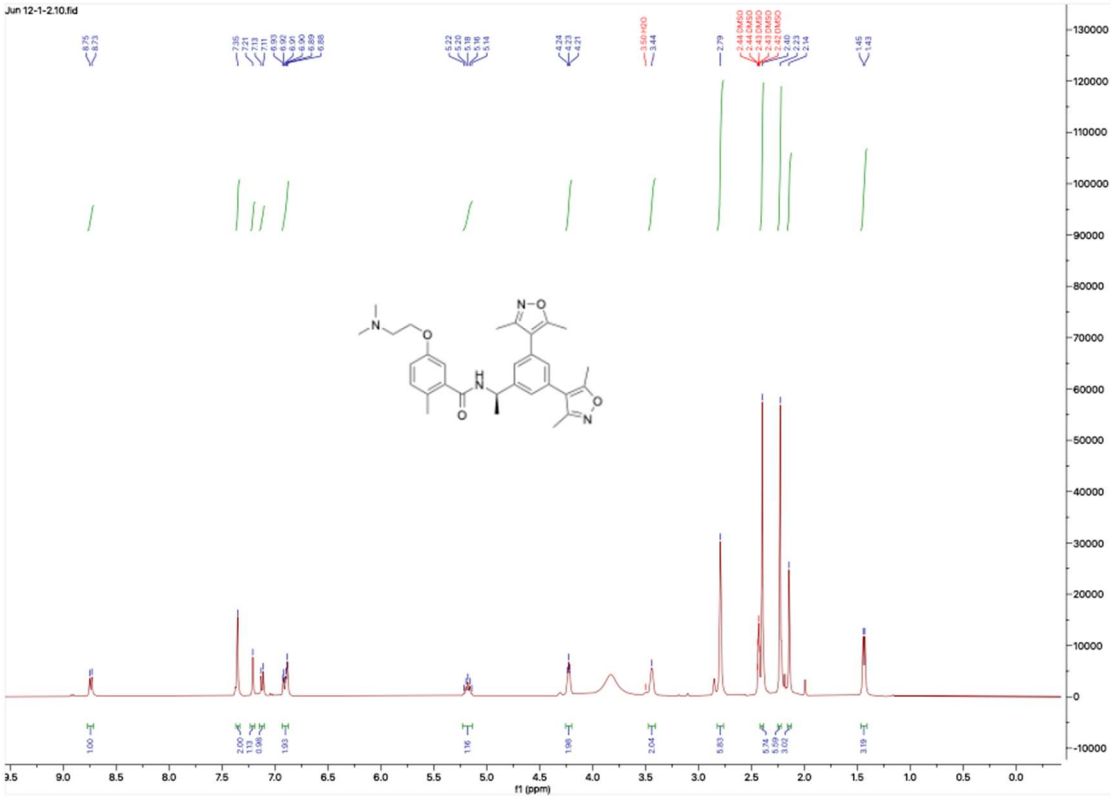

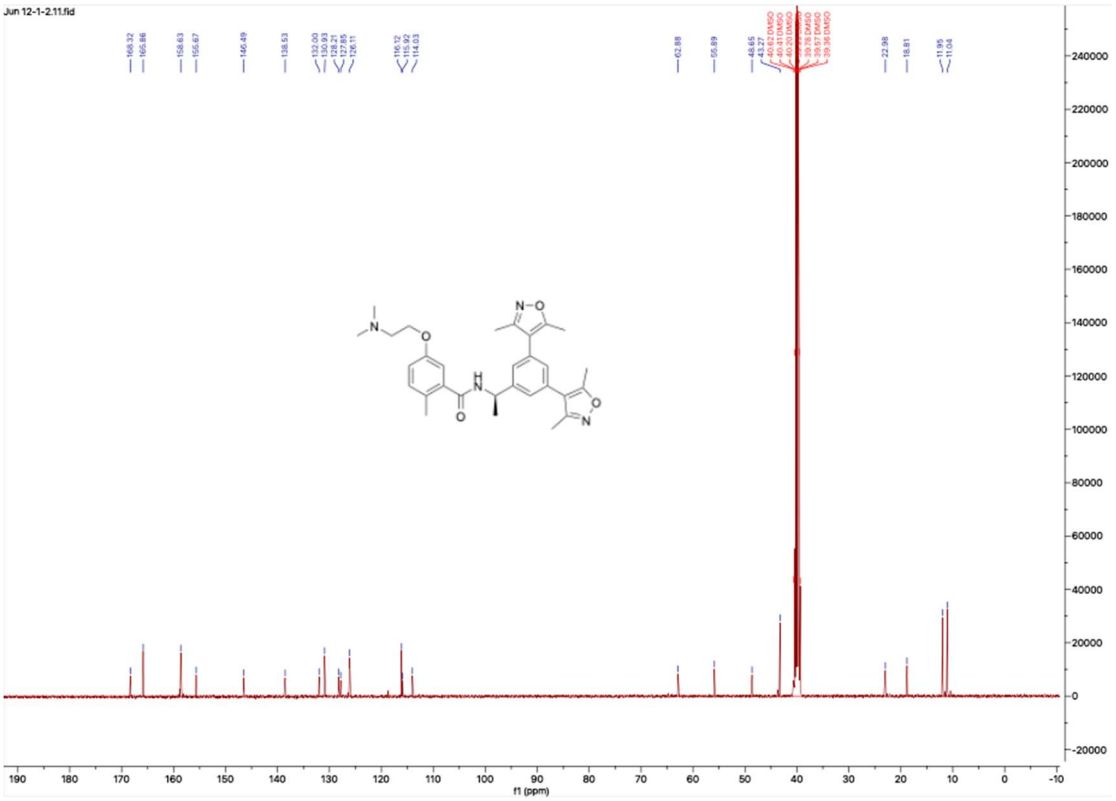

HNMR and CNMR spectra of Jun1215

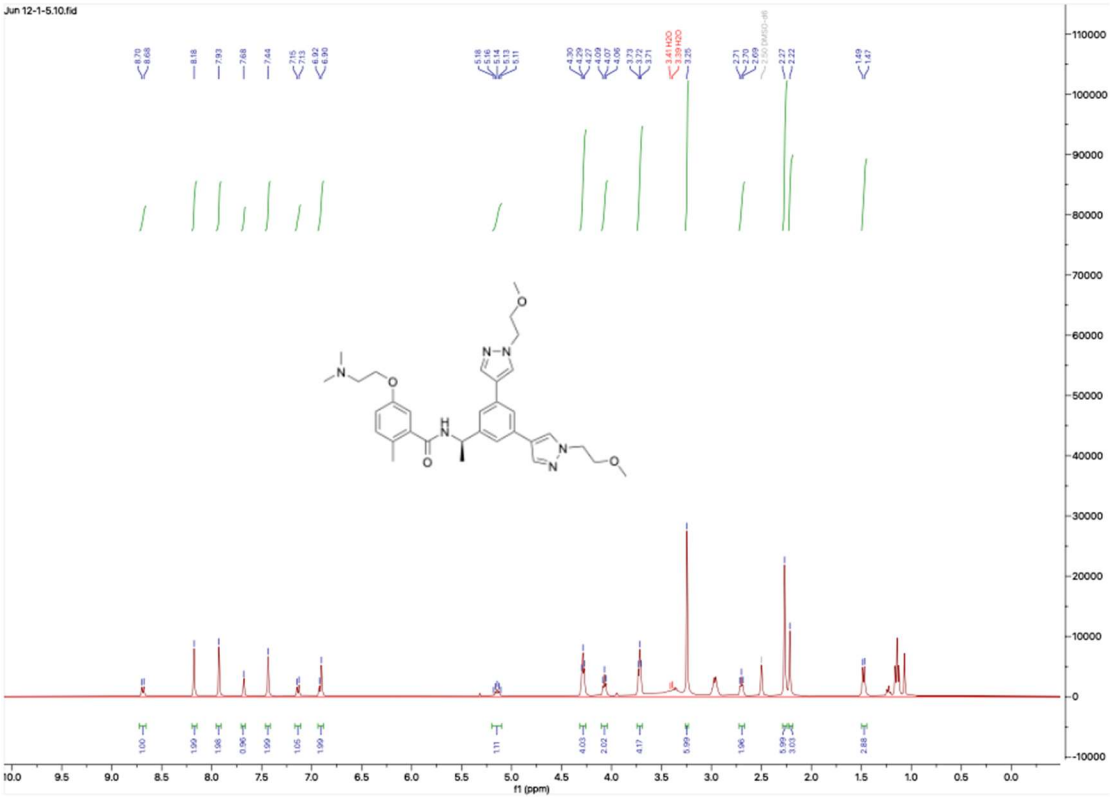

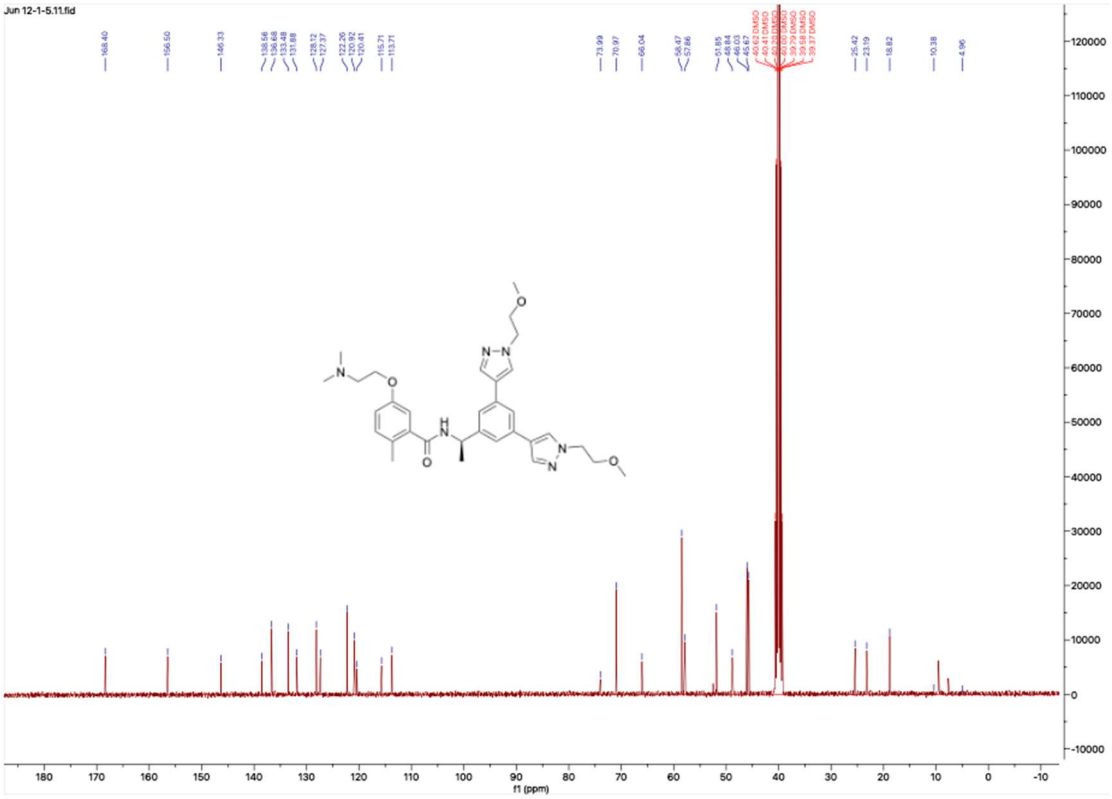

HNMR and CNMR spectra of Jun1247

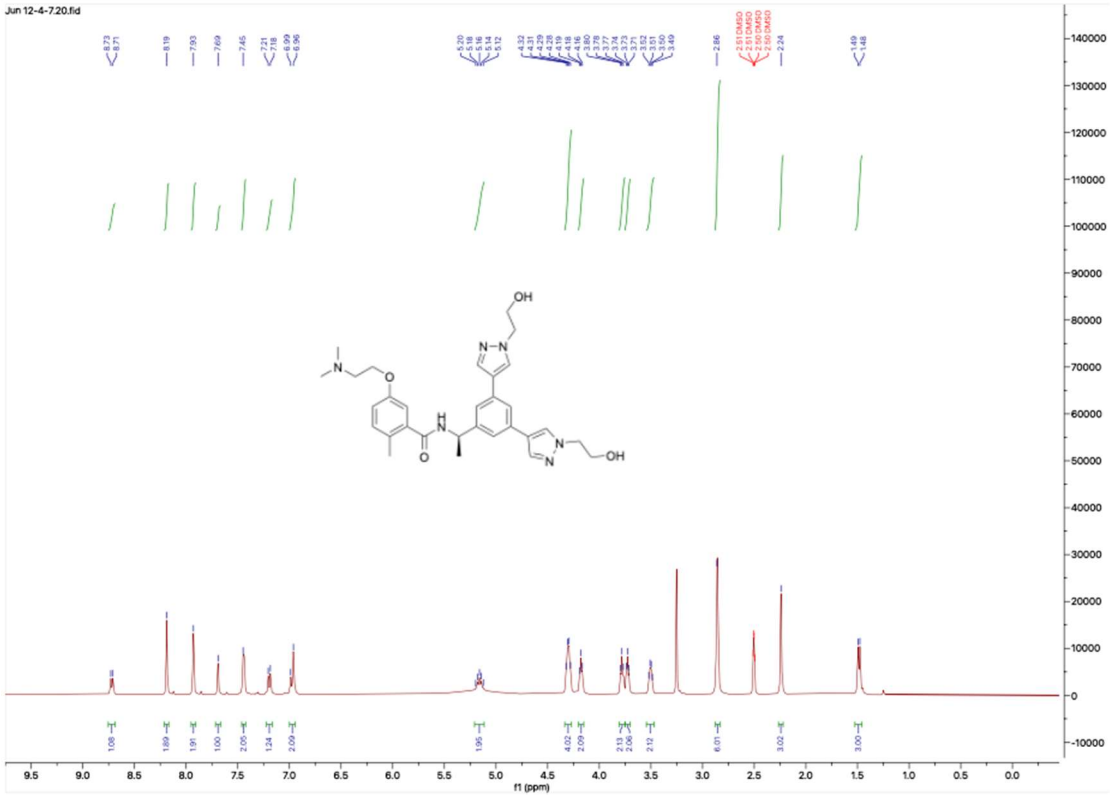

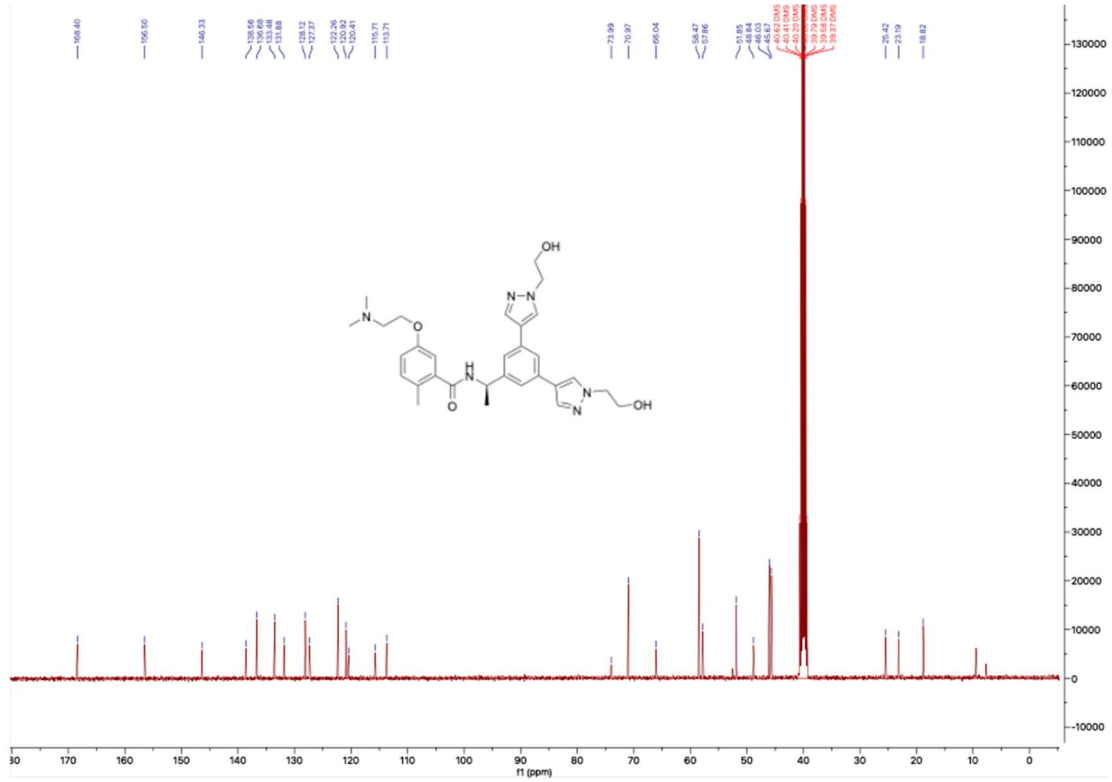

HNMR and CNMR spectra of Jun12382

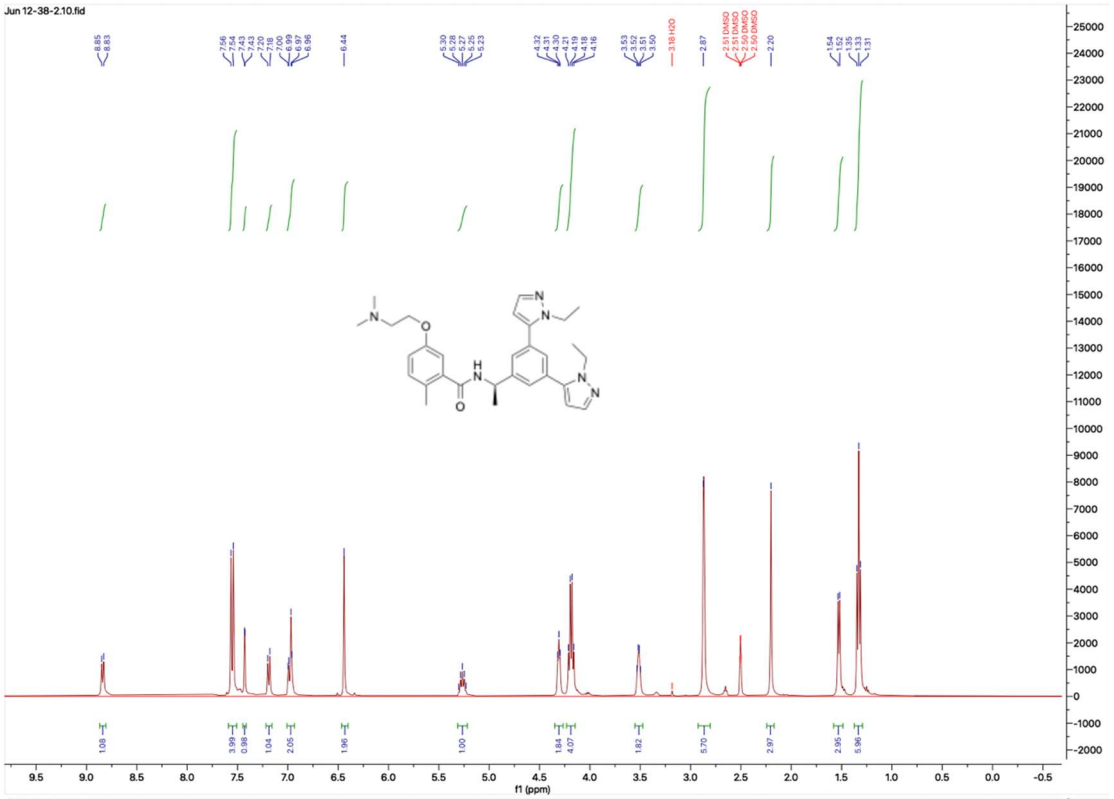

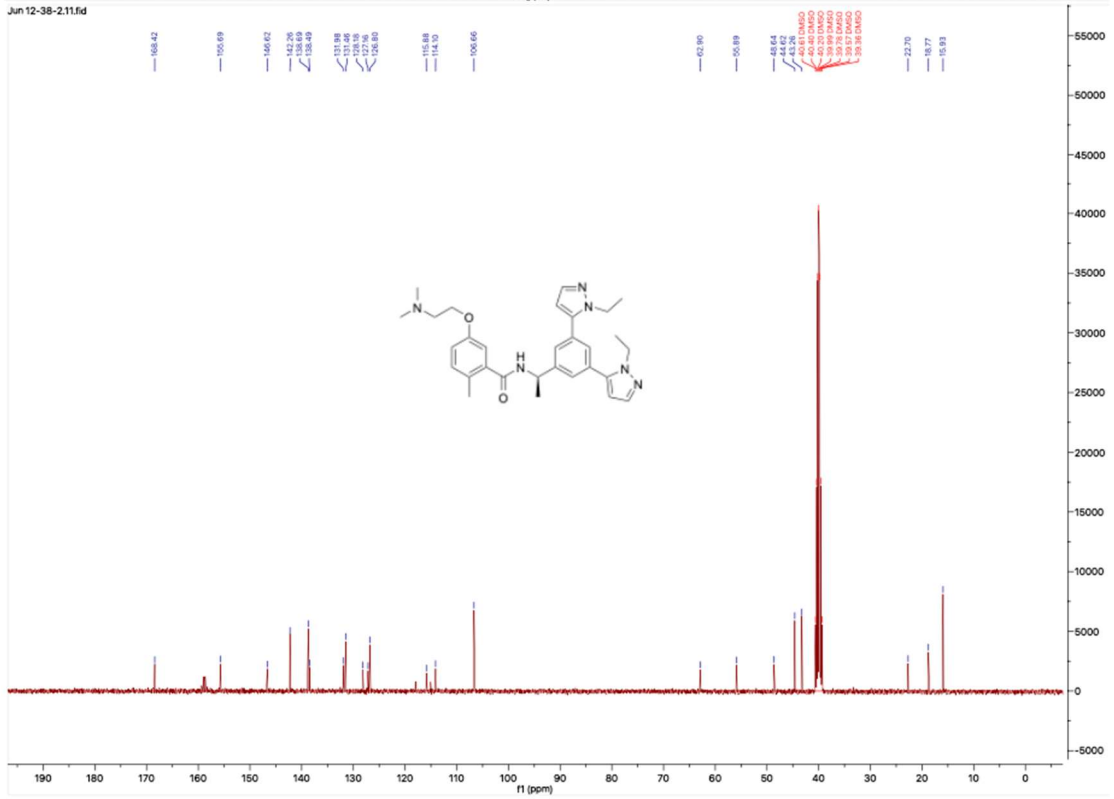

HNMR and CNMR spectra of Jun1246

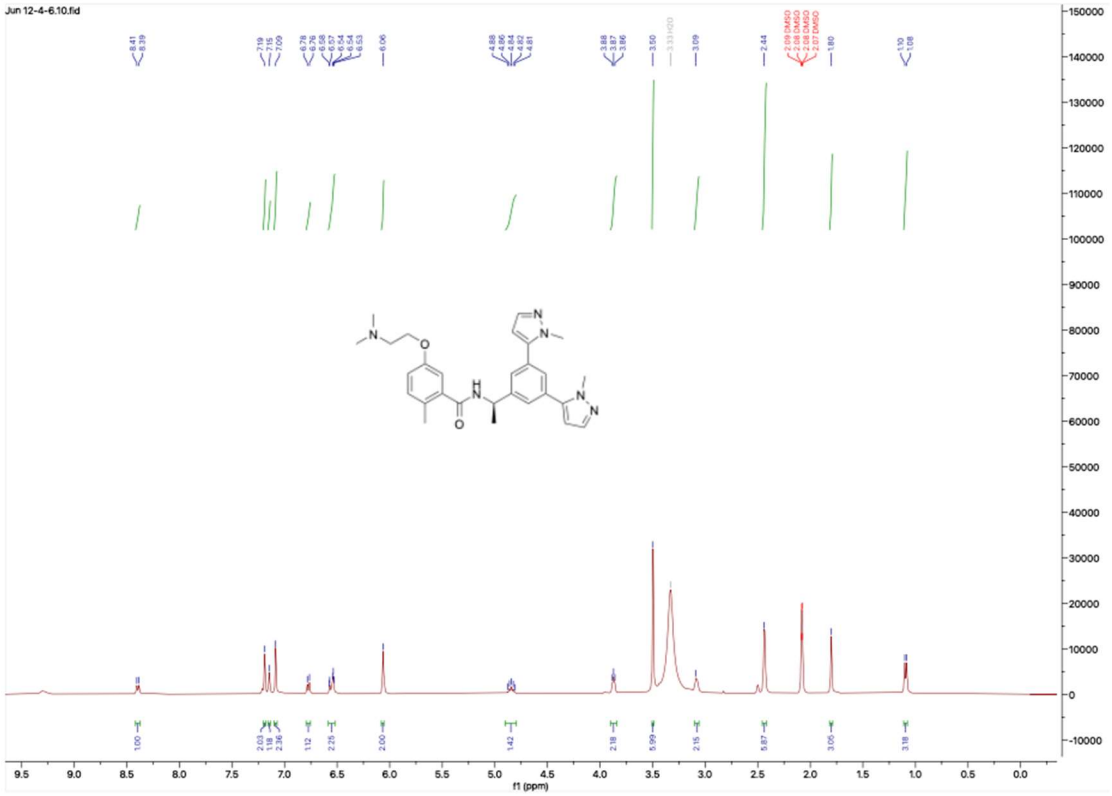

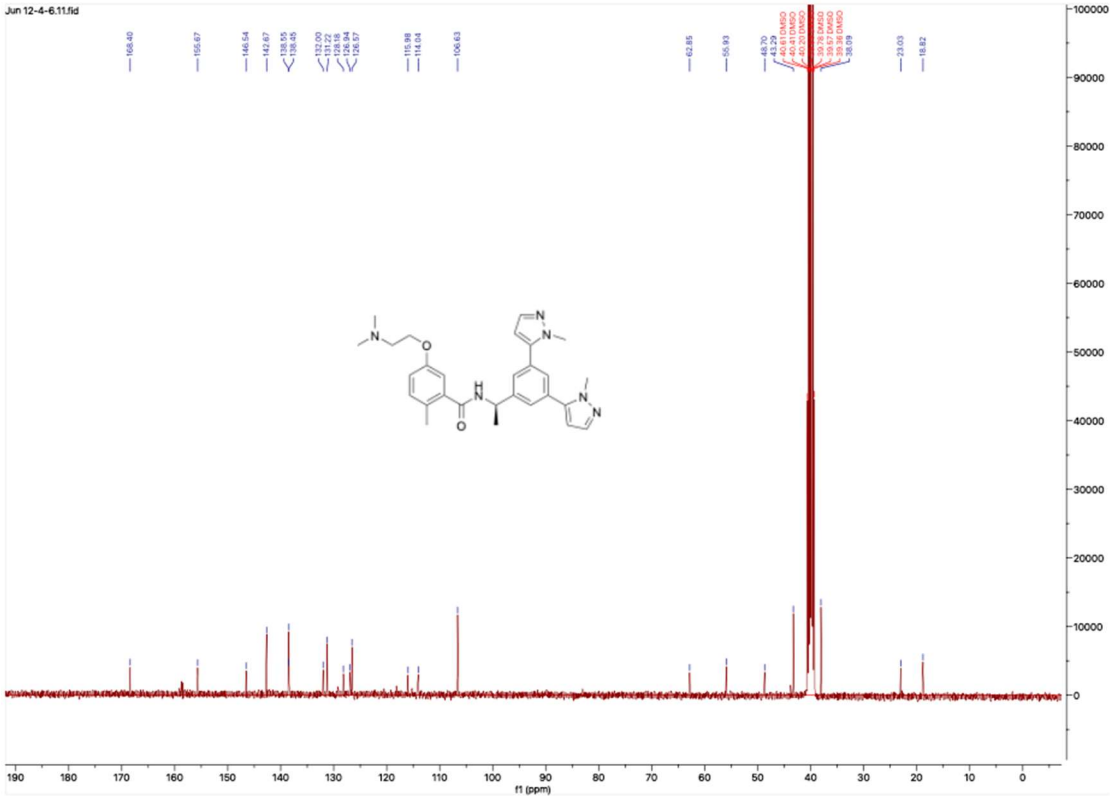

HNMR and CNMR spectra of Jun1211

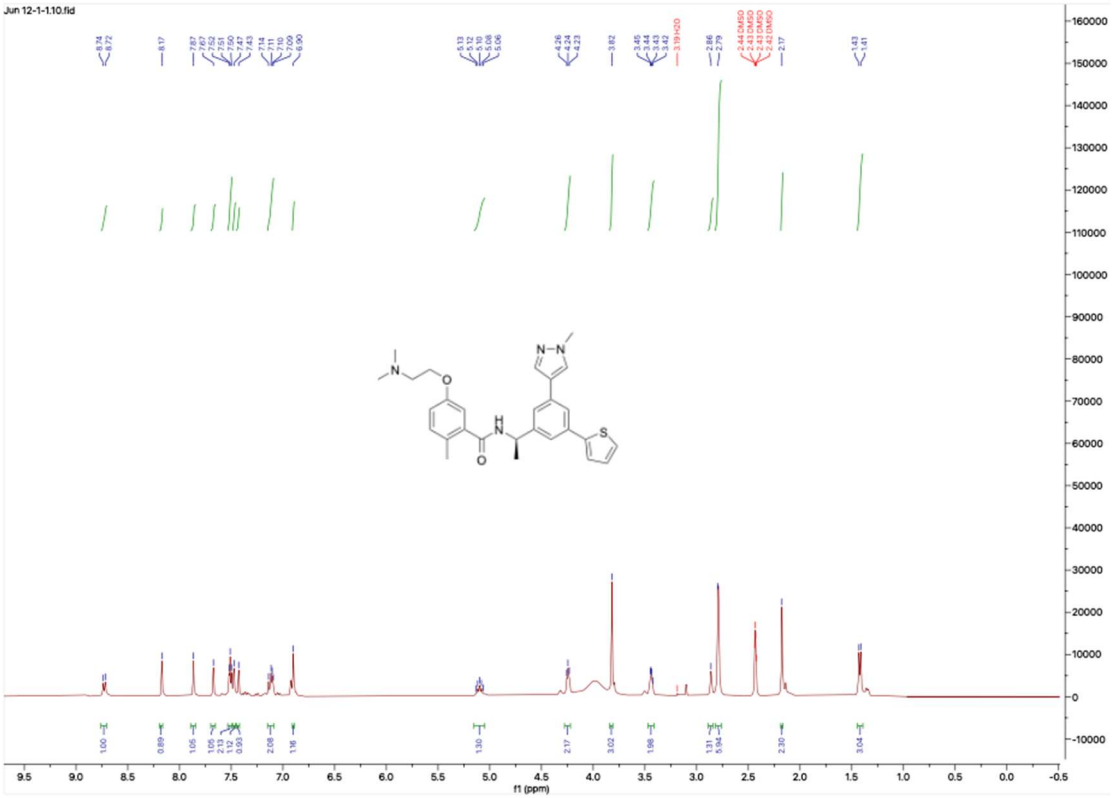

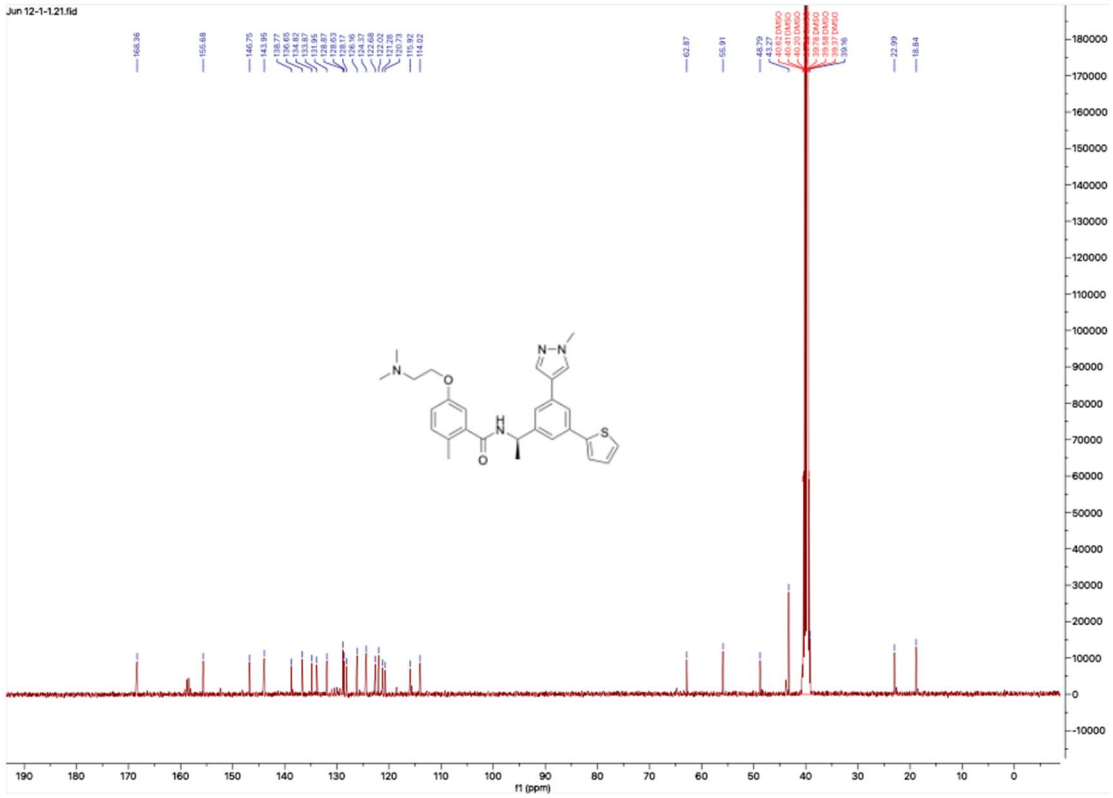

HNMR and CNMR spectra of Jun1244

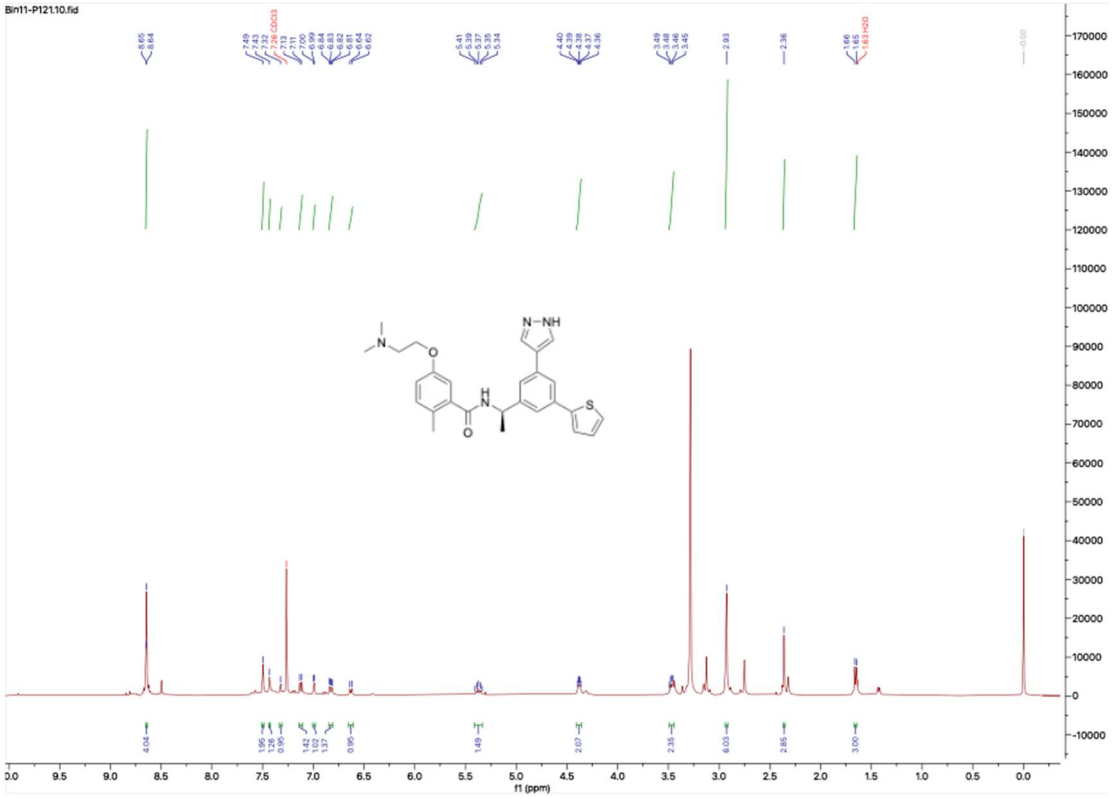

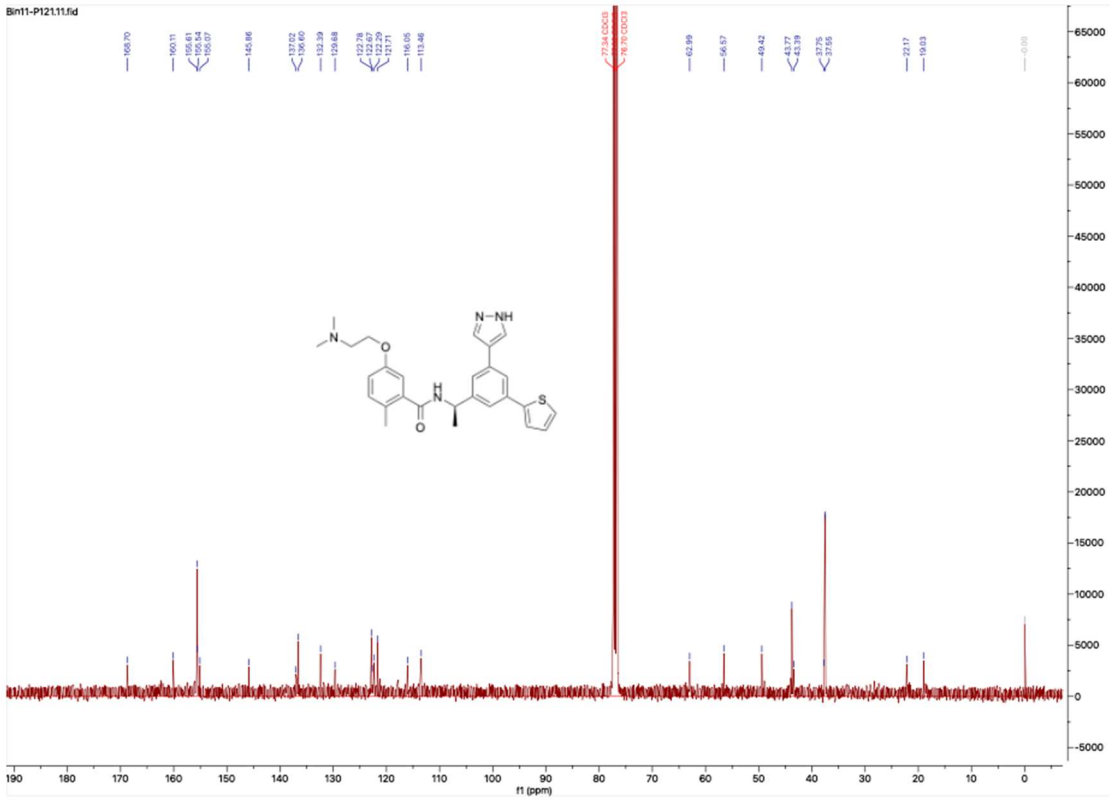

HNMR and CNMR spectra of Jun1251

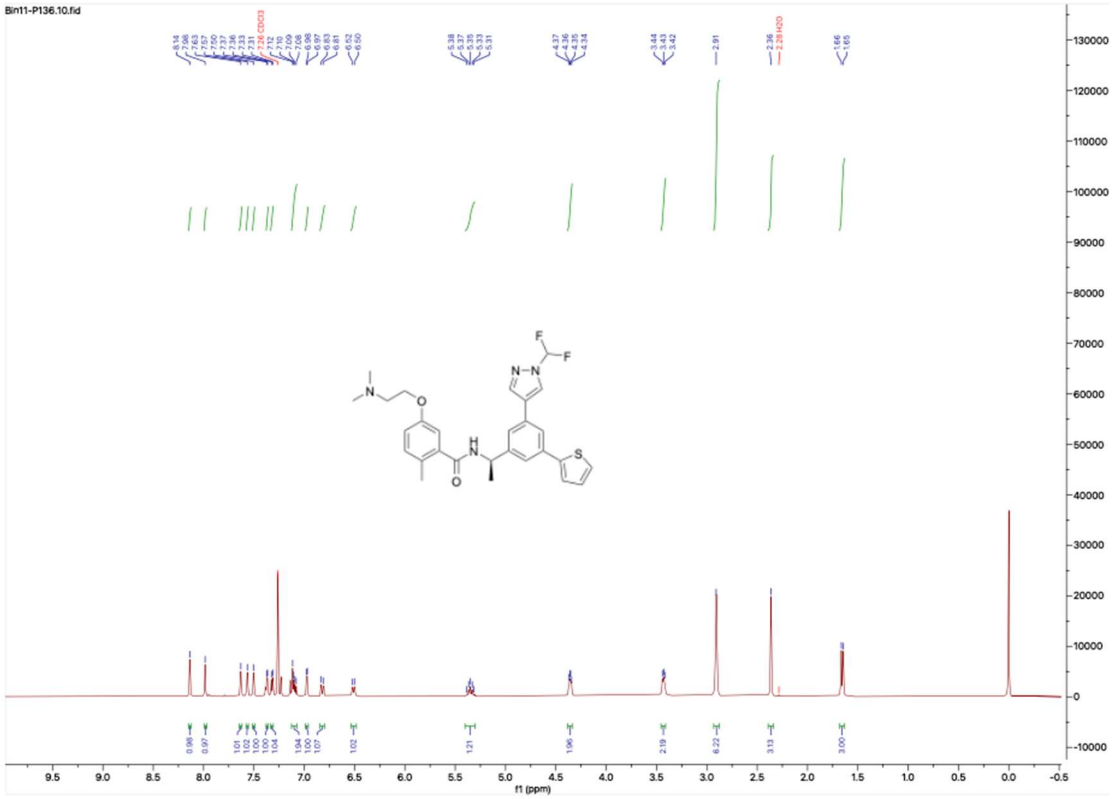

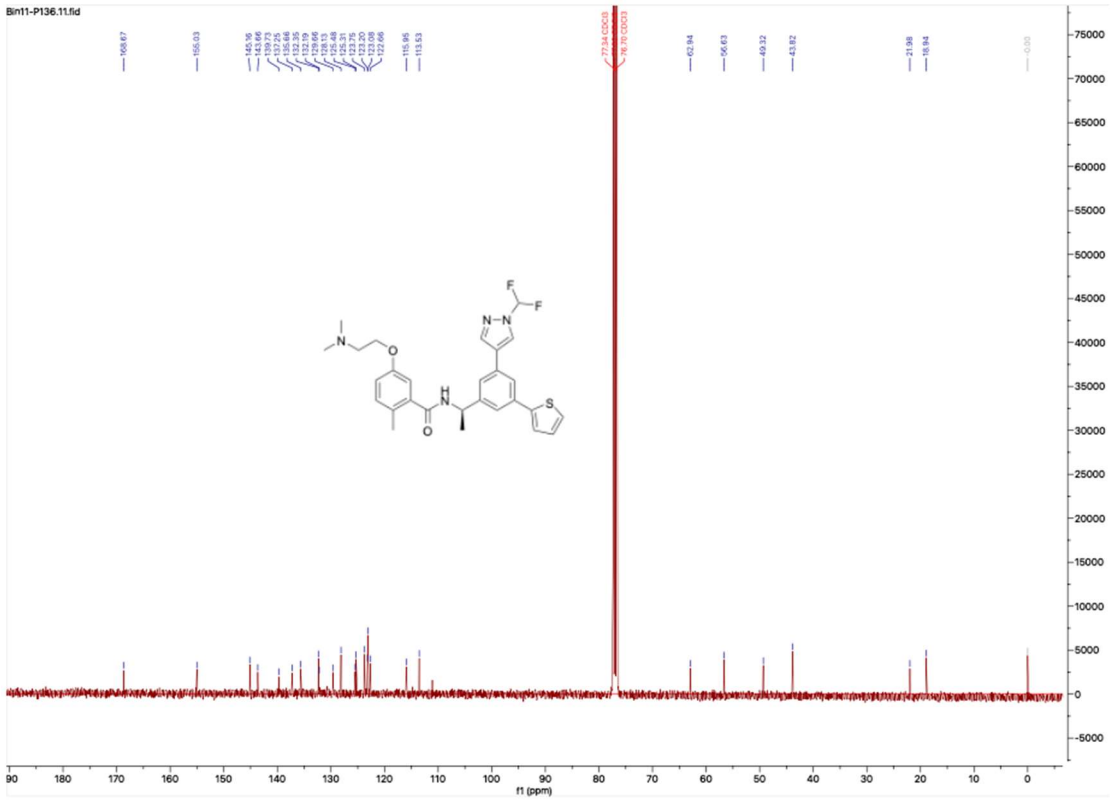

HNMR and CNMR spectra of Jun1252

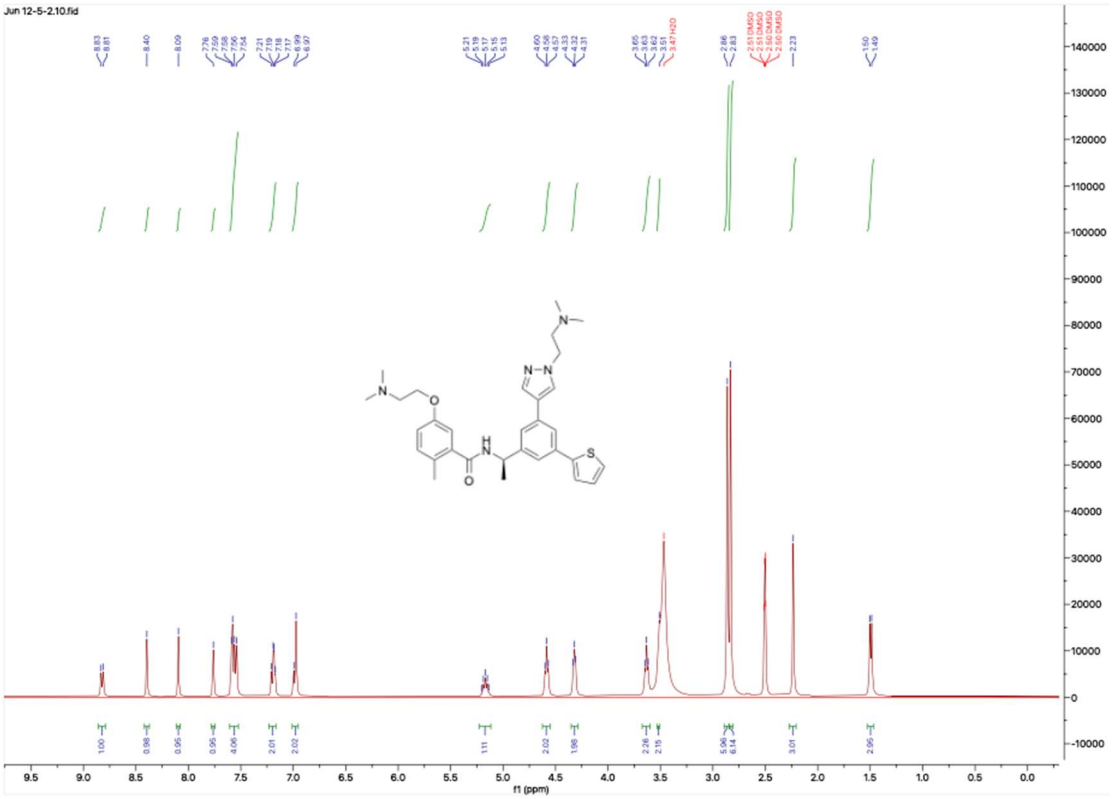

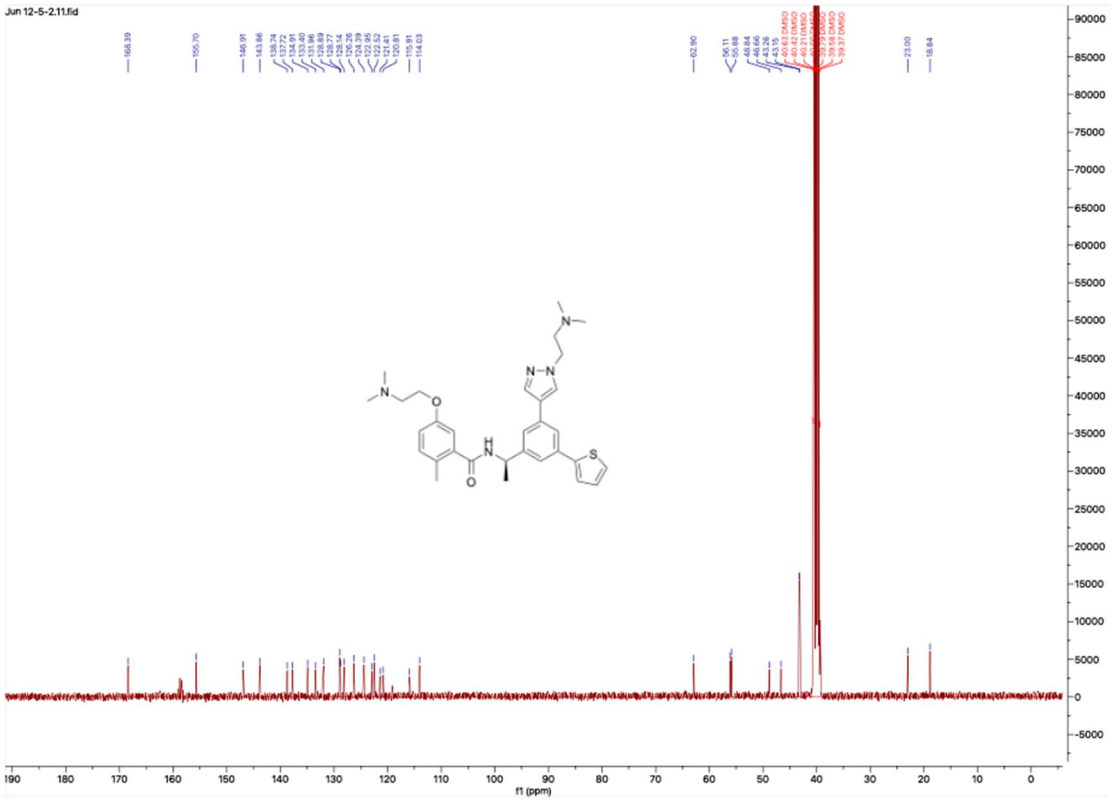

HNMR and CNMR spectra of Jun1254

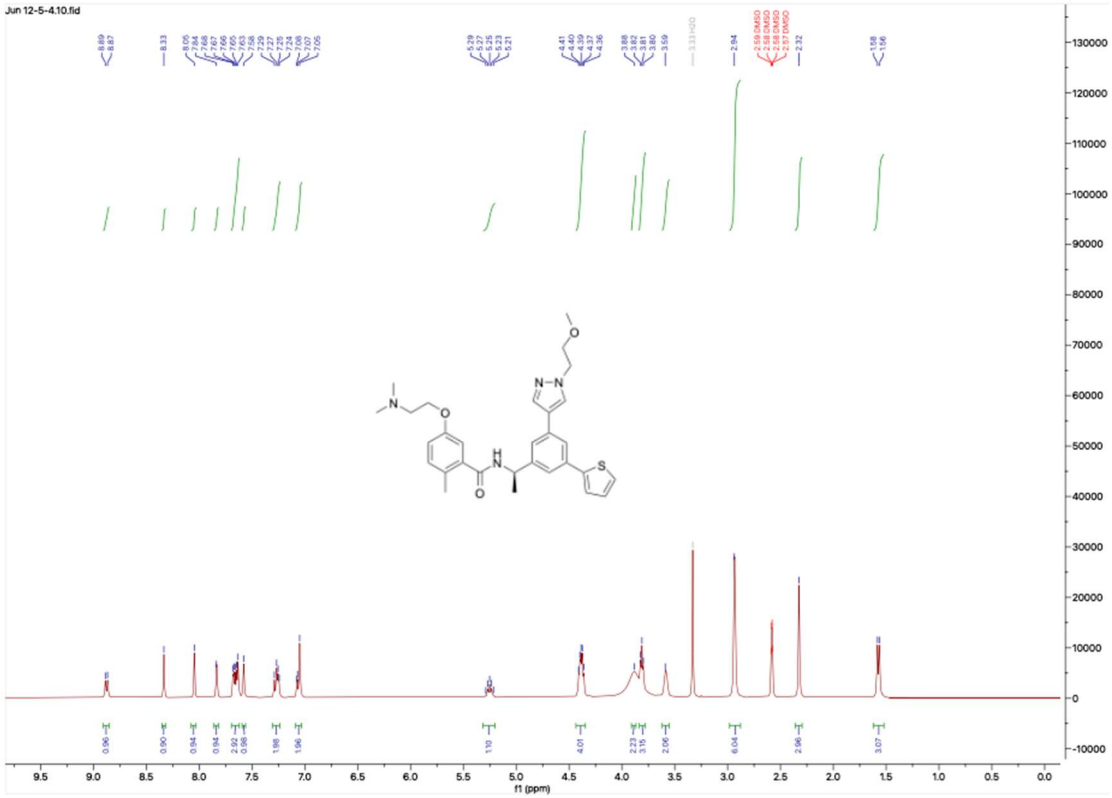

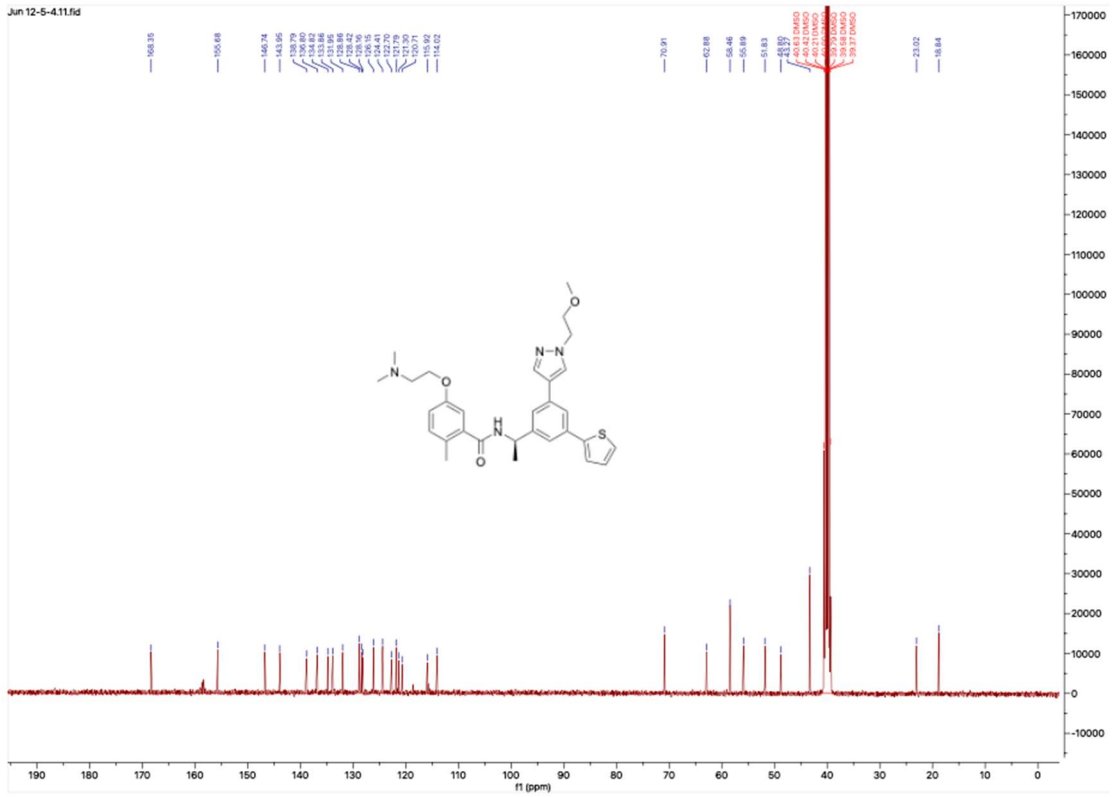

HNMR and CNMR spectra of Jun1257

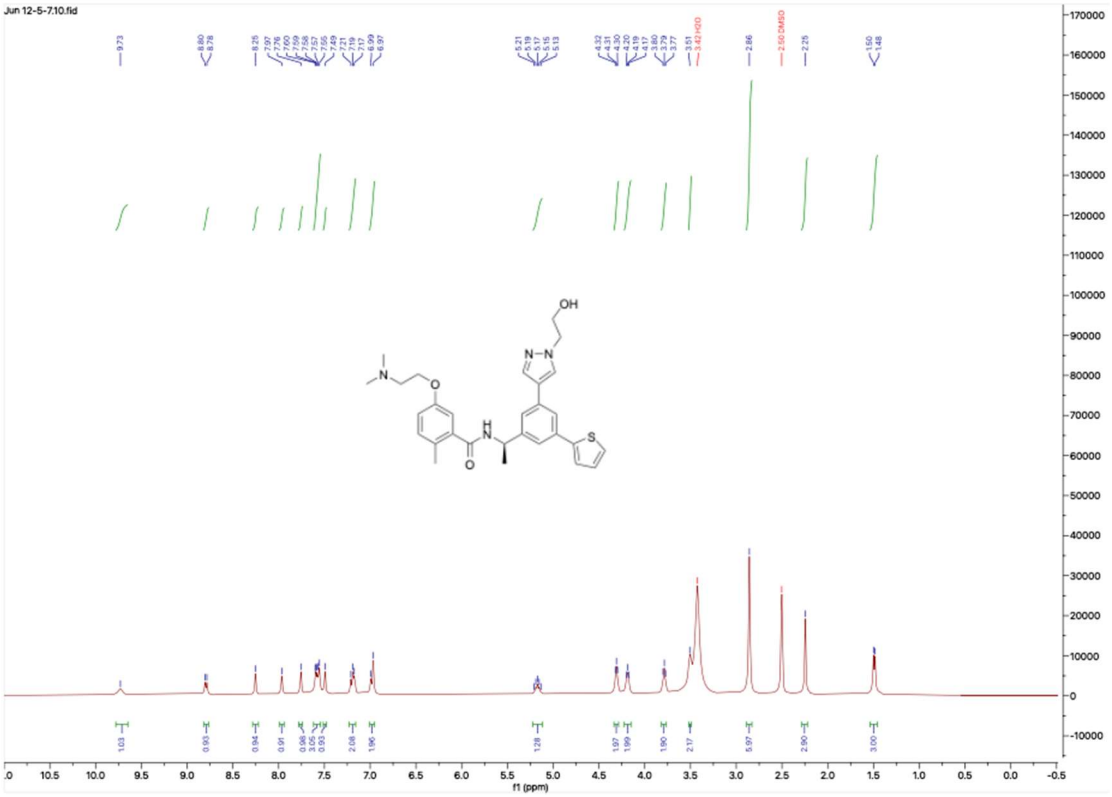

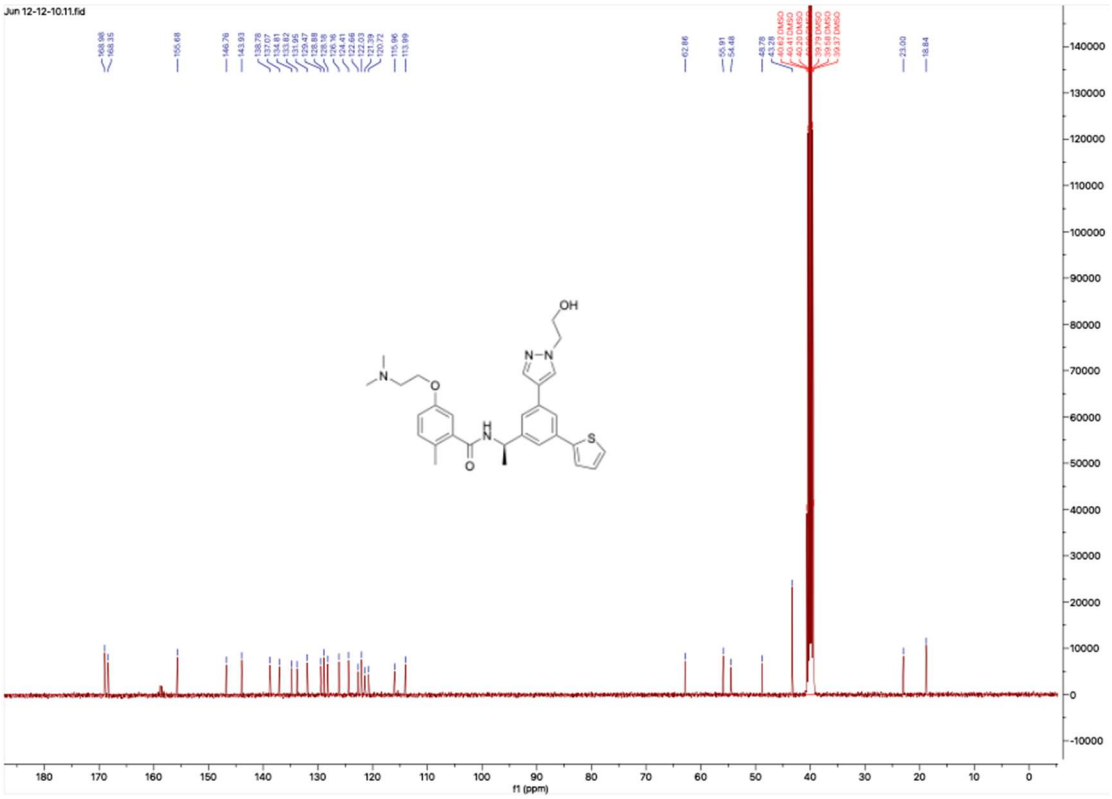

HNMR and CNMR spectra of Jun121210

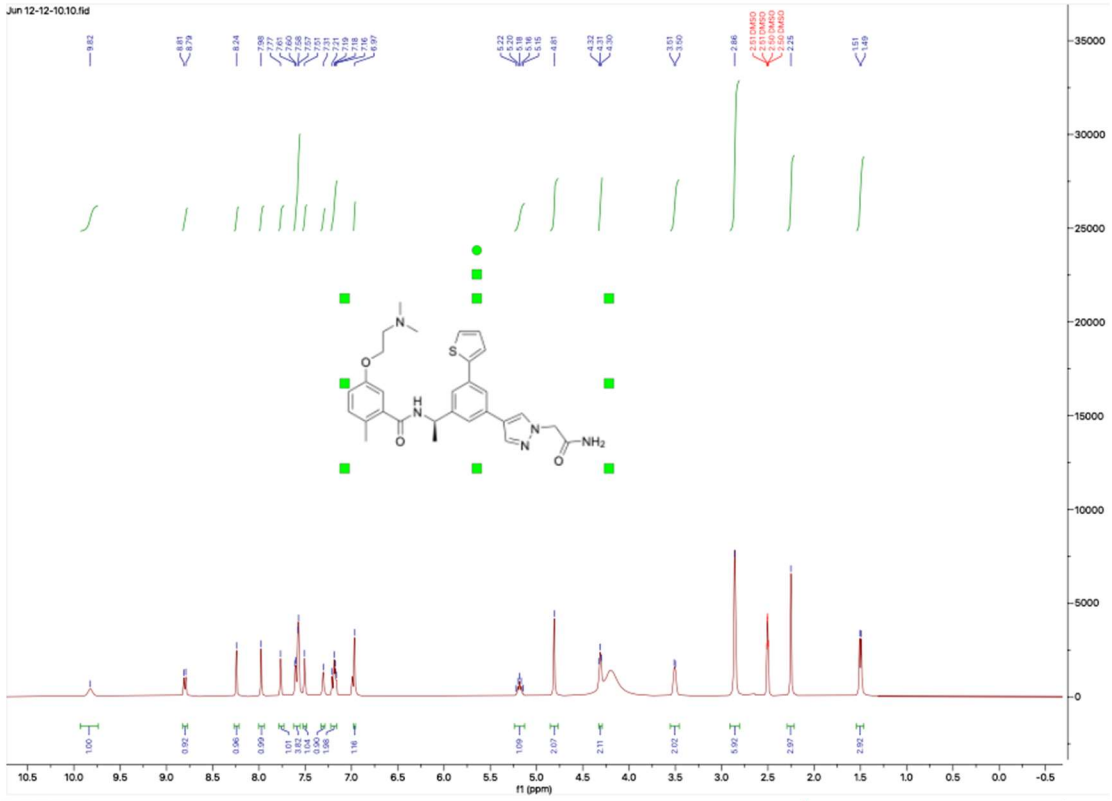

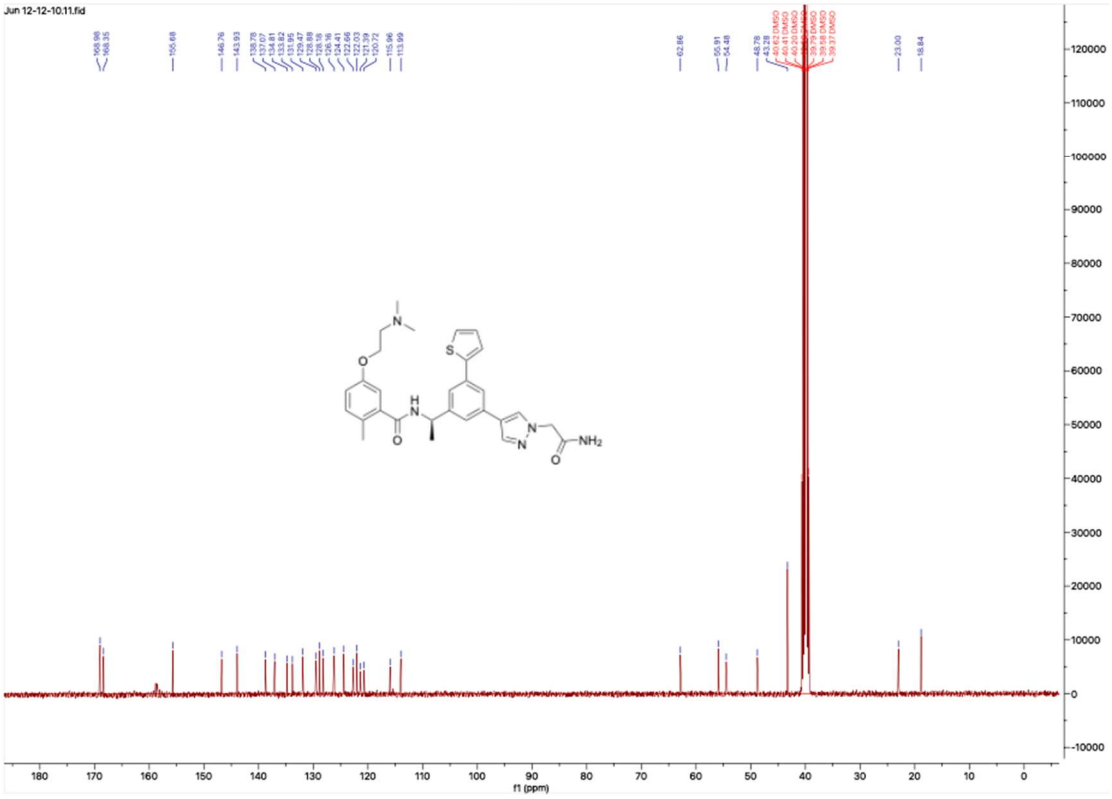

HNMR and CNMR spectra of Jun12149

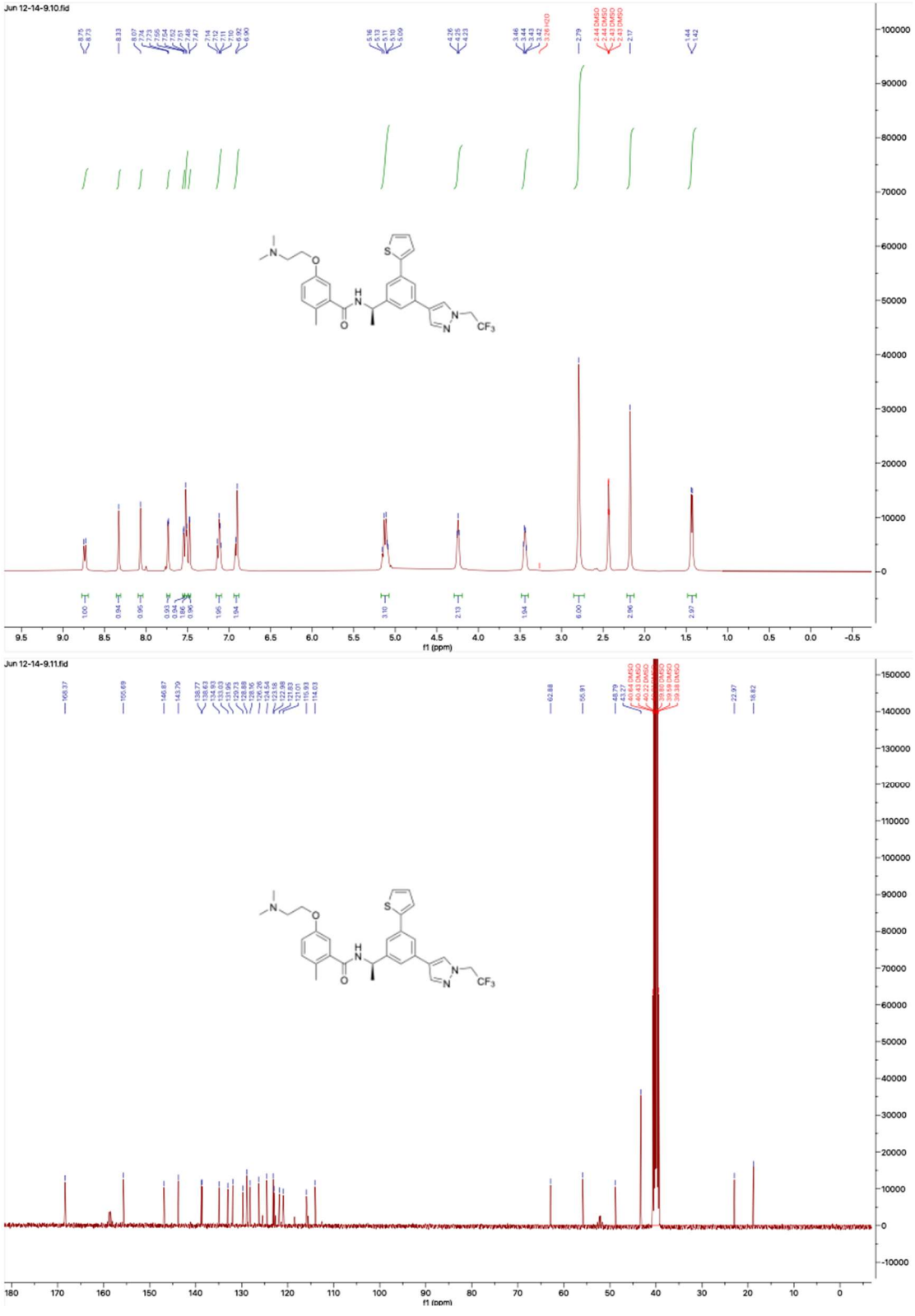

HNMR and CNMR spectra of Jun12129

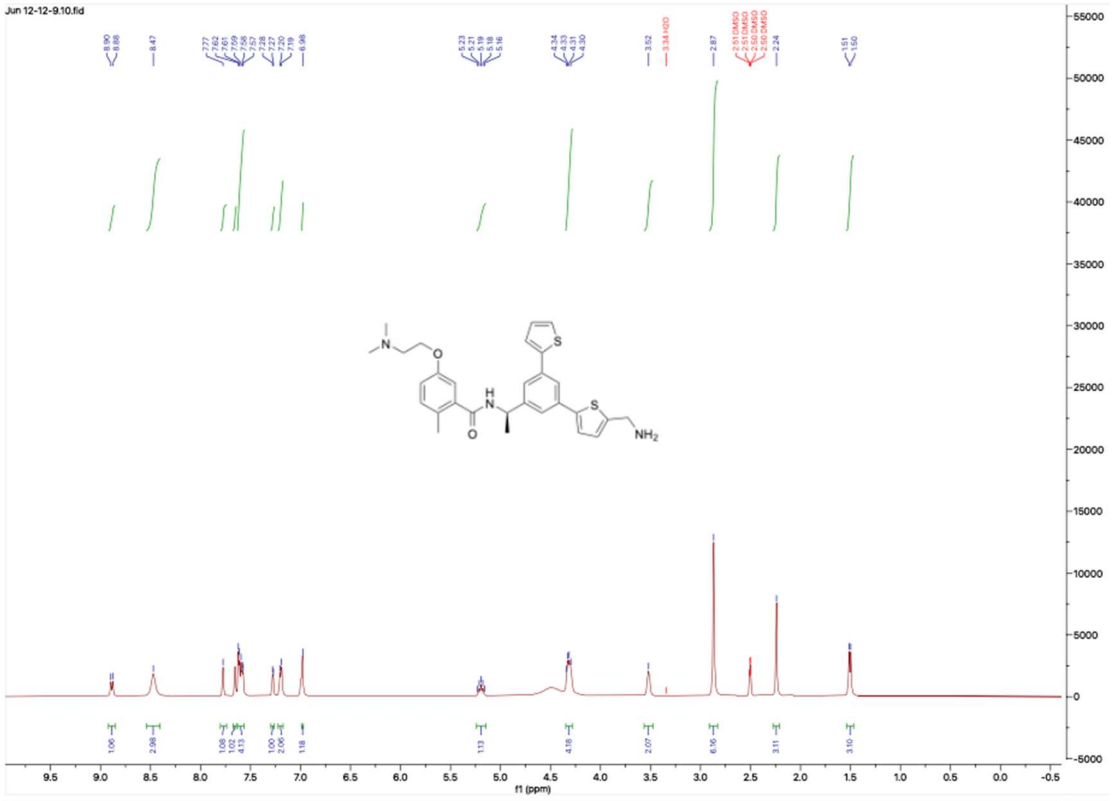

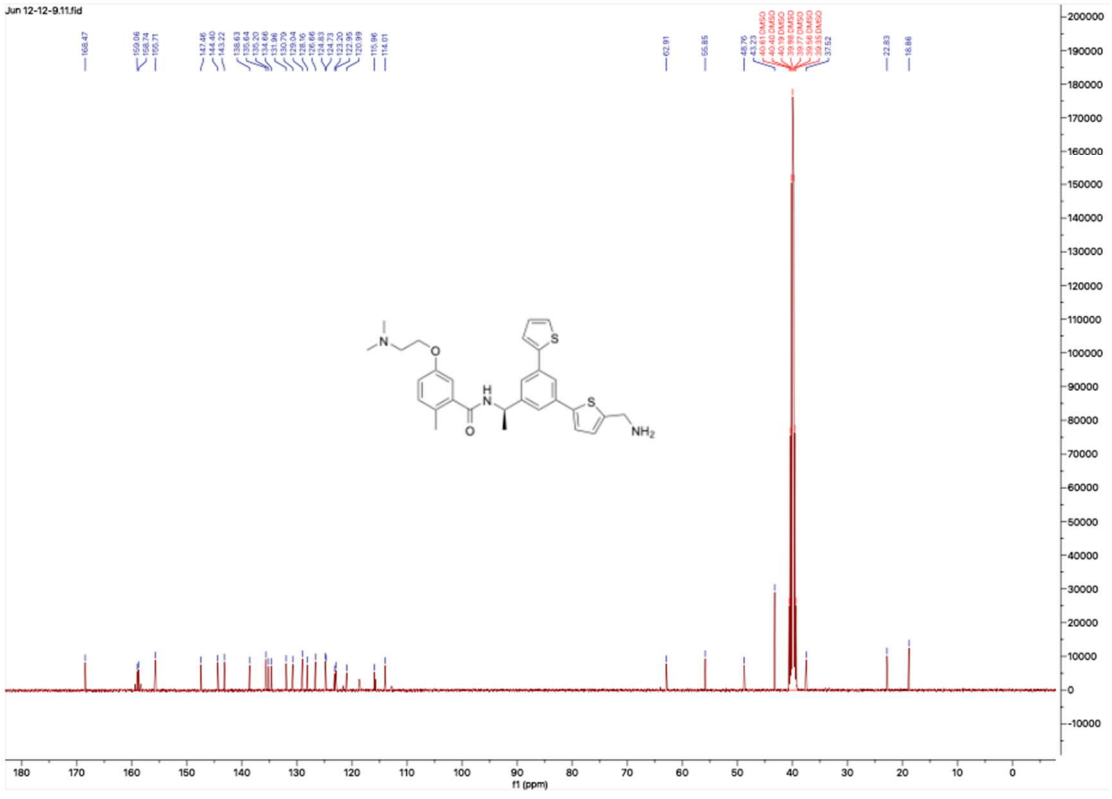

HNMR and CNMR spectra of Jun121910

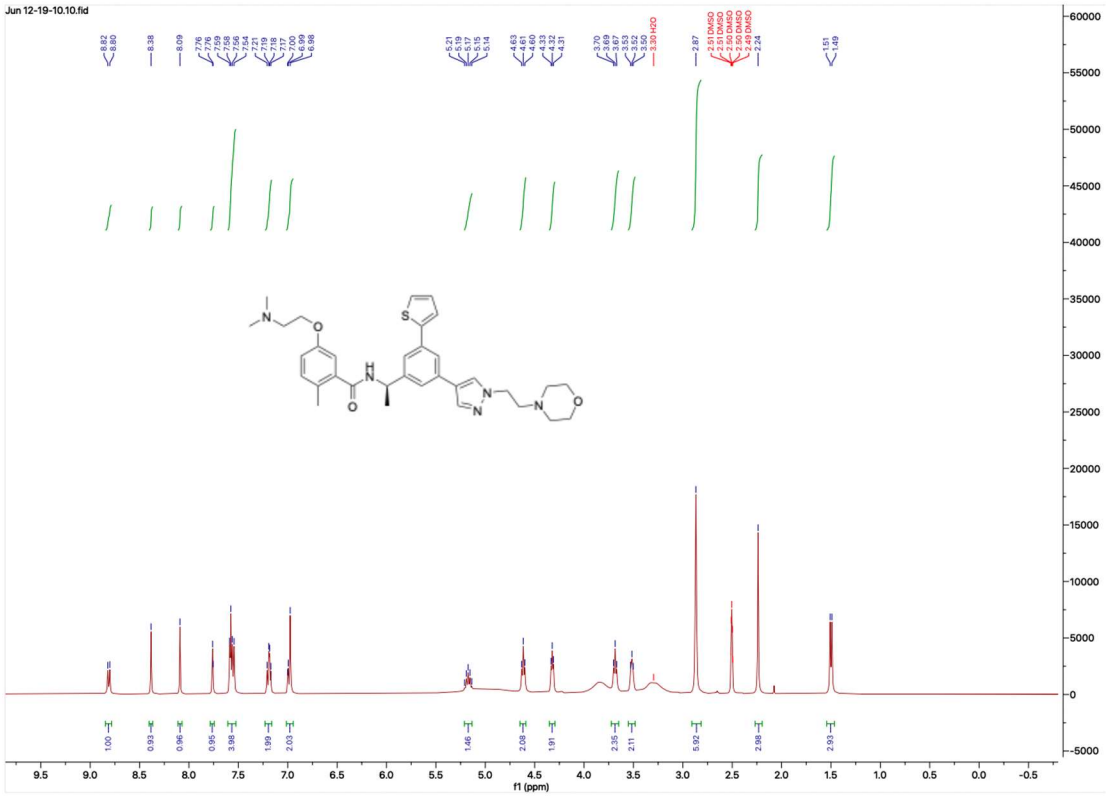

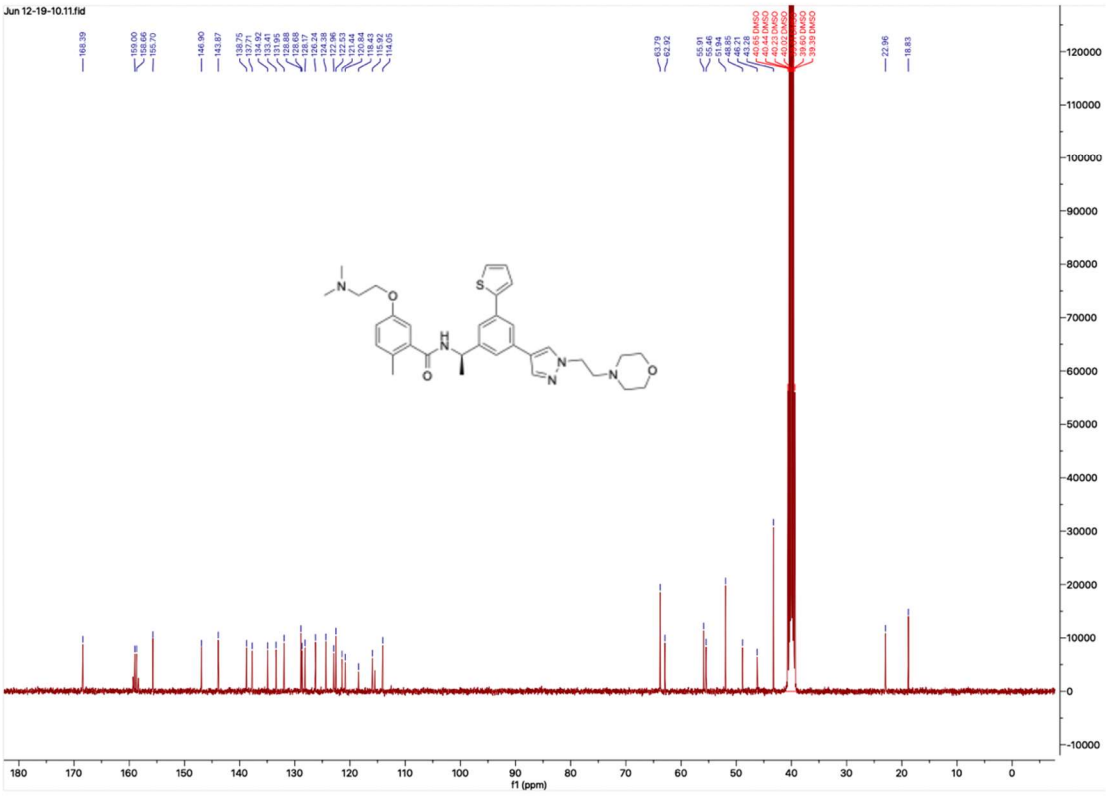

HNMR and CNMR spectra of Jun12511

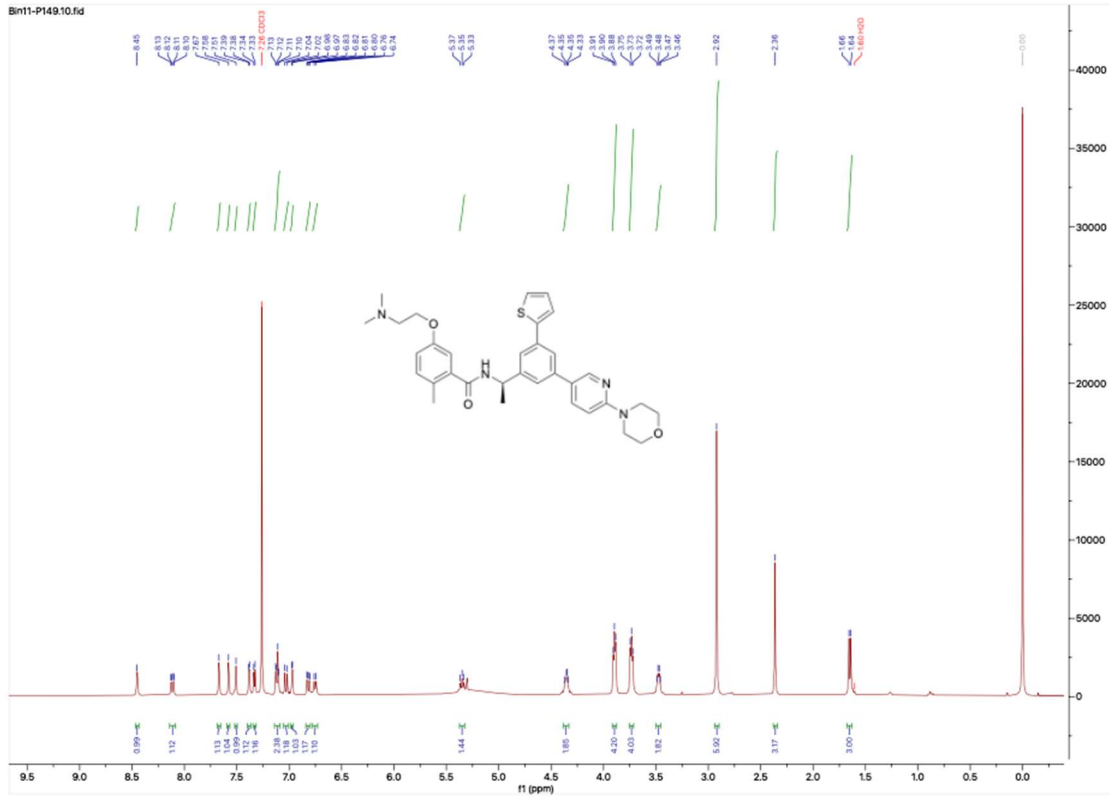

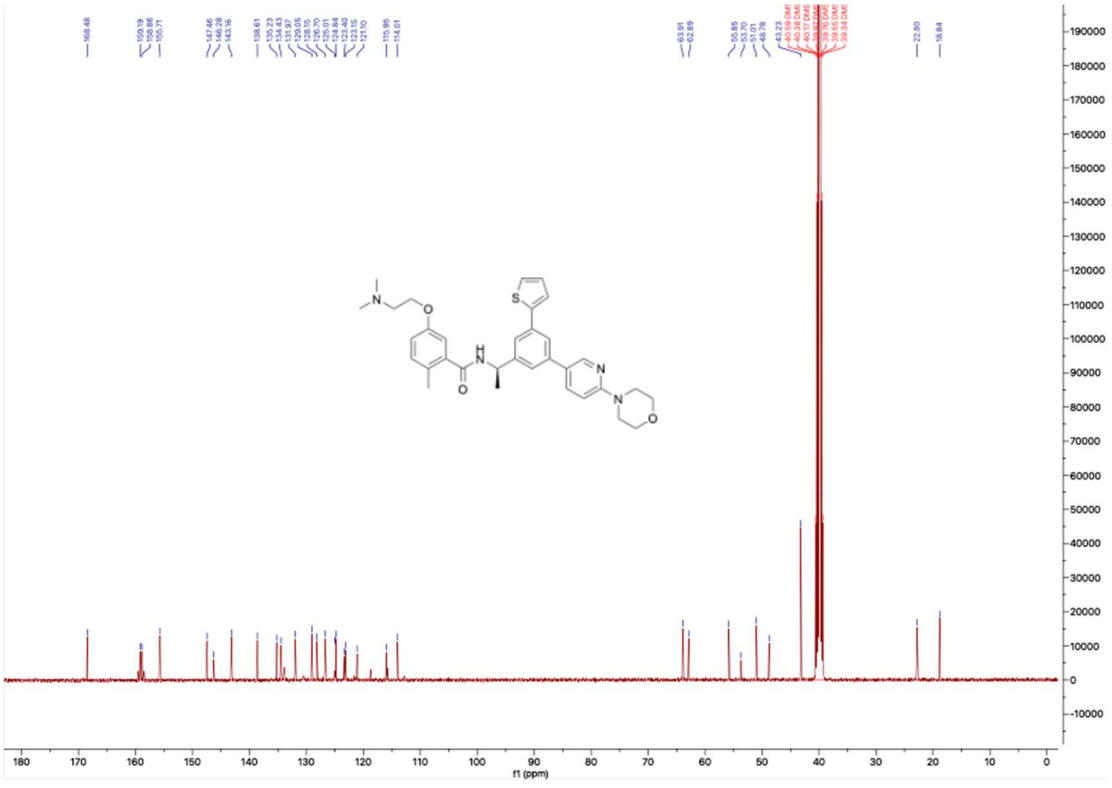

HNMR and CNMR spectra of Jun12338

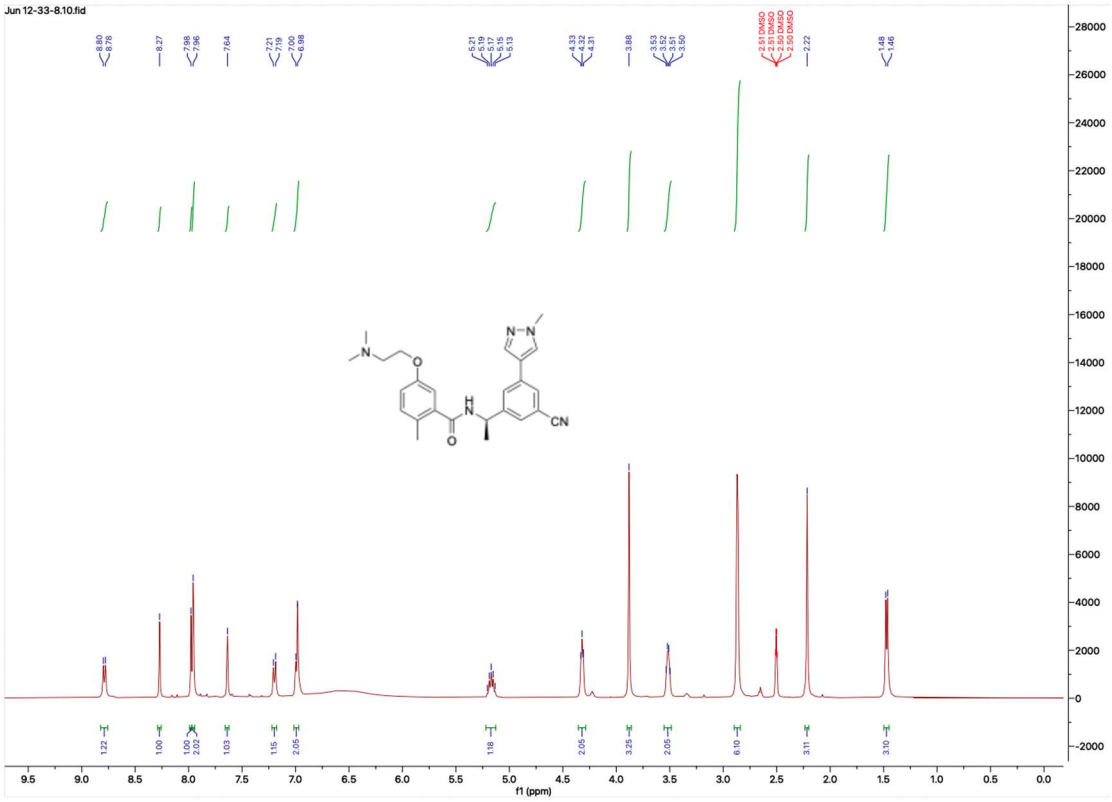

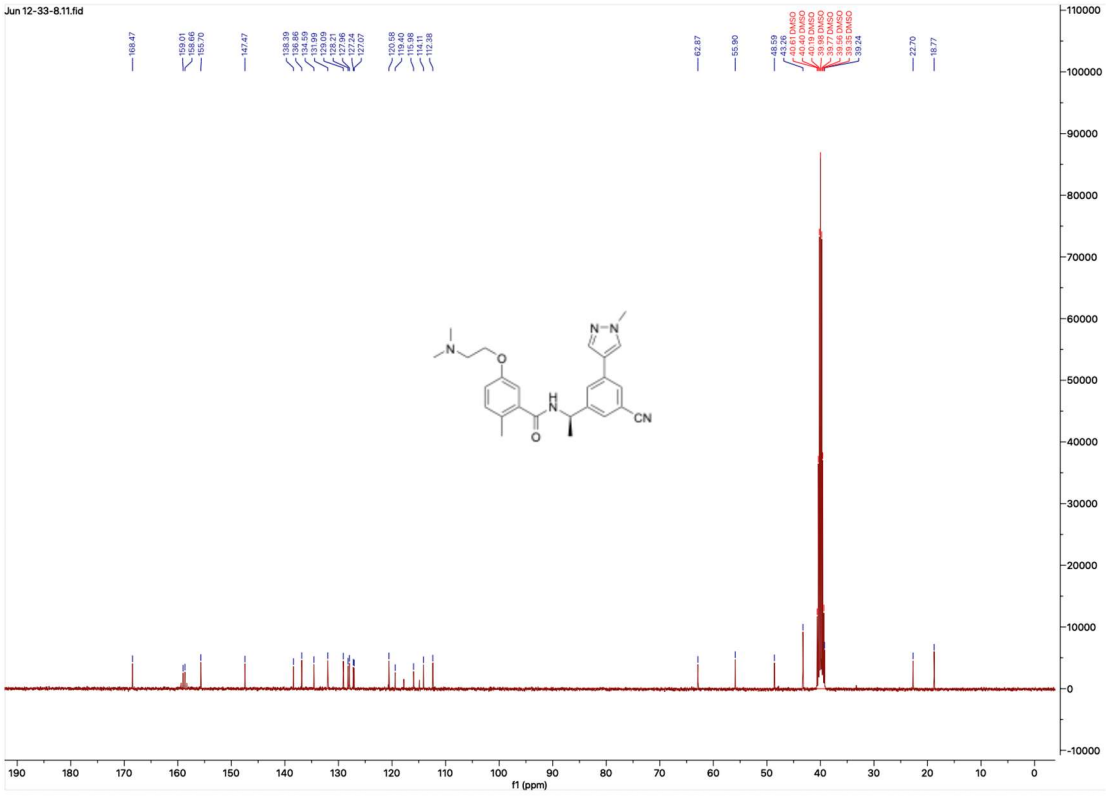

HNMR and CNMR spectra of Jun12145

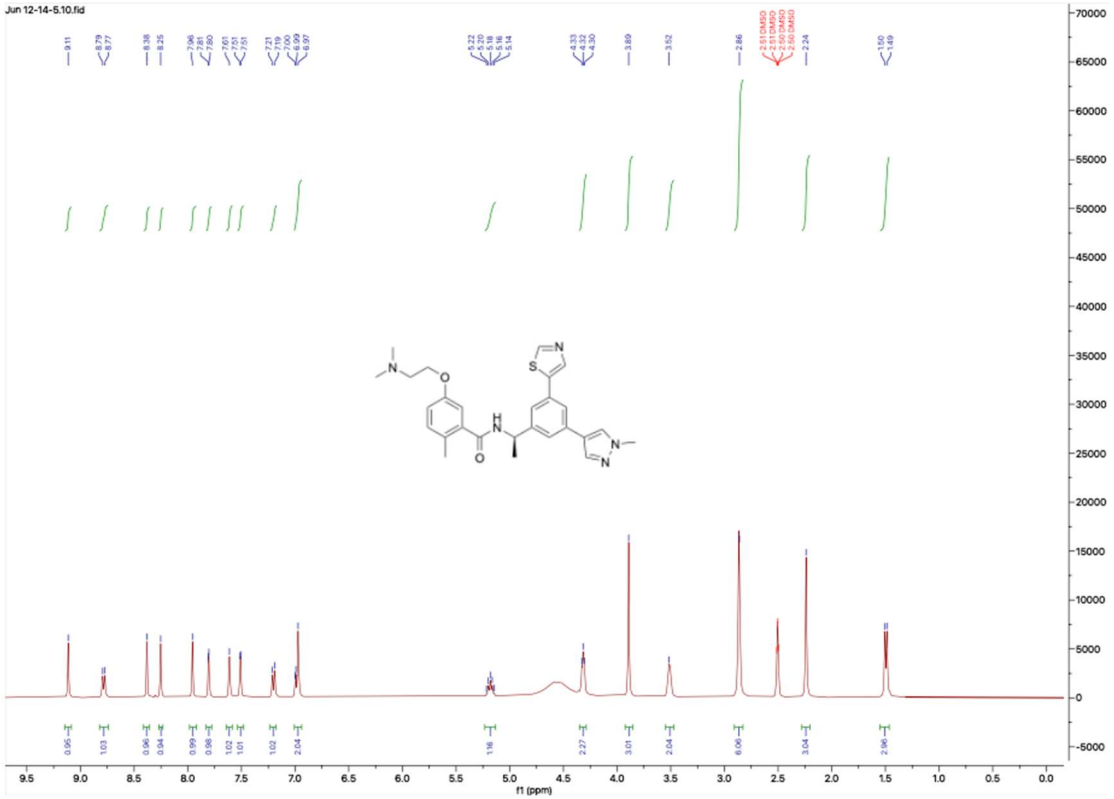

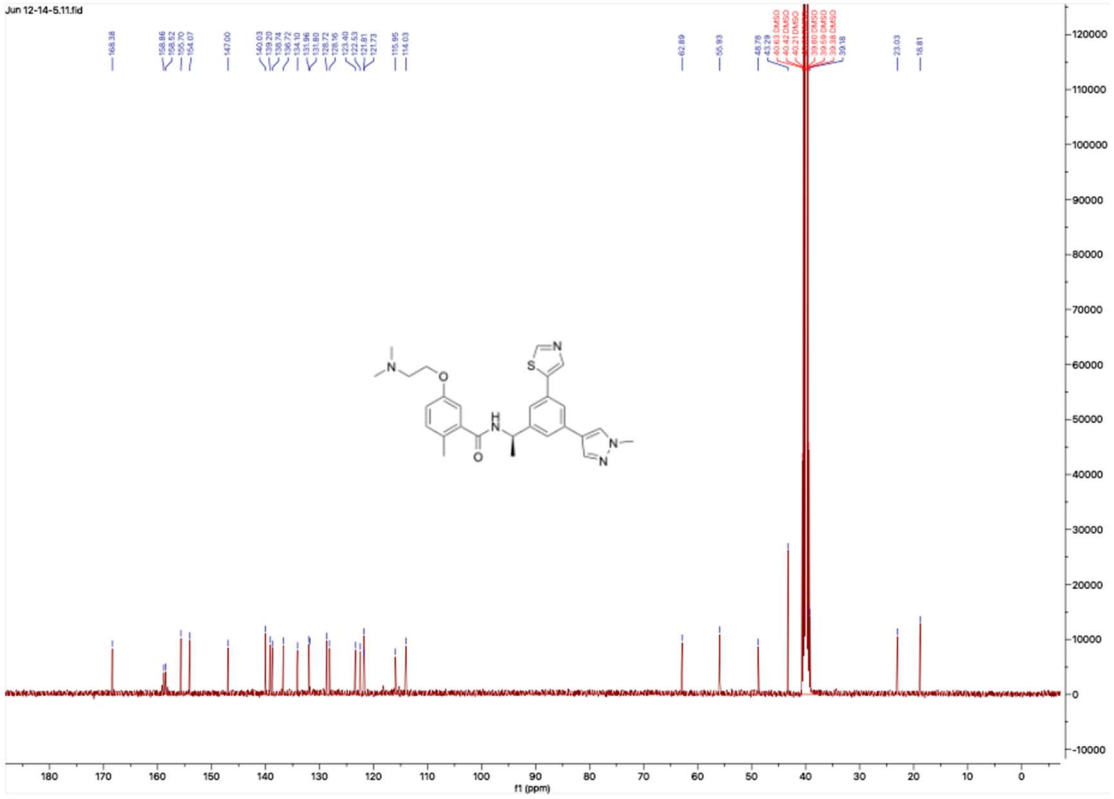

HNMR and CNMR spectra of Jun12681

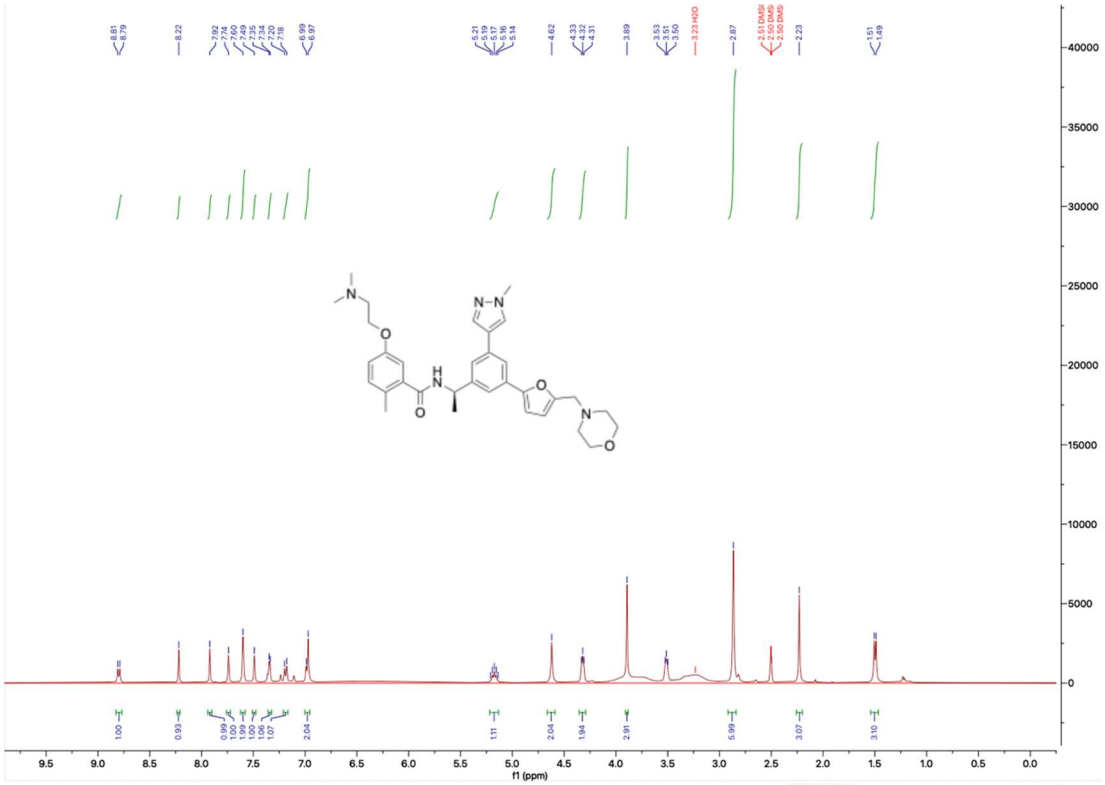

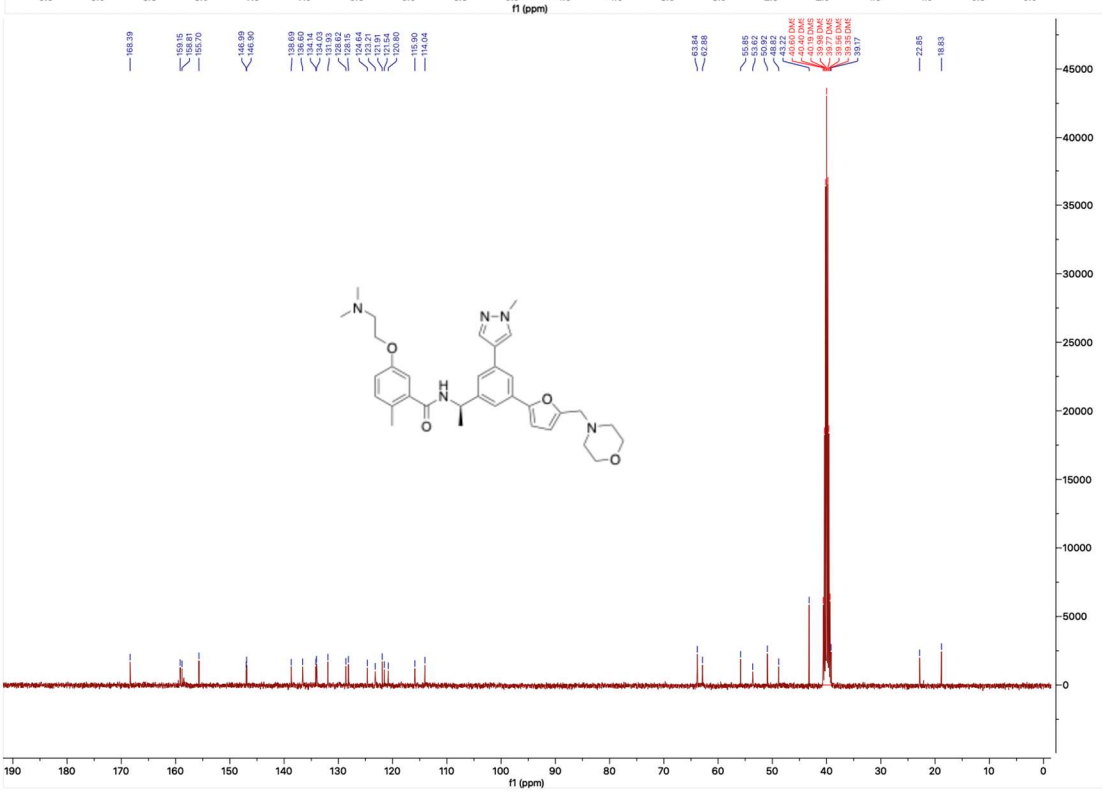

HNMR and CNMR spectra of Jun121911

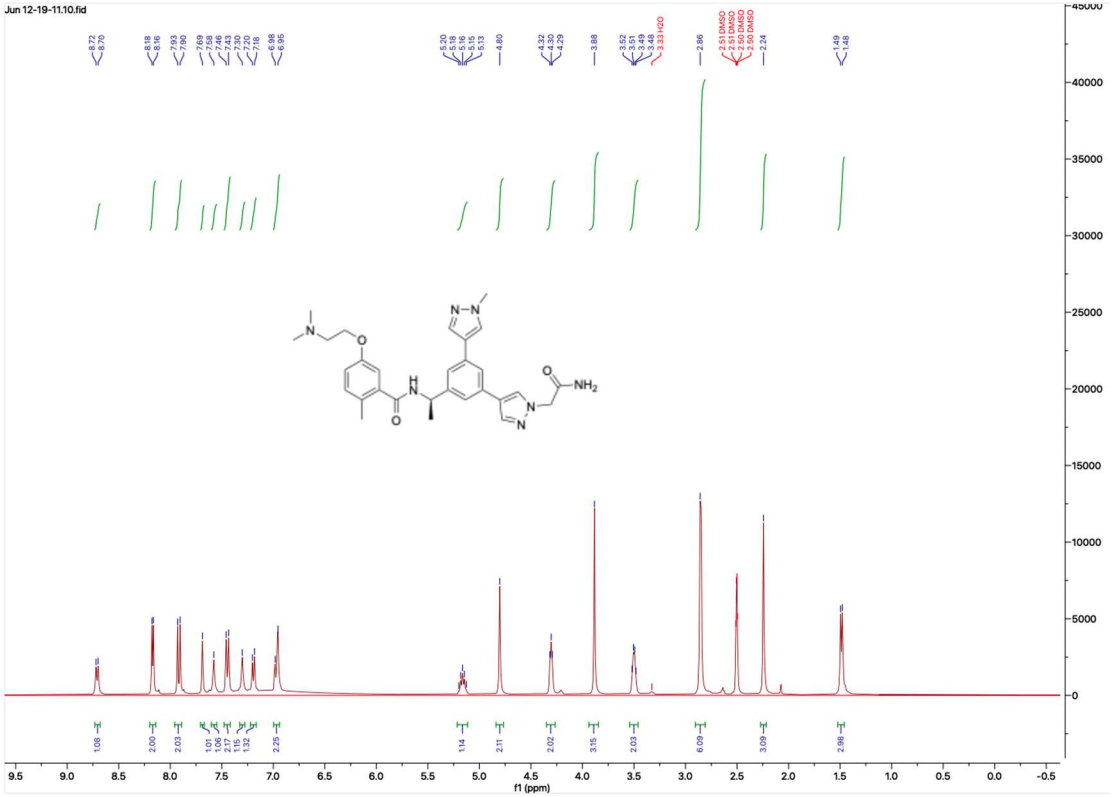

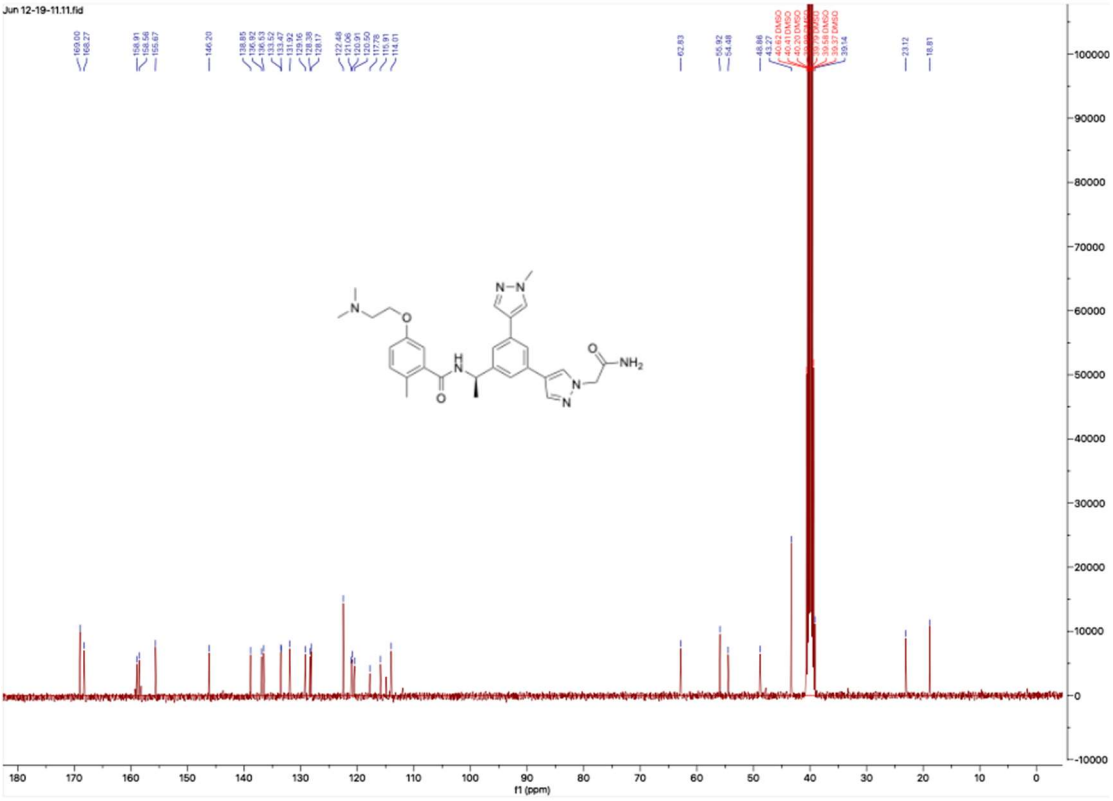

HNMR and CNMR spectra of Jun12336

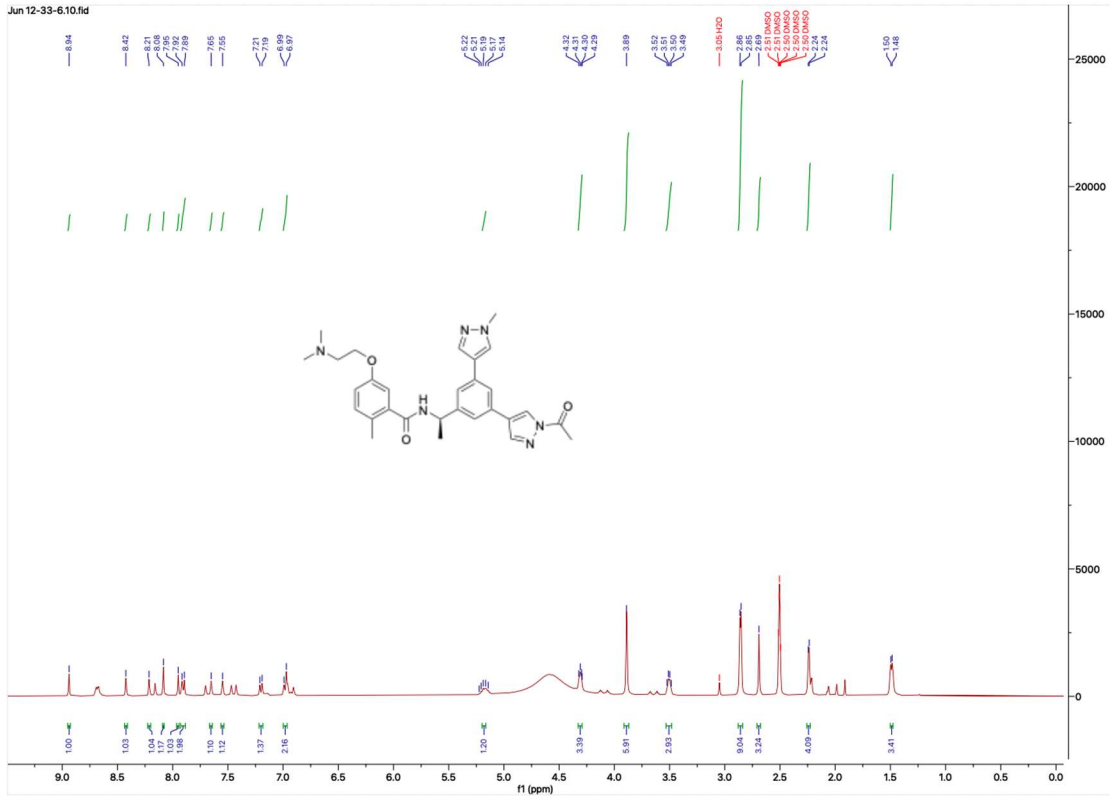

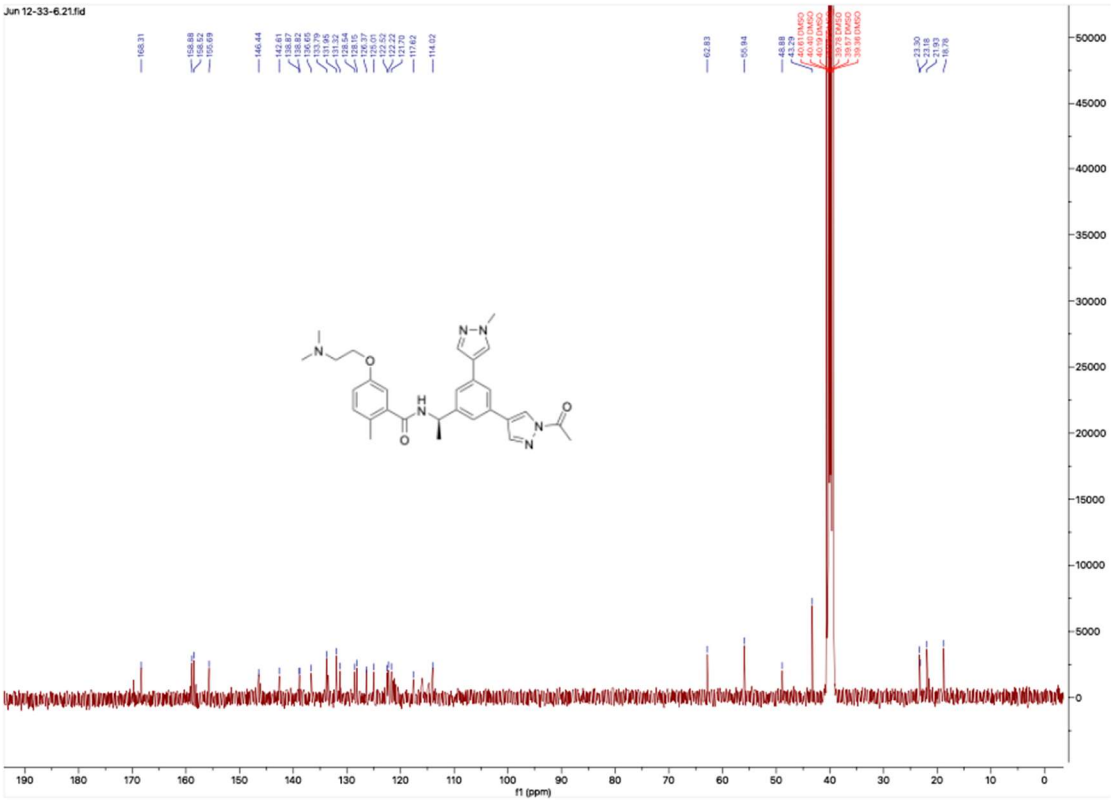

HNMR and CNMR spectra of Jun12467

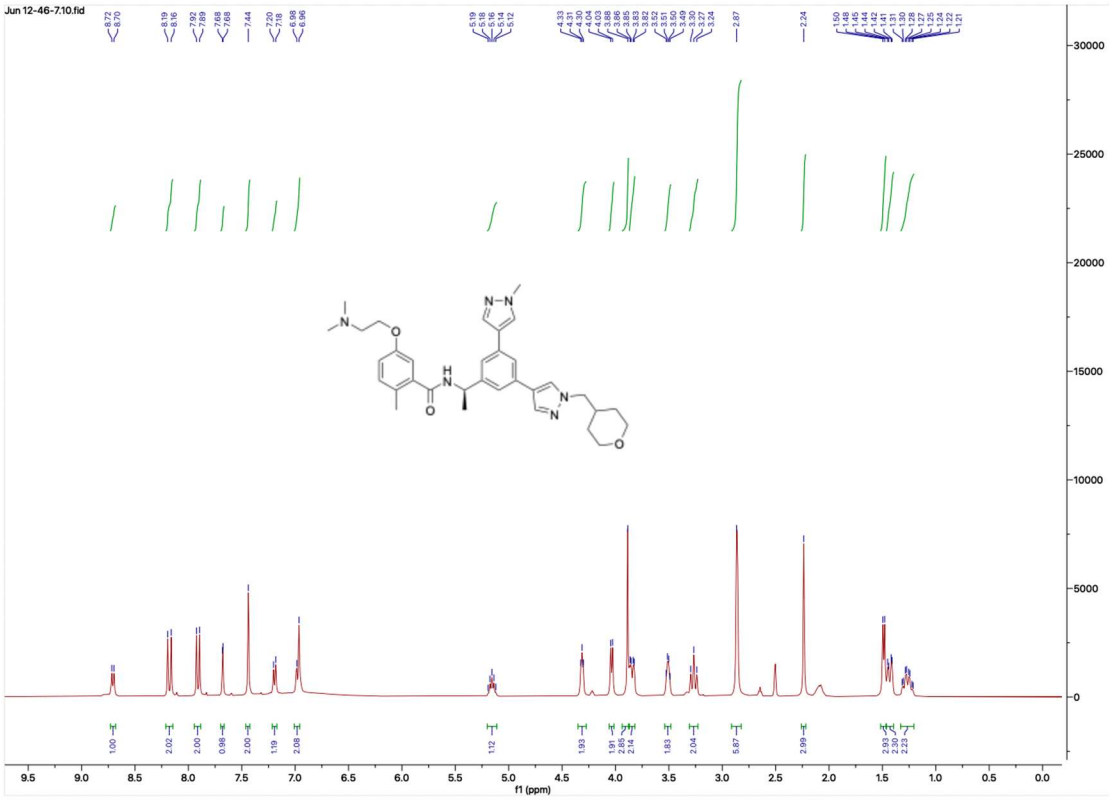

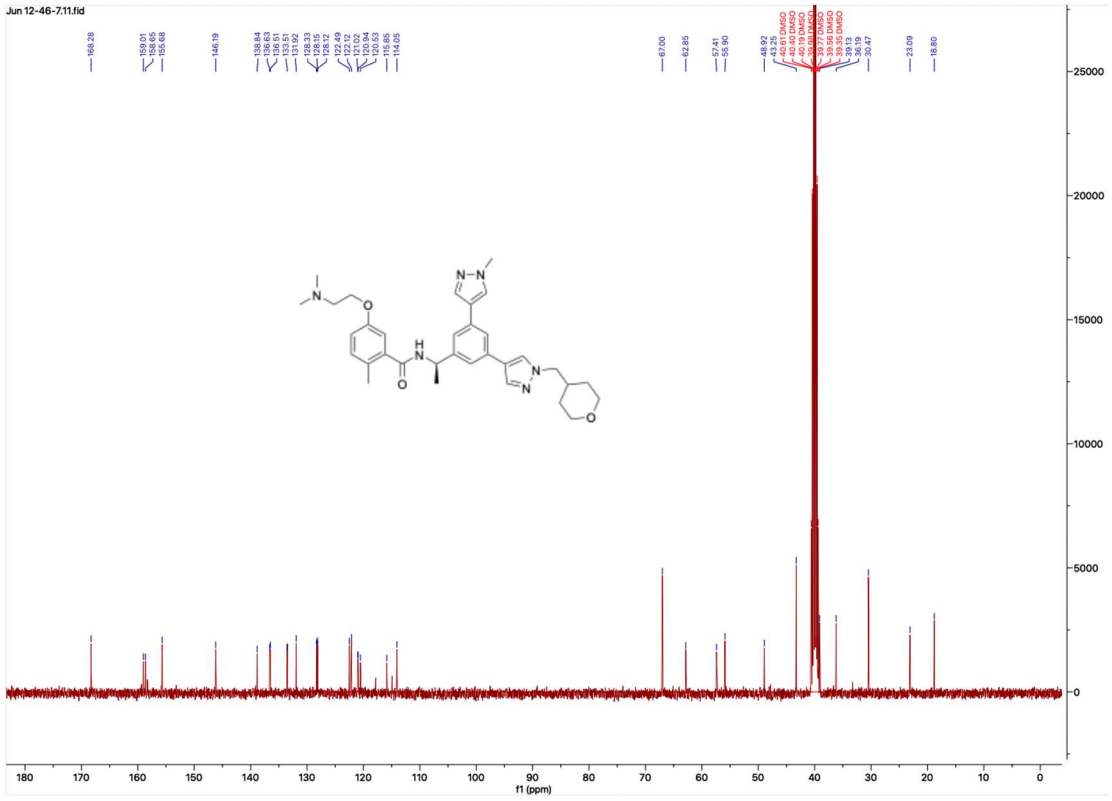

HNMR and CNMR spectra of Jun12351

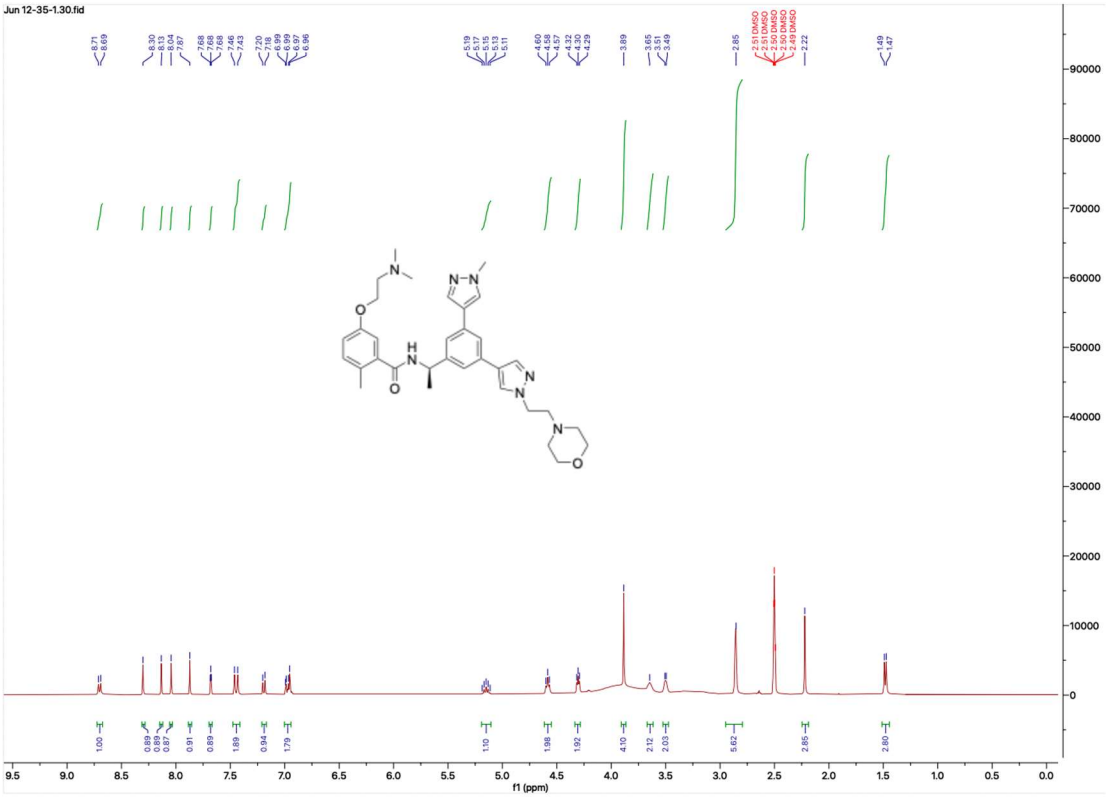

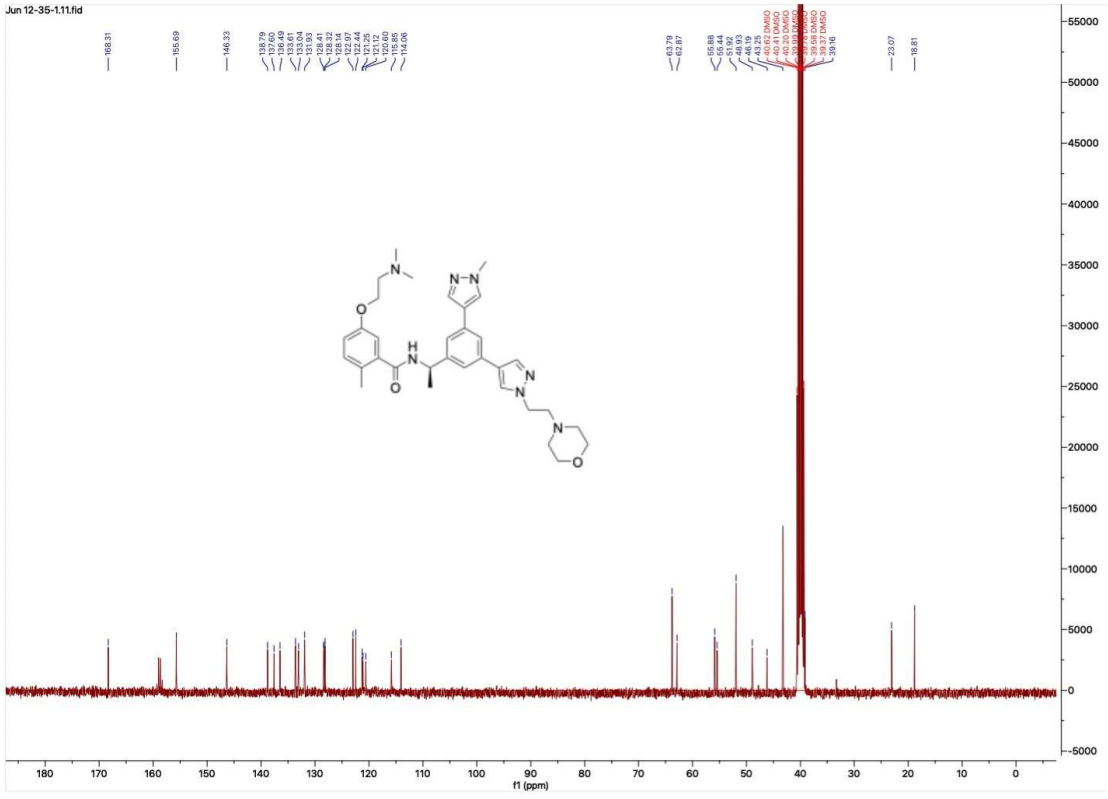

HNMR and CNMR spectra of Jun12199

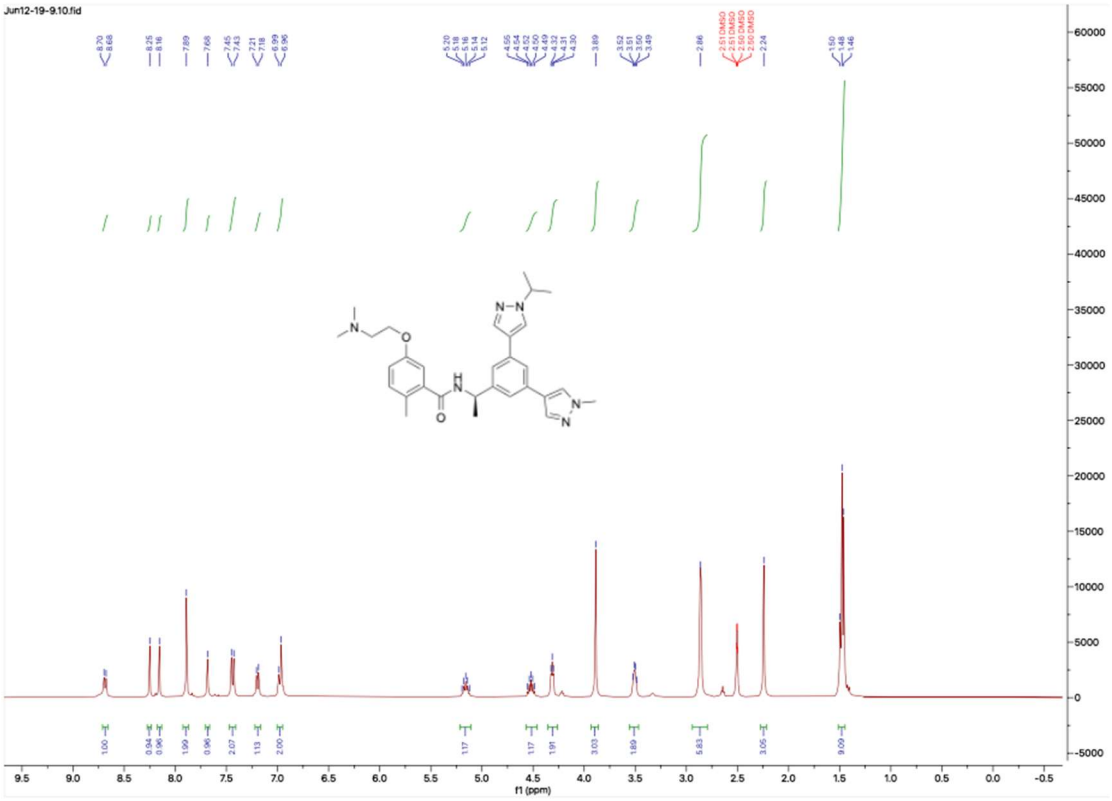

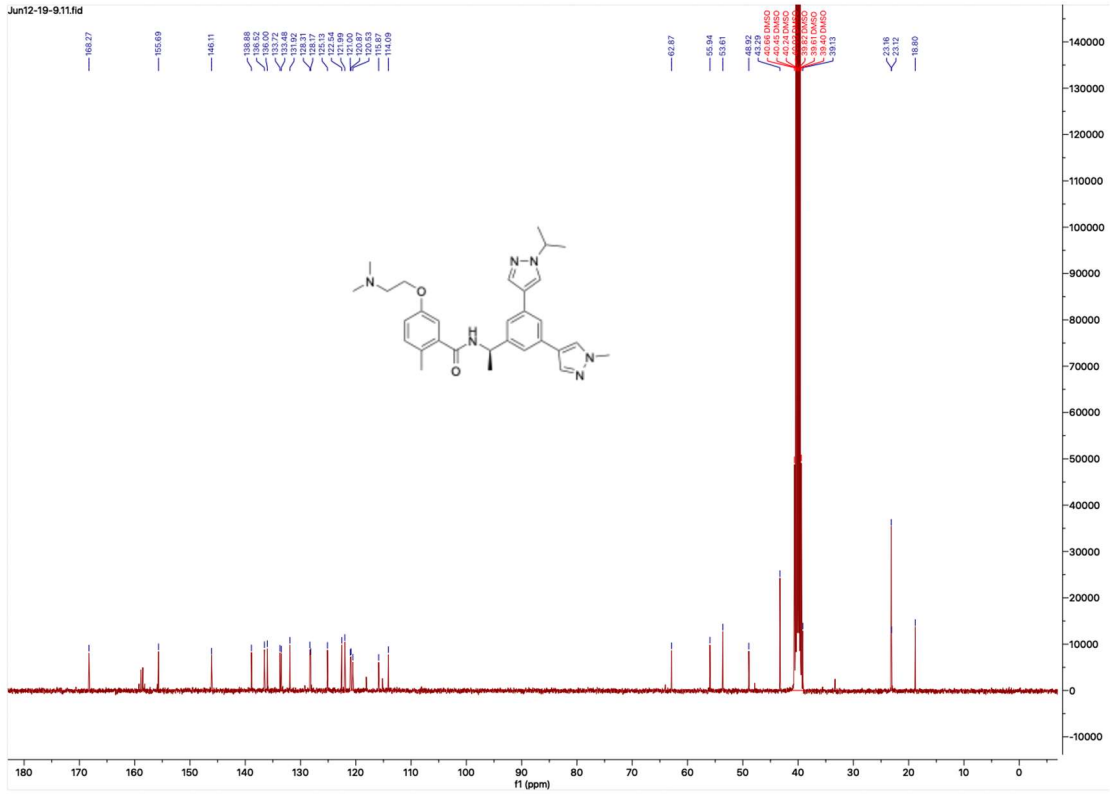

HNMR and CNMR spectra of Jun12197

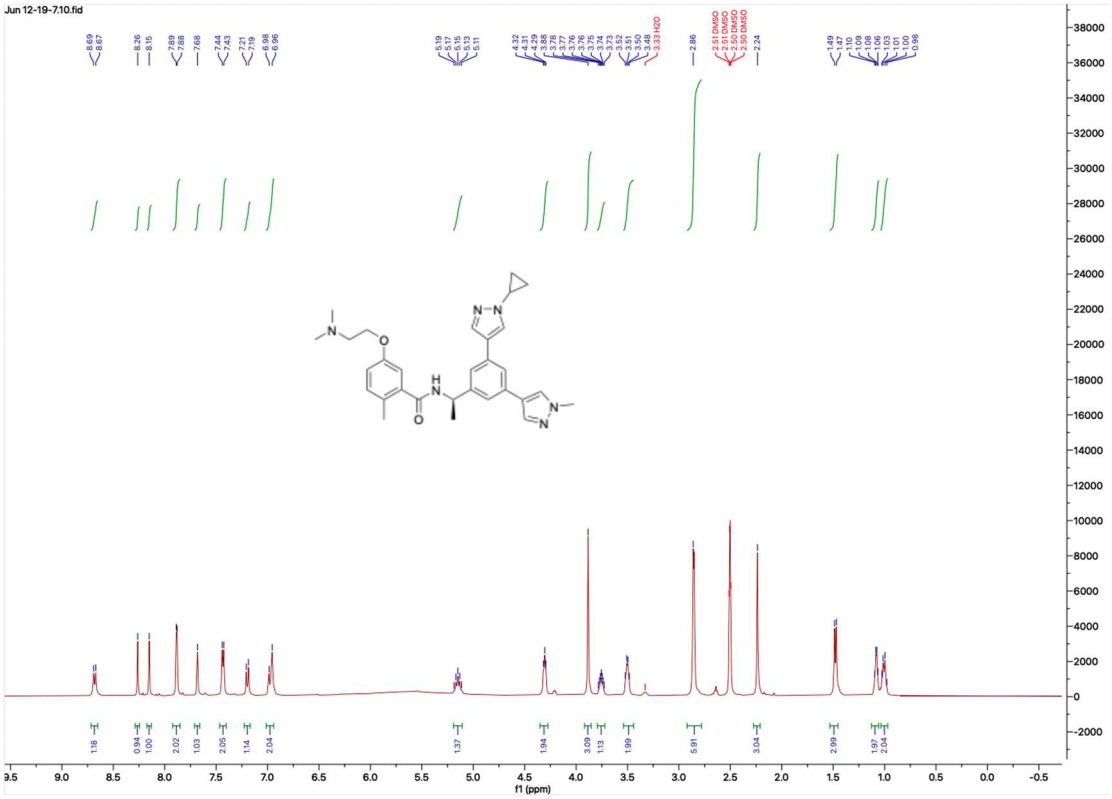

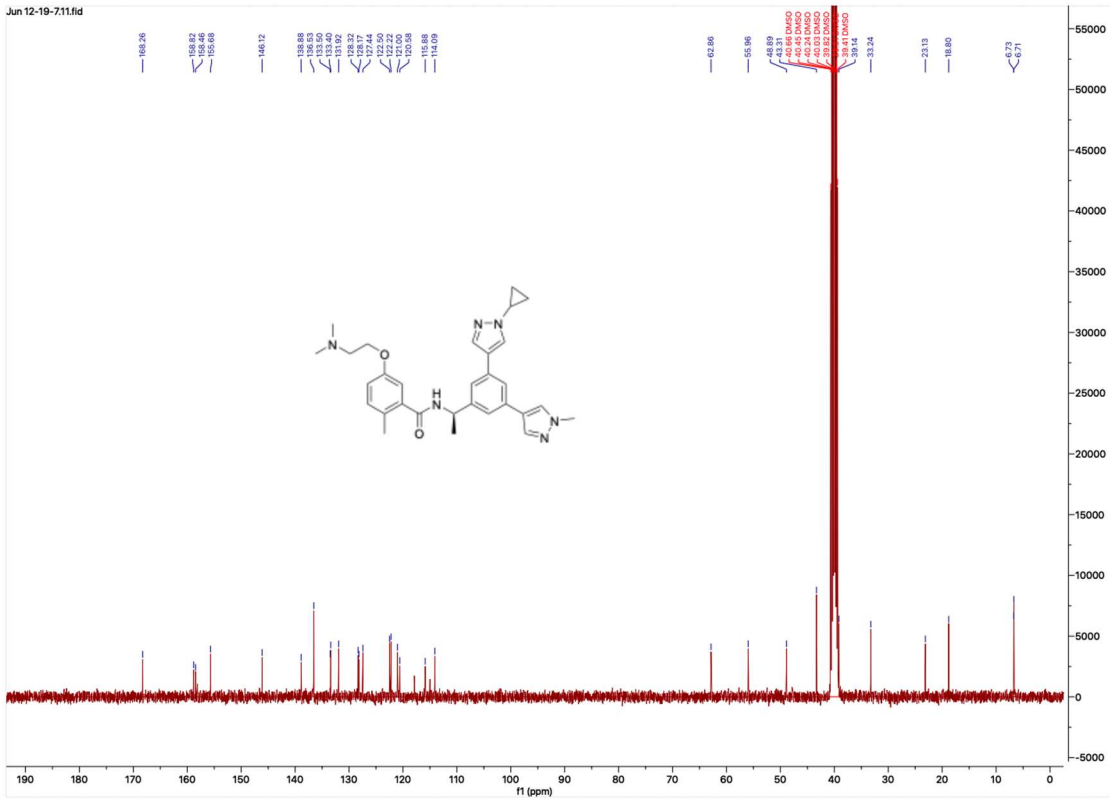

HNMR and CNMR spectra of Jun12603

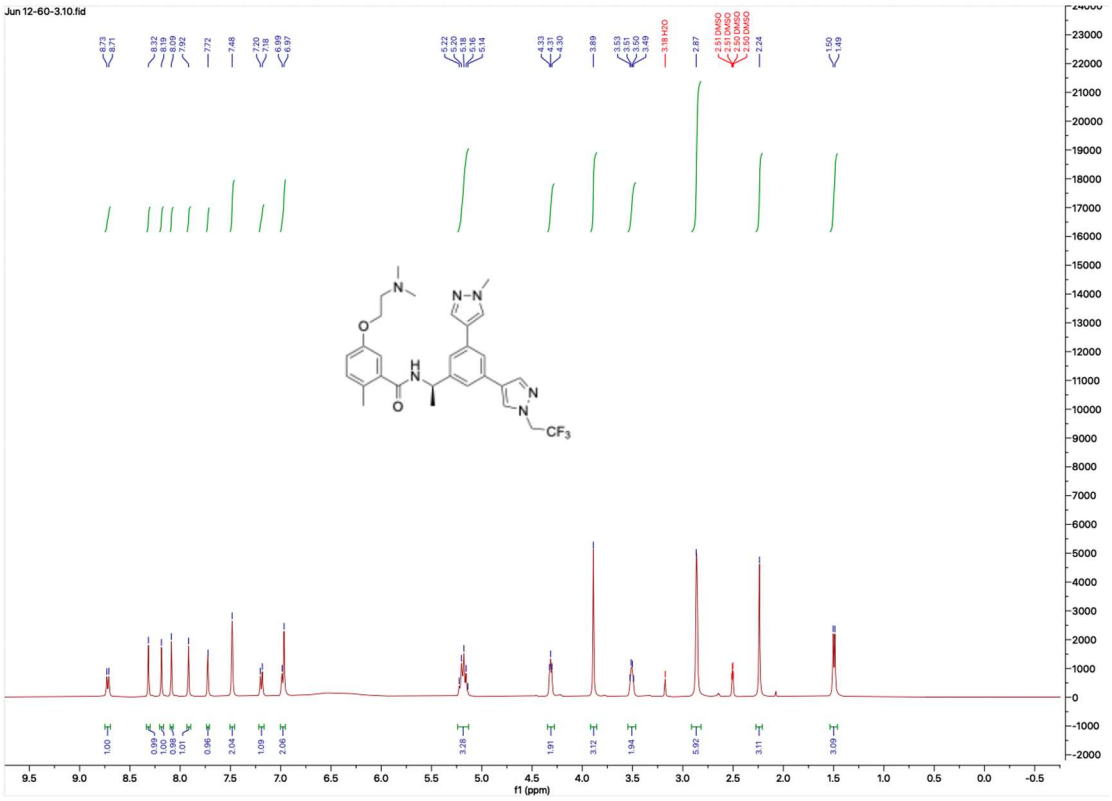

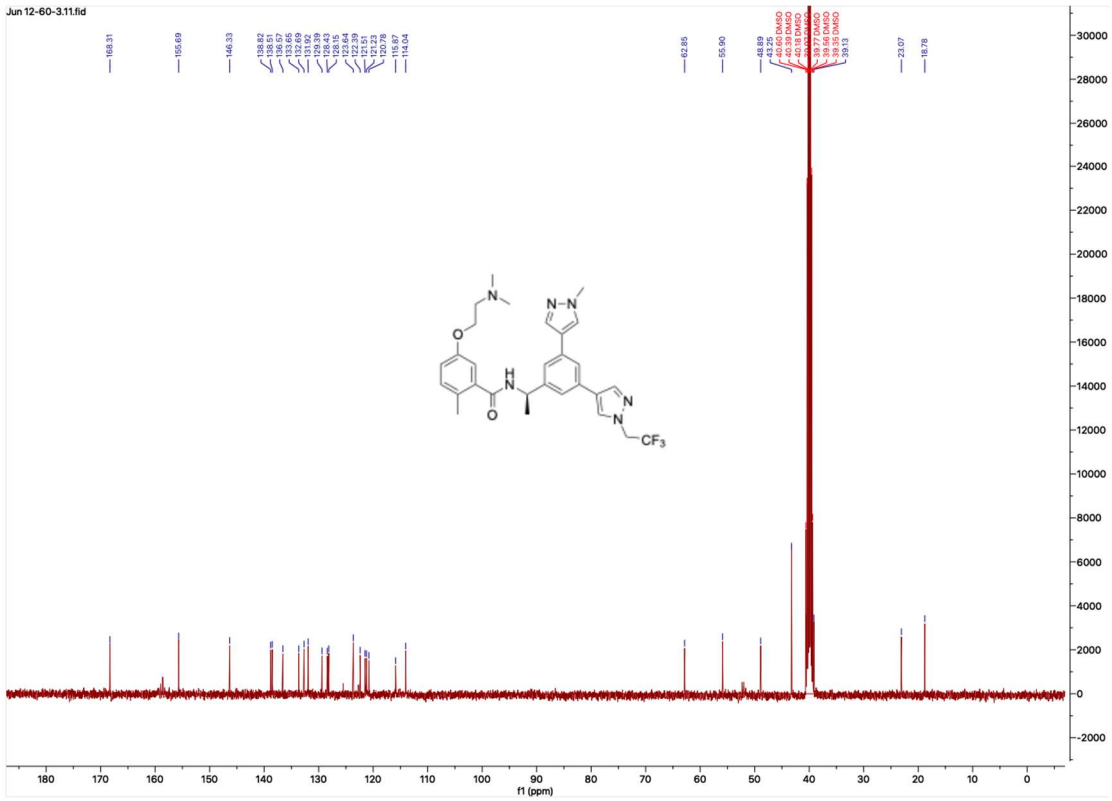

HNMR and CNMR spectra of Jun12446

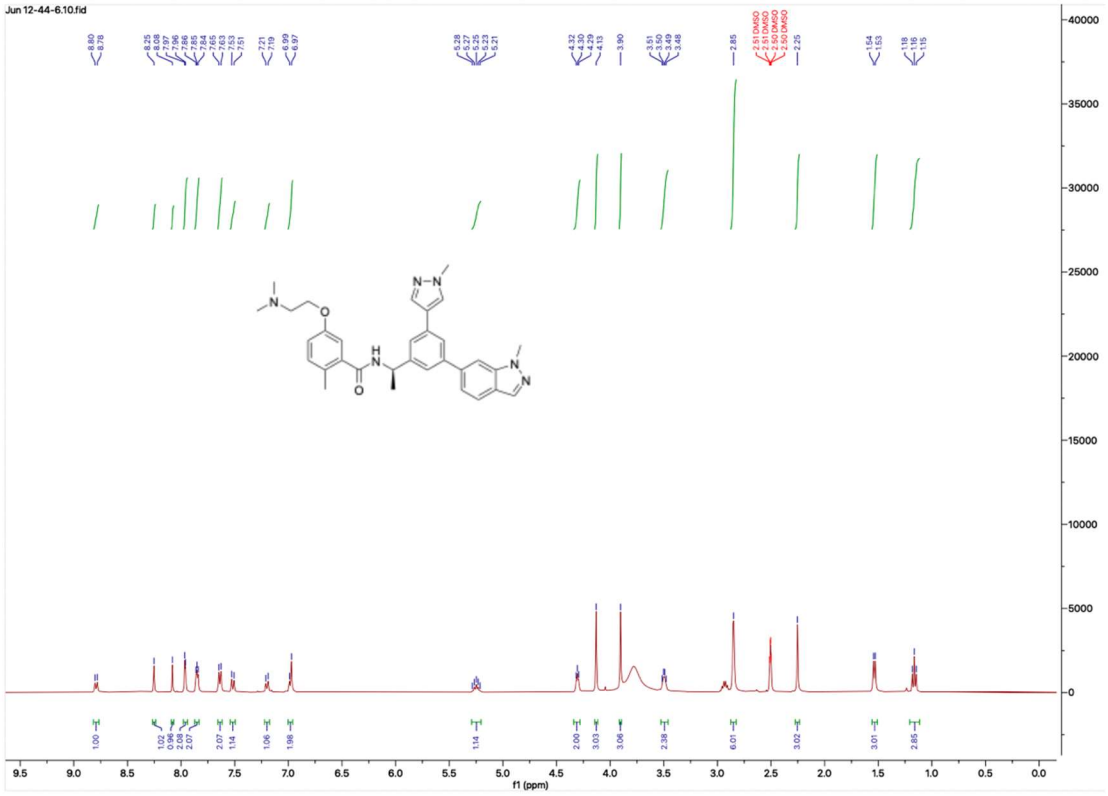

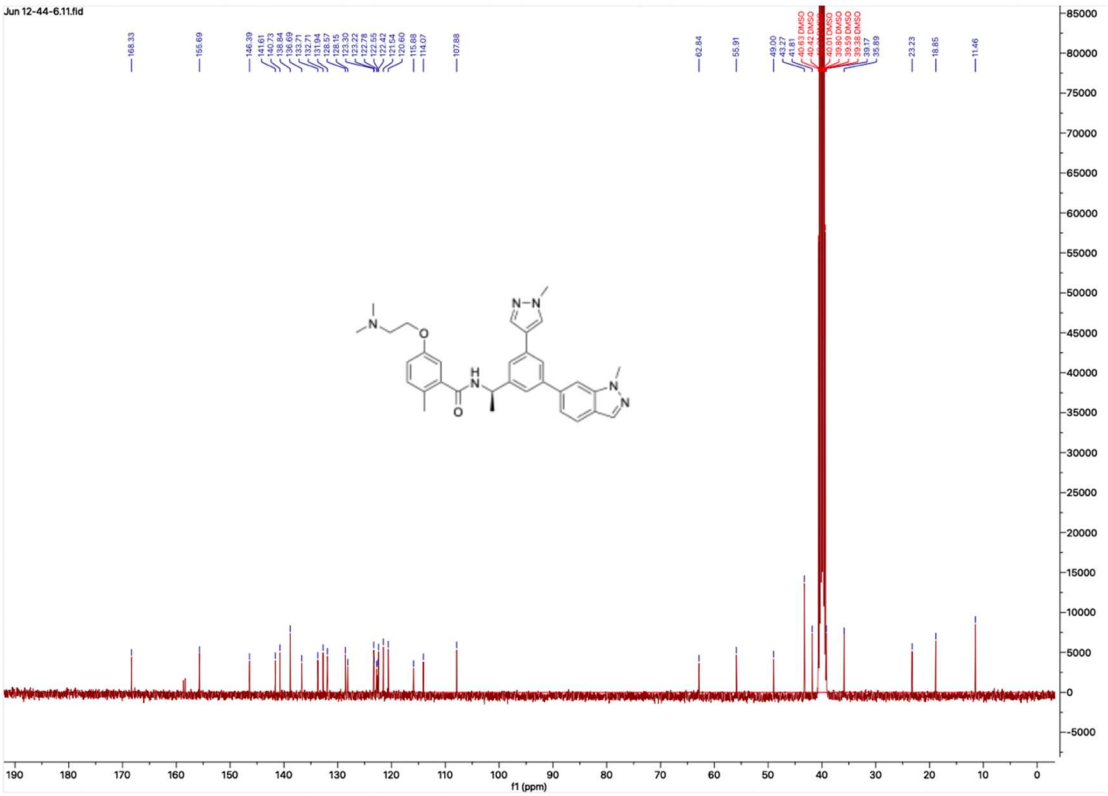

HNMR and CNMR spectra of Jun12278

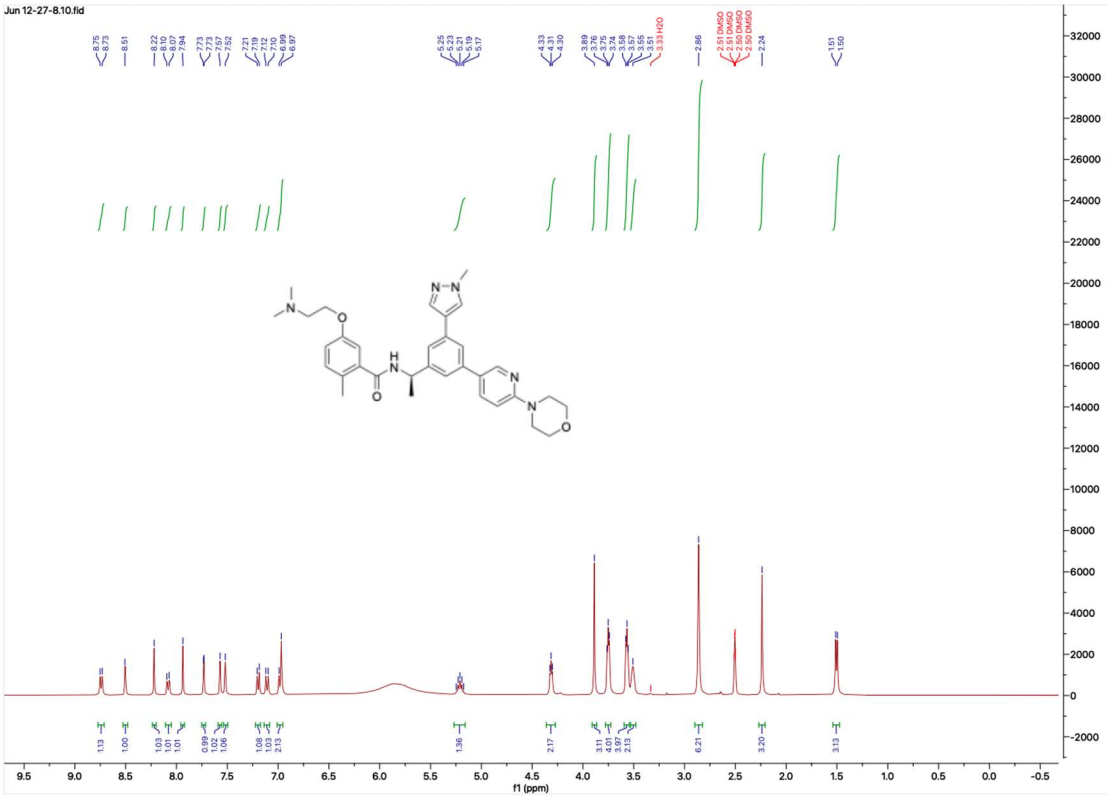

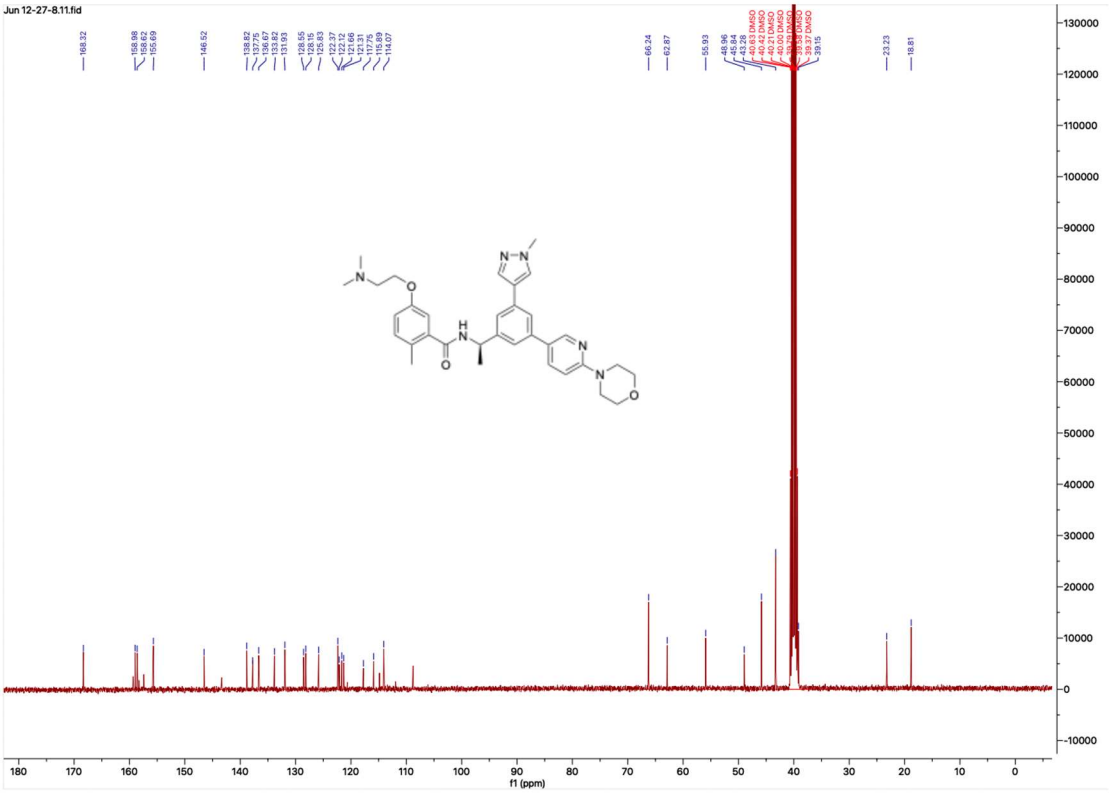

HNMR and CNMR spectra of Jun12162

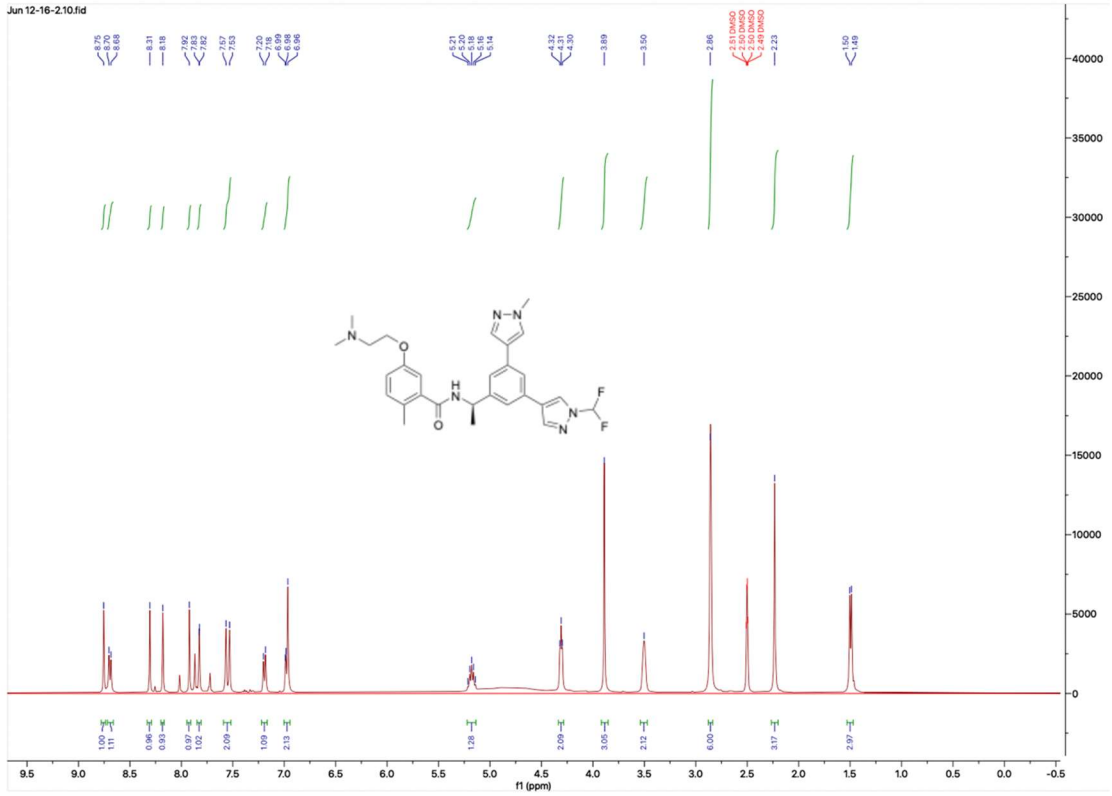

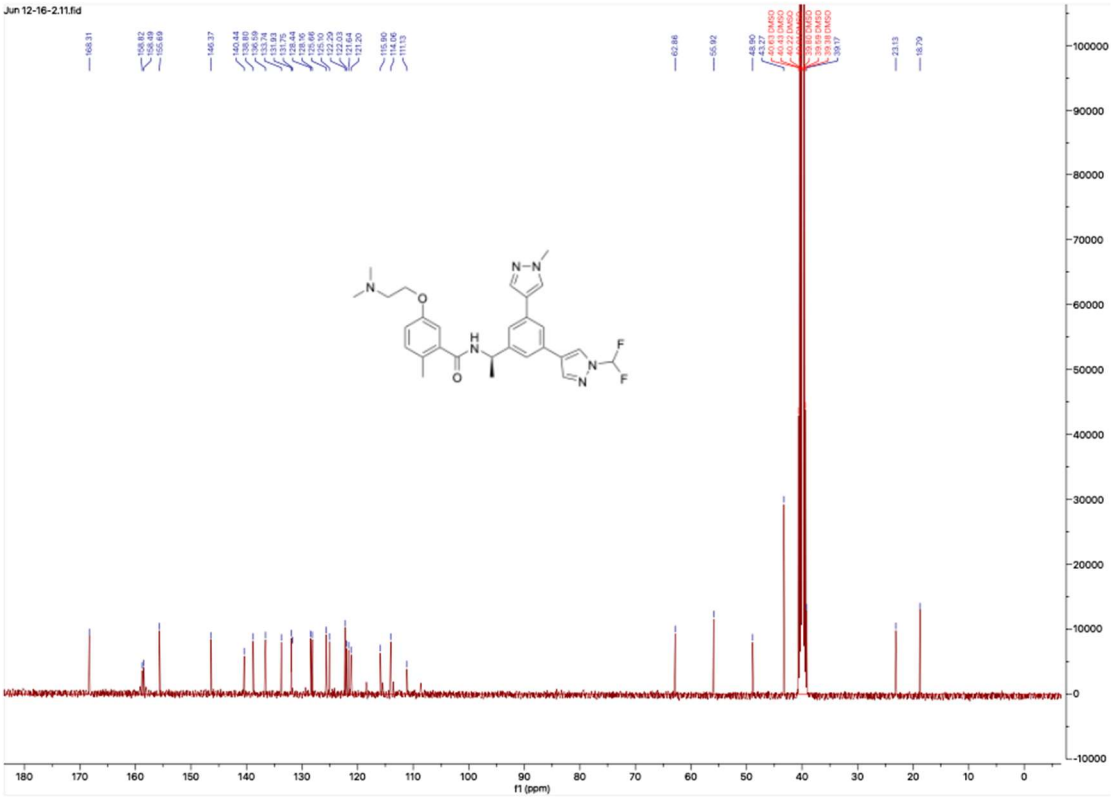

HNMR and CNMR spectra of Jun12208

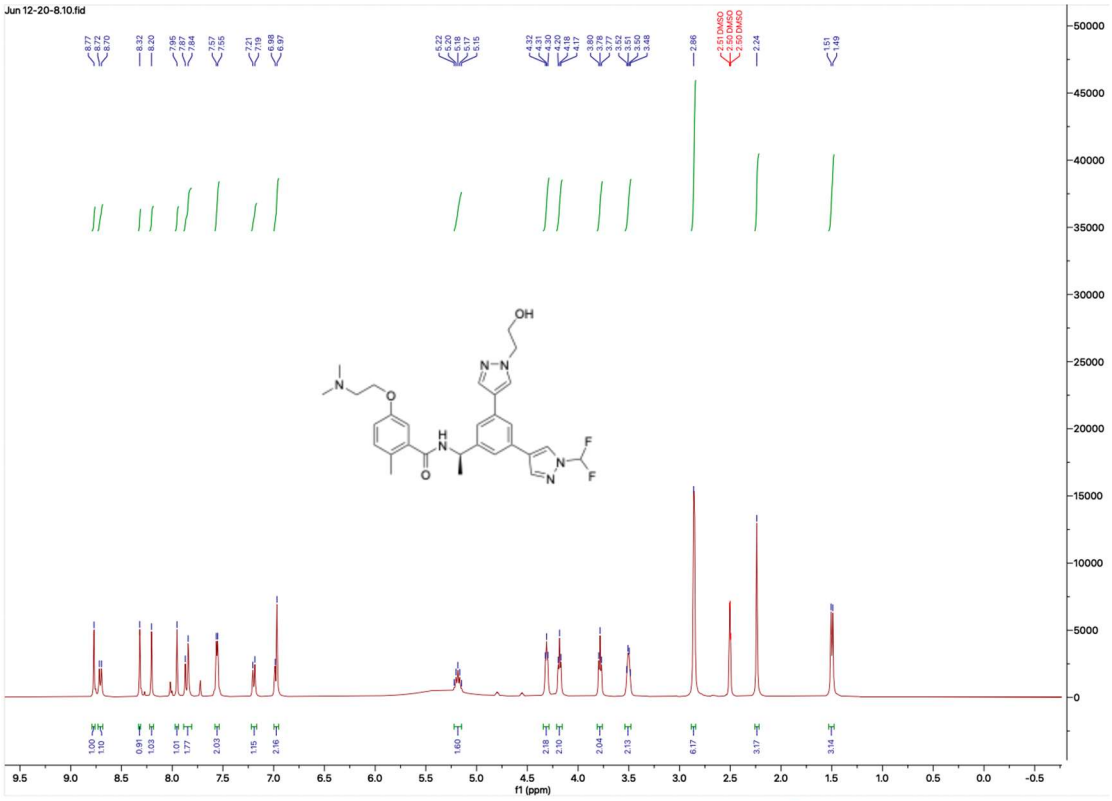

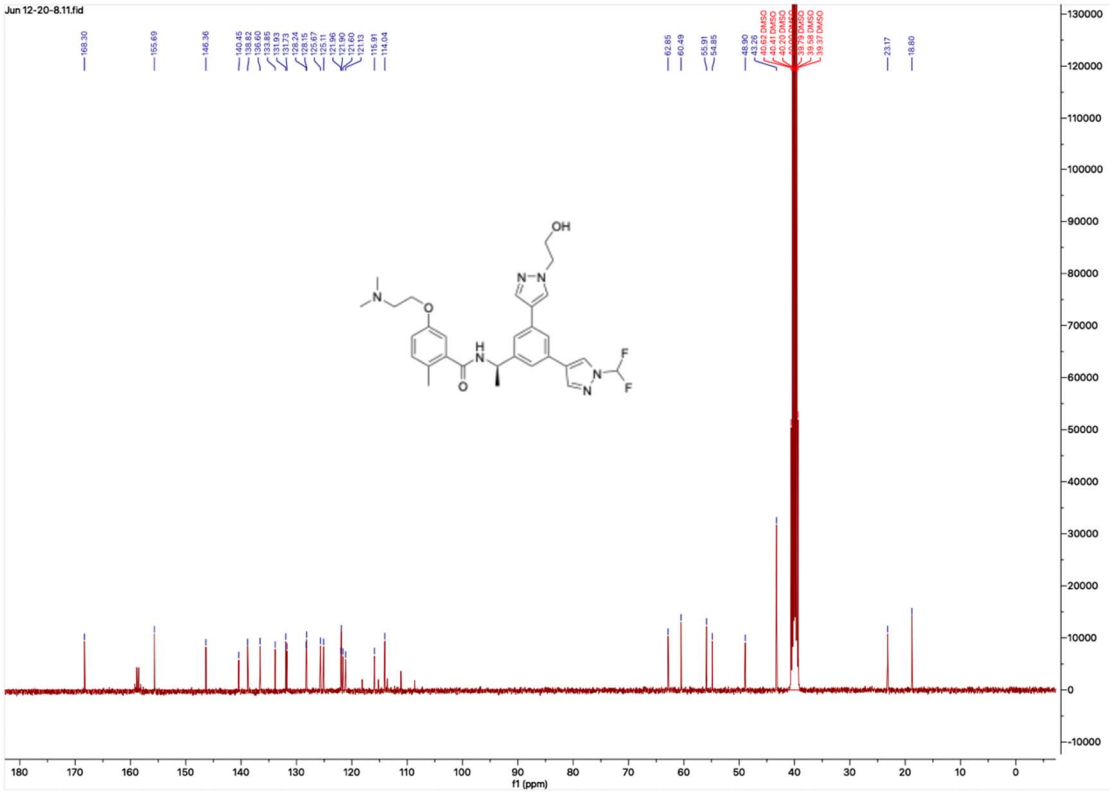

HNMR and CNMR spectra of Jun12235

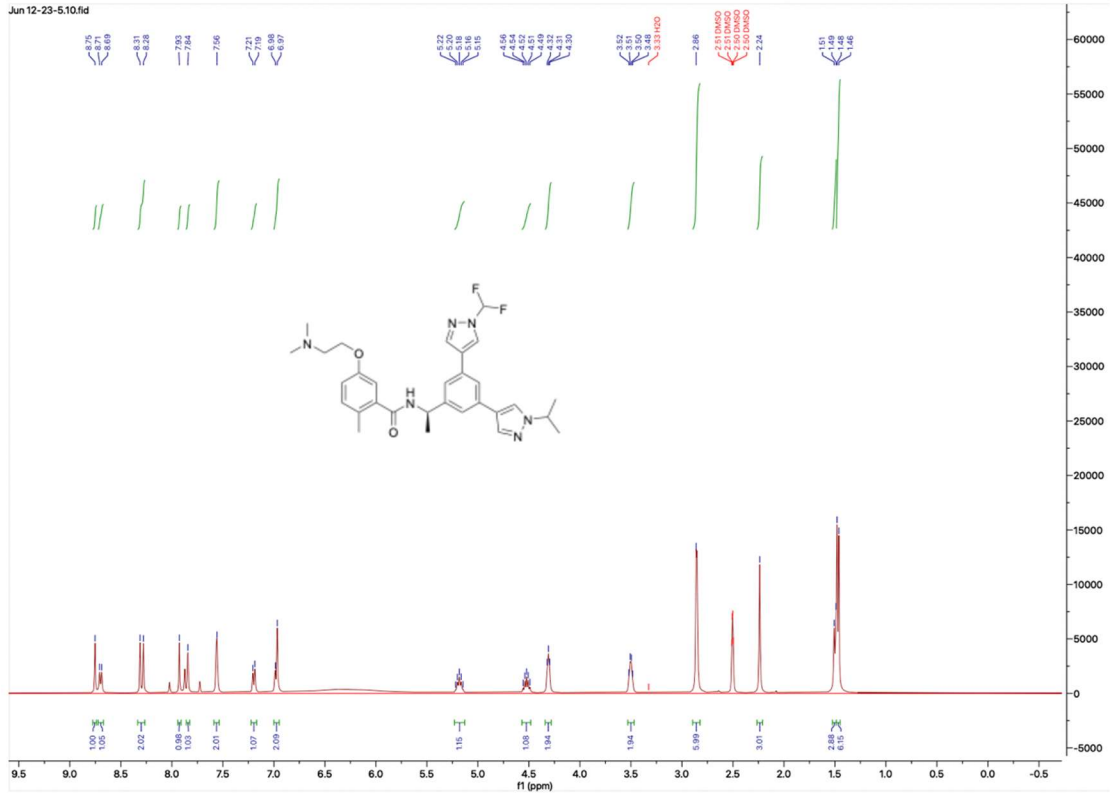

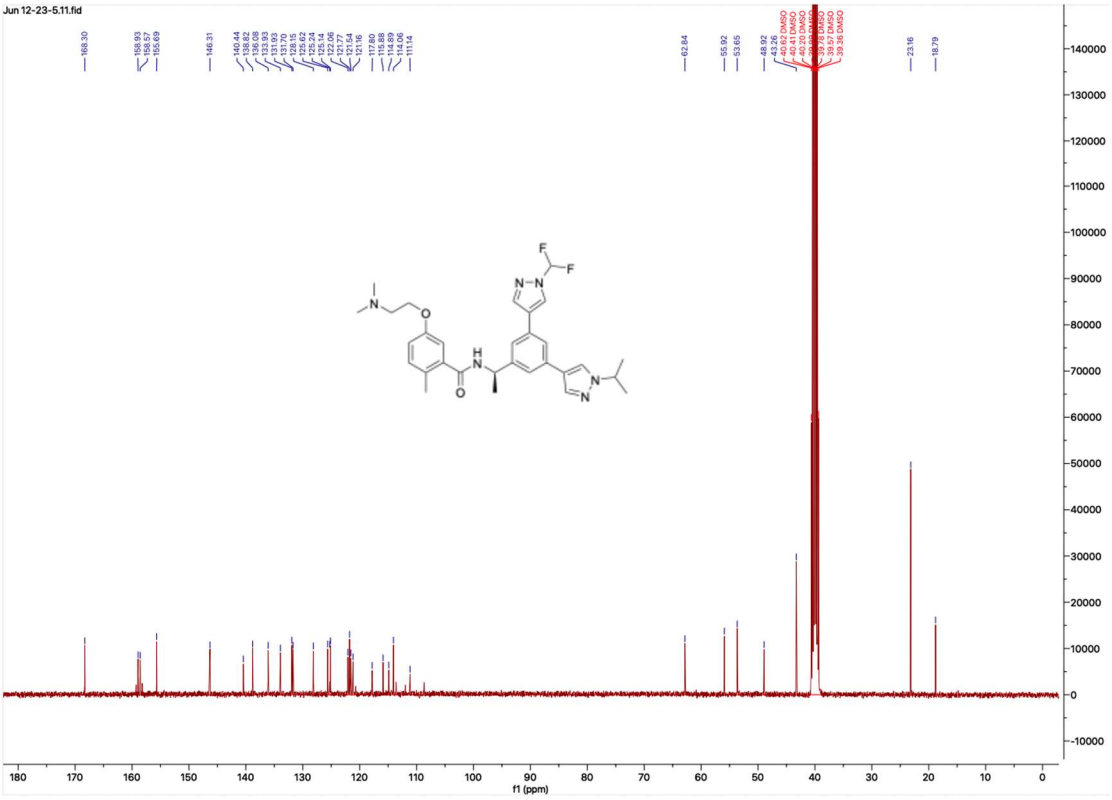

HNMR and CNMR spectra of Jun12281

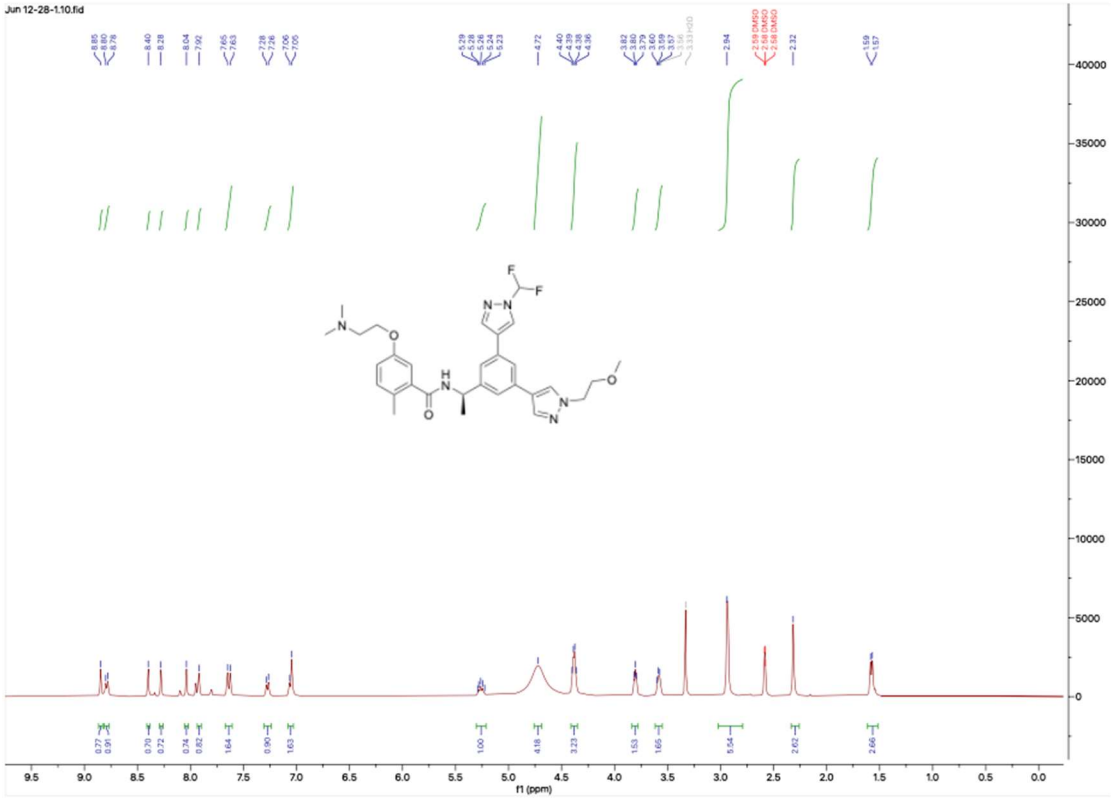

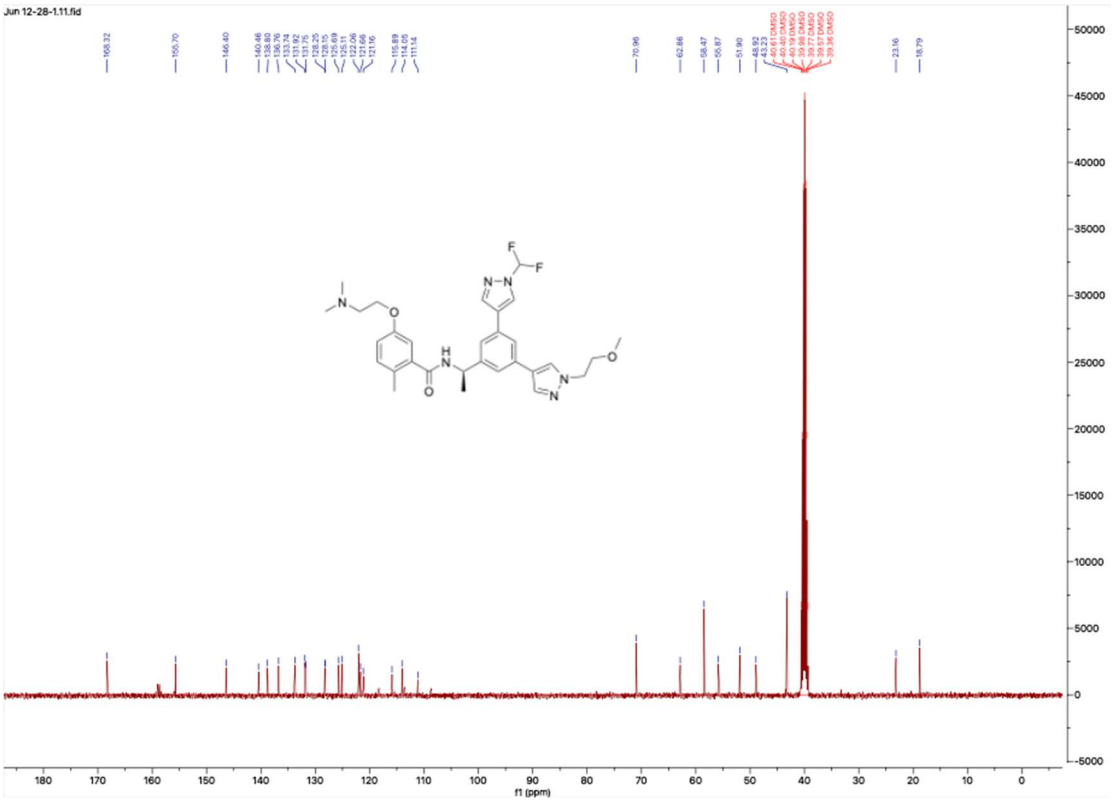

HNMR and CNMR spectra of Jun12303

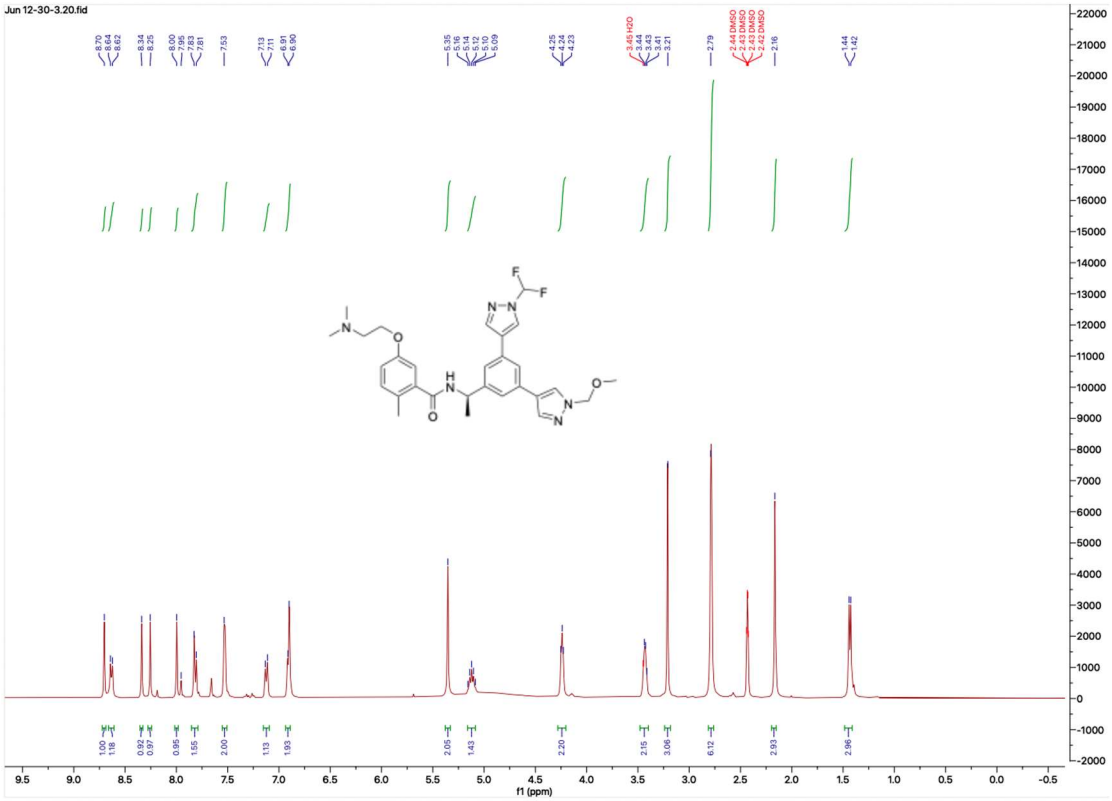

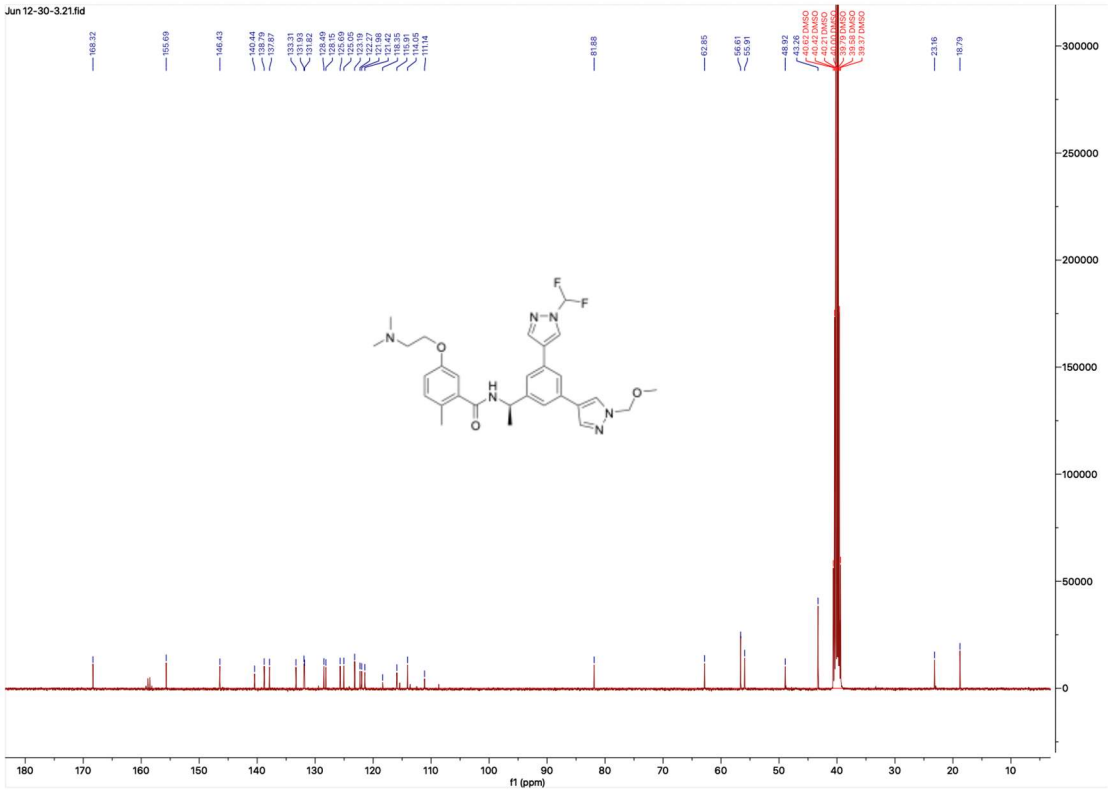

HNMR and CNMR spectra of Jun12284

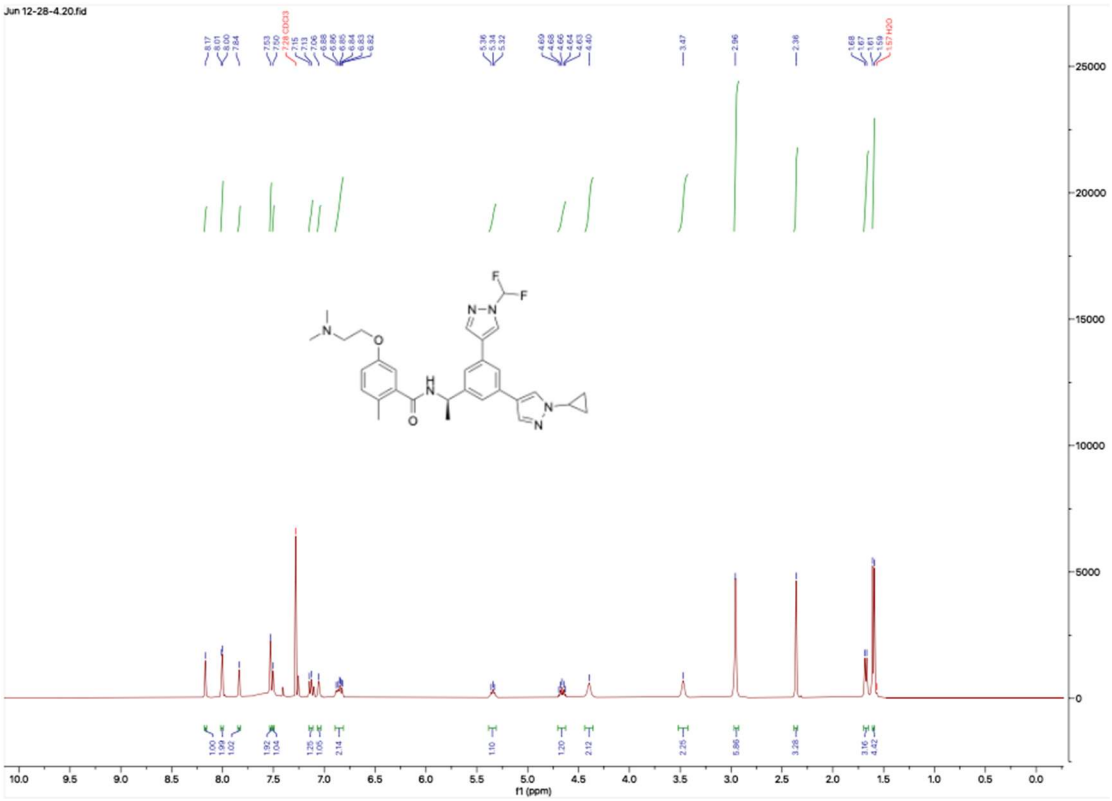

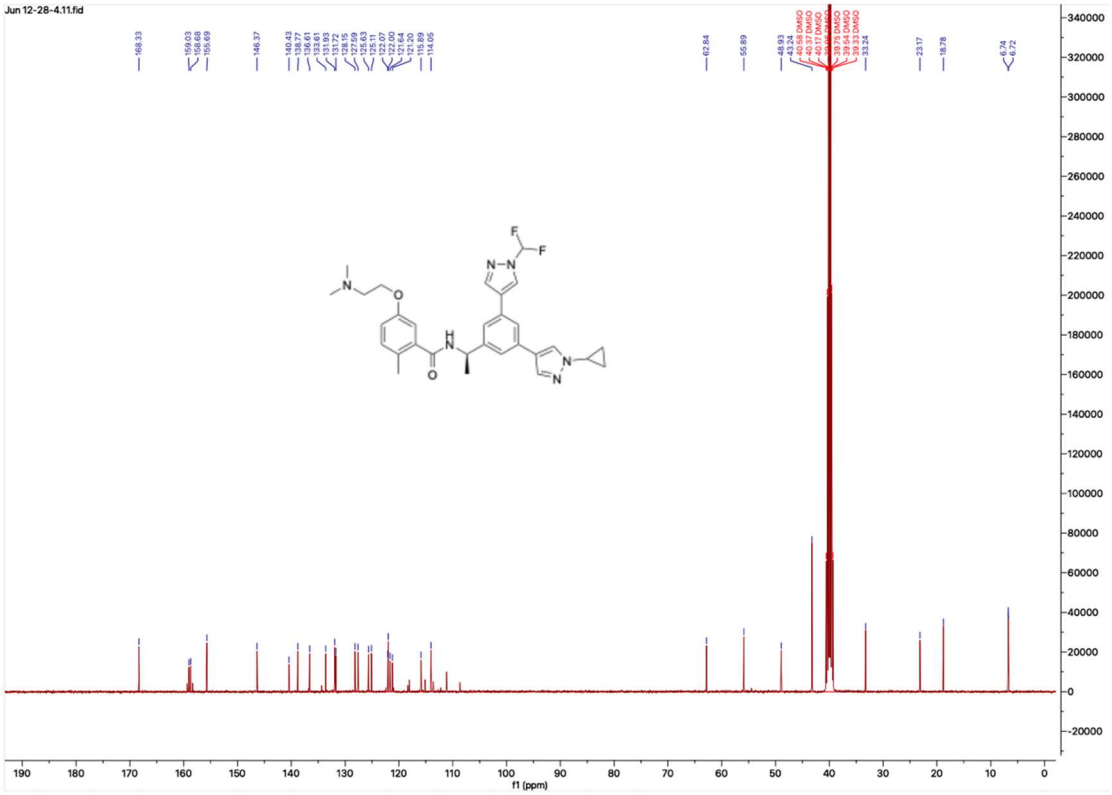

HNMR and CNMR spectra of Jun12165

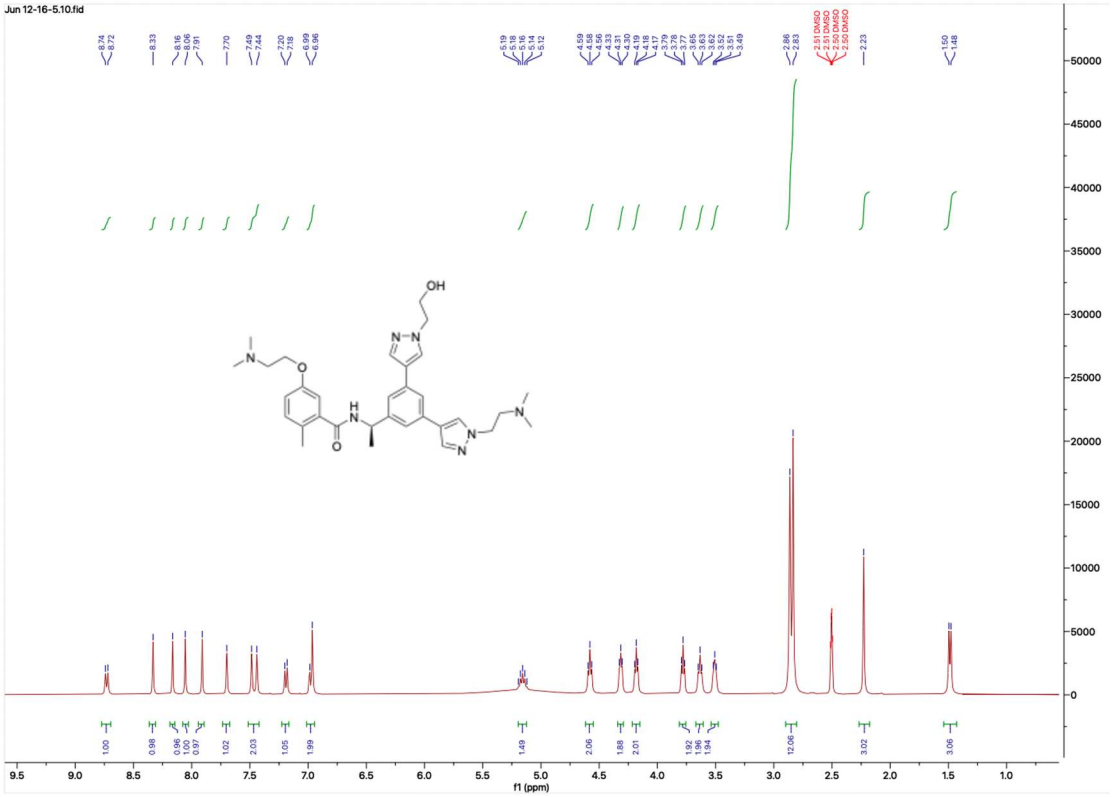

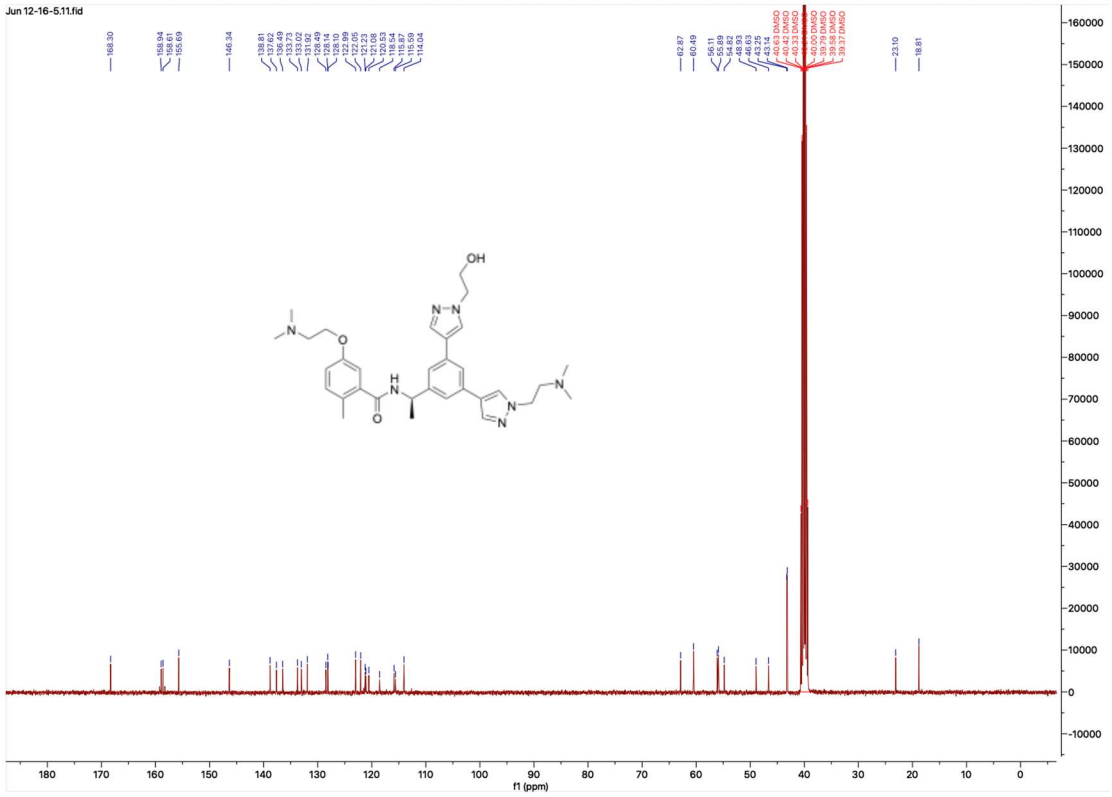

HNMR and CNMR spectra of Jun12168

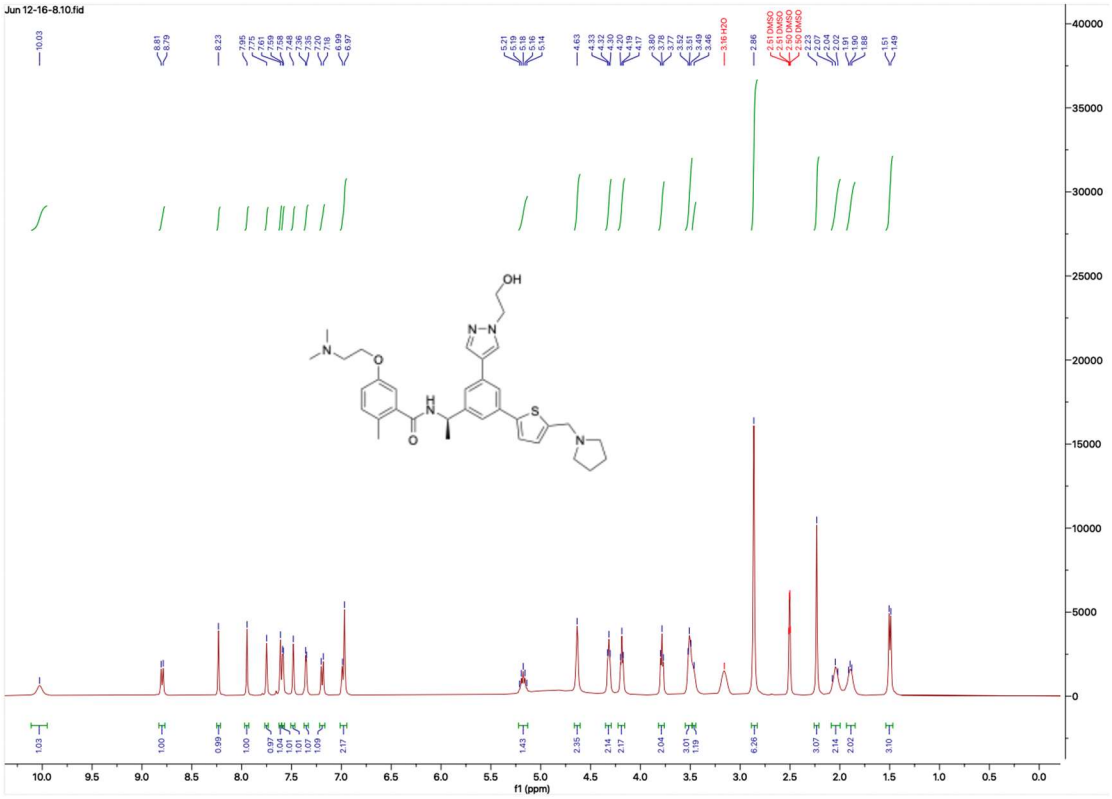

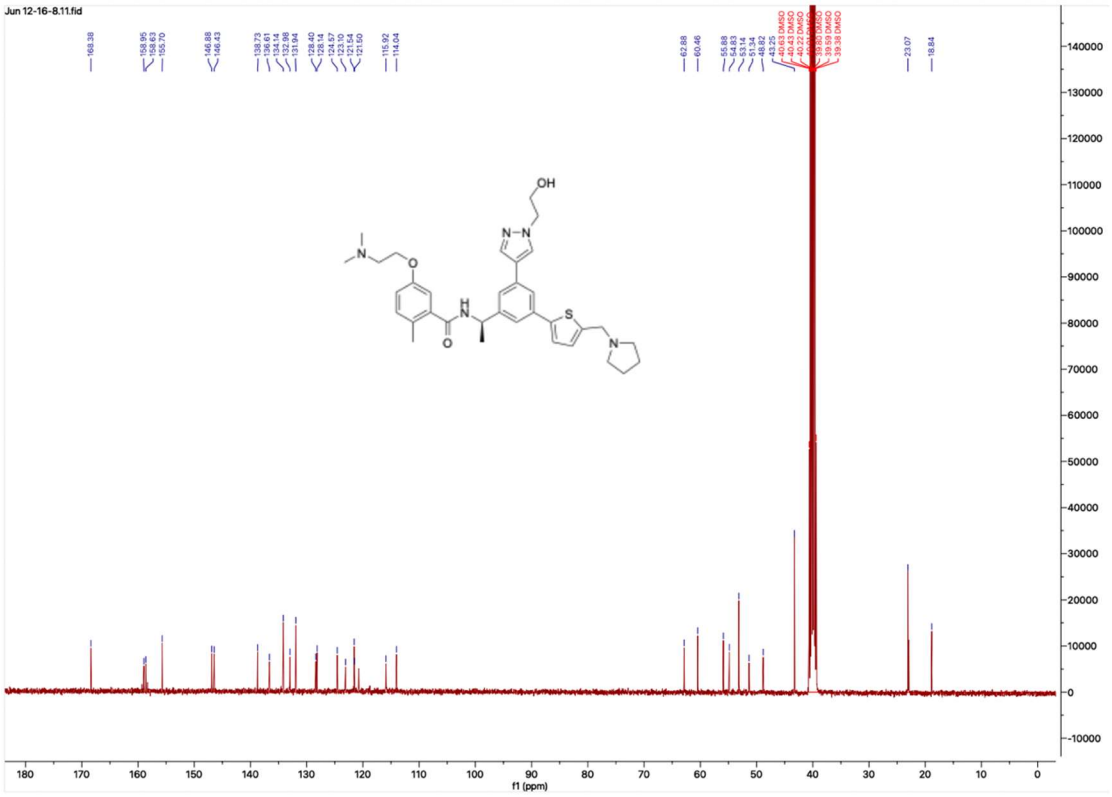

HNMR and CNMR spectra of Jun12163

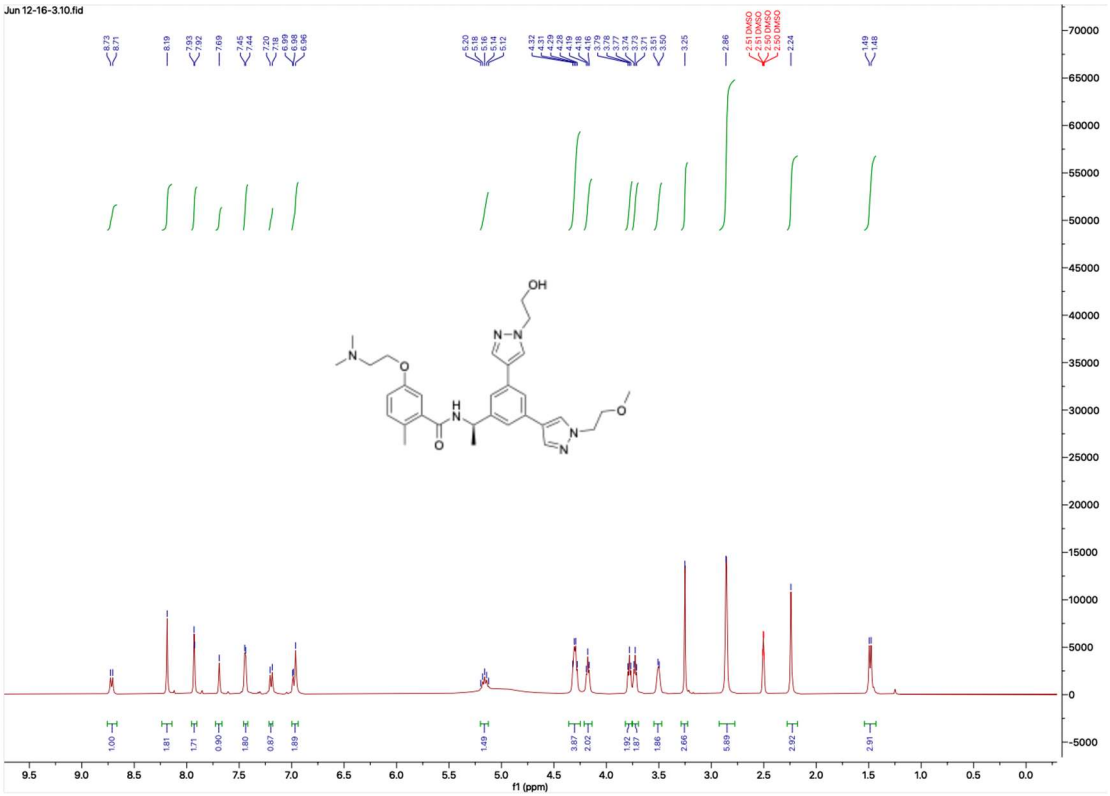

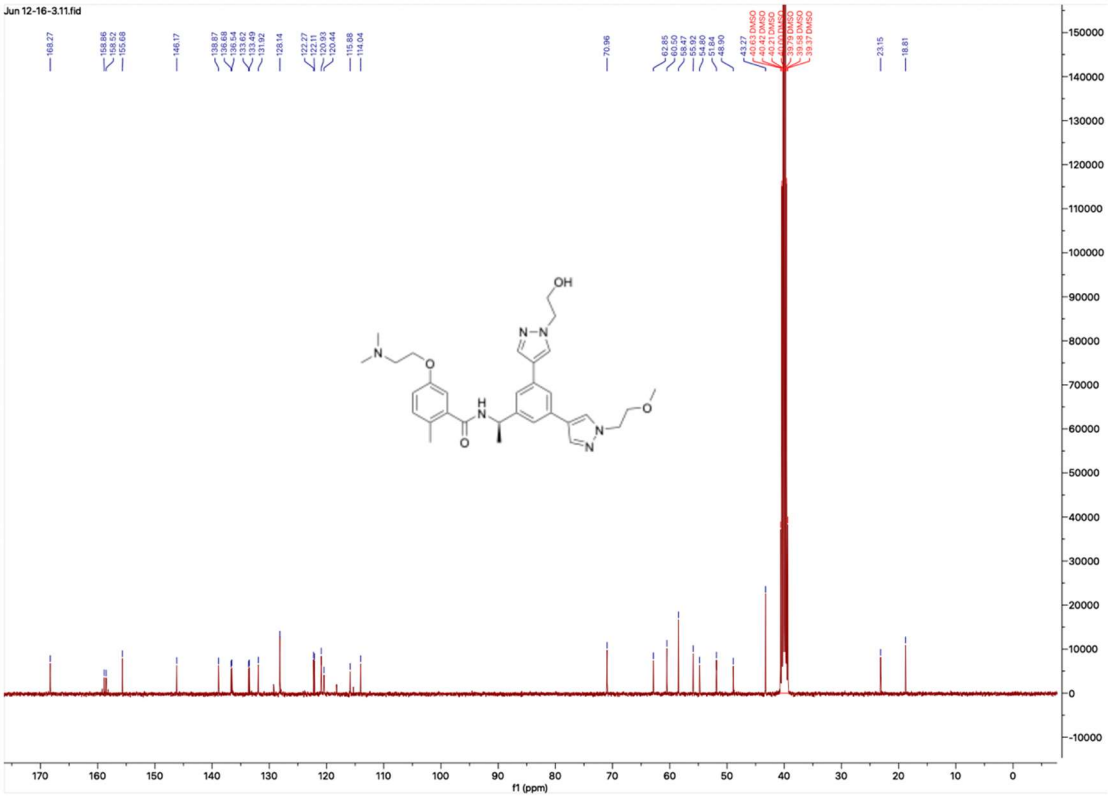

HNMR and CNMR spectra of Jun12164

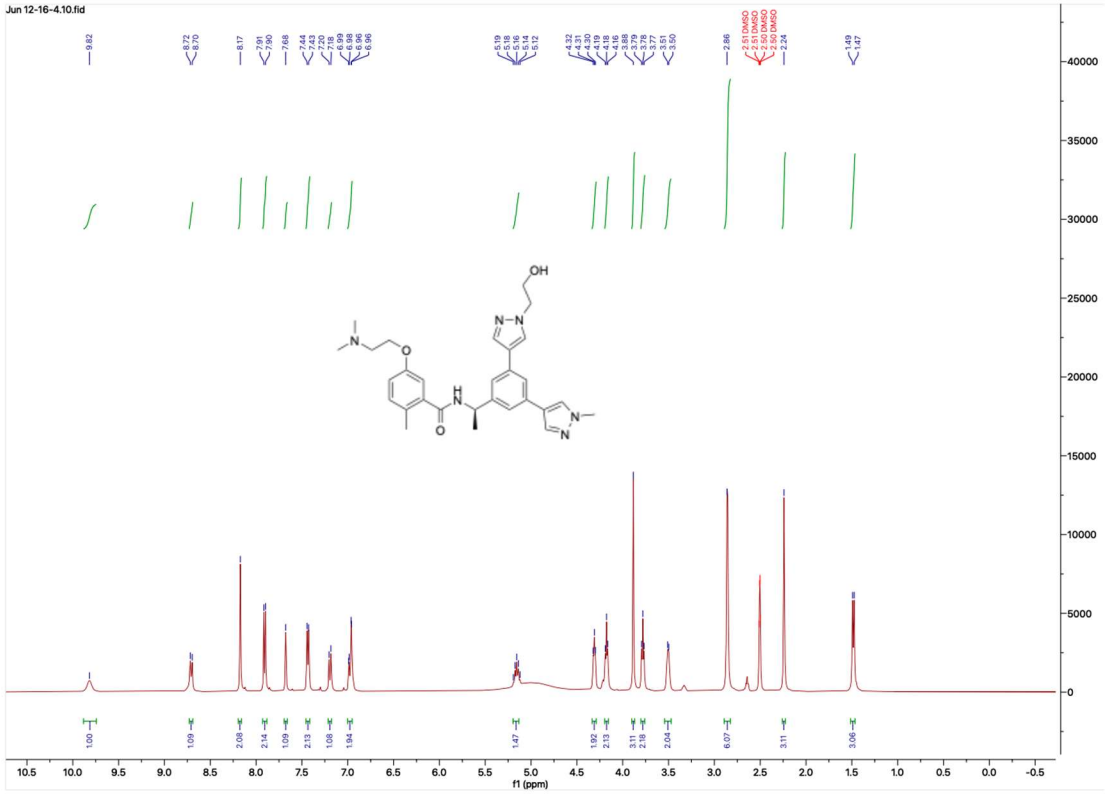

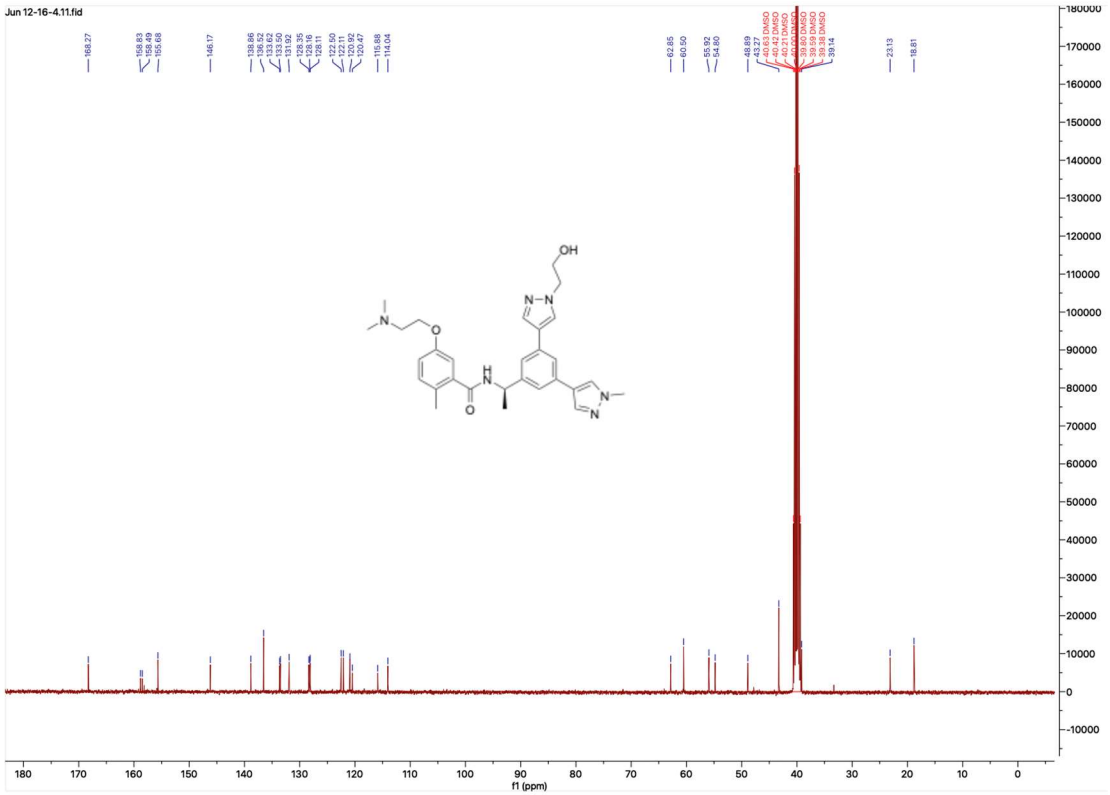

HNMR and CNMR spectra of Jun12198

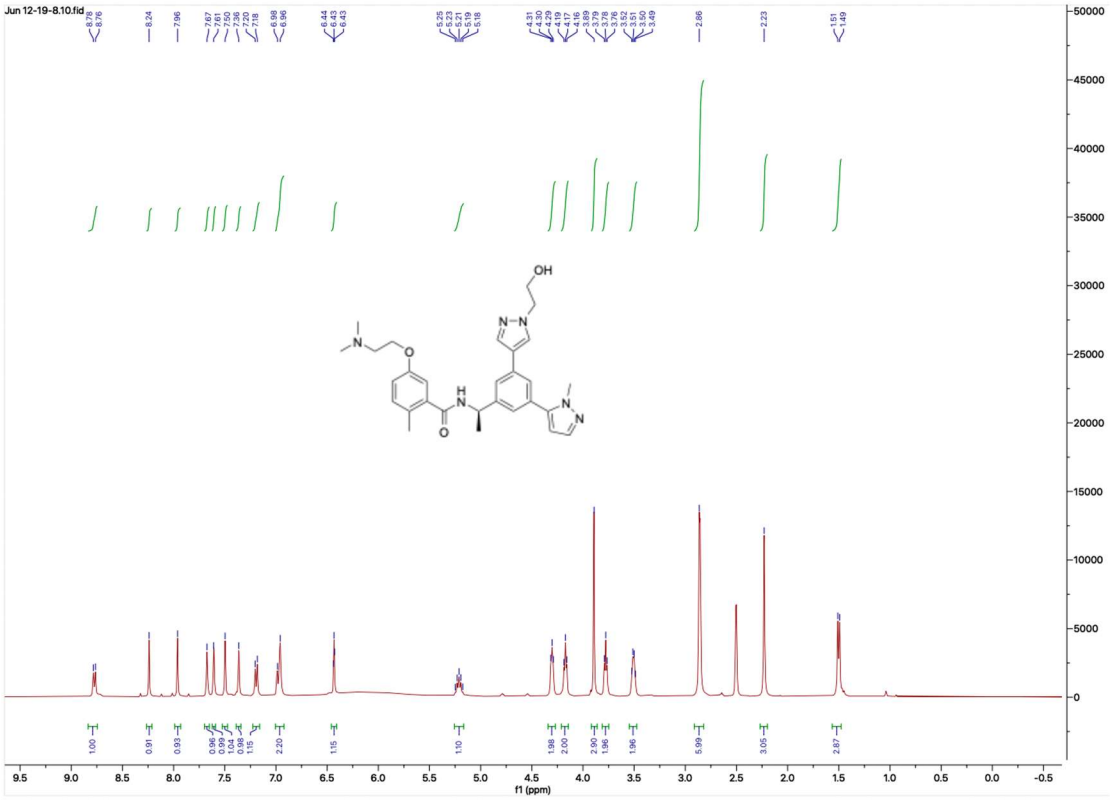

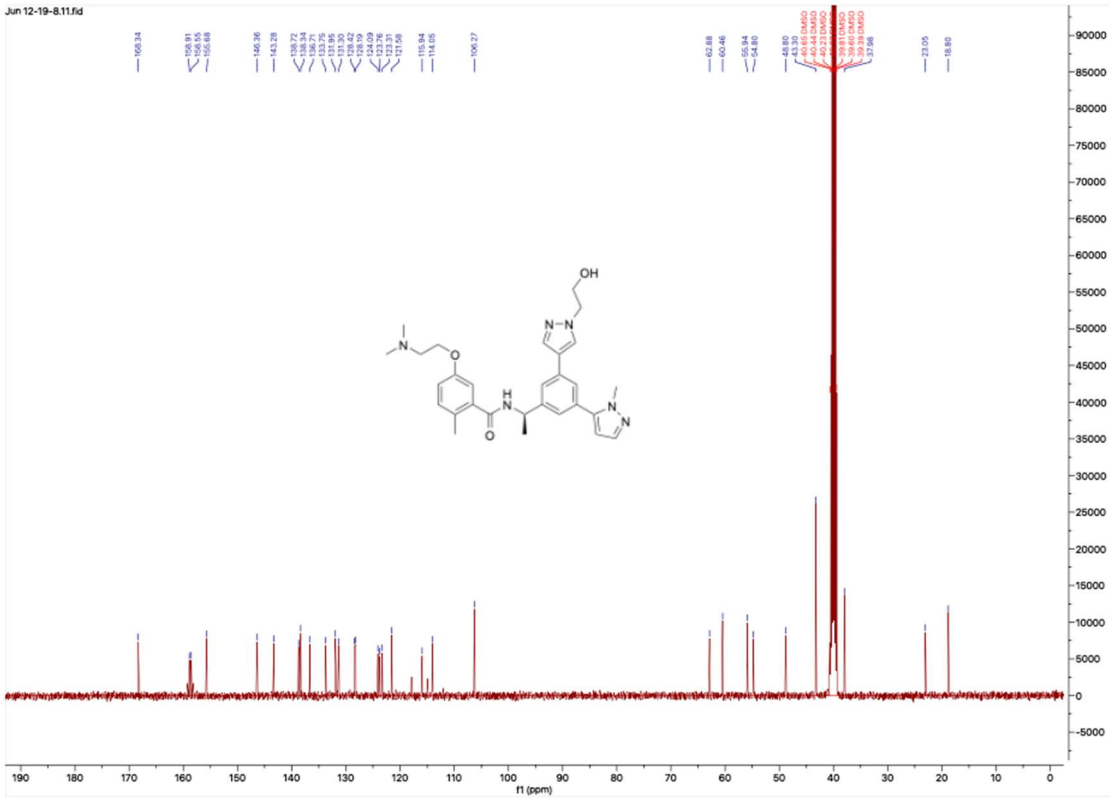

HNMR and CNMR spectra of Jun12142

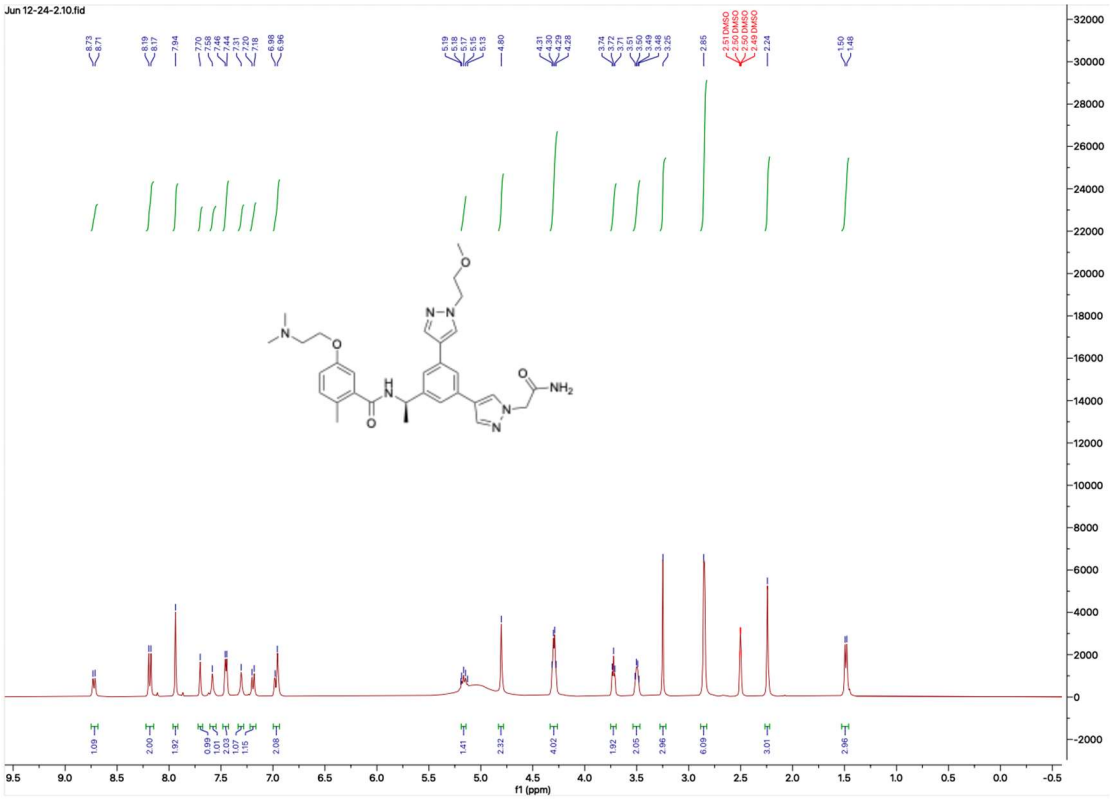

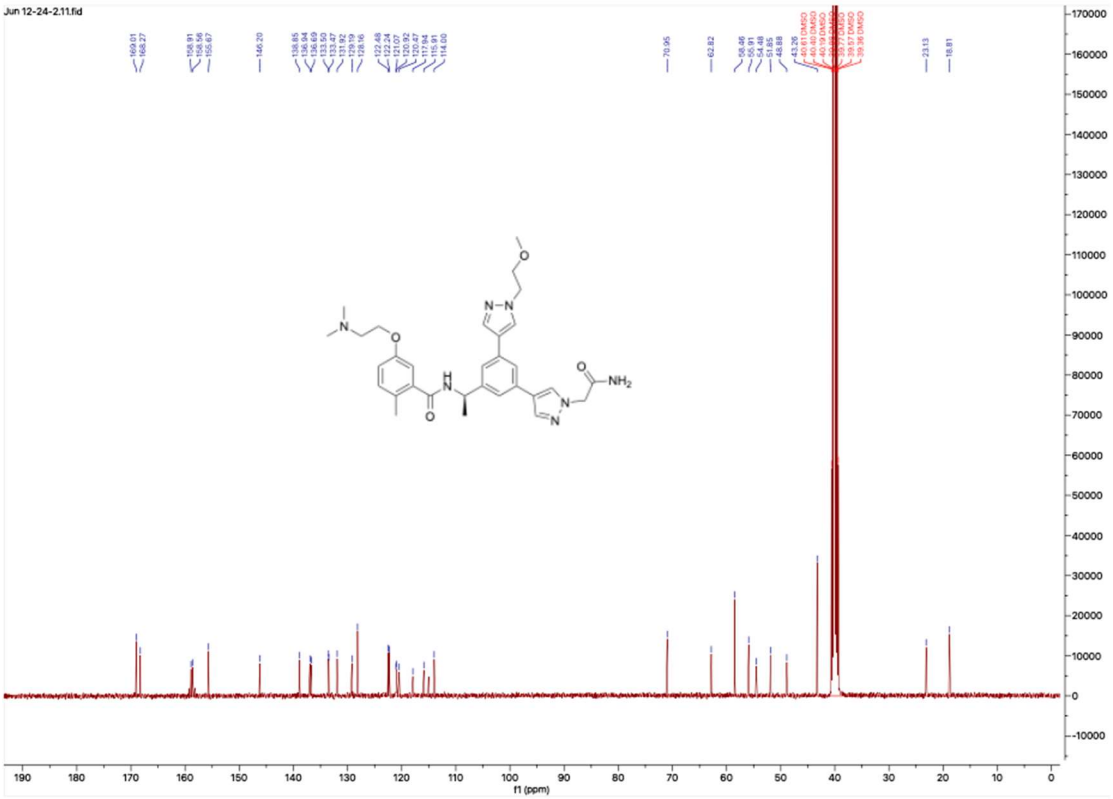

HNMR and CNMR spectra of Jun12147

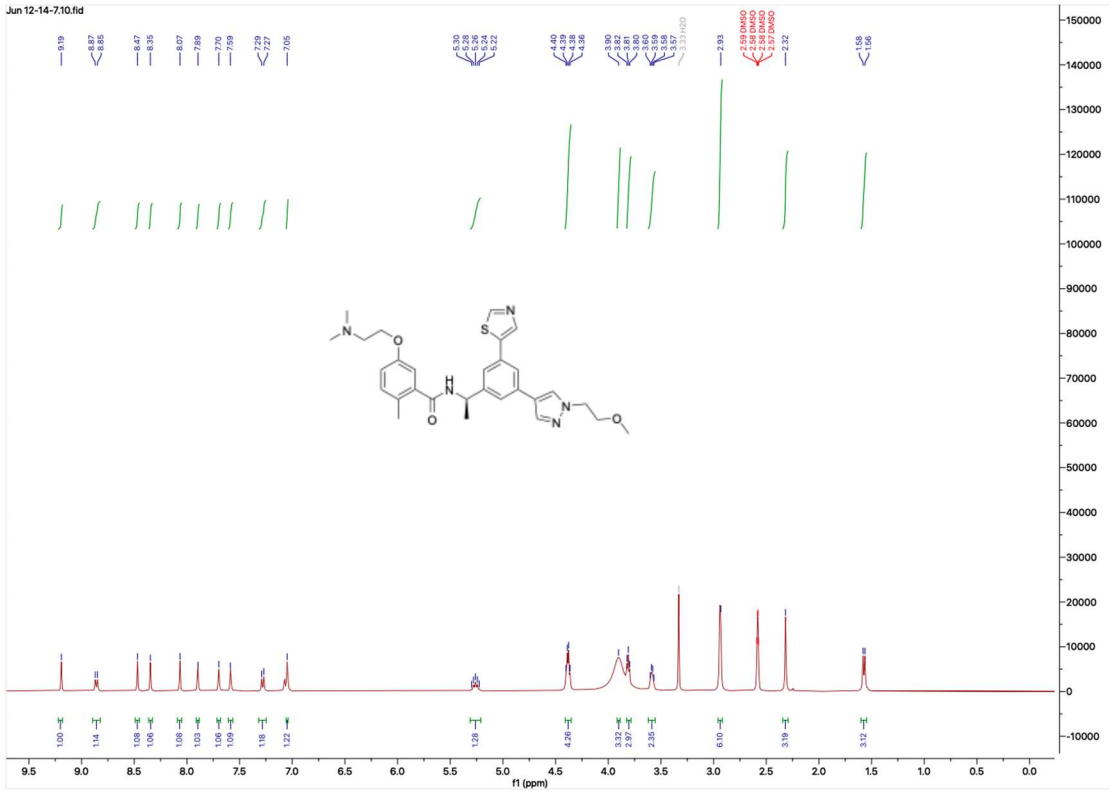

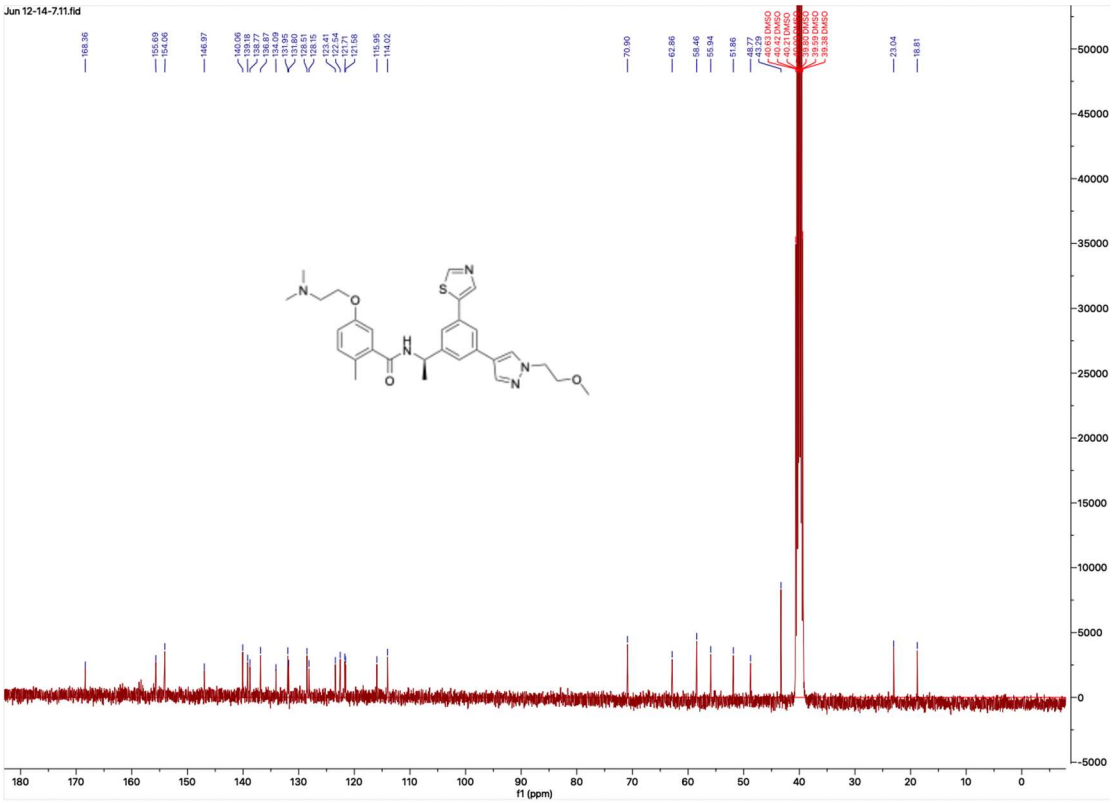

HNMR and CNMR spectra of Jun12759

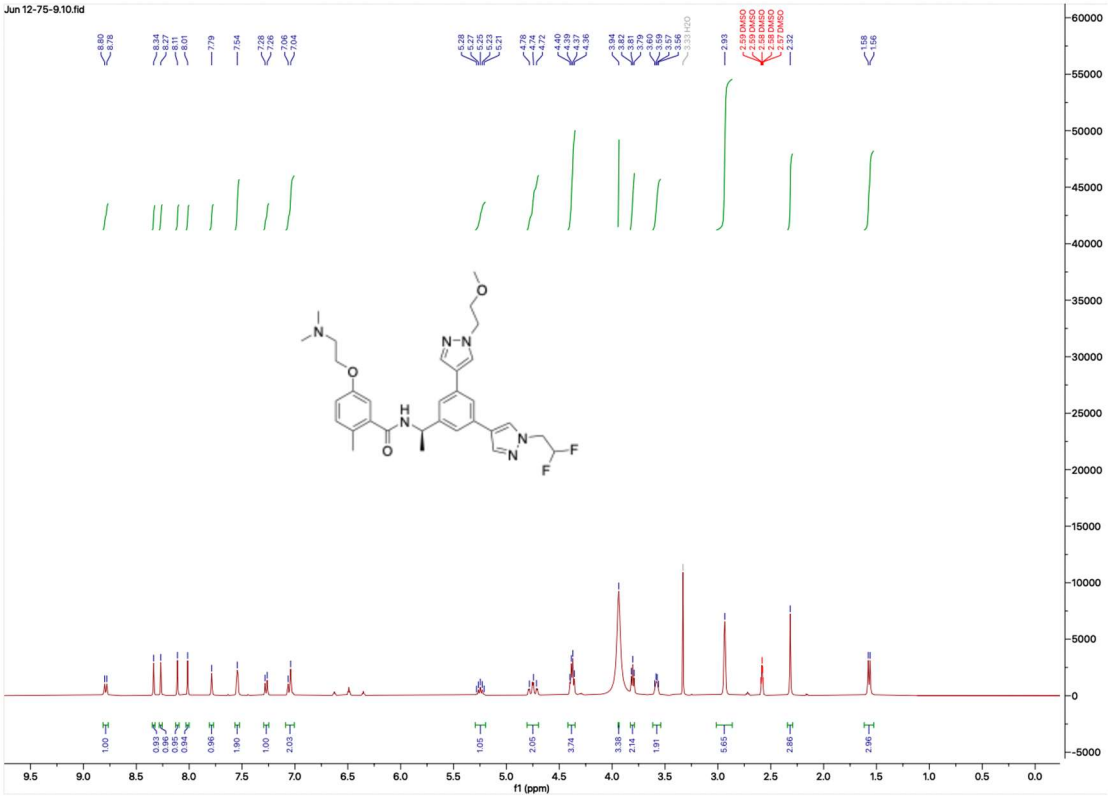

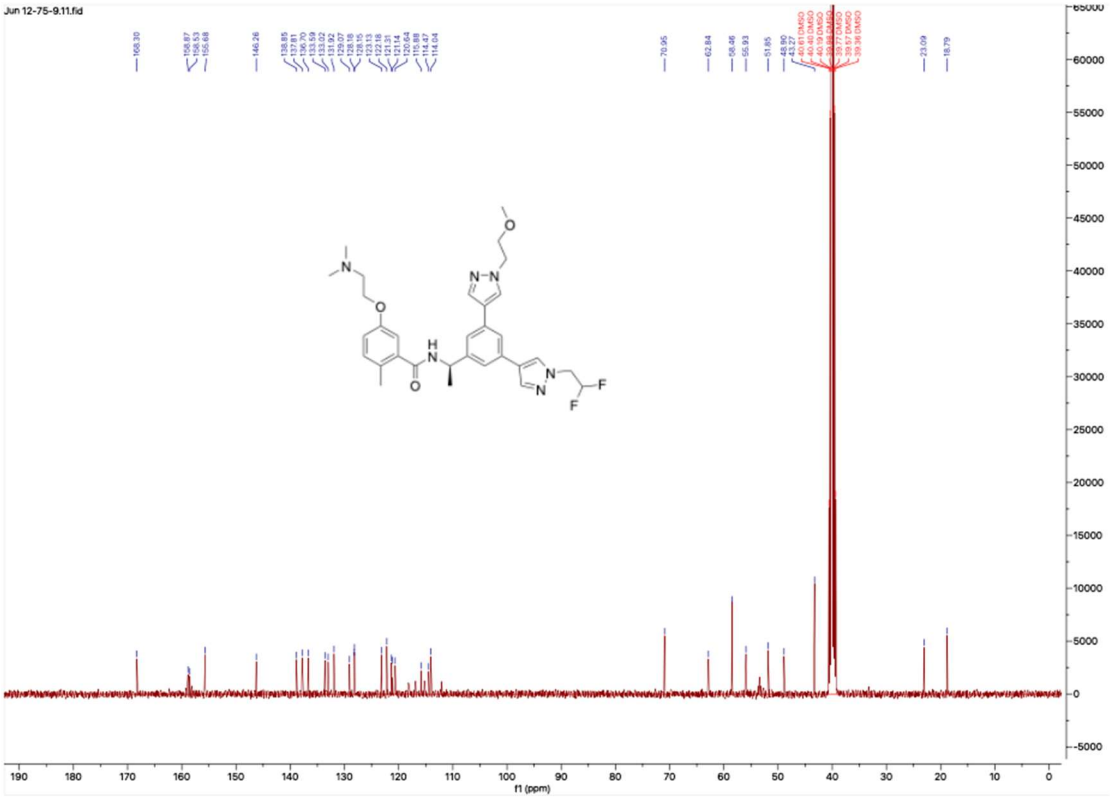

HNMR and CNMR spectra of Jun12379

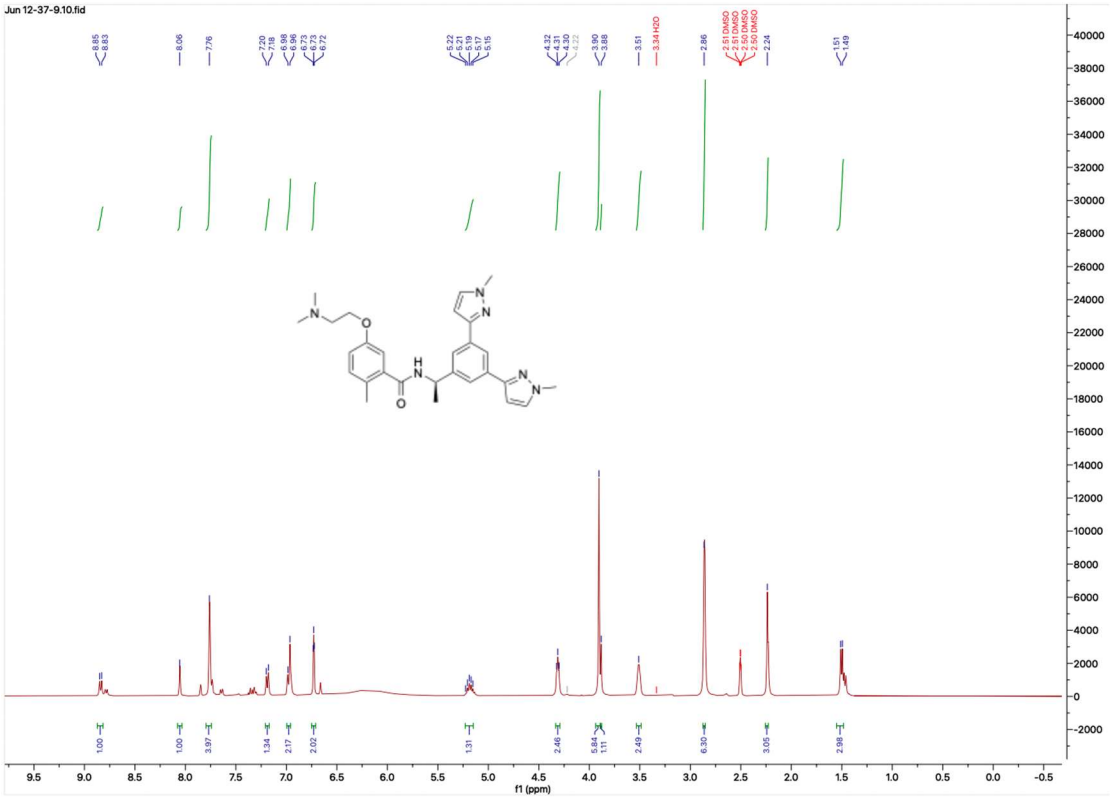

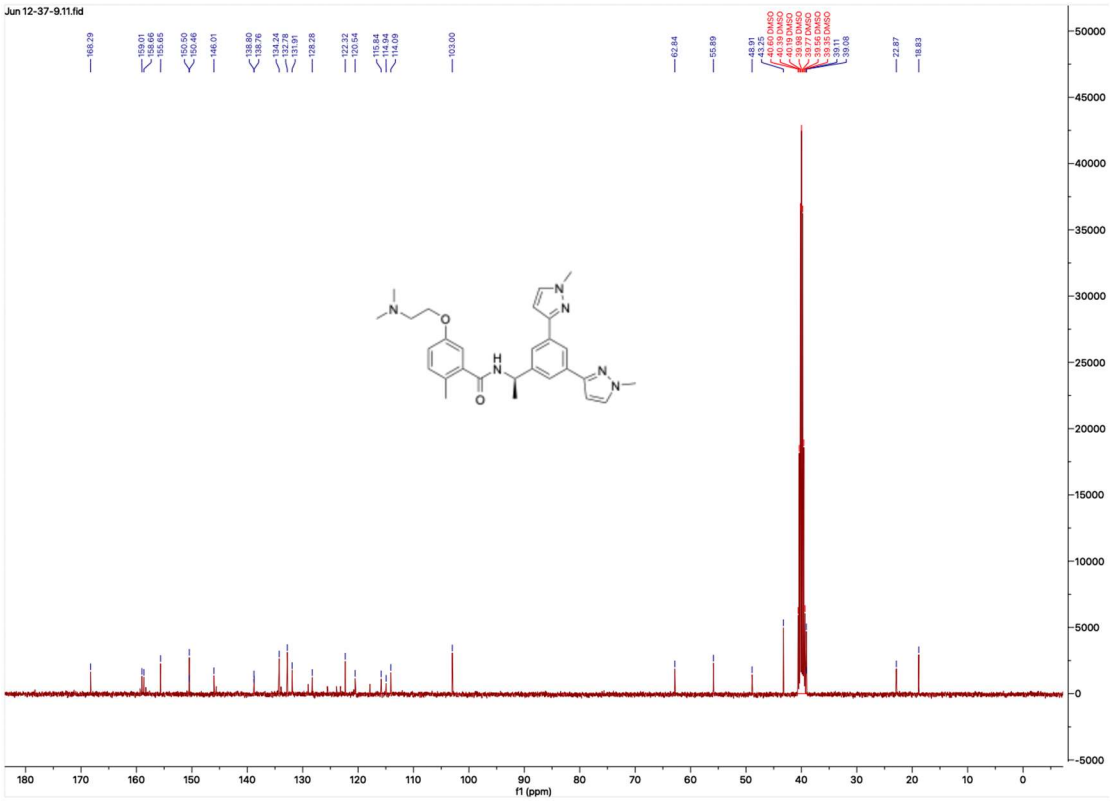

HNMR and CNMR spectra of Jun12528

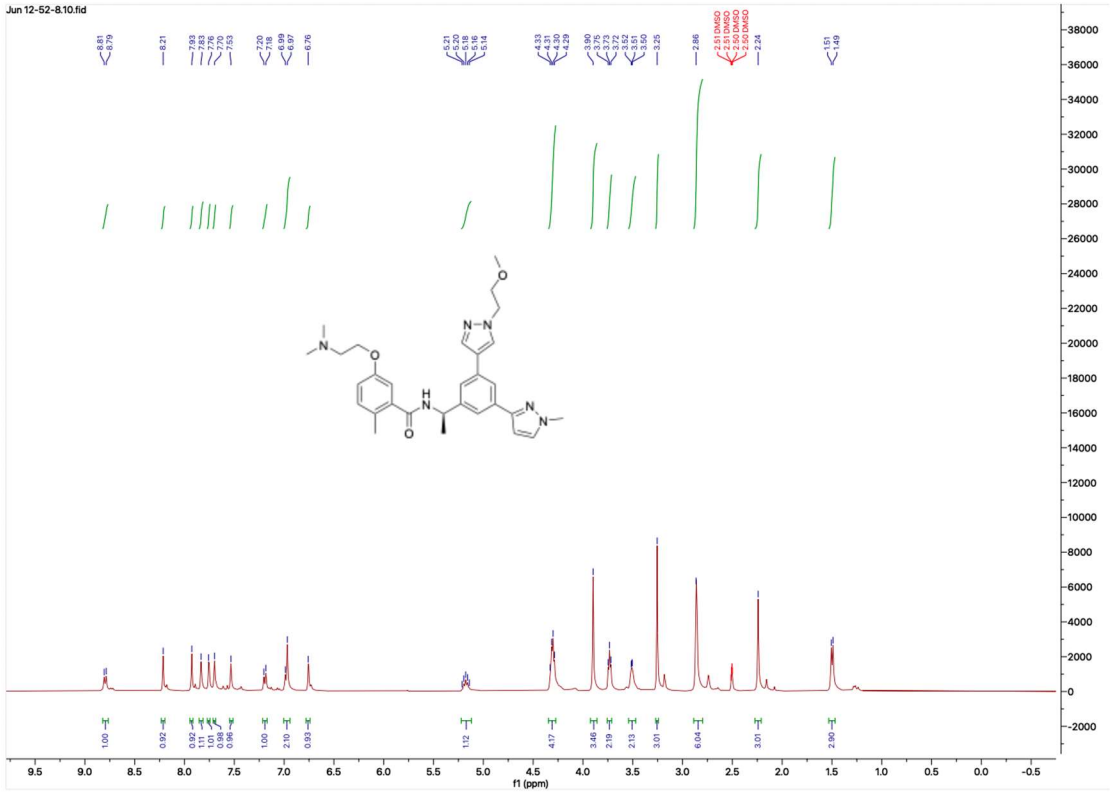

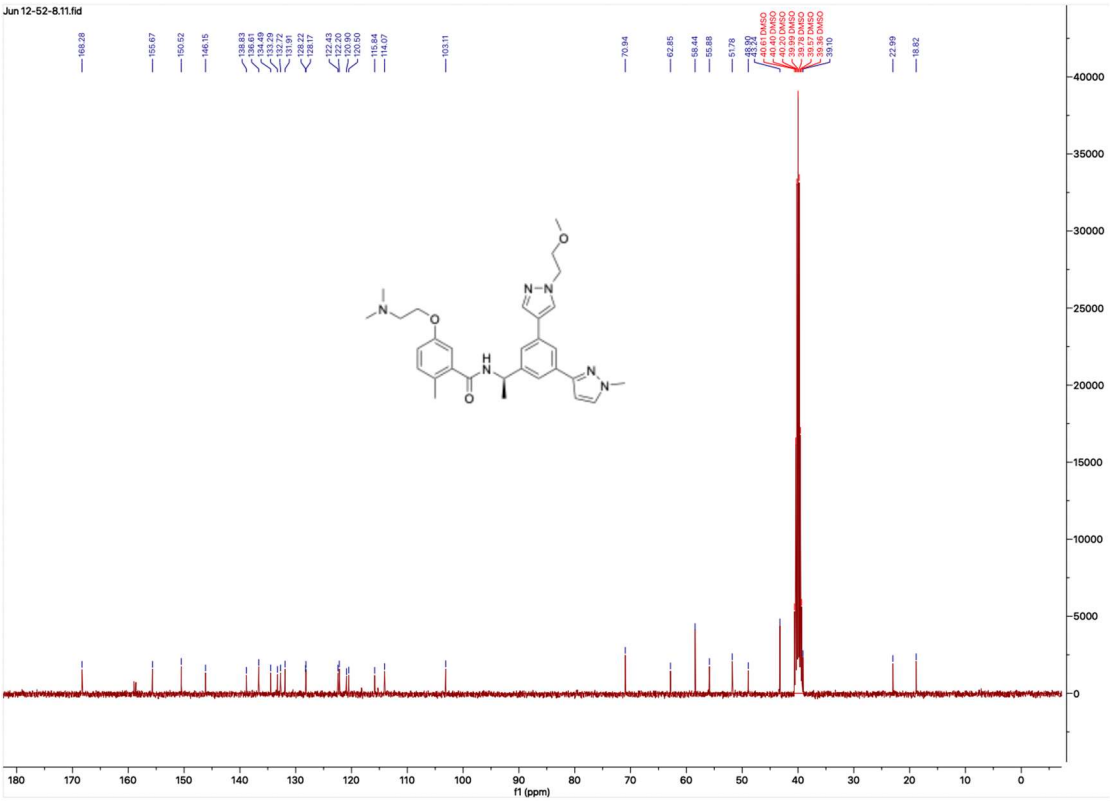

HNMR and CNMR spectra of Jun12529

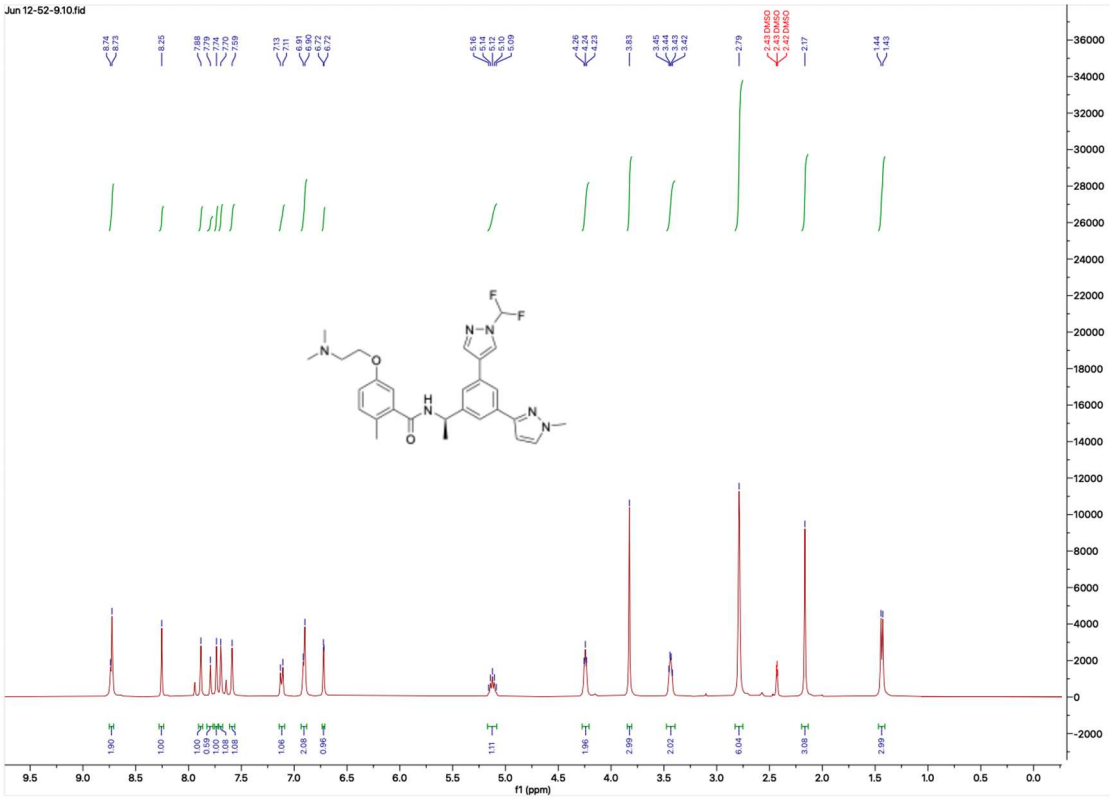

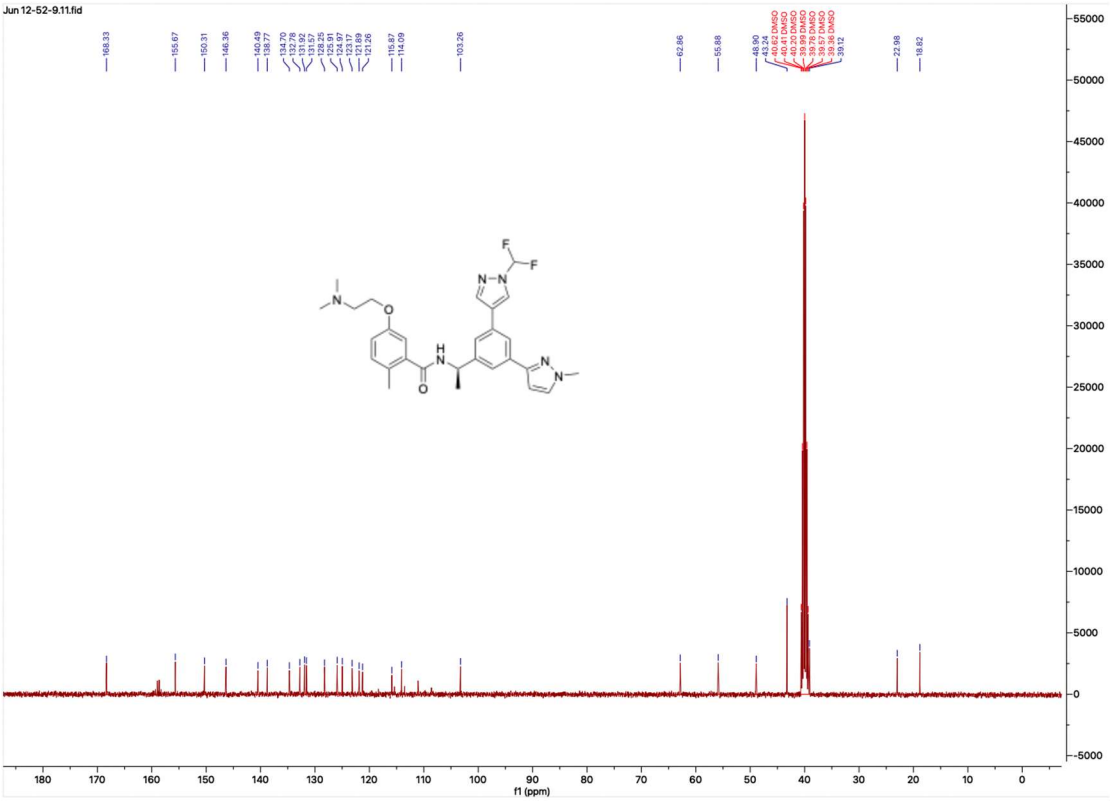

HNMR and CNMR spectra of Jun12531

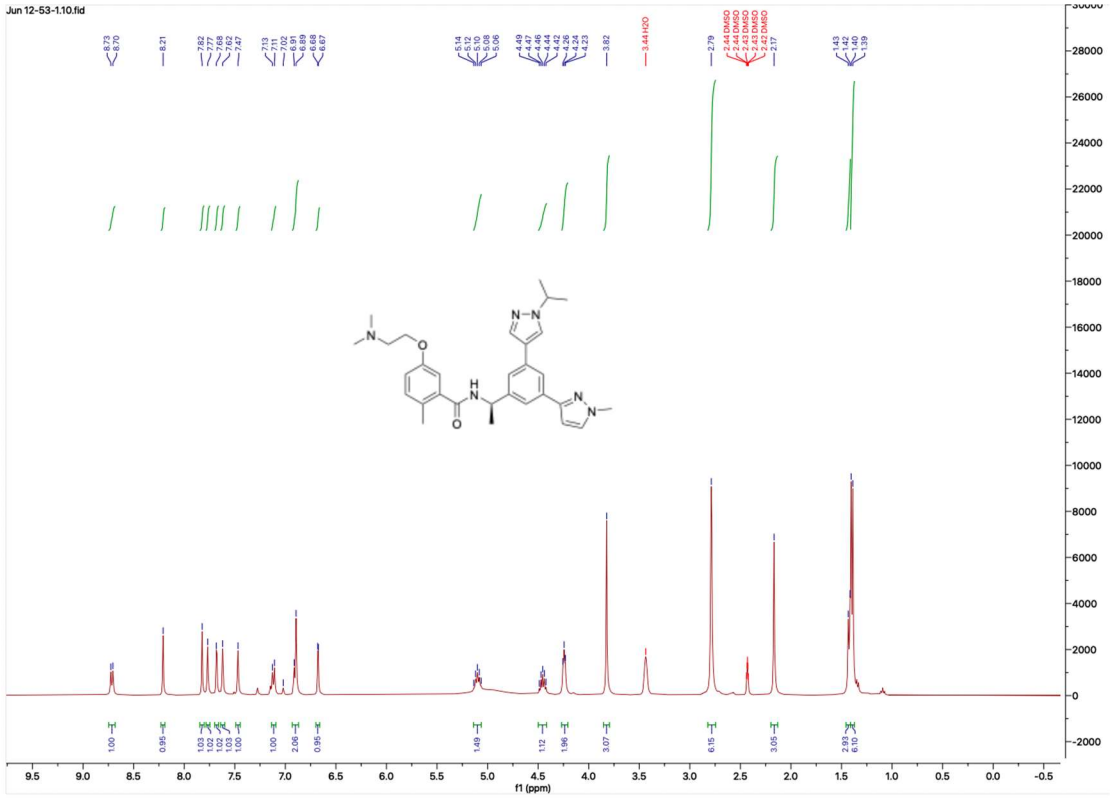

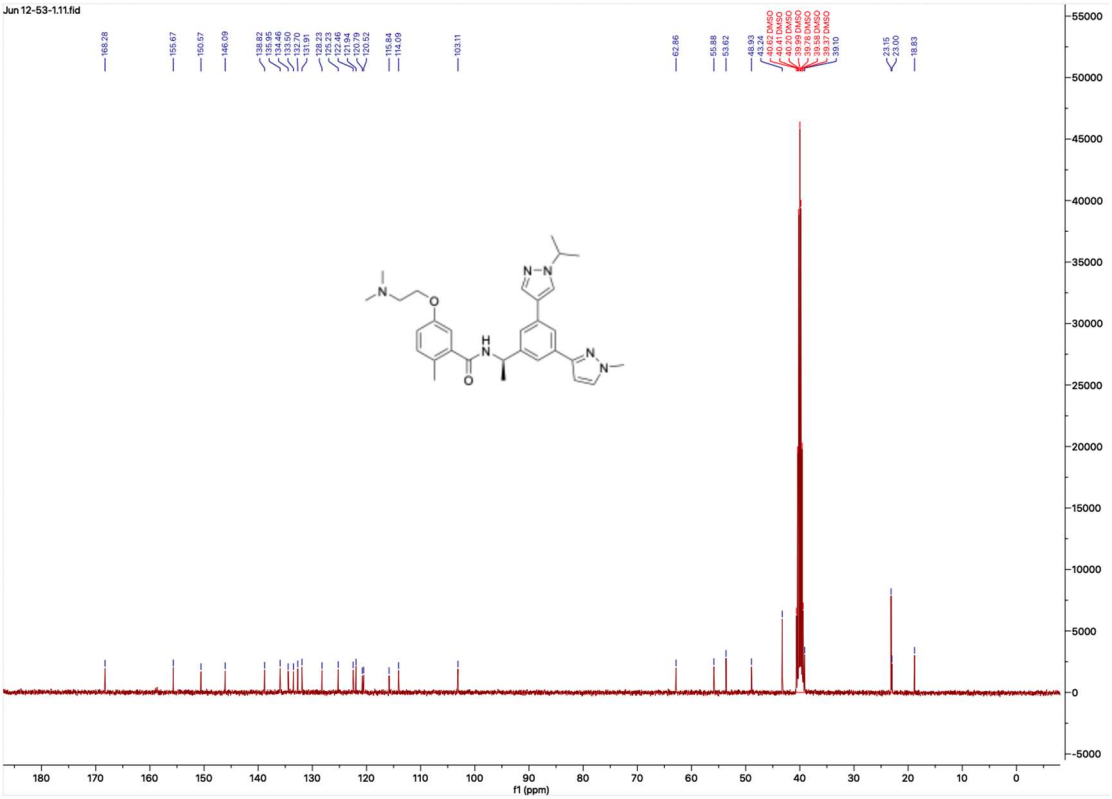

HNMR and CNMR spectra of Jun12584

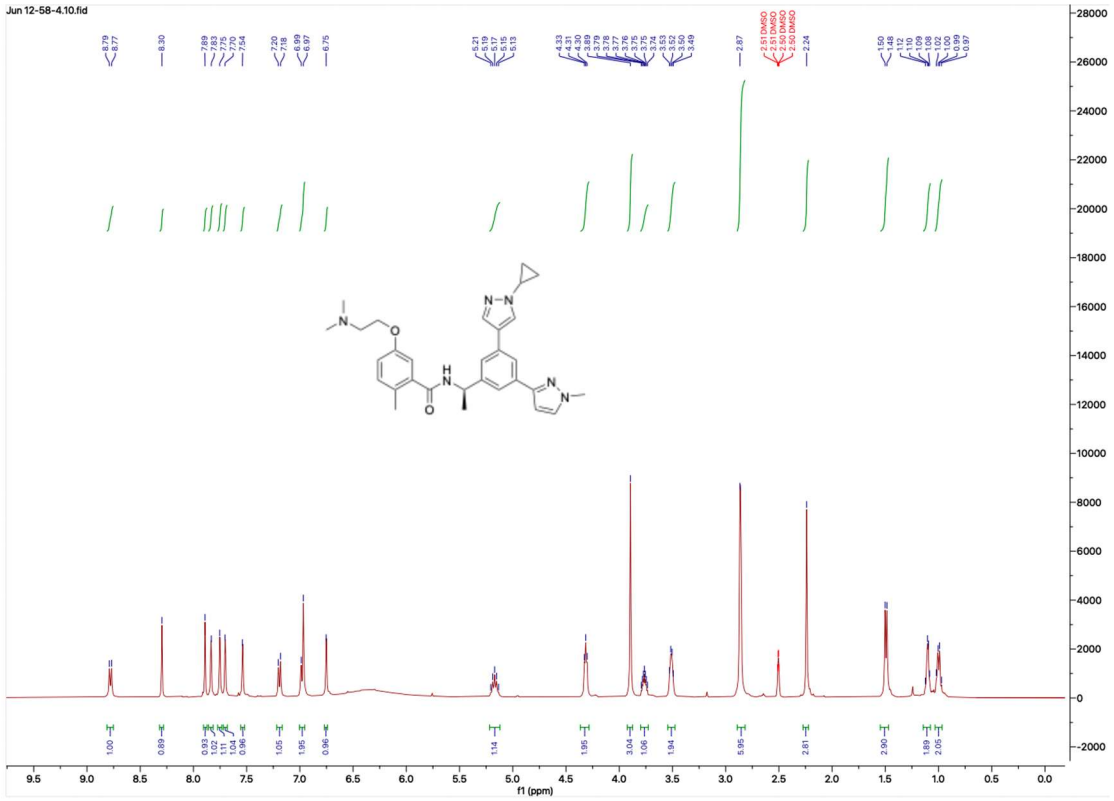

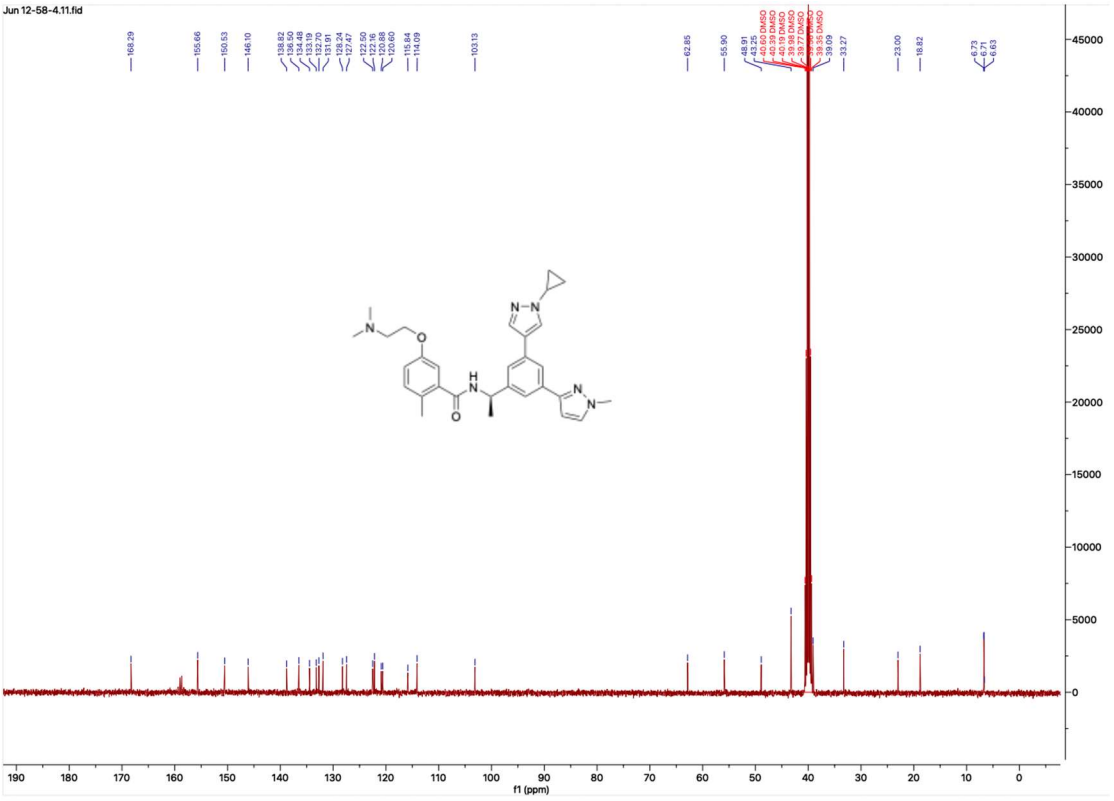

HNMR and CNMR spectra of Jun12602

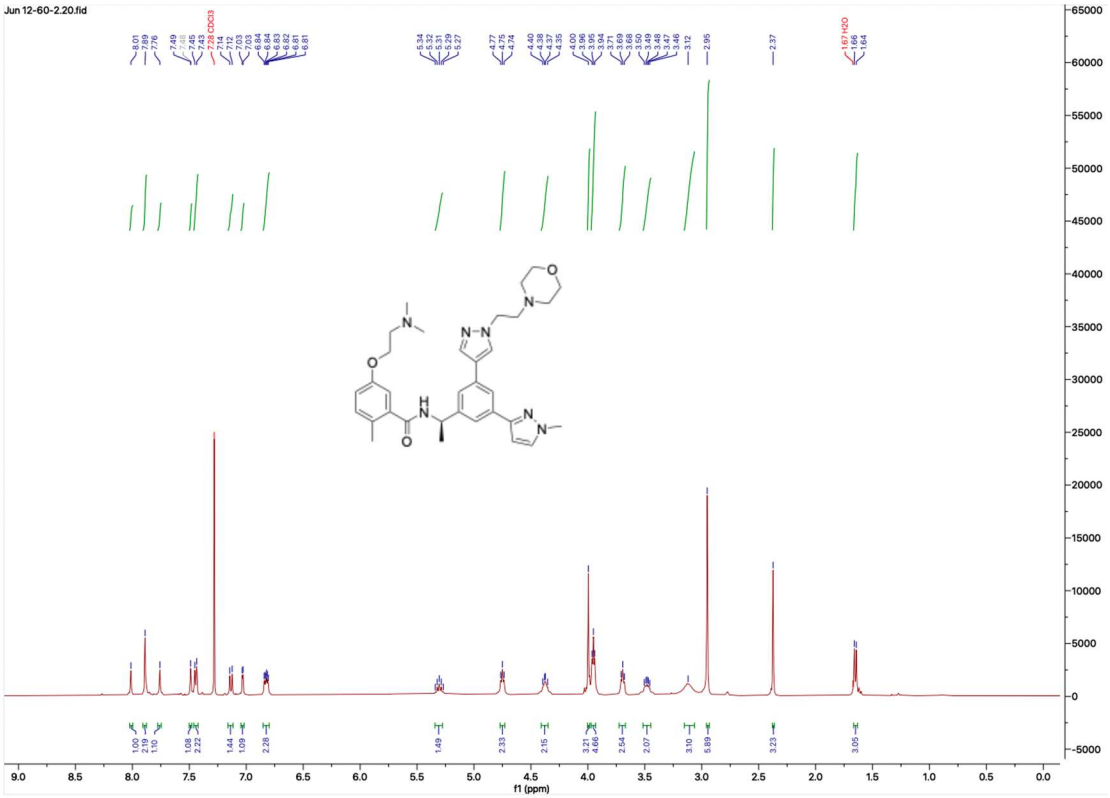

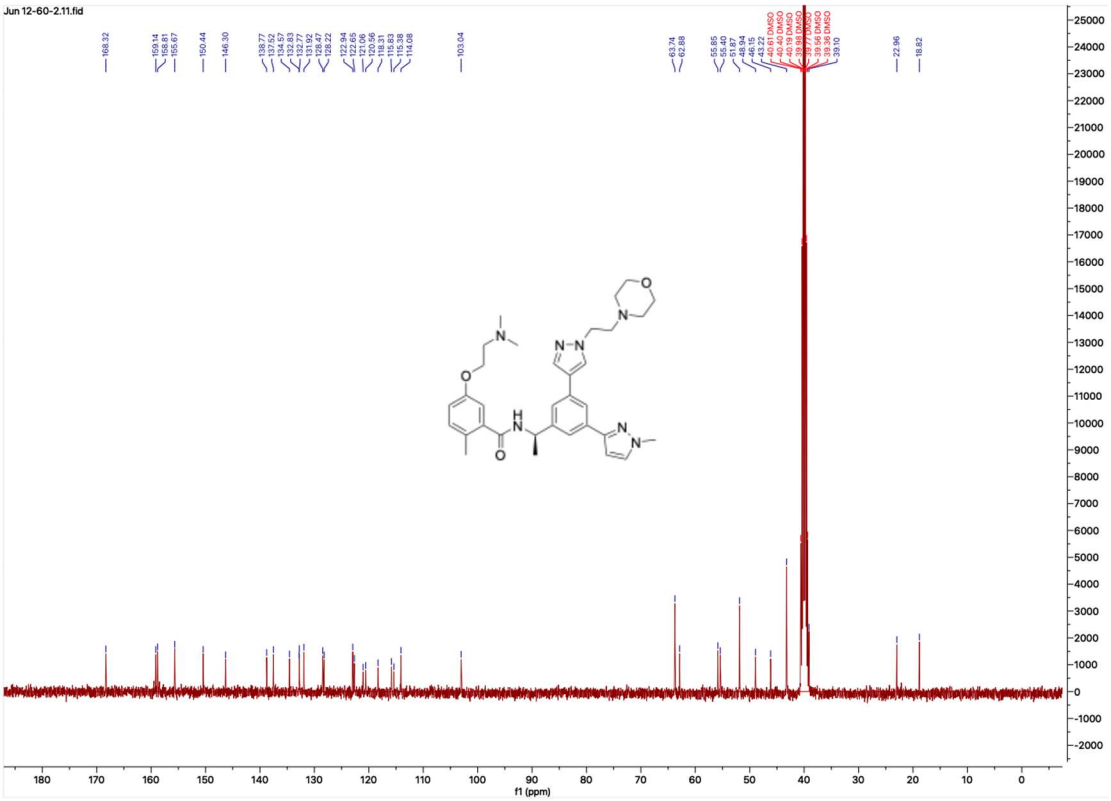

HNMR and CNMR spectra of Jun12703

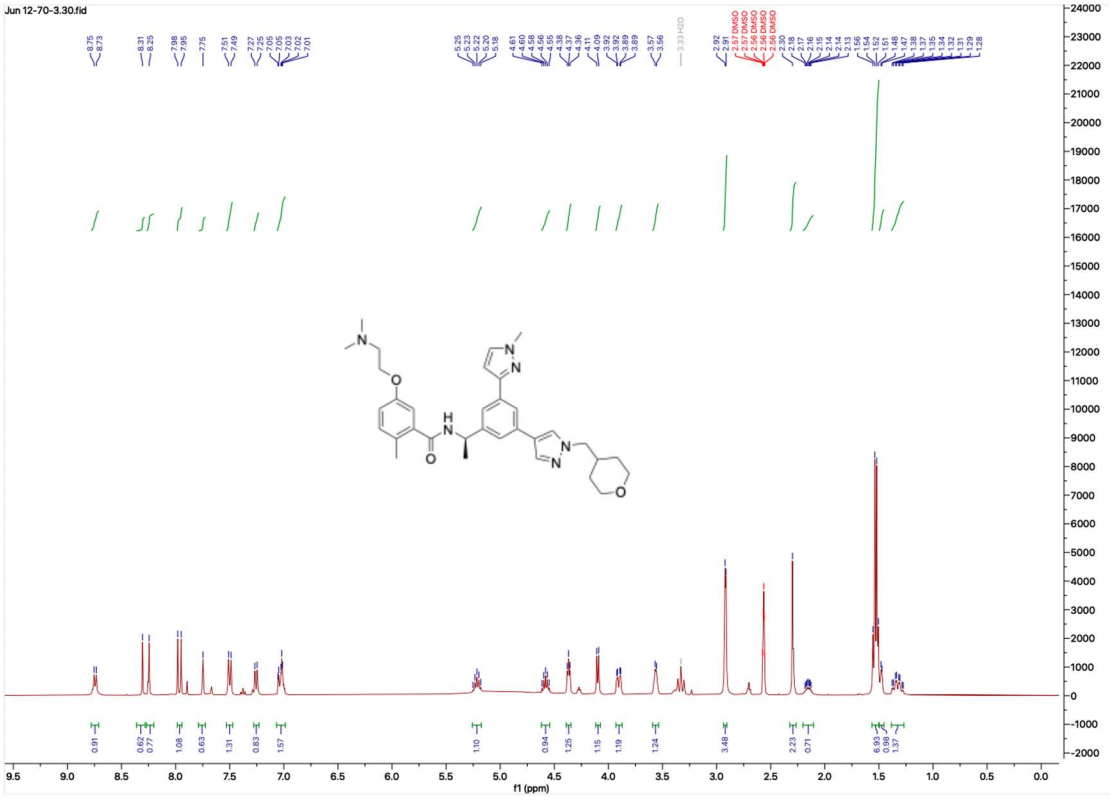

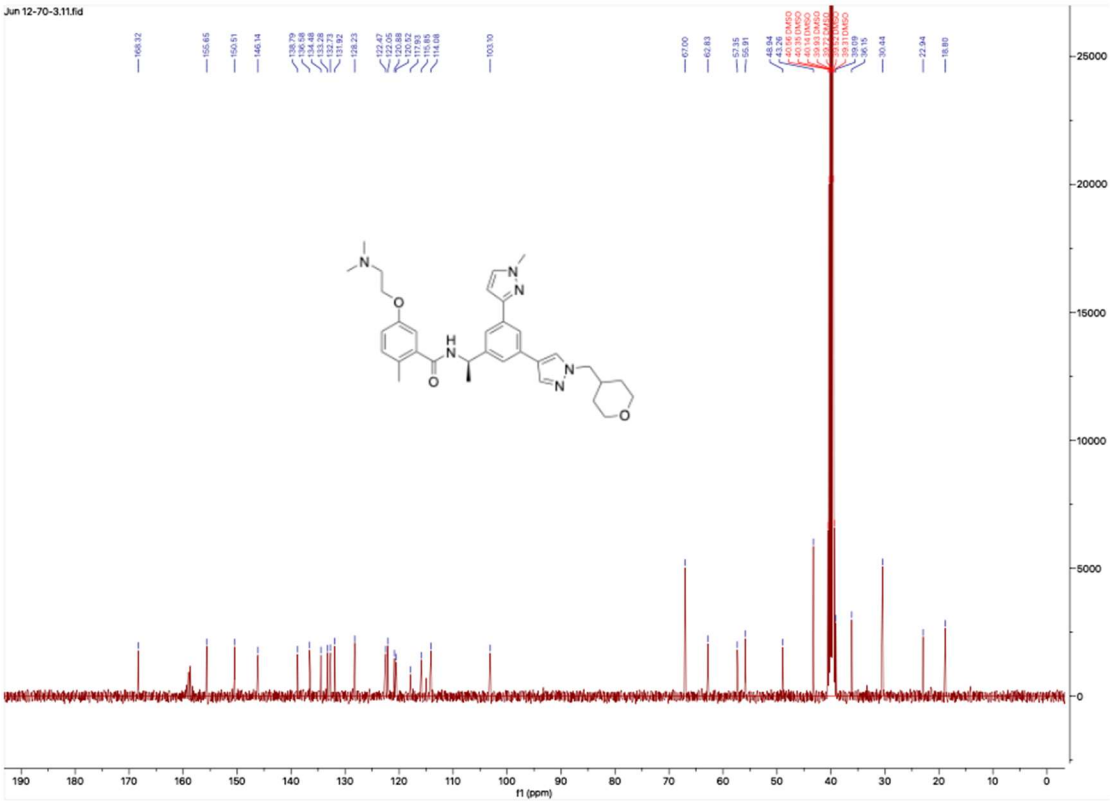

HNMR and CNMR spectra of Jun12713

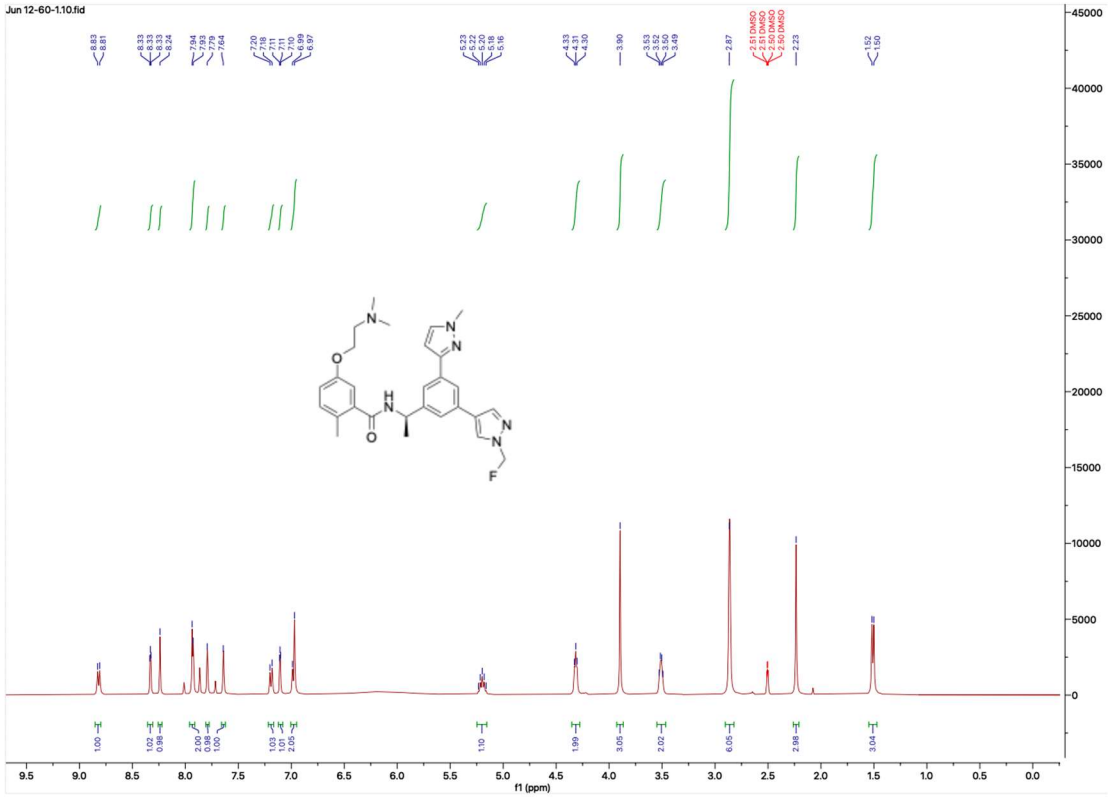

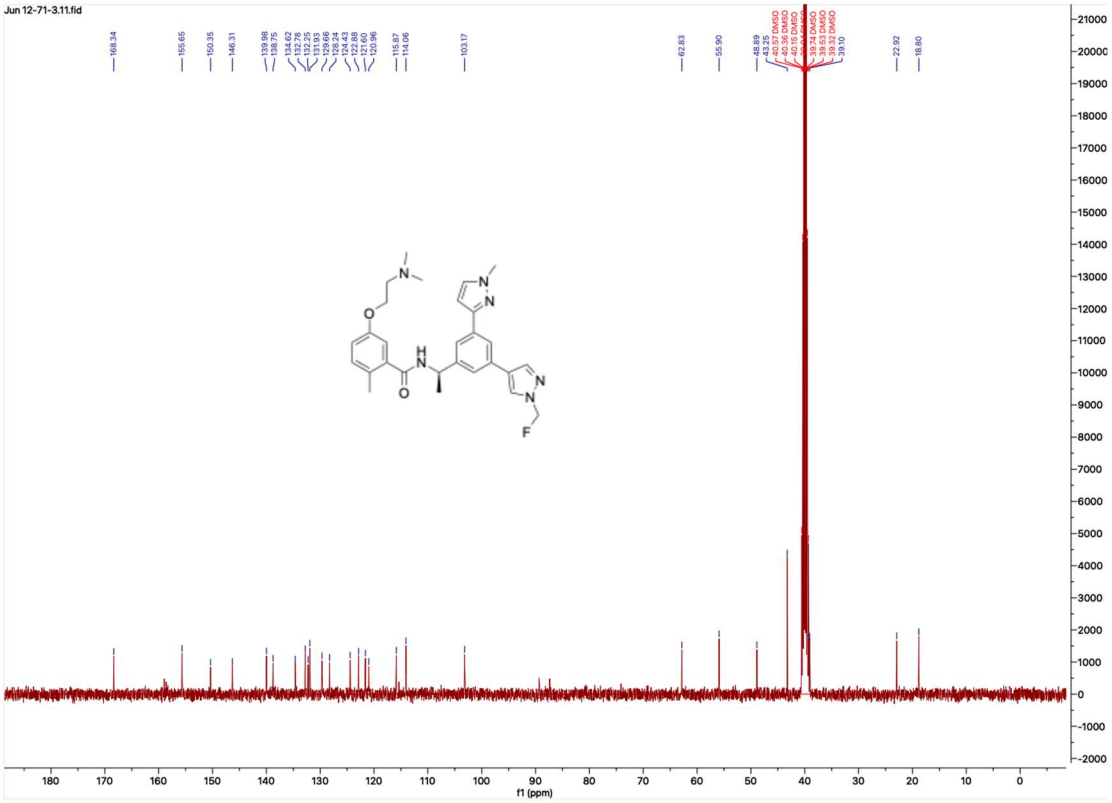

HNMR and CNMR spectra of Jun12308

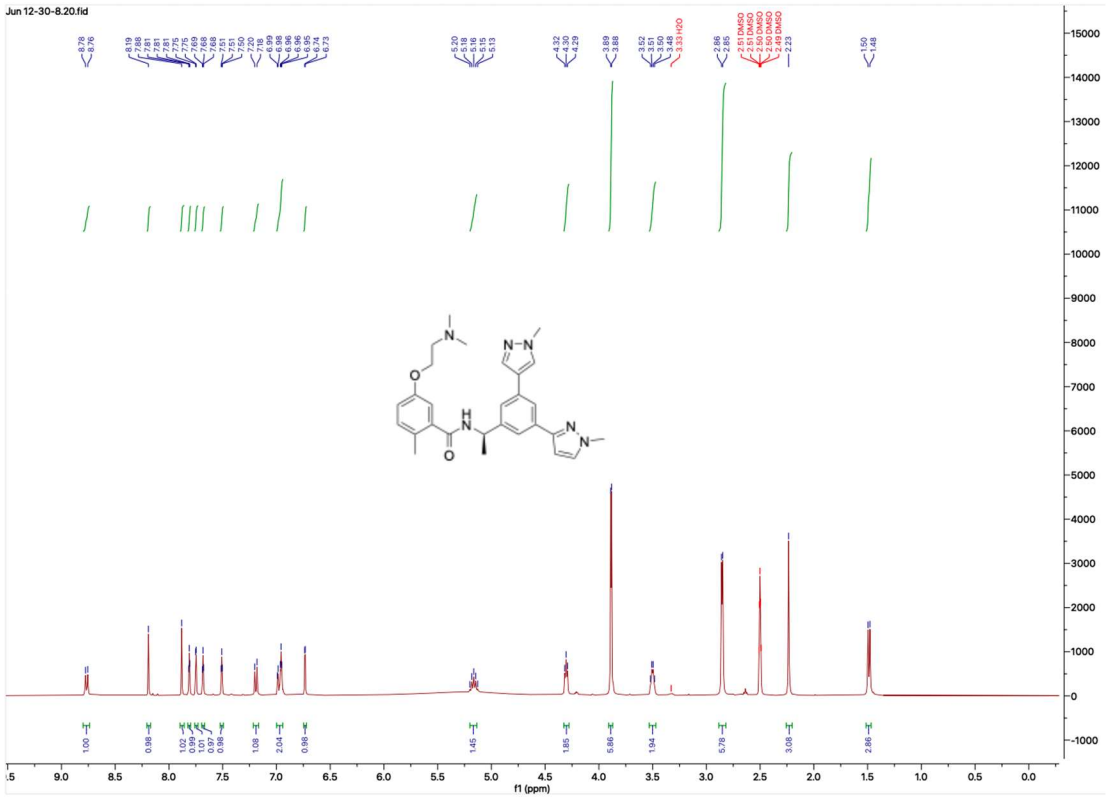

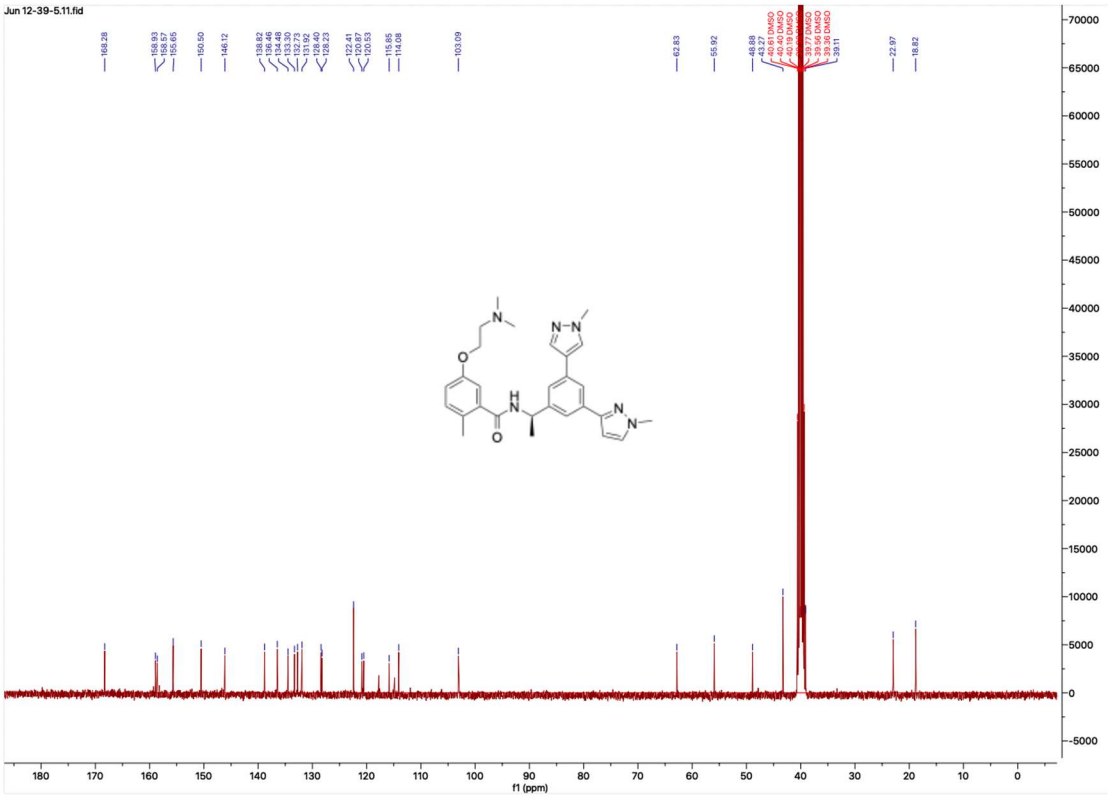

HNMR and CNMR spectra of Jun12827

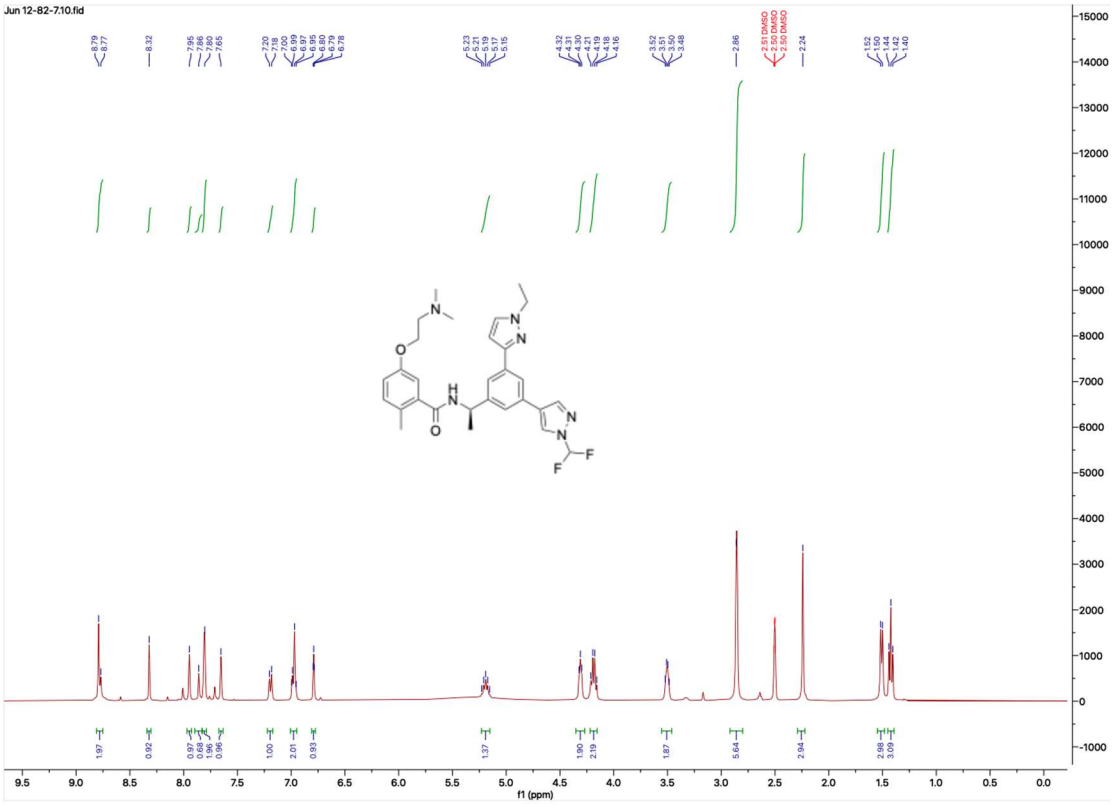

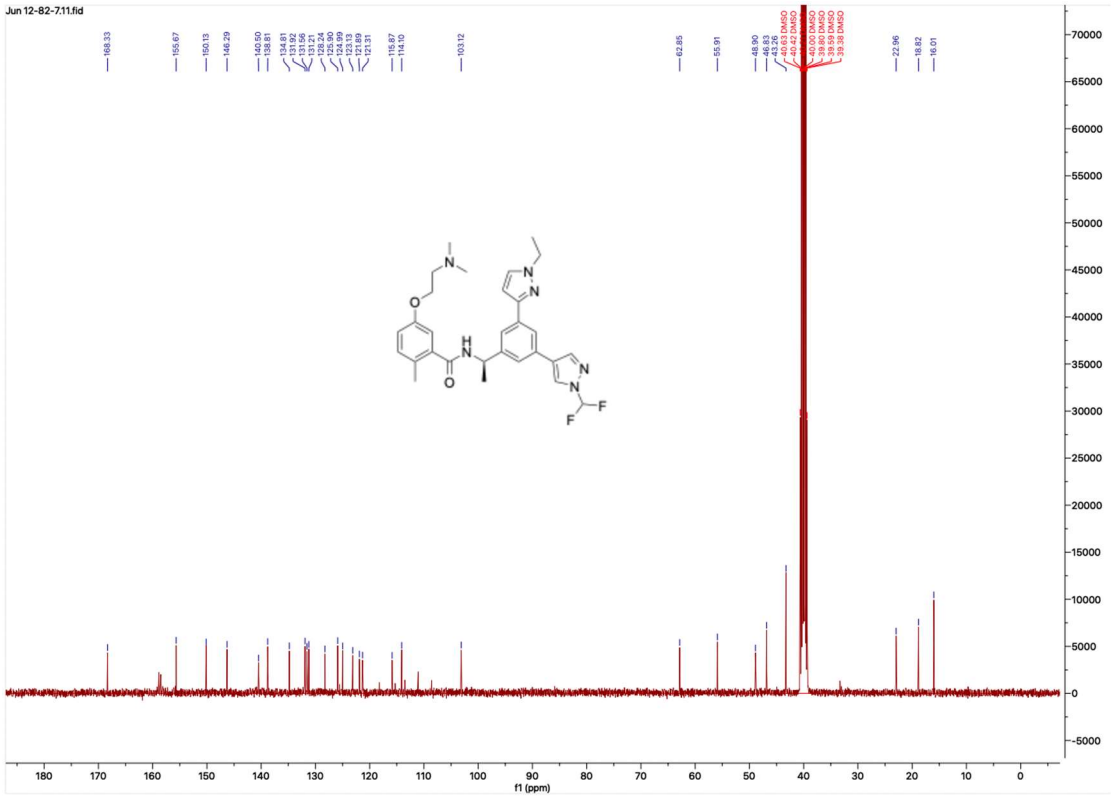

HNMR and CNMR spectra of Jun12831

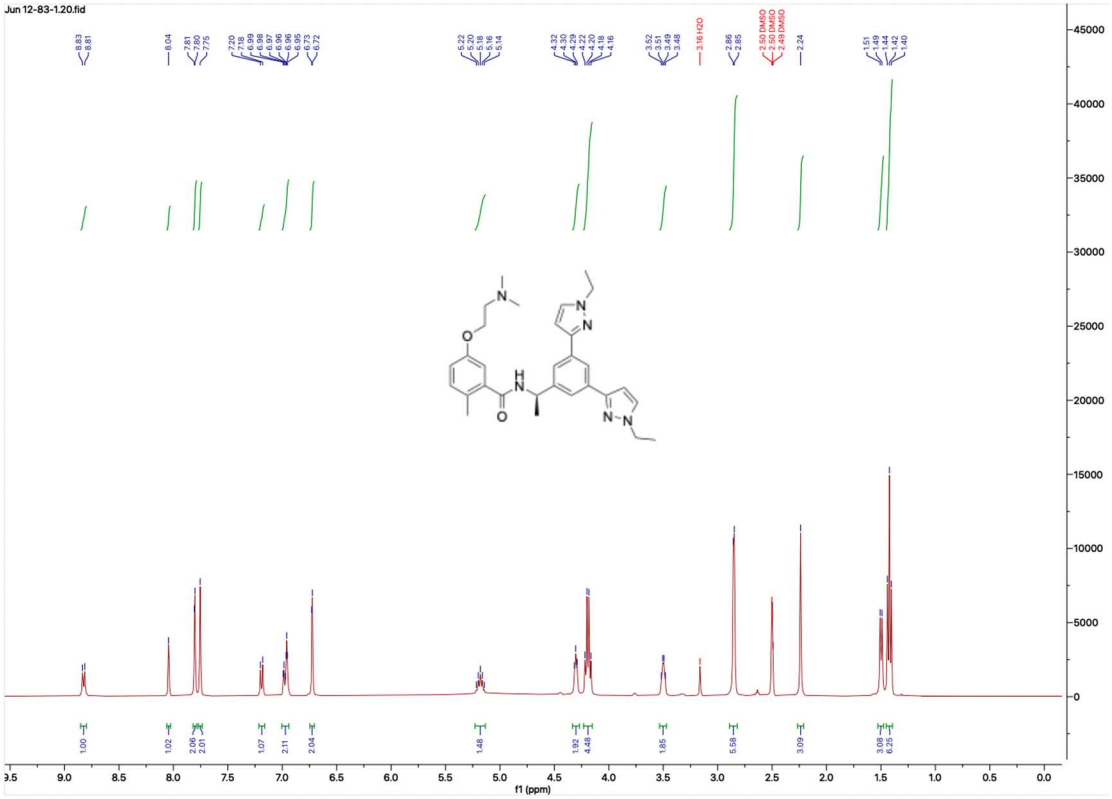

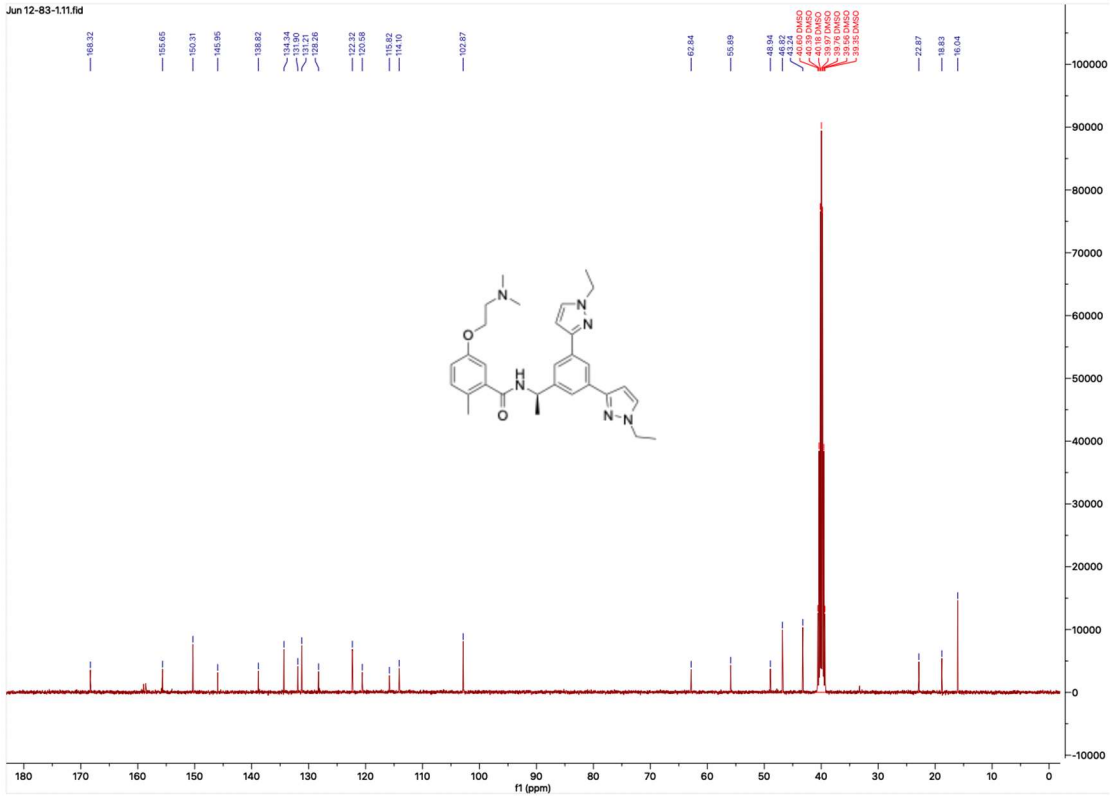

HNMR and CNMR spectra of Jun12833

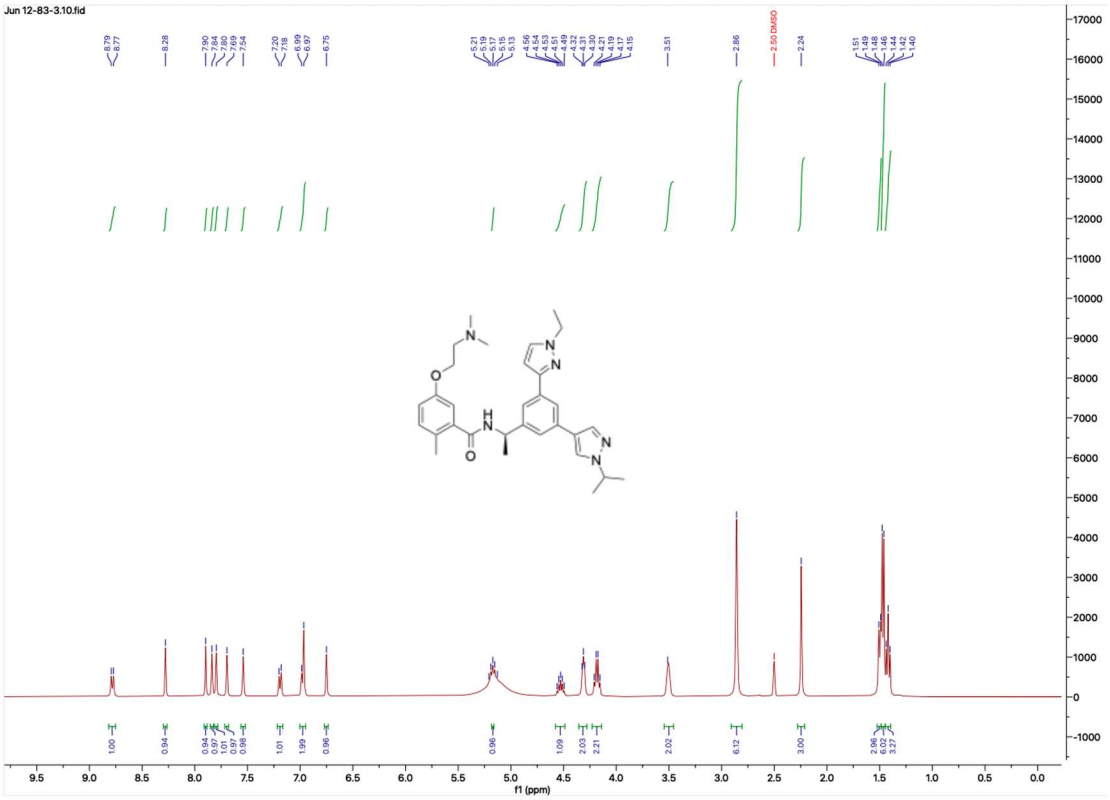

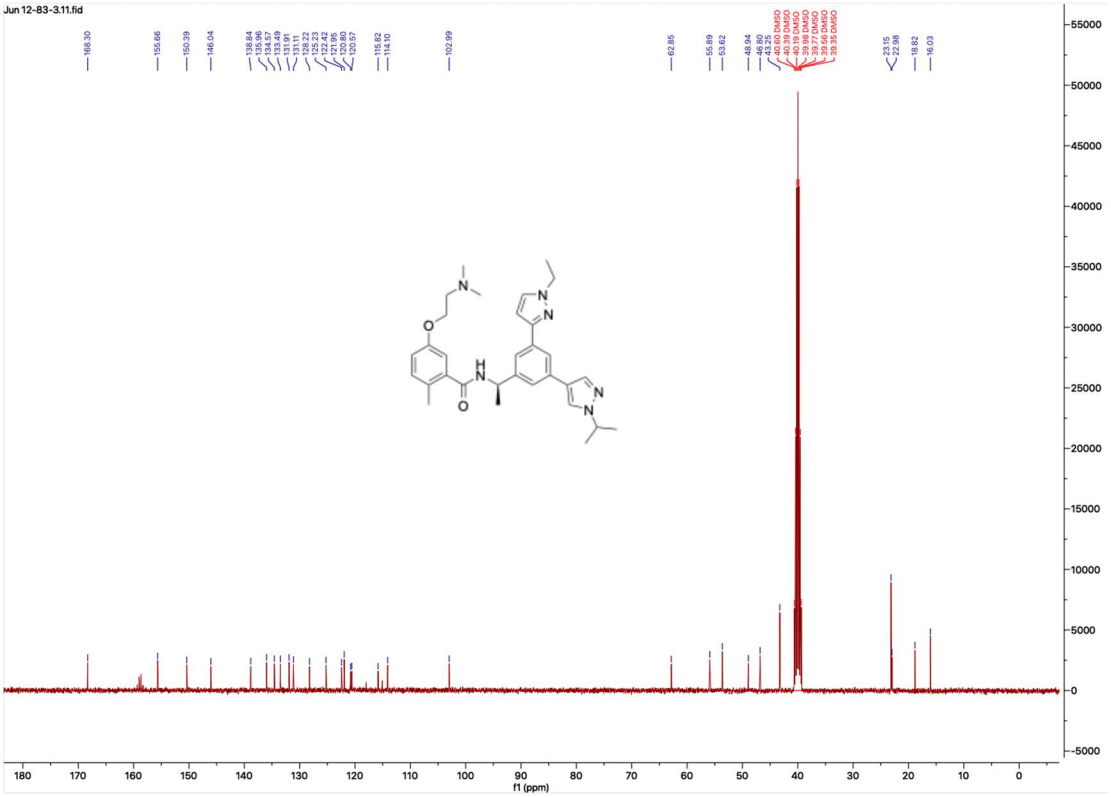

HNMR and CNMR spectra of Jun12834

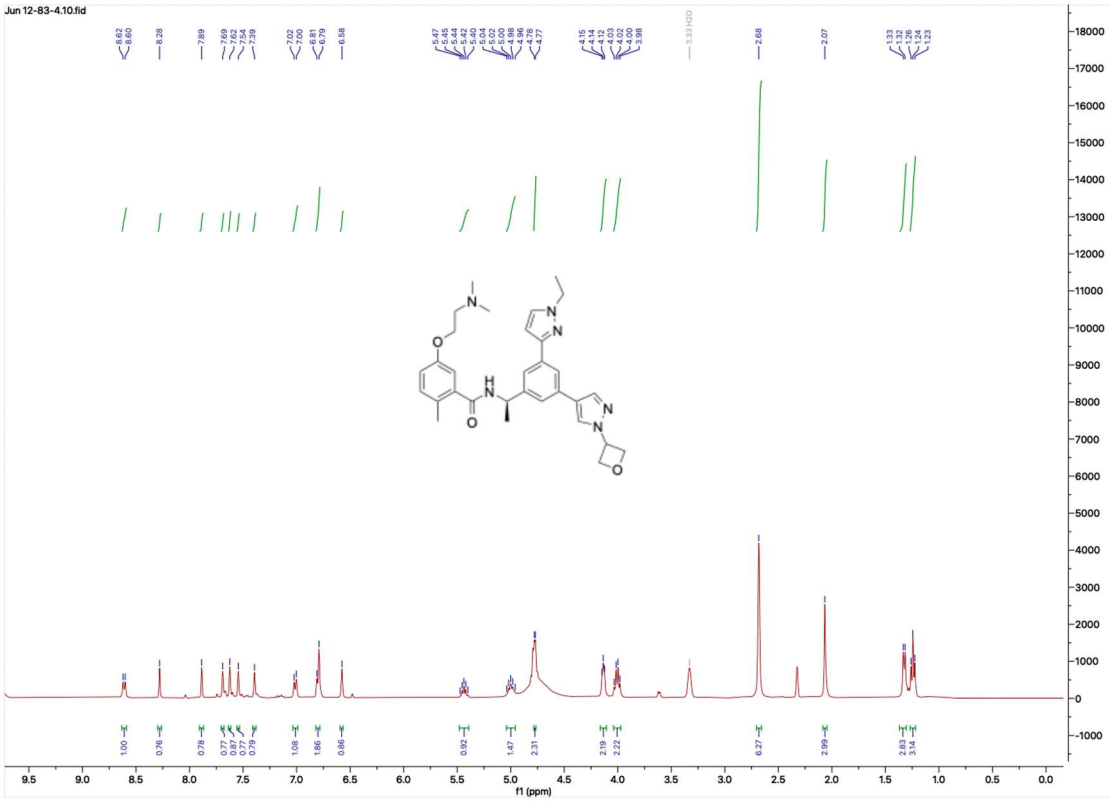

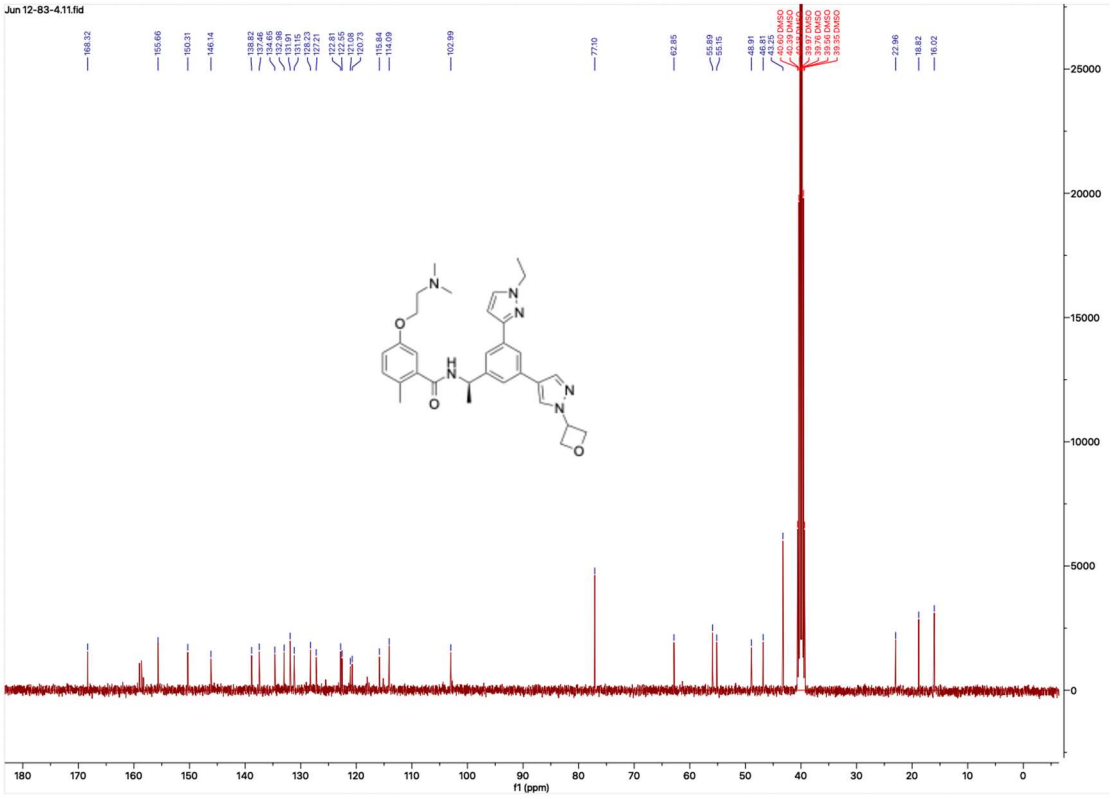

HNMR and CNMR spectra of Jun12835

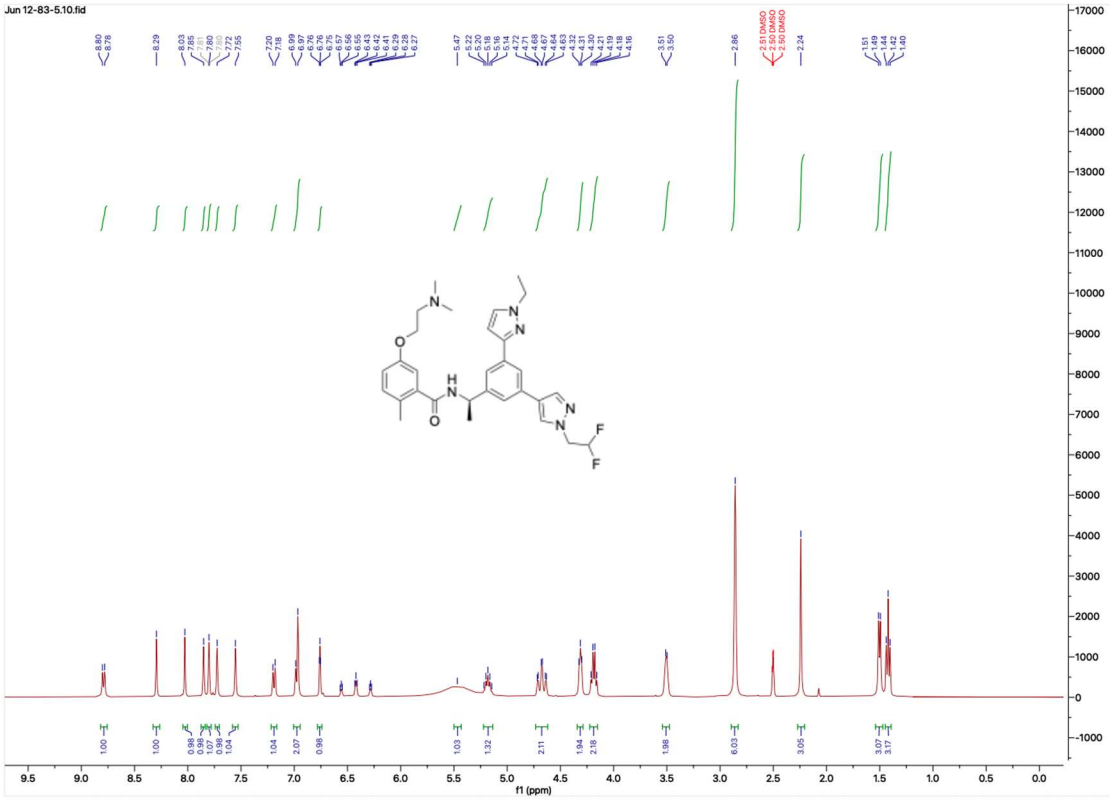

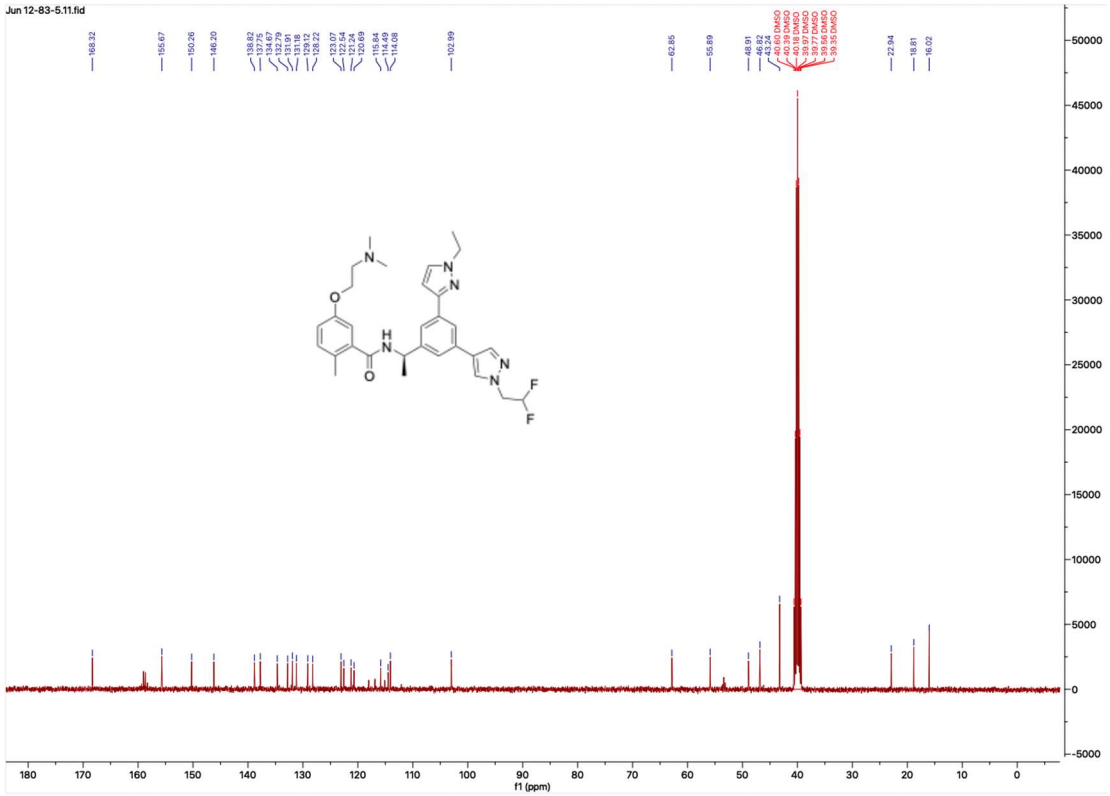

HNMR and CNMR spectra of Jun12836

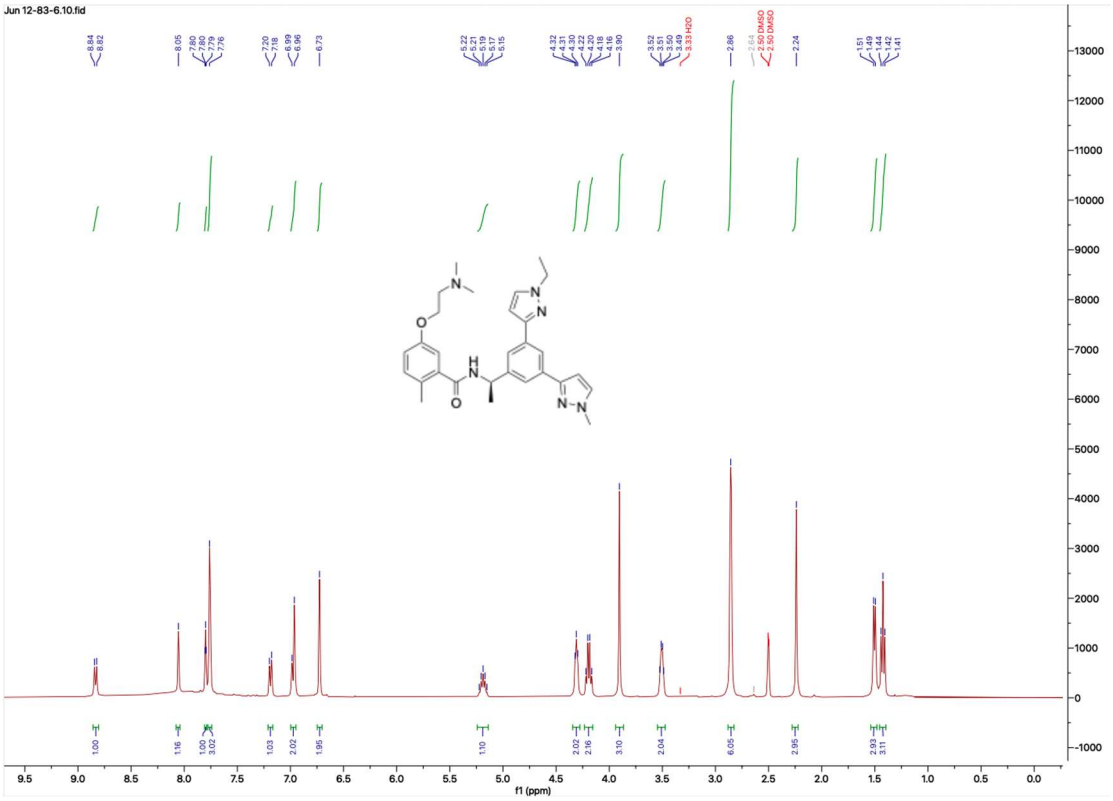

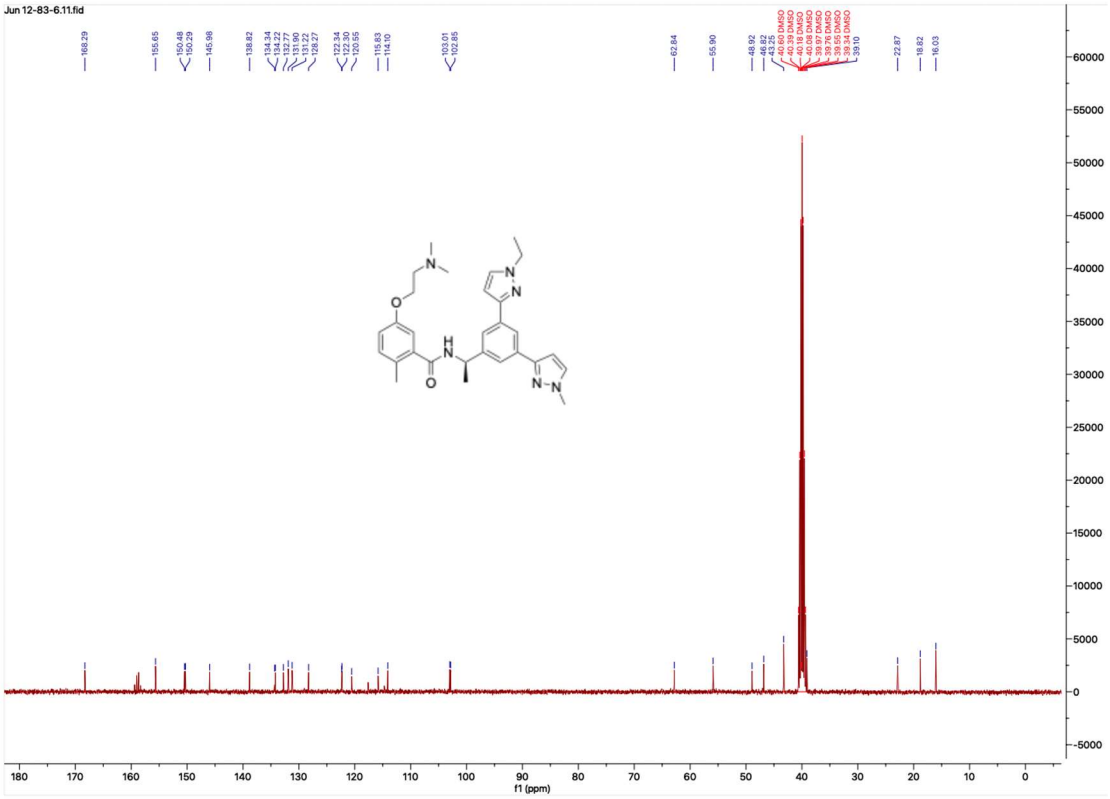

HNMR and CNMR spectra of Jun12837

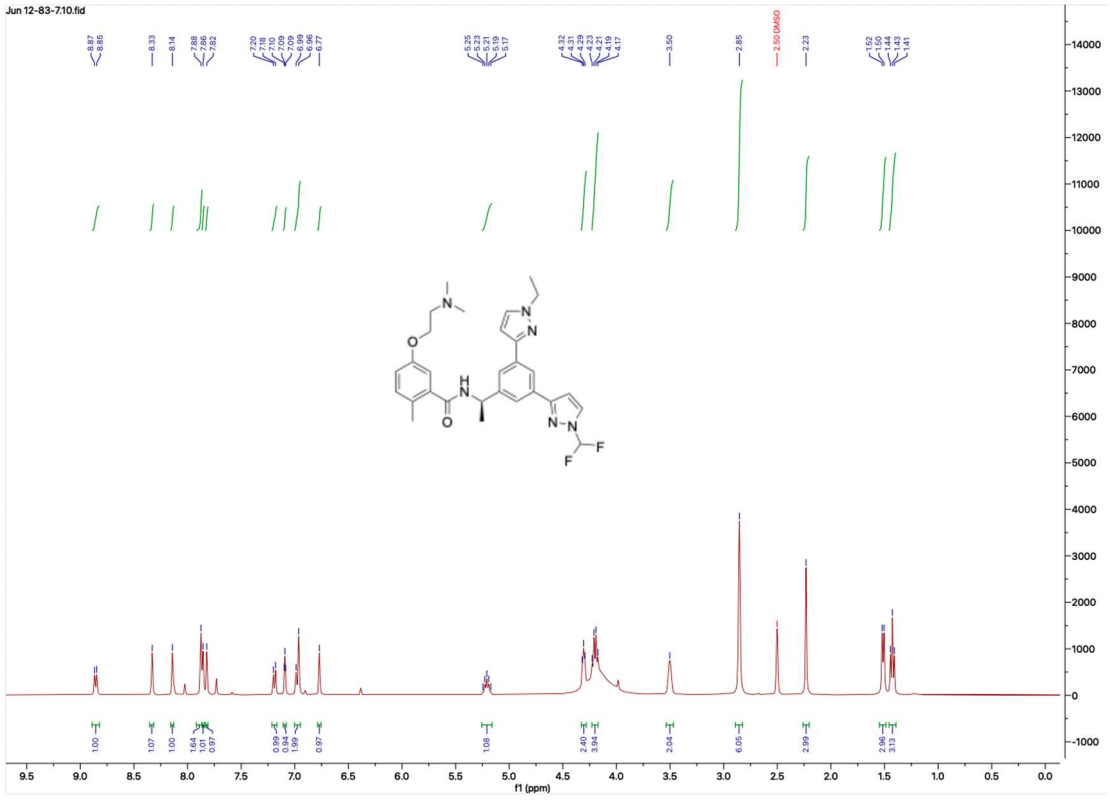

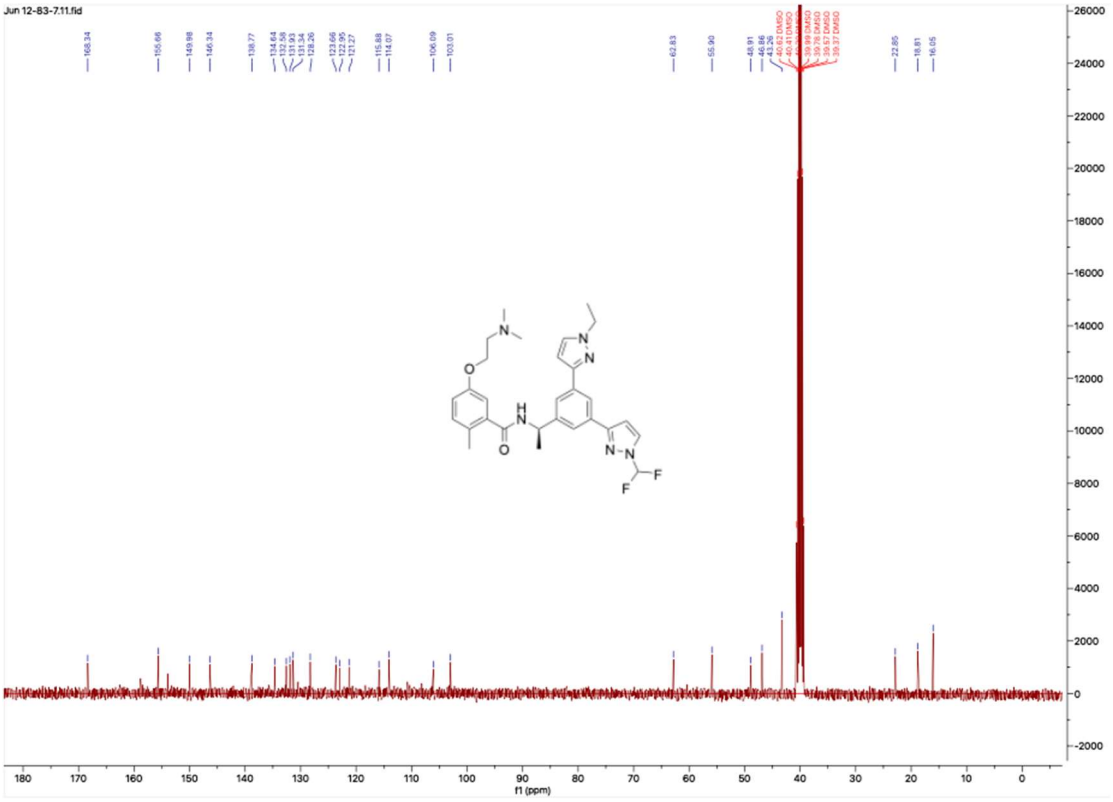

HNMR and CNMR spectra of Jun1314

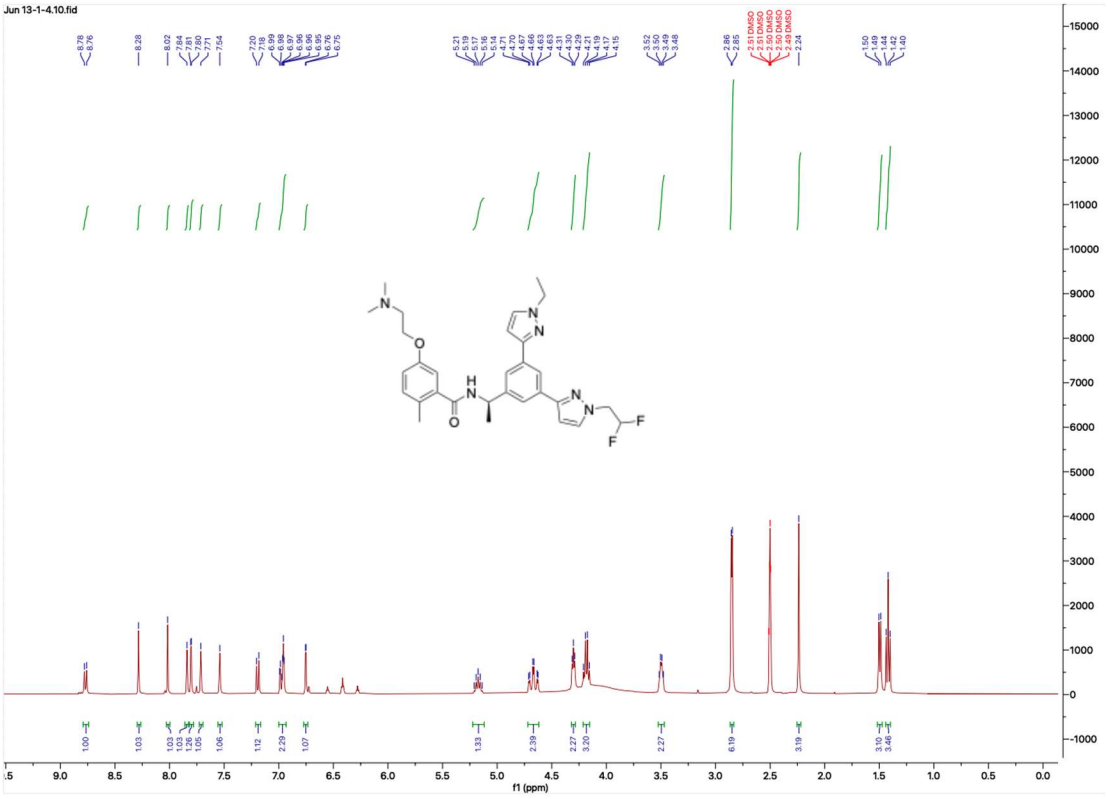

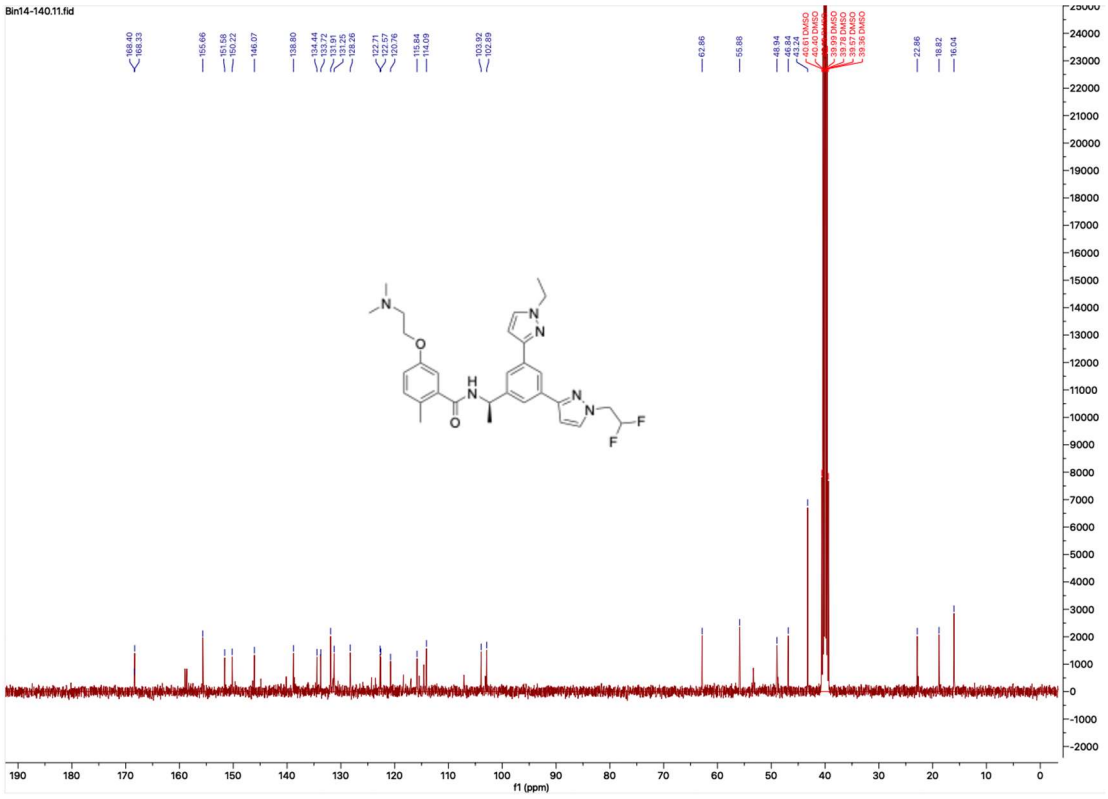

HNMR and CNMR spectra of Jun12839

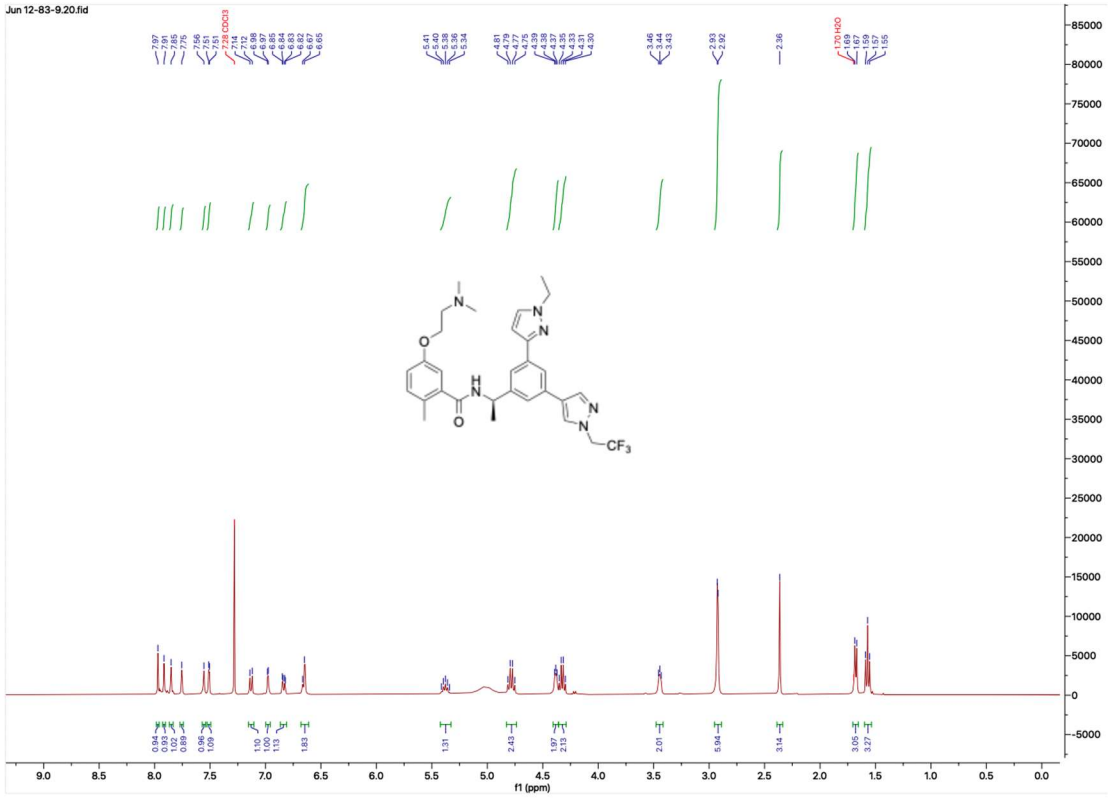

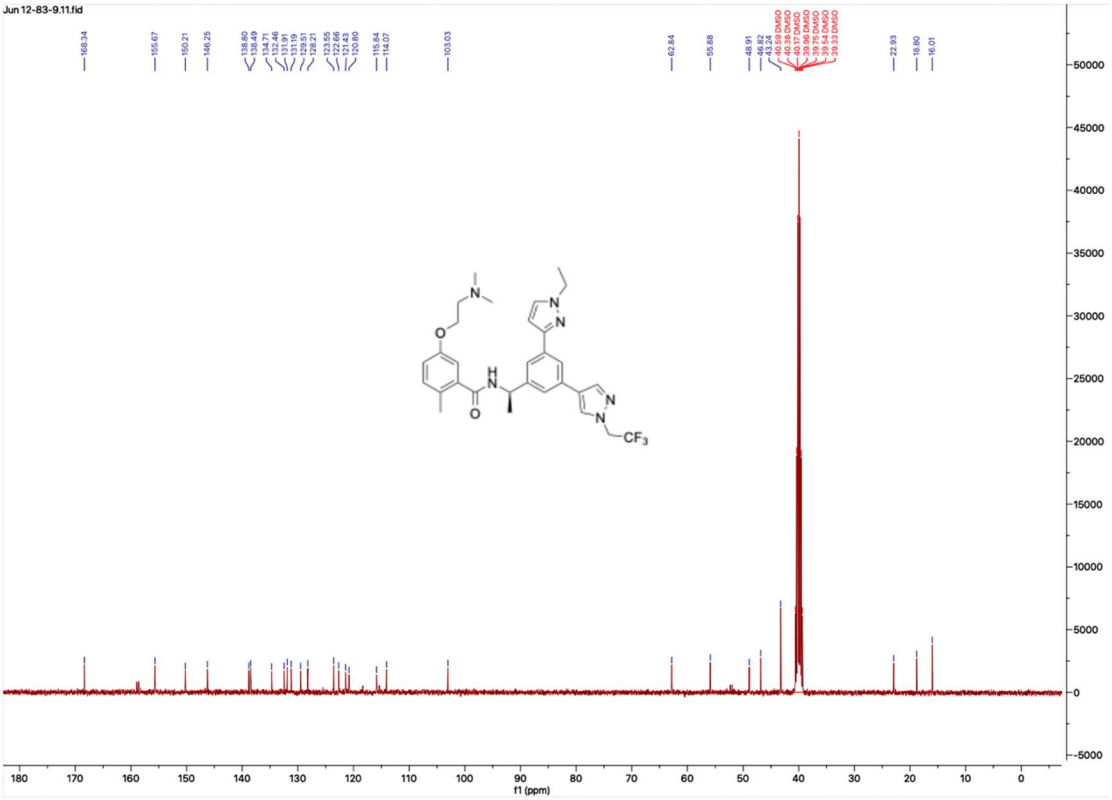

HNMR and CNMR spectra of Jun12682

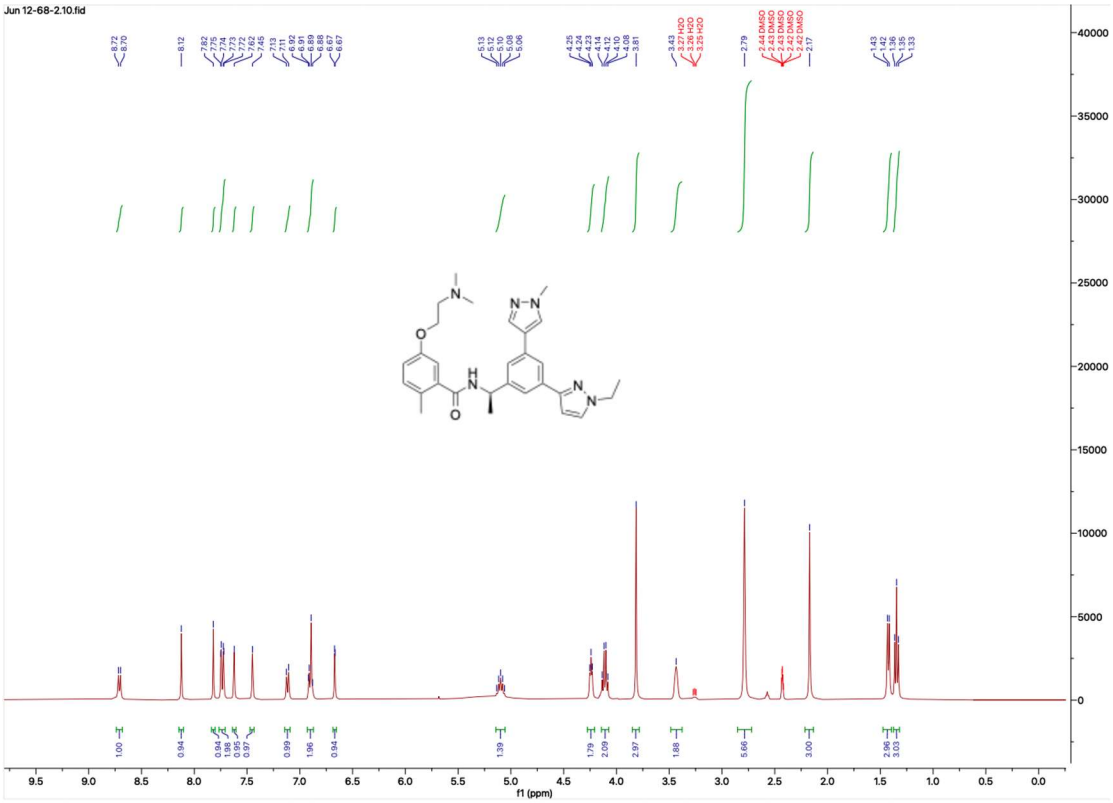

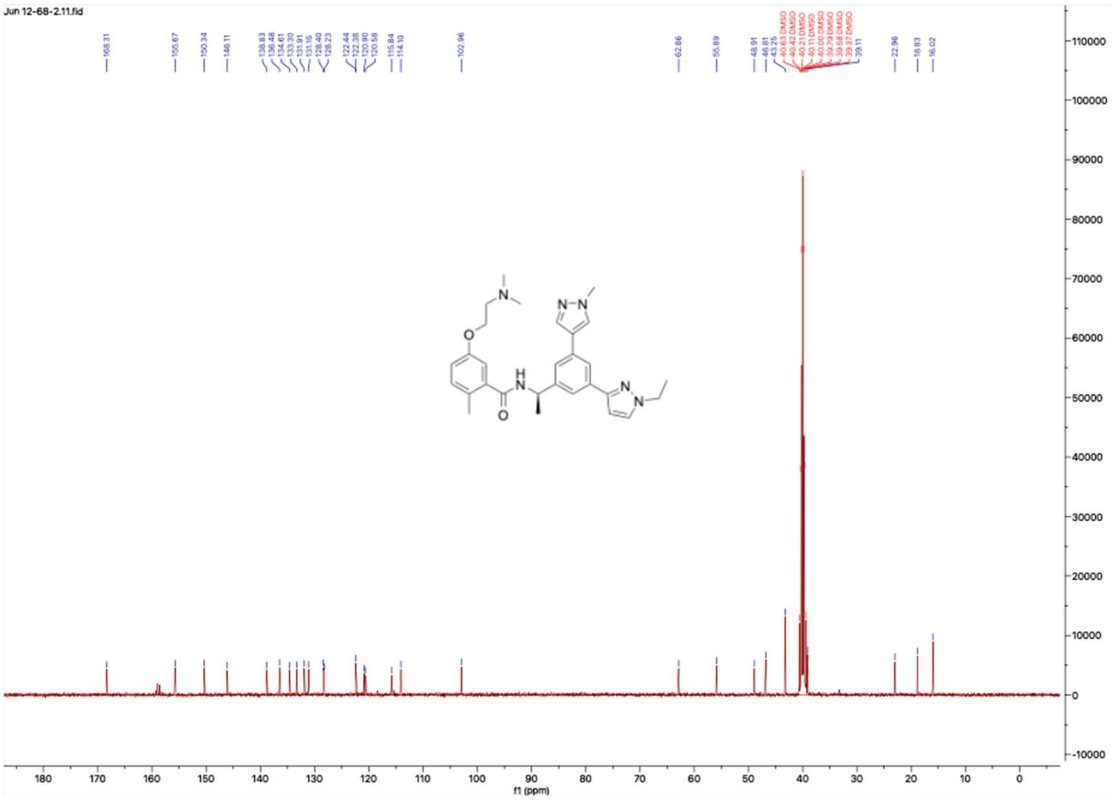

HNMR and CNMR spectra of Jun12924

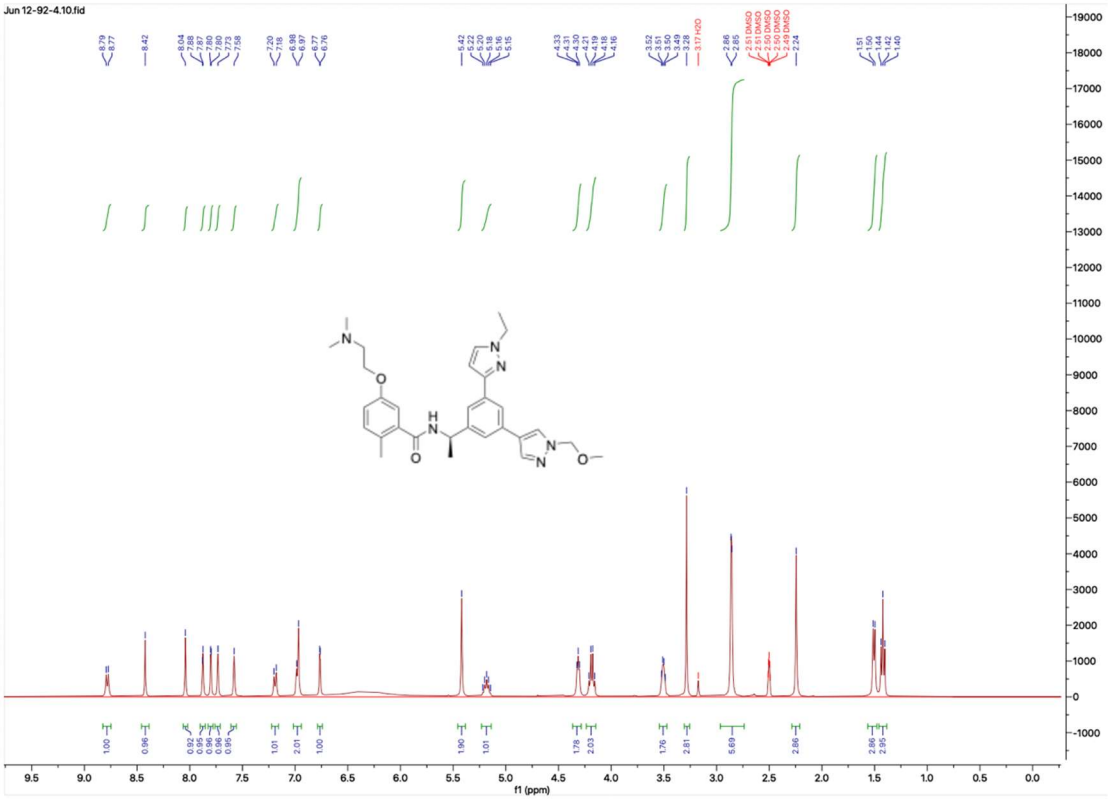

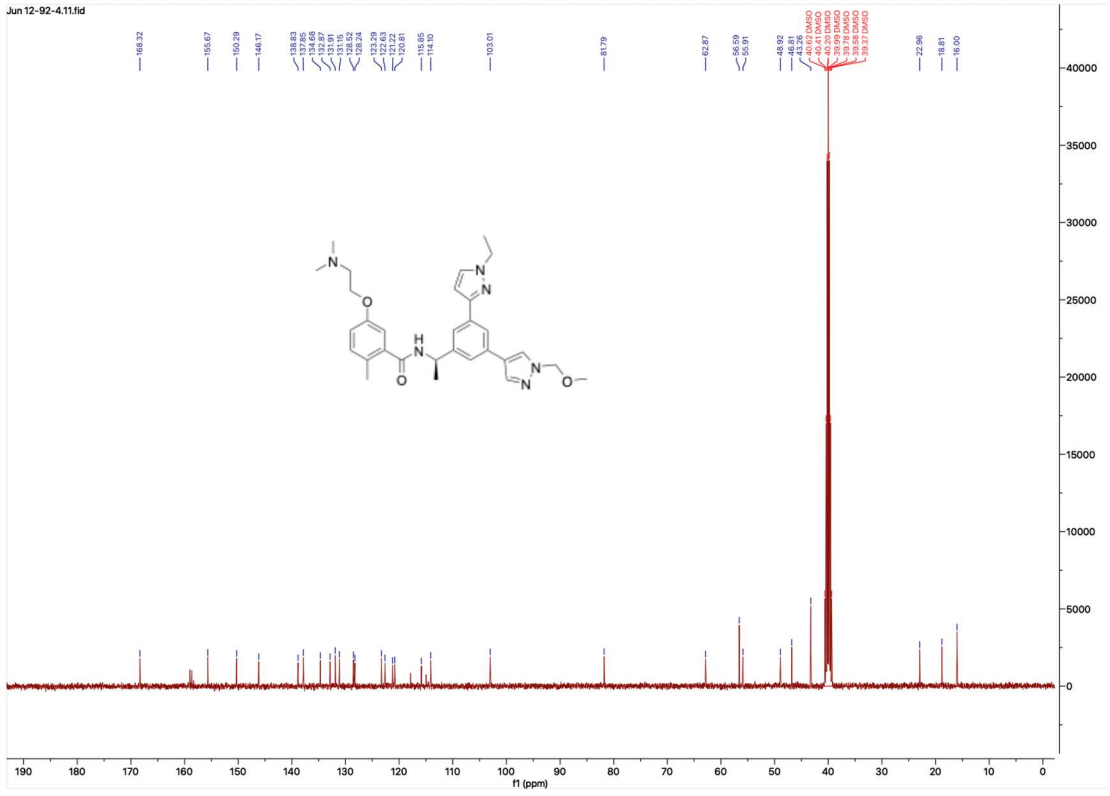

HNMR and CNMR spectra of Jun12763

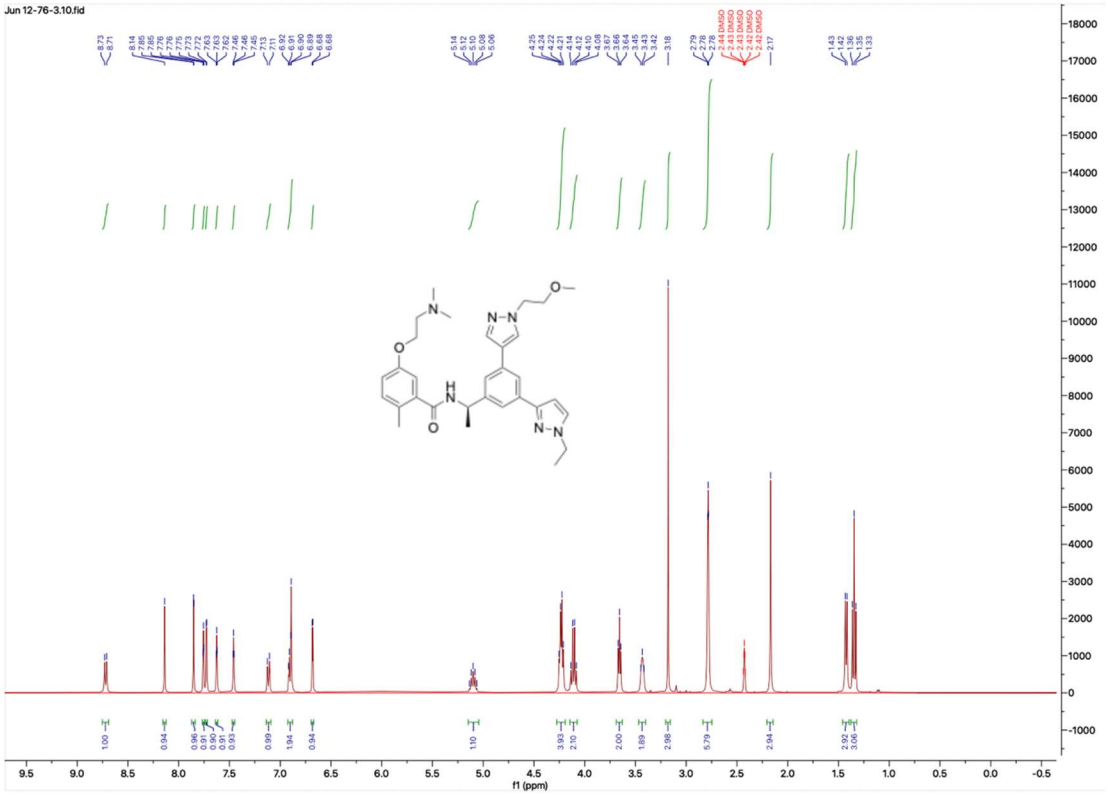

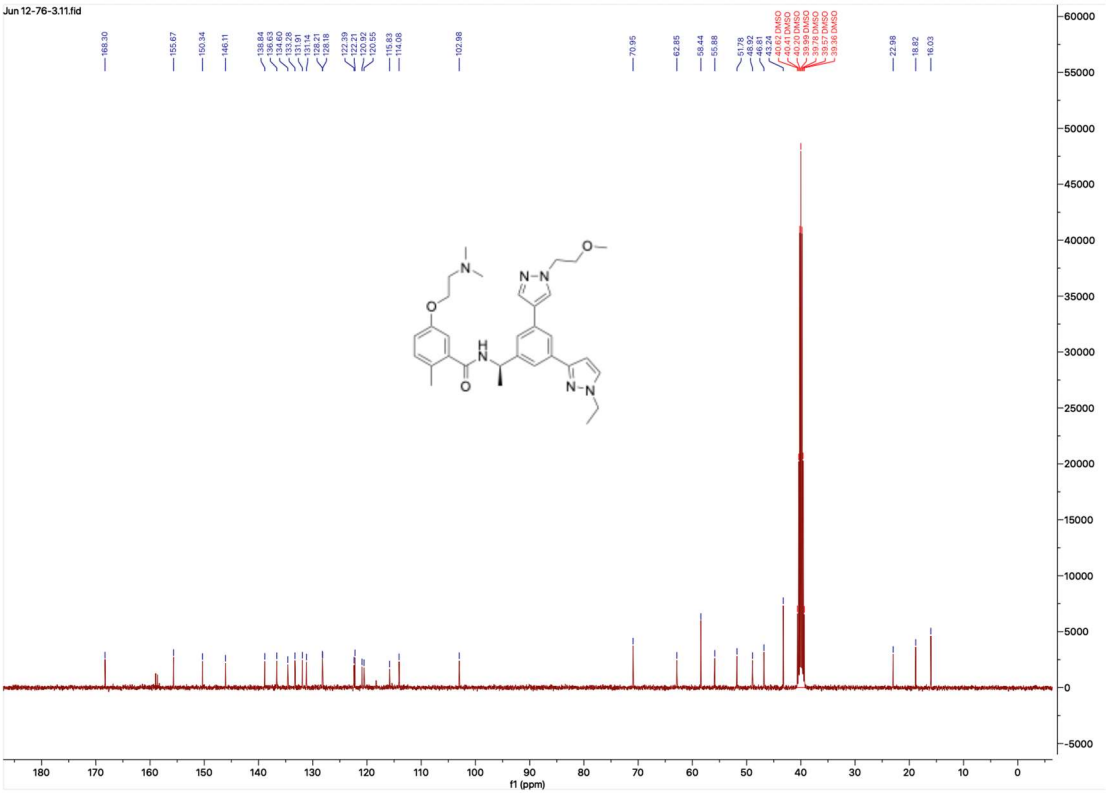

References

1. G. Li, R. Hilgenfeld, R. Whitley, E. De Clercq, Therapeutic strategies for COVID-19: progress and lessons learned. *Nat Rev Drug Discov* **22**, 449-475 (2023).
2. W. H. O. S. T. Consortium, Remdesivir and three other drugs for hospitalised patients with COVID-19: final results of the WHO Solidarity randomised trial and updated meta-analyses. *Lancet* **399**, 1941-1953 (2022).
3. L. D. Saravolatz, S. Depcinski, M. Sharma, Molnupiravir and Nirmatrelvir-Ritonavir: Oral Coronavirus Disease 2019 Antiviral Drugs. *Clin Infect Dis* **76**, 165-171 (2023).
4. D. R. Owen *et al.*, An oral SARS-CoV-2 M(pro) inhibitor clinical candidate for the treatment of COVID-19. *Science* **374**, 1586-1593 (2021).
5. Y. Unoh *et al.*, Discovery of S-217622, a Noncovalent Oral SARS-CoV-2 3CL Protease Inhibitor Clinical Candidate for Treating COVID-19. *J Med Chem* **65**, 6499-6512 (2022).
6. H. Mukae *et al.*, Efficacy and Safety of Ensitrelvir in Patients With Mild-to-Moderate Coronavirus Disease 2019: The Phase 2b Part of a Randomized, Placebo-Controlled, Phase 2/3 Study. *Clin Infect Dis* **76**, 1403-1411 (2023).
7. R. Shimizu *et al.*, Evaluation of the Drug-Drug Interaction Potential of Ensitrelvir Fumaric Acid with Cytochrome P450 3A Substrates in Healthy Japanese Adults. *Clin Drug Investig* **43**, 335-346 (2023).
8. R. Shimizu *et al.*, Safety, Tolerability, and Pharmacokinetics of the Novel Antiviral Agent Ensitrelvir Fumaric Acid, a SARS-CoV-2 3CL Protease Inhibitor, in Healthy Adults. *Antimicrob Agents Chemother* **66**, e0063222 (2022).
9. S. Iketani *et al.*, Multiple pathways for SARS-CoV-2 resistance to nirmatrelvir. *Nature* **613**, 558-564 (2023).
10. Y. Hu *et al.*, Naturally Occurring Mutations of SARS-CoV-2 Main Protease Confer Drug Resistance to Nirmatrelvir. *ACS Cent Sci* **9**, 1658-1669 (2023).
11. L. J. Stevens *et al.*, Mutations in the SARS-CoV-2 RNA-dependent RNA polymerase confer resistance to remdesivir by distinct mechanisms. *Sci Transl Med* **14**, eabo0718 (2022).
12. S. Gandhi *et al.*, De novo emergence of a remdesivir resistance mutation during treatment of persistent SARS-CoV-2 infection in an immunocompromised patient: a case report. *Nat Commun* **13**, 1547 (2022).
13. N. S. Zuckerman, E. Bucris, D. Keidar-Friedman, M. Amsalem, T. Brosh-Nissimov, Nirmatrelvir resistance - de novo E166V/L50V mutations in an immunocompromised patient treated with prolonged nirmatrelvir/ritonavir monotherapy leading to clinical and virological treatment failure - a case report. *Clin Infect Dis* doi: 10.1093/cid/ciad494, (2023).
14. C. P. Sjaarda *et al.*, Prevalence of Low-Frequency, Antiviral Resistance Variants in SARS-CoV-2 Isolates in Ontario, Canada, 2020-2023. *JAMA Netw Open* **6**, e2324963 (2023).
15. Y. Hirotsu *et al.*, Multidrug-resistant mutations to antiviral and antibody therapy in an immunocompromised patient infected with SARS-CoV-2. *Med* **4**, 813-824.e4 (2023).
16. W. Rut *et al.*, Activity profiling and crystal structures of inhibitor-bound SARS-CoV-2 papain-like protease: A framework for anti-COVID-19 drug design. *Sci Adv* **6**, eabd4596 (2020).

17. D. Shin *et al.*, Papain-like protease regulates SARS-CoV-2 viral spread and innate immunity. *Nature* **587**, 657-662 (2020).
18. P. M. Wydorski *et al.*, Dual domain recognition determines SARS-CoV-2 PLpro selectivity for human ISG15 and K48-linked di-ubiquitin. *Nat Commun* **14**, 2366 (2023).
19. Y. M. Baez-Santos, S. E. St John, A. D. Mesecar, The SARS-coronavirus papain-like protease: structure, function and inhibition by designed antiviral compounds. *Antiviral Res* **115**, 21-38 (2015).
20. H. Tan, Y. Hu, P. Jadhav, B. Tan, J. Wang, Progress and Challenges in Targeting the SARS-CoV-2 Papain-like Protease. *J Med Chem* **65**, 7561-7580 (2022).
21. J. Lei, Y. Kusov, R. Hilgenfeld, Nsp3 of coronaviruses: Structures and functions of a large multi-domain protein. *Antiviral Res* **149**, 58-74 (2018).
22. C. Ma *et al.*, Discovery of SARS-CoV-2 Papain-like Protease Inhibitors through a Combination of High-Throughput Screening and a FlipGFP-Based Reporter Assay. *ACS Cent Sci* **7**, 1245-1260 (2021).
23. A. K. Ghosh, J. L. Mishevich, A. Mesecar, H. Mitsuya, Recent Drug Development and Medicinal Chemistry Approaches for the Treatment of SARS-CoV-2 Infection and COVID-19. *ChemMedChem* **17**, e202200440 (2022).
24. Z. Shen *et al.*, Design of SARS-CoV-2 PLpro Inhibitors for COVID-19 Antiviral Therapy Leveraging Binding Cooperativity. *J Med Chem* **65**, 2940-2955 (2022).
25. B. C. Sanders *et al.*, Potent and selective covalent inhibition of the papain-like protease from SARS-CoV-2. *Nat Commun* **14**, 1733 (2023).
26. G. Platzer *et al.*, PI by NMR: Probing CH-π Interactions in Protein-Ligand Complexes by NMR Spectroscopy. *Angewandte Chemie* **59**, 14861-14868 (2020).
27. B. R. Beno, K. S. Yeung, M. D. Bartberger, L. D. Pennington, N. A. Meanwell, A Survey of the Role of Noncovalent Sulfur Interactions in Drug Design. *J Med Chem* **58**, 4383-4438 (2015).
28. H. Tan, Y. Hu, J. Wang, FlipGFP protease assay for evaluating in vitro inhibitory activity against SARS-CoV-2 M(pro) and PL(pro). *STAR Protoc* **4**, 102323 (2023).
29. T. Klemm *et al.*, Mechanism and inhibition of the papain-like protease, PLpro, of SARS-CoV-2. *EMBO J* **39**, e106275 (2020).
30. L. R. Wong *et al.*, Eicosanoid signalling blockade protects middle-aged mice from severe COVID-19. *Nature* **605**, 146-151 (2022).
31. S. A. El-Kafrawy *et al.*, SARS-CoV-2-specific immunoglobulin Y antibodies are protective in infected mice. *PLoS Pathog* **18**, e1010782 (2022).
32. L. Zhang *et al.*, Viral anti-inflammatory serpin reduces immuno-coagulopathic pathology in SARS-CoV-2 mouse models of infection. *EMBO Mol Med* **15**, e17376 (2023).
33. J. Shi *et al.*, RBD-mRNA vaccine induces broadly neutralizing antibodies against Omicron and multiple other variants and protects mice from SARS-CoV-2 challenge. *Transl Res* **248**, 11-21 (2022).
34. V. Fumagalli *et al.*, Nirmatrelvir treatment of SARS-CoV-2-infected mice blunts antiviral adaptive immune responses. *EMBO Mol Med* **15**, e17580 (2023).
35. H. Nobori *et al.*, Efficacy of ensitrelvir against SARS-CoV-2 in a delayed-treatment mouse model. *J Antimicrob Chemother* **77**, 2984-2991 (2022).
36. D. Liebschner *et al.*, Polder maps: improving OMIT maps by excluding bulk solvent. *Acta Crystallogr D Struct Biol* **73**, 148-157 (2017).

37. D. Y. Chen *et al.*, Cell culture systems for isolation of SARS-CoV-2 clinical isolates and generation of recombinant virus. *iScience* **26**, 106634 (2023).
38. X. Deng *et al.*, Breakthrough Infections with Multiple Lineages of SARS-CoV-2 Variants Reveals Continued Risk of Severe Disease in Immunosuppressed Patients. *Viruses* **13**, 1743 (2021).
39. J. R. Tyson *et al.*, Improvements to the ARTIC multiplex PCR method for SARS-CoV-2 genome sequencing using nanopore. *bioRxiv*, (2020).
40. C. Ma *et al.*, Boceprevir, GC-376, and calpain inhibitors II, XII inhibit SARS-CoV-2 viral replication by targeting the viral main protease. *Cell Res* **30**, 678-692 (2020).
41. M. D. Sacco *et al.*, Structure and inhibition of the SARS-CoV-2 main protease reveal strategy for developing dual inhibitors against M(pro) and cathepsin L. *Sci Adv* **6**, eabe0751 (2020).
42. J. Osipiuk *et al.*, Structure of papain-like protease from SARS-CoV-2 and its complexes with non-covalent inhibitors. *Nat Commun* **12**, 743 (2021).
43. Z. Otwinowski, W. Minor, Processing of X-ray diffraction data collected in oscillation mode. *Methods Enzymol* **276**, 307-326 (1997).
44. G. Winter *et al.*, DIALS as a toolkit. *Protein Sci* **31**, 232-250 (2022).
45. P. R. Evans, G. N. Murshudov, How good are my data and what is the resolution? *Acta Crystallogr D Biol Crystallogr* **69**, 1204-1214 (2013).
46. C. Vonrhein *et al.*, Data processing and analysis with the autoPROC toolbox. *Acta Crystallogr D Biol Crystallogr* **67**, 293-302 (2011).
47. A. J. McCoy *et al.*, Phaser crystallographic software. *J Appl Crystallogr* **40**, 658-674 (2007).
48. P. Emsley, K. Cowtan, Coot: model-building tools for molecular graphics. *Acta Crystallogr D Biol Crystallogr* **60**, 2126-2132 (2004).
49. P. V. Afonine *et al.*, Towards automated crystallographic structure refinement with phenix.refine. *Acta Crystallogr D Biol Crystallogr* **68**, 352-367 (2012).
50. M. F. Adasme *et al.*, PLIP 2021: expanding the scope of the protein-ligand interaction profiler to DNA and RNA. *Nucleic Acids Res* **49**, W530-W534 (2021).